Steroid Receptor Crosstalk in Breast Cancer Cells

Erin Elizabeth Swinstead

B. LabMed, B. HSc (Hons)

A thesis submitted to the University of Adelaide in the total fulfilment of the requirements for the degree of Doctor of Philosophy

School of Medicine
Department of Surgery
The University of Adelaide
Adelaide, South Australia

July, 2014

In the middle of difficulty lies opportunity

Albert Einstein

This thesis is dedicated to my Pa, Mum, and Dad

Thank you for this opportunity

CHAPTER 2: MATERIALS AND METHODS

CHAPTER 3: TREATMENT OF HUMAN BREAST CANCER CELLS WITH DIFFERING HORMONES AFFECTS CELLULAR GROWTH RATES AND RNA POLYMERASE II ACTIVATION AT SPECIFIC GENES

CHAPTER 7: GENERAL DISCUSSION

Abstract

Breast cancer is the leading cause of cancer related death in women, and approximately 1 in 11 women will develop breast cancer before the age of 75. In 2003, breast cancer was responsible for 16% of cancer related deaths in Australian women. This demonstrates that throughout the life span of the female, this organ has a high risk of developing cancer. The growth and survival of normal breast epithelial cells and breast cancer cells is promoted by estrogens and progesterone and both estrogen receptor (ER) and progesterone receptor (PR) have been shown to play prominent roles in breast cancer progression. It has also been demonstrated that co-treatment of breast cancer cells with corticosteroids and 17β-estadiol (E2) can have opposing effects on the proliferation of breast cancer cells compared with the single treatment. In addition, glucocorticoid receptor (GR) levels have been shown to have clinical implications for breast cancer cell survival. This suggests a possible role for activated GR in breast cancer development. Forkhead box protein 1 (FoxA1), a member of the forkhead class of DNA-binding proteins, has also been shown to be an important factor in breast cancer development. FoxA1 has been shown to dictate ER binding in breast cancer cells and has been deemed responsible for the rapid reprogramming of ER signalling seen in breast cancers with poor outcomes and treatment resistance. However, the effects of ER on the function of FoxA1 have been controversial. The aim of this thesis is to further investigate and characterise GR, ER, and FoxA1 crosstalk in three estrogenic breast cancer cell lines, MCF-7, ZR-75-1, and T-47D cells.

It has been determined that the combination of dexamethasone (Dex) and E2 have an altered affect on the cell proliferation of breast cancer cells, compared to the single treatment, suggesting GR can modulate the ER response. In an artificial cell model it has been demonstrated by genome-wide investigations, that activated GR and estrogen receptor (ER) can alter the binding of each other at a subset of sites, by a mechanism termed DynaLoad. In addition, it has been shown that Dex and E2 in combination can regulate a unique subset of genes in breast cancer cells. This provides evidence to indicate that Dex can oppose the growth stimulatory effects of E2 signalling, and further, in combination, Dex and E2, can alter the gene transcriptional prolife of MCF-7 breast cancer cells.

To understand how the molecular interplay between GR and ER effect breast cancer progression the genome-wide binding events of activated GR and ER have been investigated. These studies show that a GR and ER DynaLoad mechanism also exists in all three breast cancer cell lines utilised; however, there was very little crossover of binding patterns observed. This suggests that while the mechanisms of DynaLoad are present in all three cell lines, the sites altered are cell specific. Most surprisingly is the discovery of an elevated number of GR sites that are lost upon activation of ER in MCF-7 cells. However, in the other breast cancer cell lines, this finding is not as pronounced. Immunblots show that MCF-7 cells have lower GR protein levels than the other cell lines indicating that steroid receptor (SR) levels play a major role in the effect that the dual hormone treatment has on the cell. This suggests that in a highly estrogenic cell line, ER plays a strong role in modulating GR function, which could have important consequences for disease outcome.

Furthermore, and contrary to previous findings, this thesis establishes that activated ER and GR have the ability to alter the genomic response of the well-established pioneer factor FoxA1. Genome-wide analysis of FoxA1 binding, upon treatment of E2 or Dex, shows that both ER and GR can recruit FoxA1 to specific binding sites within the genome through a DynaLoad mechanism. These results indicate that there is not a specific set of pioneer factors which bind to closed chromatin and establish the binding landscape for other transcription factors (TFs). Instead this data suggests that every factor has the potential to affect the binding landscape of other TFs, depending on the chromatin context.

Overall, the findings from this thesis have provided novel insight into the crosstalk between GR, ER, and FoxA1, further highlighting the ability of activated SRs to alter the response of one another, and other TFs. In addition, it has also been determined that the outcomes of SR crosstalk is cell-specific and that differing estrogenic breast cancer cells can have altered outcomes, which are dependent on SR levels. This can have potential consequences in breast cancer disease outcomes and progression. In addition, the findings in this thesis have begun to shift our classical understanding of pioneer factors in breast cancer, demonstrating that activated GR and ER have the capabilities to recruit and alter the response of FoxA1. This has provided information on a previously unknown complexity to FoxA1 action in breast cancer cells. The studies in this thesis highlight the signalling complexity of TFs in breast cancer cells and provide the basis for further investigations into GR, ER, and FoxA1 mechanisms and the direct consequences of this on breast cancer outcomes.

Declaration

I certify that this work contains no material which has been accepted for the award of any other degree or diploma in my name in any university or other tertiary institution and, to the best of my knowledge and belief, contains no material previously published or written by another person, except where due reference has been made in the text. In addition, I certify that no part of this work will, in the future, be used in a submission in my name for any other degree or diploma in any university or other tertiary institution without the prior approval of the University of Adelaide and where applicable, any partner institution responsible for the joint award of this degree.

I give consent to this copy of my thesis, when deposited in the University Library, being made available for loan and photocopying, subject to the provisions of the Copyright Act 1968.

I also give permission for the digital version of my thesis to be made available on the web, via the University's digital research repository, the Library Search and also through web search engines, unless permission has been granted by the University to restrict access for a period of time.

Erin E. Swinstead

July 2014

Acknowledgements

First and foremost I owe my deepest gratitude to my supervisor and mentor, Dr Gordon Hager. Thank you for giving me the opportunity to join your laboratory, to undertake this project, to learn from your expertise, and for empowering me to complete this thesis. If not for you, this would not have been at all possible. Thank you for believing in my capabilities and instilling confidence in me. You were the first to do so in this long journey and I cannot thank you enough. I feel indebted to you for all you have provided me and I will always be grateful in the kindness and support you have shown me.

I would also like to express my heartfelt gratitude to my mentor, Dr Tina Miranda. You were the change I needed to get this thesis completed and I wouldn't have been able to do it without your unwavering guidance and help. Thank you for providing me technical and bioinformatical assistance and for reading and editing this thesis. Thank you for being my solid rock when the unthinkable had to be achieved and keeping me calm throughout a task deemed impossible by many. A few highlights throughout the last year were the attempts at "blinging" every ones lab benches, the realisation that tap water may in fact be essential in some cases, your twisted humour, and reminding me when all else fails to consider jumping around like a penguin or dressing up as a Jedi. I am also indebted to you for everything you did for me over these last 12 months. You mentored me right to the end, provided me with endless personal and experimental support, and I am sure if you knew what you were signing up for when you were asked to teach an Australian student DHS you would have run in the opposite direction.

I would also like to extend a special thank you to Dr Diego Presman, Dr Ido Goldstein, Dr Ty Voss, Dr Lars Grontved, Dr Josefina Ocampo, and Dr Stephanie Morris. Thank you for all the technical advice, the laughs, the support, and helping me believe I can achieve this. Thank you for the friendship and the lab excursion for burgers at a real "American" diner for lunch. I would also like to thank Ms Mary Hawkins for her technical assistance and guidance.

Thank you to the other members of LRBGE, Dr Songjoon Baek, Dr Sohyoung Kim, Dr Diana Stavreva, Dr Lou Schiltz, Dr Mia Sung, Mr Tom Johnson, Dr Lyuba Varticovski, Dr John Pooley, Dr Qizong Lao, Dr Qiuyan Wang, Dr Bethrice Thompson, Dr Mike Guertin, Dr Iain Sawyer, and Dr Akhi Nagaich. This is truly a lab full of great minds and it was an honour to have the opportunity to be a part of it.

I must thank the University of Adelaide for accepting me into the graduate program and the Australian Government for providing me with the Australian Postgraduate Award. I would also like to thank Professor Alistair Burt, the Head of the School of Medicine at the University of Adelaide for supporting my transition to the graduate partnership program at the National Institute of Health and for taking the time to ensure I was in a suitable position to complete my PhD.

Further I would like to thank Ms Lauren Giorgio from the Cancer Biology Laboratory. I think if we had both known what the last three and a half years was going to have in store for us we may have thought twice about beginning. However, the quote "there is no education like adversity" seems to have a place here. Thank you for all your help, and supporting me during the tougher times in the first two years. I can only hope I provided you with the same support while I

finished in the states. Thank you for the endless laughs during my time at the Basil Hetzel Institute. The most memorable being the quote board, the Port road park bench, the suggestion of Neptune as an alternative place for people to live, and the millions of biohazard bags that weren't strong enough to hold a single tip box. I truly hope your future career is bright and filled with success and you never again think, your treatments evaporated.

On a more personal note I would like to thank my friends and family for the support that they showed during my candidature. Ms Tamyka Penglase, thank you for the endless friendship and support you showed me during the good and tough times during my PhD. Our regular sushi dates were truly missed while in America and I also miss everything that the softball life had to offer our friendship. You always asked how my project was going and what was happening and I am thankful for the support you provided.

Ms Emma McKee and Mrs Casey Barton, you are both such special and long time friends that have always showed such an interest in my studies and have supported my PhD through to the end.

Mrs Joanna Selth, thank you for being a shoulder to cry on when I needed it most and helping me believe that I really am capable of undertaking this PhD. You completely understood the ins and outs of my project and the PhD life. Thank you to Dr Luke Selth for the support and Ms Elsie Selth for being a very good listener!

To the softball crew, there are far too many to name, but the days I spent on and off the field with you all was so important and helped me get through the first two years. I would like to make a special mention to Ms Marni Nichols, thank you for

listening to me talk about my project and PhD life while we hung out in the outfield. I really appreciated the sincere interest you showed. I would also like to thank Ms Laura Bond. From the endless dinners to the emotional support you are a great friend and always had such words of wisdom when I needed them.

To my pets, Suzie at the beginning, and Lola and Ady at the end. As different as you all were there is always something calming found in the affection from a pet. I know this was a hard task for you, Lola!

To my new family; Cliff, Susan, Blair, and Juan. Thank you for the support and enthusiastic interest into my project and PhD. I hope I have done justice to a topic that you also have a personal connection to.

Michelle; my little sister, thank you for always showing an interest in my studies and knowing when to give me the advice of "this is the year to get this darn thing done" when I needed it. The FaceTime chats really kept me going until the end.

Pa, unfortunately you left us before I submitted and had the chance to tell you of this amazing opportunity I was presented with after my first trip to the states in 2012. Without your unwavering love and financial assistance I would never have made it here to begin with. Thank you for the message of "use it wisely," I hope I did just that. Also thank you for telling Mum before you passed "that girl is going to achieve great things just mark my words" just what I needed to hear to make it to the end. Thank you for always believing I was a lot smarter than I ever realised.

Mum and Dad, thank you from the bottom of my heart for guiding me into the person I have become today. You both raised me to take every opportunity

presented to me with both hands, to never give up, and keep on trying. I truly believe that is one of the main reasons I made it through this PhD. Without you both supporting me financially, and in my decision to move I would not have been able to complete this. Mum, your fight with breast cancer was a driving force into the reasons I undertook this project and I hope I did you proud with this body of work.

Lastly, to my husband Reed. I'm not quite sure I have the words to thank you like I should but I don't know what I would have done without you. Your unconditional support and acceptance of this PhD was unwavering and I drew on your patience and optimism repeatedly. Thank you for bearing down and editing this thesis, and understanding that tumour is spelt with a u in Australia! Thank you for listening to the stresses, taking an interest into my project, however foreign it sounded, keeping me calm when the unthinkable had to be achieved, and for being there for me always. You never demonstrated any frustration toward me during this last year as frustrating as it was at times. You made life that much easier for me, especially while I was writing up and I will forever be thankful. I will never forget how kind and supportive you truly have been. Thank you, I would have been lost without you in the end. I love you.

Abbreviations

17β-HSD	17β-hydroxysteroid dehydrogenase
3β-HSD	3β-hysroxysteroid dehydrogenase
ac	acetylation
AF-1	transcriptional activation function 1
AF-2	transcriptional activation function 2
AP-1	activating protein 1
AR	androgen receptor
Aromatase	aromatase cytochrome P-450 enzyme
bp	base pair
BSA	bovine serum albumin
CTCF	CCCTC-binding factor
ChIP	chromatin immunoprecipitation assay
ChIP-chip	tiled oligonucleotide microarrays
ChIP-seq	chromatin immunoprecipitation sequencing
cHRT	combined hormone replacement therapy
CO_2	carbon dioxide
CSS	charcoal stripped fetal bovine serum
C/EBP	CCAAT/enhancer binding protein
DBD	DNA-binding domain
DCIS	ductal carcinoma *in situ*
Dex	dexamethasone
DHEA	dehydroepiandrosterone
DHEA-S	dehydroepiandrosterone sulphate

DHS	DNase I hypersensitivity
DHT	dihydrotestosterone
DMEM	Dulbecco's Modified Eagle Medium
DNA	deoxyribonucleic acid
DNase I	deoxyribonuclease I
DynaLoad	dynamic assisted loading
E2	17β-estradiol
EDTA	ethylenediaminetetraacetic acid
EGTA	ethylene glycol tetraacetic acid
EMT	epithelial-to-mesenchymal transition
ENCODE	The Encyclopedia of DNA Elements
ER	estrogen receptor
ERE	estrogen receptor response element
ERα	estrogen receptor alpha
ERβ	estrogen receptor beta
FAIRE	formaldehyde-assisted isolation of regulatory elements
FBS	fetal bovine serum
FDR	false discovery rate
FIMO	finding individual motif occurrences
FLIP	fluorescence loss in photobleaching
FoxA1	forkhead box protein 1
FRAP	fluorescence recovery after photobleaching
g	gram
GR	glucocorticoid receptor
GRE	glucocorticoid response element

H	histone
h	hour
H_2O	water
HATs	histone acetyltransferase complexes
HCl	hydrogen chloride
HDACs	histone deacetylases
Helix 1	N-terminal helix
Helix 2	C-terminal helix
Her2	human epidermal growth factor receptor
Homer	Hypergeometric Optimization of Motif Enrichment
HRE	hormone response element
HRT	hormone replacement therapy
IDC	invasive ductal carcinoma
ILC	invasive lobular carcinoma
JunD	jun D proto-oncogene
K	lysine
kb	kilobase
KCl	potassium chloride
L	liter
LBD	ligand-binding domain
LCIS	lobular carcinoma *in situ*
LINE	long interspersed repetitive elements
M	molar
me1	monomethylation

me2	dimethylation
me3	trimethylation
MeV	Multiple Experiment Viewer
min	minute
mL	milliliter
mm	millimetre
mM	millimolar
MMTV array	mouse mammary tumour virus promoter
MMTV LTR	mouse mammary tumour virus long terminal repeat
MMTV-Luc	mouse mammary tumour virus promoter luciferase
MR	mineralocorticoid receptor
mRNA	message ribonucleic acid
MYC	v-myc avian myelocytomatosis viral oncogene homolog
NaCl	sodium chloride
P4	progesterone
PAD2	peptidylarginine deiminase 2
PBS	Dulbecco's phosphate buffered saline
PI	protease inhibitors
PR	progesterone receptor
qPCR	quantitative polymerase chain reaction
R	arginine
RO	reverse osmosis
rpm	revolutions per minute
RNA	ribonucleic acid
RNA PolII	RNA polymerase II

sec	second
SDS	sodium dodecyl sulphate
SR	steroid receptor
STR	short tandem repeats
T	testosterone
TAE	tris-acetate-EDTA
TF	transcription factor
trypsin-EDTA 0.25%	trypsin
TSS	transcription start site
ug	microgram
uL	microlitre
uM	micromolar
UV	ultraviolet
V	volts
WHI	Women's Health Initiative

Other:

ºC	degree Celsius
%	percentage
>	greater than
<	less than
≥	greater than or equal too
≥	less than or equal too

Chapter 1

Introduction

1.1 Introduction

The mammary gland is an organ present in female mammals, with its function being to produce milk for offspring. Breast cancer originates from the breast tissue, is the most frequently diagnosed malignancy, and the leading cause of cancer related death in women worldwide. Approximately 1 in 9 women are diagnosed with breast cancer in their life time and the disease accounts for 23% of all invasive new cancer cases (Jemal, Bray et al. 2011). This demonstrates that throughout the life span of females this organ is at high risk of developing cancer.

1.1.1   Structure of the mammary gland.

The development of the mammary gland progresses in stages and is in part controlled by the production of the hormones estrogens (Russo and Russo 2006), progesterone (P4) (Aupperlee, Kariagina et al. 2005), prolactin (Horseman 1999, Aupperlee, Kariagina et al. 2005) and androgens (Birrell, Hall et al. 1998, Labrie 2006). Human mammary tissue is comprised of both glandular and stromal compartments. Glandular tissue is enclosed within a basement membrane and functions to produce milk (Hayes 1993). The mammary gland begins to develop at the prenatal stage when the ectoderm thickens. This is often referred to as the milk line that extends from the neck to the inguinal region of the foetus. As development of the foetus continues, the milk buds form along the milk line and the glandular mammary epithelium originates (Larson 1978). The milk buds continue to develop forming the nipple, and further extend into the mammary fat pad. This extension is in the structure of a series of branching ducts (Larson 1978). To begin, this process is relatively slow up until puberty when the process is accelerated due to the increase in female hormone production. The branching

ducts fill the mammary pad and form a number of separate structures, termed lobes, which in turn comprise of smaller elements called terminal branches, also referred to as lobules. These lobules contain alveoli, lined by epithelial cells, and under the control of the hormone prolactin, produce milk and are often referred to as lactiferous ducts (Donegan 1995). One of the branching ducts forms the lactiferous sinus which narrows and terminates at the nipple (Tortora 1995). The functional component of the mammary gland is called the terminal ductal lobular unit or the TDLU and contains the extralobular terminal ducts, intralobular terminal ducts, and lobules (Figure 1.1) (Cardiff 1998). The mammary gland develops further during pregnancy, and upon increased exposure to P4 the lobules undergo proliferation forming side buds that branch into alveoli. The result of the extensive branching is the entire gland primarily composed of epithelial cells (Larson 1978, Donegan 1995). This state remains until post-lactation, where the mammary gland regresses and undergoes atrophy. However, while the lobules decrease in size, it is not to the extent of a nulliparous female (Larson 1978, Hayes 1993). At menopause the breast glandular tissue undergoes atrophy entirely while in some parts of the breast the lobules disappear and only ducts remain (Hayes 1993).

1.1.2   Breast Cancer.

Breast cancer is the leading cause of cancer related deaths in women (WHO 2008). Approximately 1 in 11 women will develop breast cancer before the age of 75, and in 2003, breast cancer was responsible for 16% of cancer related deaths in Australian women (AIHW 2007). Breast cancer predominantly arises in the epithelial cells lining the lobules or ducts. The earliest detectable form of breast

cancer is localised, pre-invasive lesions termed *in situ* carcinoma, which consist of neoplastic growths confined within individual ducts. The next stage in breast cancer progression is invasive carcinoma and involves the neoplastic cells breaching the basement membrane and invading into the stroma and other parts of the breast tissue (Roses 1999). The last stage of breast cancer progression is when the malignant epithelial cells have the potential to metastasise. This occurs when the cells move from the primary tumour site via the blood stream or the lymphatic vessels to the lymph nodes and then to further organs. In breast cancer, metastases are more commonly found in the brain, liver, and bones (Hayes 1993) (Figure 1.2).

1.1.3 Breast cancer risk factors.

The most important risk factor for breast cancer in women is increasing age, with a maximal incidence observed at 55-64 years (NCI 2007). Family history accounts for approximately 5-10% of all breast cancers (Fackenthal and Olopade 2007) with the best characterised susceptibility genes being BRCA1 and BRCA2 (Miki, Swensen et al. 1994). Obesity in post-menopausal women has been demonstrated as a risk factor for breast cancer development; however, this does not appear to apply in the case of pre-menopausal women (Hsieh, Trichopoulos et al. 1990, Harvie, Hooper et al. 2003). Another risk factor is exposure to hormones. Estrogens promote the growth of breast cancer and increasing the life time exposure of a female to estrogens by early menarche, late menopause, late age at first full-term pregnancy, and nulliparity increases the risk of breast cancer (Clemons and Goss 2001). A more recent risk factor for breast cancer

development is the use of combined hormone replacement therapy (cHRT) in postmenopausal women due to increasing a women's exposure to estrogens.

A large randomised controlled clinical trial with 16,600 women, and 5 year follow-up, was conducted by the Women's Health Initiative (WHI) (Chlebowski, Hendrix et al. 2003). This trial concluded that women on cHRT (i.e. estrogen and progestin in combination) had an increased risk of invasive breast cancer compared with placebo treated women, with an incidence of 0.38% and 0.3% respectively (Rossouw, Anderson et al. 2002). Further, between 1996 and 2001, 1,084,100 women were enrolled in the Million Women Study in the United Kingdom. This study revealed that women on hormone replacement therapy (HRT) (i.e. estrogen alone) or cHRT were at a higher risk of developing breast cancer compared to women that had not used, or were not currently using either of these therapies. Relative risk values were at 2.0 and 1.3 respectively (Beral 2003). However, these results remain controversial, as the findings of the Million Women Study have been questioned due to selection bias on the basis of prescribing practices that may have affected risk estimates (Beral 2003). Re-analysis of the WHI data suggested that women have an increased breast cancer risk while taking cHRT, but that risk decreased during the post intervention stage (Chlebowski, Kuller et al. 2009, Chlebowski, Anderson et al. 2010). More recent analysis of the WHI data has concluded that increased breast cancer mortality can be expected in the future. This being due to the finding that women who are diagnosed while on cHRT have a similar prognosis to women who are not (Chlebowski, Manson et al. 2013). It seems possible from the data that cHRT, but not HRT (i.e. the presence of progestins and elevated estrogen), increases the risk of breast cancer development.

1.1.4   <u>Hormones in breast cancer</u>.

From historic studies we know that estrogen, 17β-estradiol (E2), is required for the development, growth, and homeostatic maintenance of normal and malignant breast tissue (Wittliff 1984, Labrie, Poulin et al. 1990, Mauvais-Jarvis, Kuttenn et al. 1990). Over 100 years ago it was demonstrated that removal of the ovaries can suppress the growth of breast cancer (Beatson 1983), which was later found to be due to a reliance of breast cancer cells on ovarian hormones. In premenopausal women, the ovaries are responsible for P4, testosterone (T), and the majority of circulating estrogen, the most abundant estrogen being E2, under the influence of follicle stimulating hormone (FSH) and luteinising hormone (LH) from the pituitary gland (Dowsett, Folkerd et al. 2005). Another source of estrogen in females is the peripheral tissues where E2 is produced from T and androstenedione via the aromatase cytochrome P-450 enzyme (aromatase). Further, 17β-hydroxysteroid dehydrogenase (17β-HSD) converts estrone to E2 (Simpson 2003).

In postmenopausal women the ovaries cease to function. P4 and T are produced by the adrenal glands and estrogens are produced locally from hormonal precursors also produced by the adrenal glands. Here the adrenal androgen dehydroepiandrosterone (DHEA) and dehydroepiandrosterone sulphate (DHEA-S) are converted to androstenedione via 3β-hydroxysteroid dehydrogenase (3β-HSD), and then T via 17β-HSD which can be aromatised to E2 by aromatase or dihydrotestosterone (DHT) via 5α-reductase. Alternatively, androstenedione can be converted to estrone and further to E2 via aromatase (van Landeghem,

Poortman et al. 1985, Simpson and Davis 2001, Labrie, Luu-The et al. 2003, Simpson 2003, Labrie 2006).

Recently it has been demonstrated that cotreatment of breast cancer cells with corticosteroids and E2 can have opposing effects on the proliferation of breast cancer cells compared with the single treatments. This suggests a possible role for corticoids in breast cancer (Zhou, Bouillard et al. 1989, Rhen and Cidlowski 2006, Cvoro, Yuan et al. 2011, Whirledge, Dixon et al. 2012). Cortisol, a glucocorticoid is synthesised from cholesterol in the adrenal gland. Cholesterol is a 27-carbon sterol that is cleaved to pregnenolone and can be converted to either P4 by 3β-HSD or 17α-hydroxypregnenolone by 17α-hydroxylase. Both P4 and 17α-hydroxypregnenolone are further converted to 17α-hydroxprogesterone then 11-deoxyxortisol and lastly to cortisol by 11β-hydroxylase (Ghayee and Auchus 2007).

1.2 Nuclear Receptors and Cancer

1.2.1   The nuclear receptor family and signalling.

The nuclear receptor super family involves a multitude of transcription factors (TFs) that include evolutionarily related steroid receptors (SRs) as well as orphan receptors. The cellular actions of E2, P4, and glucocorticoids are mediated primarily via binding to and activation of their SRs, estrogen receptor (ER), progesterone receptor (PR), and glucocorticoid receptor (GR) respectively. These hormones can pass through the cell plasma membrane and bind to the SRs resulting in signal transduction. ER, PR, and GR are referred to as class I SRs,

which also includes mineralocorticoid receptor (MR) and the androgen receptor (AR) (Laudet 1997).

SRs contain two structural subunits, the C-terminal ligand-binding domain (LBD) which is moderately conserved and the highly conserved DNA-binding domain (DBD) (Birnbaumer, Schrader et al. 1983, Wrange, Okret et al. 1984, Bain, Heneghan et al. 2007). The LBD is the largest domain and has a number of crucial functions. It consists of an interior binding pocket specific for its cognate ligand. Further it contains a domain crucial for recruiting coactivation proteins termed the ligand-regulated transcriptional activation function (AF-2). This renders coactivators capable of interacting with chromatin-remodeling proteins and transcriptional activation machinery (Xu and Li 2003). Lastly, it is involved in dimerisation or tetramerisation which is necessary for binding to high-affinity deoxyribonucleic acid (DNA) response elements (Kumar and Chambon 1988).

The DBD serves to dock the SRs to the hormone response element (HRE) and is mainly responsible for DNA binding specificity. It further acts as a transmitter of information to other regions of the receptor molecule (Bain, Heneghan et al. 2007). The DBD contains two zinc-finger structures coordinated by four cysteine residues that are necessary to retain a stable structure and function that allows protein folding and DNA-binding activity (Freedman, Luisi et al. 1988). Within the structure are also two α-helics, the N-terminal helix (helix 1) and the C-terminal helix (helix 2). Helix 1 interacts with the major groove of the DNA half-sites and helix 2 overlays helix 1 contributing to stabilisation of the protein structure (Bain, Heneghan et al. 2007). Further there is a D-box and P-box structure. As the DBD can undergo DNA-induced dimerisation upon binding an

inverted repeat HRE, the D-box is responsible for making up the dimer interface and the P-box is critical to sequence-specific DNA binding (Archer, Hager et al. 1990, Meijsing, Elbi et al. 2007). The DBD and LBD is connected by a short amino acid sequence called the hinge region which has the ability to be phosphorylated and this has been identified to be involved in increased transcriptional activity (Knotts, Orkiszewski et al. 2001, Lee, Choi et al. 2006). In addition to the LBD and the DBD there is an N-terminal region which contains a constitutionally active transactivation region called the transcriptional activation function (AF-1). In contrast to the AF-2, the AF-1 sequence demonstrates weak sequence conservation within the SR family (Takimoto, Tung et al. 2003)

The mediators of estrogens are the estrogen receptor alpha (ERα) and estrogen receptor beta (ERβ). The ERα was cloned in 1986 (Green, Walter et al. 1986, Greene, Gilna et al. 1986) and later in 1996 ERβ was cloned from the rat prostate (Kuiper, Enmark et al. 1996) with both being encoded by separate genes on different chromosomes (Balfe, McCann et al. 2004). The *ERα* gene has 8 exons and is localised to chromosome 6q24-27 while the protein is 595 amino acids in length and has a molecular weight of 66 kDa (Greene, Gilna et al. 1986). In comparison, the ERβ protein has a molecular weight of approximately 61.2 kDa (Kuiper, Enmark et al. 1996, Kuiper and Gustafsson 1997) and is 530 amino acids long (Ogawa, Inoue et al. 1998). Further, the *ERβ* gene is localised to chromosome 14q23-2 and is also 8 exons in length (Kuiper, Enmark et al. 1996, Kuiper and Gustafsson 1997). One of the most well characterised E2-regulated genes is the PR, which is mediated by P4 and expressed in two isoforms. These two isoforms are transcribed from the same gene: *PR-A* and *PR-B*, is localised to chromosome 11q22-q23, and is 8 exons in length. PR-A has a protein size of 94

kDa and PR-B 116 kDa (Rousseau-Merck, Misrahi et al. 1987, Kastner, Krust et al. 1990, Kraus, Montano et al. 1993). PR-B is generally a much stronger activator of transcription than PR-A (Giangrande and McDonnell 1999, Richer, Jacobsen et al. 2002), which can be explained in part by the presence of an additional 165 amino acids at the N-terminal end, referred to as the B-upstream segment or AF-3 (Sartorius, Melville et al. 1994, Leonhardt, Boonyaratanakornkit et al. 2003). PR was first cloned from chicken oviduct in 1986 (Jeltsch, Krozowski et al. 1986). The GR was first cloned in rat in 1984 (Miesfeld, Okret et al. 1984), is activated by glucocorticoids, and is 94 kDa in length and 777 amino acids long (Hollenberg, Weinberger et al. 1985, Weinberger, Hollenberg et al. 1985). The gene is localised to chromosome 5q11-q13 and contains 9 exons (Hollenberg, Weinberger et al. 1985) (Figure 1.3).

In the absence of hormone, ER and PR are predominantly localised in the nucleus where as GR is located in the cytoplasm. The receptors are in an inactive complex with chaperones including heat shock protein 90 and heat shock protein 70 (Pratt and Toft 1997). Upon ligand binding to the receptors the complex dissociates and the receptor translocates into the nucleus where they classically form homodimers which bind with high affinity to HREs, which is a consensus sequence of two palindromic hexanucleotide half-sites. While it is known that the structure of the HRE is conserved, ER recognises a consensus sequence of AGGTCA whereas GR and PR recognise a consensus AGAACA sequence (Evans 1988, Tsai, Carlstedt-Duke et al. 1988, Umesono and Evans 1989). The DNA bound receptors recruit transcription machinery factors and mediate transcription responsive genes (Yamamoto 1985, Beato 1989, Hall, Couse et al. 2001, Heldring, Pike et al. 2007) (Figure 1.4).

1.2.2   Role of ER, PR, and GR in breast cancer.

The roles of ER and PR in breast cancer progression are well known and have been highly defined however the involvement of GR in breast cancer homeostasis and development is only beginning to be uncovered. ER is expressed in approximately 55-80% of primary breast cancers, while PR is expressed in 45-82% (McGuire 1978, Rosa, Caldeira et al. 2008). The expression of these receptors in combination is currently used to predict the patient's response to endocrine therapies (Creighton, Kent Osborne et al. 2009). Loss of ER and PR expression is associated with a more aggressive, treatment resistant breast cancer (Fisher, Redmond et al. 1983, Fisher, Wickerham et al. 1983). For these women anti-estrogen therapy will not be effective, limiting the available treatment options. It has long been understood that estrogens promote the growth and proliferation of breast cancer cells. Further, the actions of synthetic progestins and the effect they have on proliferation of breast cancer cell lines has also been intensively investigated. In ZR-75-1 and T-47D breast cancer cells, R5020 (a synthetic progestin) alone has no effect on cell proliferation, however, in combination with E2, causes a significant decrease in proliferation driven by E2 alone. These effects can be reversed by RU486, which is a PR and GR antagonist (Hissom and Moore 1987, Moore, Hagley et al. 1988, Gill, Tilley et al. 1991), as well partially by the AR antagonist hydroxyflutamide (Poulin, Dufour et al. 1989). Likewise, in MCF-7 breast cancer cells several synthetic progestins have no effect on cell proliferation alone, but in combination with E2 cause a significant reversal of E2-induced proliferation. However, interestingly these results cannot be reversed via RU486 unlike previously observed in ZR-75-1 and T-47D cells (van der Burg, Kalkhoven et al. 1992). In a further assessment of cell

behaviour, it has been demonstrated that P4 and medroxyprogesterone 17-acetate (MPA) (a synthetic progestin) enhance migration and invasion in T-47D breast cancer cells, and this can be inhibited via the use of a PR antagonist, ORG 31710 (Fu, Giretti et al. 2008). It was later demonstrated that E2 and P4 cotreatment resulted in a decrease in cell migration and invasion in comparison to E2 alone (Fu, Giretti et al. 2008).

Glucocorticoids are well known to play an essential role in embryonic development and tissue homeostasis. Further, they have anti-inflammatory and immunosuppressive properties (Franchimont 2004). It has been shown that the addition of glucocorticoids to chemotherapy in advanced breast cancer treatment initially resulted in an increased response rate; however; there was no observed effect on one year survival. This perhaps isn't a surprising phenomenon due to the increasing evidence suggesting that glucocorticoids can indeed improve cancer cell survival. This has been shown to be a result of glucocorticoids increasing cancer cells ability to evade apoptosis (Herr and Pfitzenmaier 2006, Redondo, Tellez et al. 2007). It is increasingly becoming apparent that GR signalling may play a critical role in breast cancer development (Vaidya, Baldassarre et al. 2010, Vilasco, Communal et al. 2011). In MCF-7 cells it has been observed that dexamethasone (Dex), a synthetic glucocorticoid, inhibits the proliferative effects of E2. It was also shown that this inhibition is alternated by RN486 (Zhou, Bouillard et al. 1989). A study investigating GR transcription demonstrated that grade 3 breast cancers when compared with normal breast tissue or 1 and 2 grade tumours had overexpressed levels of GR (Smith, Lea et al. 2003). It has also been demonstrated that GR message ribonucleic acid (mRNA) levels were significant increase in the stroma when compared with normal tissue,

suggesting a possible role for GR in stromal and tumour epithelial interactions (Smith, Lea et al. 2007). Moreover, it has been shown that high levels of GR expression is significantly correlated with shorter relapse free survival in patients with ER negative breast cancers. Furthermore, it has been noted that ER positive breast cancers with high GR expression levels are associated with better outcomes compared to breast cancers with low GR expression (Pan, Kocherginsky et al. 2011). While it is becoming very apparent that GR appears to play an important role in breast cancer alone with the well understood role of ER and PR, what has not been investigated in depth is how ER, PR, and GR act together, and how they might act mechanistically to affect cellular responses.

1.2.3   Nuclear receptor crosstalk in cancer.

Genome-wide investigations have provided important information on SRs functions. However, most have been performed in control environments where only one receptor is activated at a time. We know in a physiological context that multiple receptors are activated at one single time due to all cells being exposed to a mixture of hormones. It is becoming apparent that co-activation of SRs can effect each other's functions and change cellular responses. It has been demonstrated that co-activation of ER and GR reprograms the binding landscape resulting in a rearrangement of SR binding in mouse mammary cells. Specifically, activation of GR allows ER to bind to specific sites in the genome. Moreover, activation of ER can affect the chromatin structure of GR sites that are estrogen dependent resulting in a new subset of GR binding sites. Co-activation of both ER and GR can also result in a loss of specific binding sites for each receptor (Miranda, Voss et al. 2013). It also has been previously reported in

MCF-7 cells stably transfected with mouse mammary tumour virus promoter luciferase (MMTV-Luc) E2 significantly inhibits GR mediated MMTV-Luc transcription. E2 has also been demonstrated to inhibit the known glucocorticoid induction of p21 suggesting a role for GR and ER crosstalk (Kinyamu and Archer 2003).

Further to the studies observed in breast cancer cells it has also been shown that AR and GR have similar binding patterns in prostate cancer cells. In addition, GR regulates a large number of genes that are originally considered AR pathway specific (Sahu, Laakso et al. 2013). Recently it has been demonstrated that GR substitutes for AR in prostate cancer cells to activate a group of genes and was required to maintain a castrate resistant phenotype. This suggests that GR primes cells to drive an AR phenotype during AR blockade, resulting in a new mechanism of castrate resistance by GR and AR crosstalk (Arora, Schenkein et al. 2013).

1.3 Binding and recruitment of nuclear receptors to chromatin

---

1.3.1   <u>Dynamic binding of nuclear receptors</u>.

It has been shown that chromatin structure is important for SRs binding and recruitment and therefore plays an important role in SRs crosstalk. Classically the binding of SRs to HRE has been considered to be a long-term process with residency at the chromatin lasting for minutes (min) to hours (h). This long-term residency was reflected to result in the stable assembly of cofactors and TFs (Becker, Gloss et al. 1986, Schaffner 1988). However, further studies have elucidated that SRs rapidly exchange with DNA. Utilising a tandem array of the

mouse mammary tumour virus promoter (MMTV array) (Walker, Htun et al. 1999, McNally, Muller et al. 2000) a green florescent protein-tagged GR in live cell fluorescence microscopy has shown to stably integrate with the MMTV array rapidly. By fluorescence recovery after photobleaching (FRAP) and fluorescence loss in photobleaching (FLIP), this dynamic exchange observed at the MMTV array has been found to be at a magnitude of seconds (Htun, Barsony et al. 1996, Walker, Htun et al. 1999, McNally, Muller et al. 2000, Becker, Baumann et al. 2002). The same phenomena has been observed for ER (Reid, Hubner et al. 2003, Sharp, Mancini et al. 2006), AR (Klokk, Kurys et al. 2007), nuclear factor kappa-B (Bosisio, Marazzi et al. 2006), and RNA polymerase II (RNA PolII) (Becker, Baumann et al. 2002, Dundr, Hoffmann-Rohrer et al. 2002). This paradigm shifted our understanding of SRs dynamics. In contrast to the notion that SRs had long term residency on chromatin, it is now understood that receptors continuously cycle and transiently interact with chromatin. This mode of action has been termed the "hit-and-run" model for binding (McNally, Muller et al. 2000).

The analysis of SRs function has long been limited to promoters of well investigated genes. Advances in technology now allow investigation on an unprecedented scale. The earlier studies utilising chromatin immunoprecipitation assay (ChIP) DNA hybridised to tiled oligonucleotide microarrays (ChIP-chip) to a single chromosome surprisingly revealed that ER and AR were found distal to gene transcription start sites (TSS) which at times were up to 200 kilobase (kb) away (Carroll, Liu et al. 2005, Wang, Li et al. 2007). These findings were later confirmed using genome-wide analysis via ChIP-chip and chromatin immunoprecipitation sequencing (ChIP-seq). These studies have shown that

more than 60% of binding events are located distal to promoter regions, located in intergenic and intronic domains (Carroll, Meyer et al. 2006, So, Chaivorapol et al. 2007, Reddy, Pauli et al. 2009, Welboren, van Driel et al. 2009).

SR interact with chromatin with the chromosomal architecture largely restricting the access of SRs to their HRE. It has been shown that SRs interact with chromatin that is accessible prior to hormone signalling (John, Sabo et al. 2008, Hurtado, Holmes et al. 2011, John, Sabo et al. 2011, He, Meyer et al. 2012). Specifically, genome-wide studies of chromatin accessibility and GR binding events have demonstrated that approximately 95% of GR binding is located at are pre programmed chromatin. The remaining 5% of GR binding events occurred at classical *de novo* sites (John, Sabo et al. 2011). This suggests that perhaps the chromatin is primed by other factors to maintain SR binding (Voss, Schiltz et al. 2011).

1.3.2   <u>Role of histone modifications and histone variants</u>.

Transcription factors interact with chromatin to elucidate a transcriptional response and the chromatin landscape is critical to regulate gene expression. Histones are proteins found in the cell nuclei that package DNA in to nucleosomes. There are five major histones; H1/H5, H2A, H2B, H3, and H4. Histones H2A, H2B, H3, and H4 are known as the core histones while H1 and H5 are the linker histones. A stable nucleosome complex comprises of two H2A-H2B dimers associated on either side of a H3-H4 tetramer and this forms the octameric nucleosome core particle (Luger, Mader et al. 1997, Wolffe and Hayes 1999). There is 147 base pairs (bp) of DNA wrapped around the nucleosome core (Luger, Mader et al. 1997). The linker histone H1 attaches the nucleosome to the

DNA which in turn allows the development of the higher order structure. This higher order structure consists of wrapping DNA around nucleosomes with approximately 50 bp of DNA between each nucleosome. The interaction of DNA with nucleosomes as well as the interaction with linker histone H1 compacts DNA but also inhibits DNA sequences of regulatory factors (Orphanides and Reinberg 2000, Orphanides and Reinberg 2002). The N-terminal of histone H3 and histone H2B forms a tail and passes through the major groove of the DNA double strand approximately every 20 bp. The N-terminal tail of histone H4 forms an interaction with the histone H2A-H2B dimer complex of another nucleosome. The histone tails provide a site for chemical modifications to occur, that being phosphorylation, acetylation, methylation, or ubiquitylation. These chemical post-translational modifications alter chromatin structure and the recruitment of chromatin-modifying factors. It has been demonstrated that the modification of histones can regulate transcription via altering the chromatin structure (Shogren-Knaak, Ishii et al. 2006).

Histone acetylation can occur at lysine residues on histone H3 and H4 which is involved in active transcription and in turn can regulate TF binding to nucleosomal DNA (Lee, Hayes et al. 1993). A vast number of proteins regulate the acetylation state of histones. Histone acetyltransferase complexes (HATs) mediate histone acetylation and the removal of acetyl marks is partially mediated by histone deacetylases (HDACs) (Nagy, Kao et al. 1997, Chen, Ma et al. 1999). It has been proposed that the acetylation of histones is a result in weakened octomer:DNA interactions which in turn marks the nucleosomes for remodelling via chromatin remodelling complexes (Ito, Ikehara et al. 2000, Chandy, Gutierrez et al. 2006). Histone modifications are often present in promoter and 5' and 3'

ends as well as distal regulatory regions including enhancers (Heintzman, Stuart et al. 2007, Heintzman, Hon et al. 2009).

Further to histone modifications, histone variants have been shown to affect transcriptional regulation. It has been demonstrated that histone H2A and H3 can be exchanged with histone variants H2A.Z and H3.3 respectively. This incorporation into the chromatin is independent of DNA replication and requires ATP-dependent chromatin remodelling mechanisms or histone chaperones (Mizuguchi, Shen et al. 2004, Schwartz and Ahmad 2005, John, Sabo et al. 2008, Gevry, Hardy et al. 2009, Hardy, Jacques et al. 2009). When both variants are incorporated into the nucleosomes there is an increase in instability which can alter interactions with linker histones and in turn chromatin remodelling complexes (Jin and Felsenfeld 2007). Further, genomic analysis of H3.3 and H2A.Z containing nucleosomes has demonstrated that nucleosomes containing both variants are associated with regions depleted of nucleosomes in active promoter and enhancer regions (Jin, Zang et al. 2009). This suggests that the double-variant nucleosome can permit TF access to active regulatory elements resulting in gene transcription (Ng and Gurdon 2008) (Figure 1.5).

<div style="border:1px solid">

1.4 Role of other TF on recruitment of receptors to binding sites

</div>

1.4.1   <u>Activating protein 1 (AP-1) on GR and ER recruitment</u>.

While it has long been understood that SRs interact with DNA by binding primarily to their HRE, it is now becoming apparent that they can also be recruited to the DNA by interactions with other TFs(Schule, Muller et al. 1988, Carroll, Liu et al. 2005, Norris, Chang et al. 2009, Voss, Schiltz et al. 2011). It

has been demonstrated recently that AP-1 plays a mechanistic role in mediating GR and ER response (Uht, Anderson et al. 1997, Voss, Schiltz et al. 2011, Miranda, Voss et al. 2013). Classically, it has been described that interactions between GR and AP-1 occur through direct protein-protein interactions on chromatin. It has also been demonstrated that on promoters of genes regulated by AP-1, GR is found to repress transcription through interaction with AP-1 in the absence of glucocorticoid response element (GRE). This DNA independent repression is described to involve tethering mechanisms of GR to AP-1 (Jonat, Rahmsdorf et al. 1990, Schule, Rangarajan et al. 1990, Yang-Yen, Chambard et al. 1990, Ponta, Cato et al. 1992). It has been shown that GR binding events genome-wide are generally associated with open chromatin, that being chromatin opened prior to hormone treatment. This suggests a role for other DNA binding proteins having the ability to prime the chromatin landscape and facilitate the recruitment of TFs, in this case GR (John, Sabo et al. 2011). It has been later demonstrated that AP-1 can aid GR access to specific sites in the genome by maintaining an open chromatin state by AP-1 and GR co-localisation to the same elements in 51% of GR binding sites. This thereby provides a new understanding of AP-1 and GR mechanisms whereby one TF primes the chromatin for the recruitment of a secondary factor (Voss, Schiltz et al. 2011). While it has been demonstrated that GR can inhibit AP-1 activated transcription (Ponta, Cato et al. 1992), conversely, it has been shown that ER can stimulate AP-1 transcription (Gaub, Bellard et al. 1990, Webb, Lopez et al. 1995). It has further been shown via *de novo* motif analysis some ER sites require AP-1 for binding and this recruitment could be through a tethering mechanism (Miranda, Voss et al. 2013).

1.4.2   Forkhead box protein 1 (FoxA1) on nuclear receptor recruitment.

FoxA1 has been demonstrated to act as a pioneer factor and a nuclear receptor regulatory protein. Pioneer factors are class of proteins that are a critical transcription apparatus (Zaret and Carroll 2011). Once FoxA1 has bound to chromatin, nucleosomal rearrangement is induced which can in turn result in an increase in the accessibility of DNA binding elements. This results in the recruitment of other transcriptional regulators and SRs (Cirillo, McPherson et al. 1998, Eeckhoute, Lupien et al. 2009, Hurtado, Holmes et al. 2011, He, Meyer et al. 2012). Utilising formaldehyde-assisted isolation of regulatory elements (FAIRE) it has been shown that FoxA1 binding events in MCF-7 cells are enriched in regions with high FAIRE signal, which represents nucleosome-depleted domains indicating an increase in chromatin accessibility upon FoxA1 binding (Eeckhoute, Lupien et al. 2009, Hurtado, Holmes et al. 2011). Further, in MCF-7 cells it has been shown that the forkhead motifs is enriched at 56% of ER bound DNA and approximately 50% of ER binding sites overlap with FoxA1 binding sites. In addition it has been shown that FoxA1 occupies these regions prior to ER activation. This suggests there is significant co-occupancy between ER and FoxA1 and that FoxA1 acts as a pioneer factor for ER which facilitates an open chromatin structure even in the absence of hormone (Carroll, Liu et al. 2005, Eeckhoute, Carroll et al. 2006, Lupien, Eeckhoute et al. 2008, Lupien and Brown 2009, Hurtado, Holmes et al. 2011). FoxA1 requirement on AR binding has also been investigated in breast and prostate cancer cell lines demonstrating similar results observed with ER suggesting FoxA1 is a required factor in AR recruitment to DNA (Wang, Li et al. 2009, Ni, Chen et al. 2011, Robinson, Macarthur et al. 2011, Sahu, Laakso et al. 2011, Sahu, Laakso et al. 2013). Further, the role of FoxA1 in GR recruitment has been briefly investigated suggesting FoxA1 plays a

mechanistic role along with other TFs on GR DNA recruitment (Belikov, Astrand et al. 2009, Belikov, Holmqvist et al. 2012, Sahu, Laakso et al. 2013).

Lastly, while PR genome-wide studies have been limited it has been shown upon activation with progestin, a high percentage of PR binding sites contain a FoxA1 binding motif suggesting an interaction between the two proteins in T-47D cells (Clarke and Graham 2012).

1.5 Dynamic assisted loading (DynaLoad)

In addition to a tethering mechanism as described above, TFs can be recruited to specific sites by a mechanism termed DynaLoad (Voss, Schiltz et al. 2011). This mechanism has the ability to allow a factor that doesn't have chromatin access to exert its response. A TF that has chromatin access can bind and recruit chromatin remodelling complexes to specific sites in the genome, which results in reprogramming of the chromatin structure. This in turn allows a secondary factor with a response element in the remodelled area to bind to sites that are previously deemed unavailable. Utilising a mutant ER, ER pBox, that binds to a GRE in the MMTV array instead of an estrogen receptor response element (ERE), it has been demonstrated that when both GR and ER pBox are simultaneously activated there is not a competition for binding. In fact, it has been found that ER pBox can only bind at certain sites when GR is first activated. Further, these sites have an increase in deoxyribonuclease I (DNase I) digestion, demonstrating an increase in DNaseI hypersensitivity (DHS) after GR activation, suggesting that GR recruits chromatin modifiers to these sites before ER pBox is recruited (Voss, Schiltz et al. 2011). It has also been shown that AP-1 can maintain an open chromatin state,

which facilitates the selective access of GR to specific sites by a DynaLoad mechanism. Expression of a dominant negative form of AP-1 prevents changes in chromatin state and inhibits GR binding at the DynaLoad sites (Voss, Schiltz et al. 2011). In a mouse mammary cell line, it has been shown that ER and GR can influence each other's binding at specific sites through a DynaLoad mechanism. Co-activation of ER and GR reprograms the chromatin landscape resulting in a global shift of their binding patterns. It has been observed that activation of GR allows the selective access of ER to specific sites by maintaining an open chromatin structure at theses specific response elements. The same phenomenon is observed for activation of ER, resulting in a changed chromatin structure at some GR binding sites. This indicates that the DynaLoad mechanism can function in both directions (Miranda, Voss et al. 2013).

1.6 Objectives of this thesis

There has been extensive investigation into the genome-wide localisation of nuclear receptor binding sites further widening our understanding of SR action in cell environments. The role ER and PR play in breast cancer development is well understood and recently GR is beginning to emerge as a potential player in breast cancer progression. While genome-wide investigations have provided vital information into SR function these studies have often been performed in settings where one receptor is activated by the addition of hormone treatments. Physiologically, cells are maintained in an environment where a multitude of hormones are present which in turn allows for activation of multiple SRs at any given time. It is becoming apparent that crosstalk and the newly proposed idea of DynaLoad plays an important role in SR function. It has recently been

demonstrated that co-activation of GR and ER reprograms the chromatin landscape and results in global rearrangement of SR binding. However, these studies have been performed in an artificial cell line engineered to over express both GR and ER. Therefore, the functional consequences of GR and ER crosstalk on binding and transcriptional response are still unknown in a cancer setting as well as the potential role other well established TFs play in this potential crosstalk. Furthermore, while it is well known that ER and PR contribute to breast cancer development, the mechanistic role of ER and PR crosstalk is still very unclear. Therefore the overall objectives of this study are to determine the effects of GR and ER signalling in breast cancer epithelial cells as well as ER and PR crosstalk. In addition, this study strives to further investigate the role of FoxA1 under GR, ER, and PR responses.

Specifically, the aims of this thesis are:

1. Characterise the effects that co-activation of ER and GR or ER and PR has on cell proliferation, transcription, and the genome-wide binding patterns of the nuclear receptors in three cell line models of breast cancer.

2. Determine the effects that Dex, P4, and E2 has on FoxA1 binding genome-wide.

3. Determine if there are common binding patterns for ER, GR, and FoxA1 upon hormone treatments in three different breast cancer cell line models.
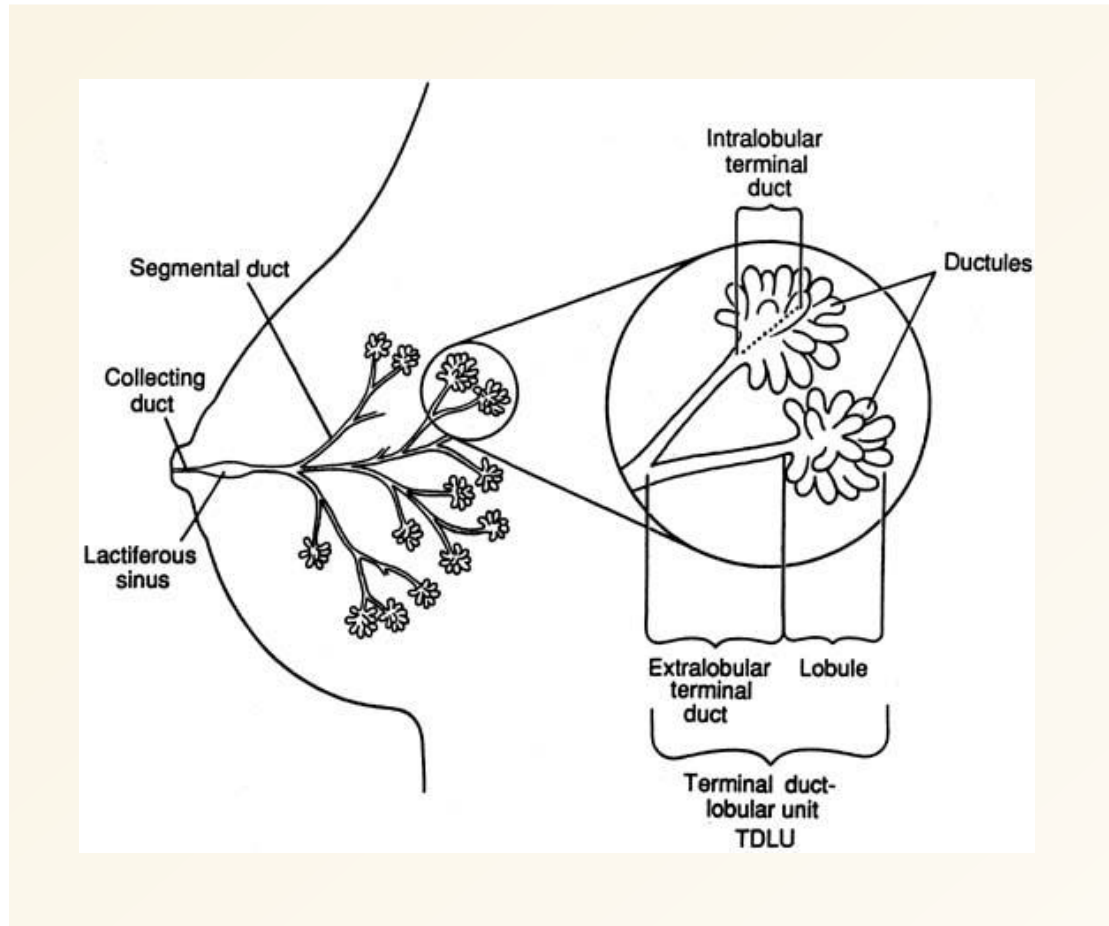
Figure 1.1: Diagram of the human mammary gland. The mammary gland consists of branching ducts which form separate structures called lobes with one of the branching ducts forming the lactiferous sinus. The functional component of the mammary gland is the terminal ductal lobular unit which consists of extralobular terminal ducts, intralobular terminal ducts, and lobules (Hindle 2009).
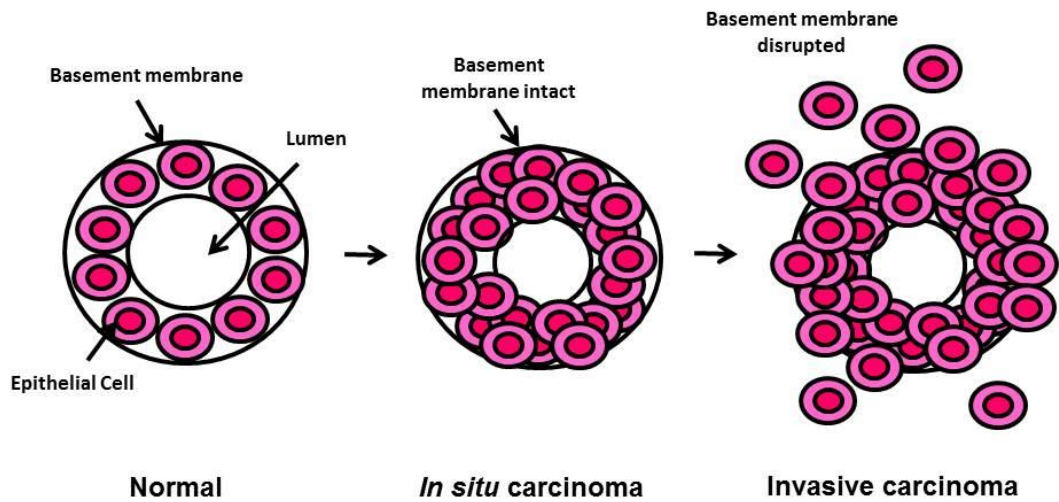
Figure 1.2: Diagram of breast cancer progression. *In situ* carcinoma consists of neoplastic growth confined within the basement membrane of individual ducts. Invasive carcinoma occurs when the cells breach the basement membrane and invade the stroma and other parts of the breast tissue.
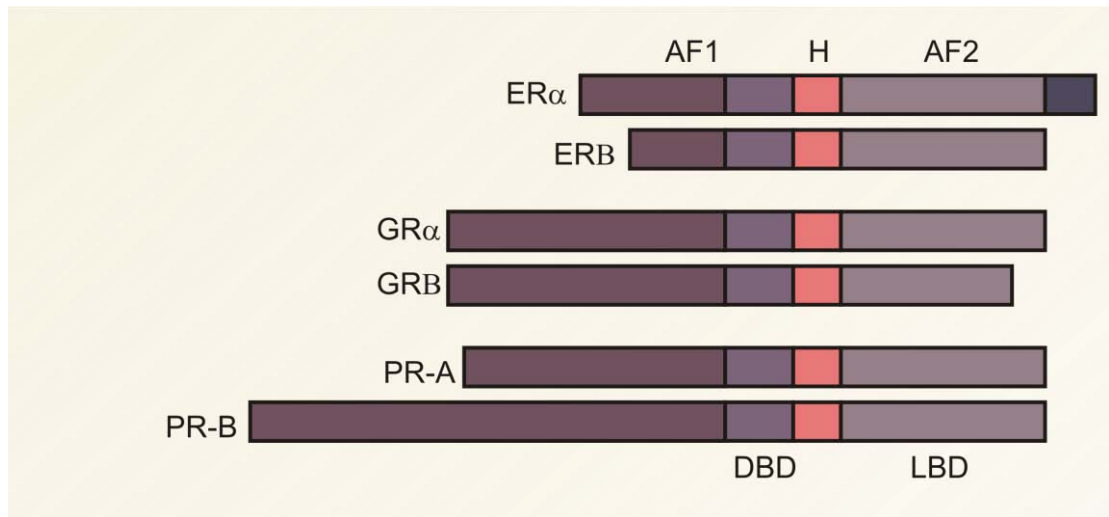
Figure 1.3: Representation of ERα, ERβ, GRα, GRβ, PR-A, and PR-B. ERα, ERβ, GRα, GRβ, PR-A, and PR-B contain DNA binding domain (DBD), hinge region (H), and ligand binding domain (LBD). The activation function 1 (AF-1) is located in the NTD and activation function 2 (AF-2) is location in the LBD.
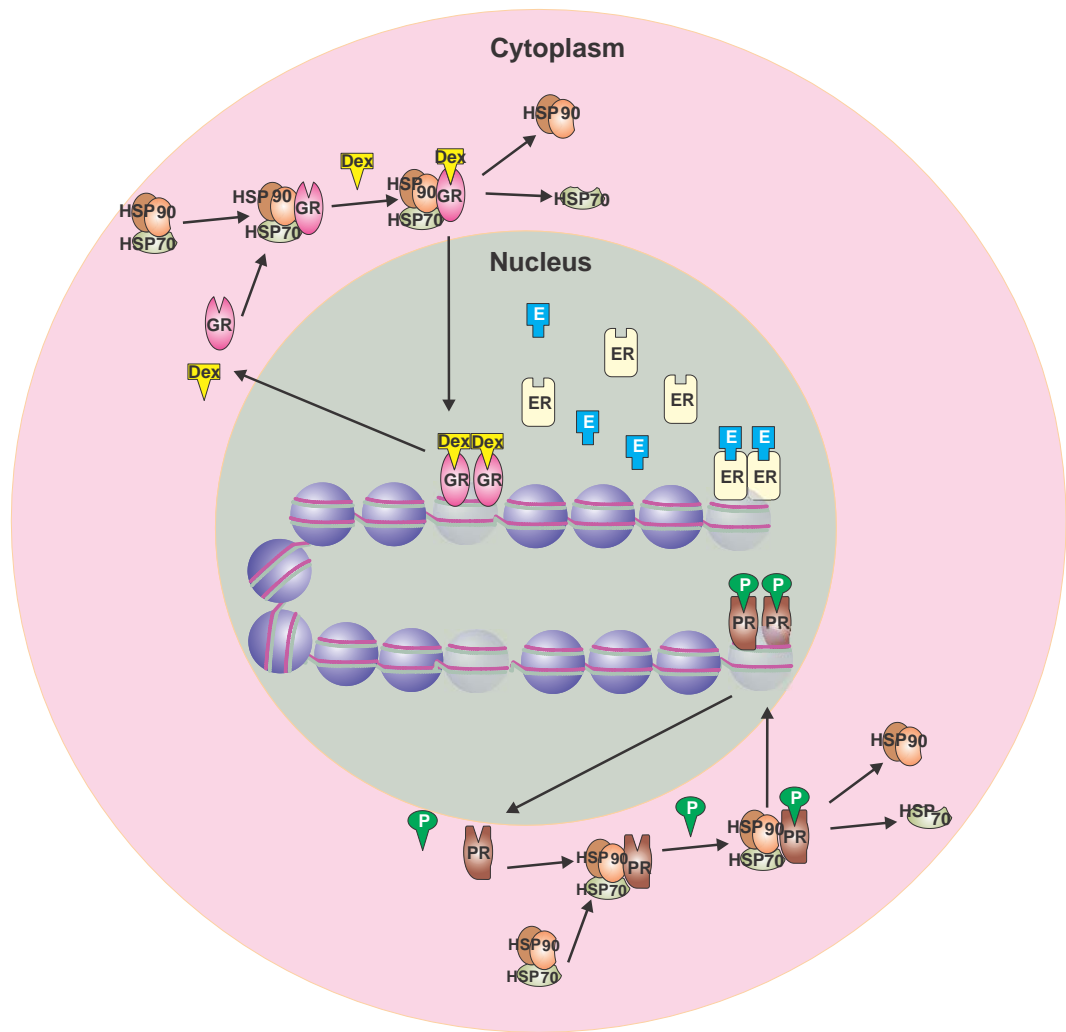
Figure 1.4: Estrogen, progesterone, and glucocorticoid signalling pathways.
In the absence of hormone PR and GR reside in the cytoplasm, where as ER is
located in the nucleus. The receptors interact with cofactors including heat shock
proteins 70 and 90. Upon hormone binding the receptors dissociate from the heat
shock proteins. In the nucleus, the receptors bind as homodimers to response
elements. This process is dynamic resulting in regular movement of receptors.
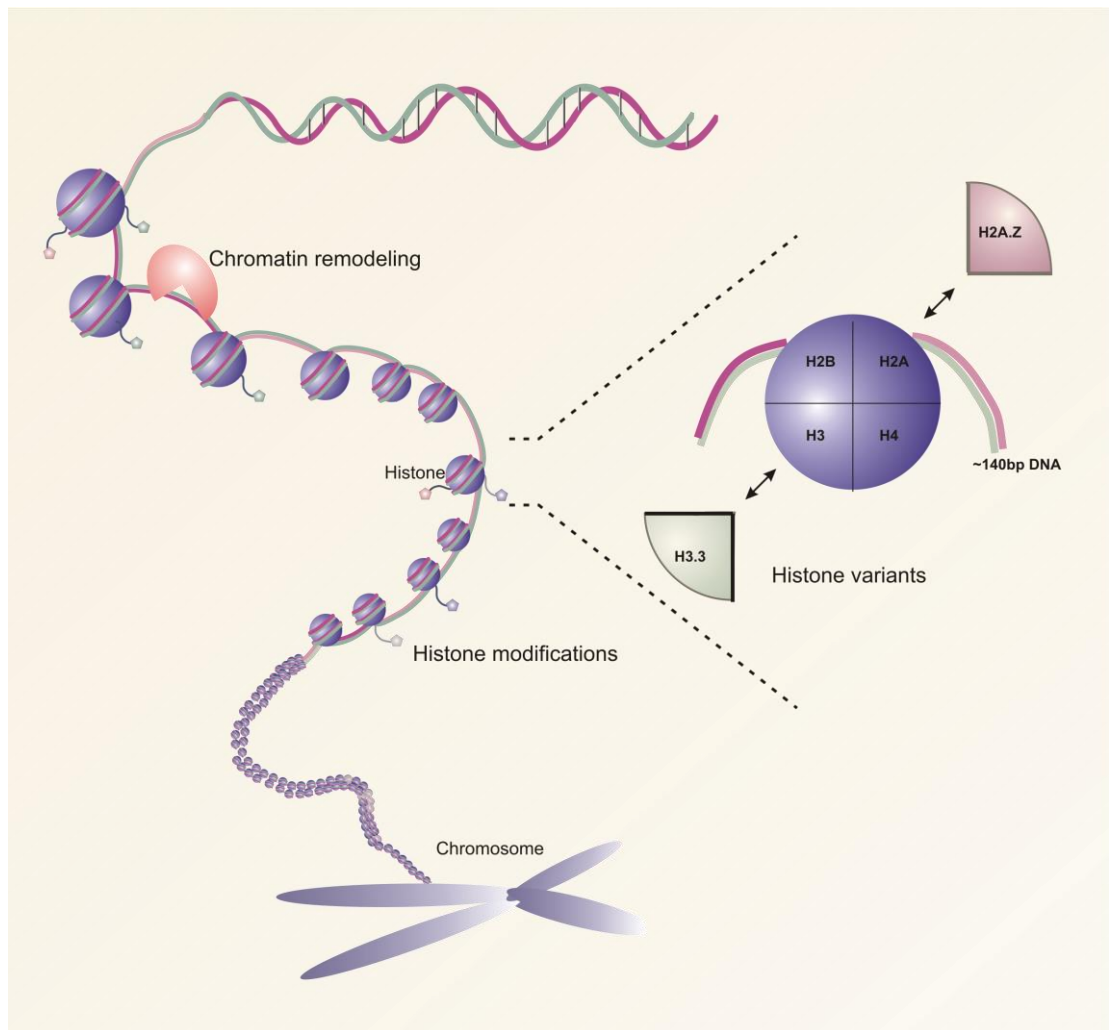
Figure 1.5: Diagram of the critical mechanisms involved in gene transcription. The chromatin landscape is critically involved in gene expression. Histones are located in the cell nuclei and package DNA into nucleosomes. A stable nucleosome complex comprises of two H2A-H2B dimers associated on either side of a H3-H4 tetramer forming the nucleosome core particle. Histone modifications can occur marking nucleosomes for chromatin remodelling. Histone variants also alter transcriptional processes.

Chapter 2

Materials and Methods

2.1 Materials

2.1.1 General reagents and buffers.

Reagent	Company
Acetic Acid	Sigma-Aldrich (St Louis, MO, USA)
Agarose UltraPure	Invitrogen (Carlsbad, CA, USA)
Bradford Protein Assay	Bio-Rad (Hercules, CA, USA)
Bromophenol Blue	Sigma-Aldrich (St Louis, MO, USA)
Bovine serum albumin (BSA)	New England BioLabs (Beverly, MA, USA)
Charcoal stripped fetal bovine serum (CSS)	Gibco (Grand Island, NY, USA)
Dulbecco's Modified Eagle Medium (DMEM) (containing 4.5g/L D-Glucose)	Gibco (Grand Island, NY, USA)
Dulbecco's Phosphate Buffered Saline (PBS) 1X	Gibco (Grand Island, NY, USA)
Ethylenediaminetetraacetic acid (EDTA) 0.5M pH 8.0	Quality Biological Inc. (Gaithersburg, MD, USA)
Ethylene glycol tetraacetic acid (EGTA) 0.5M pH8.0	bioPLUS Fine Research Chemicals (New Brunswick, NJ, USA)
Ethanol 200 proof	The Warner-Graham Company (Cockeysville, MD, USA)
Extra Thick Blot paper	Bio-Rad (Hercules, CA, USA)
Fetal bovine serum (FBS)	Gibco (Grand Island, NY, USA)
Formaldehyde soultion	Sigma-Aldrich (St Louis, MO, USA)
GelRed Nucleic Acid Stain	Biotium Inc. (Hayward, CA, USA)

GelStair Nucleic Acid Stain Gel Stain	Lonza (Rockland, ME, USA)
Glycerol	Sigma-Aldrich (St Louis, MO, USA)
Glycogen	Invitrogen (Carlsbad, CA, USA)
Glycine	Sigma-Aldrich (St Louis, MO, USA)
HiMark Pre-Stained HMW protein standard	Invitrogen (Carlsbad, CA, USA)
Igepal CA-630	Sigma-Aldrich (St Louis, MO, USA)
Immuno-Blot LF PVDF membrane	Bio-Rad (Hercules, CA, USA)
Isopropanol	J.T Baker (phillipsburg, NJ, USA)
L-Glutamine 200mM (100x)	Gibco (Grand Island, NY, USA)
Lithium Chloride	Sigma-Aldrich (St Louis, MO, USA)
MassRuler 1kb DNA ladder Mix	Fermentas (Pittsburgh, PA, USA)
MEM Non-essential Amino Acid (100X)	Gibco (Grand Island, NY, USA)
100% Methanol	The Warner-Graham Company (Cockeysville, MD, USA)
NuPAGE LDS Sample Buffer 4X	Invitrogen (Carlsbad, CA, USA)
NuPAGE 3-8% TAE gel	Invitrogen (Carlsbad, CA, USA)
20X NuPAGE Tris Acetate SDS Running Buffer	Invitrogen (Carlsbad, CA, USA)
Penicillin Streptomycin	Gibco (Grand Island, NY, USA)
Phenol-chloroform-isoamyl alcohol	Sigma-Aldrich (St Louis, MO, USA)
Phenol red free Dulbecco's Modified Eagle Medium (DMEM) (containing 4.5g/L D-Glucose)	Gibco (Grand Island, NY, USA)
Phenol red free RPMI 1640 medium (containing L-Glutamine)	Gibco (Grand Island, NY, USA)

KCl 1M	Quality Biological Inc. (Gaithersburg, MD, USA)
Ponceau S	Sigma-Aldrich (St Louis, MO, USA)
Protease Inhibitors (PI) Cocktail	Invitrogen (Carlsbad, CA, USA)
Proteinase K	Ambion (Grand Island, NY, USA)
H_2O Nuclease Free	Ambion (Grand Island, NY, USA)
iQ SYBR® Green Supermix	Bio-Rad (Hercules, CA, USA)
10X TBS HCl pH 7.2	Quality Biological Inc. (Gaithersburg, MD, USA)
Tris-acetate-EDTA (TAE) 10X	Crystalgen Innovation solutions for science (Commack, NYC, USA)
10X Tris Glycine Transfer Buffer	Quality Biological Inc. (Gaithersburg, MD, USA)
Tris-HCl 1M pH 7.5	Quality Biological Inc. (Gaithersburg, MD, USA)
Tris-HCl 1M pH 8	Quality Biological Inc. (Gaithersburg, MD, USA)
Trypan Blue solution 0.4%	Sigma-Aldrich (St Louis, MO, USA)
Trypsin-EDTA 0.25% 1X (trypsin)	Gibco (Grand Island, NY, USA)
Tween20	Sigma-Aldrich (St Louis, MO, USA)
RPMI 1640 medium (containing L-Glutamine)	Gibco (Grand Island, NY, USA)
SDS (sodium dodecyl sulphate) 10%	KSD Scientific Inc. (Ellicott city, MD, USA)
Skim milk powder	Nestle (Glendale, CA, USA)
Super Signal West Pico Chemiluminescent Substrate	Thermo Fisher Scientific (Waltham, MA, USA)
NaCl 5M	Quality Biological Inc. (Gaithersburg, MD, USA)
Sodium deoxycholate	Sigma-Aldrich (St Louis, MO, USA)

Sodium pyruvate 100mM 100X	Gibco (Grand Island, NY, USA)
Xylene cyanol FF	Sigma-aldrich (St Louis, MO, USA)

2.1.2 <u>Cell lines</u>.

The MCF-7 cell line is a human breast epithelial cell line purchased from American Type Culture Collection (Manassas, VA, USA). The cell line is derived from a pleural effusion obtained from a 69 year old female diagnosed with adenocarcinoma of the breast (Soule, Vazguez et al. 1973).

The ZR-75-1 cell line is a human breast epithelial cell line purchased from American Type Culture Collection (Manassas, VA, USA). The cell line is derived from an ascites obtained from a 63 year old female diagnosed with ductal carcinoma of the breast (Engel, Young et al. 1978).

The T-47D cell line is a human breast epithelial cell line purchased from American Type Culture Collection (Manassas, VA, USA). The cell line is derived from a pleural effusion obtained from a 54 year old woman diagnosed with infiltrating ductal carcinoma of the breast (Keydar, Chen et al. 1979).

2.1.3 <u>Hormones</u>.

Hormone	Company
Dex	Sigma-Aldrich (St Louis, MO, USA)
E2	Sigma-Aldrich (St Louis, MO, USA)
P4	Sigma-Aldrich (St Louis, MO, USA)

2.1.4   Antibodies.

Antibody	Company
ER (human) Ab-10 (MA1-12692) mouse monoclonal	Thermo Fisher Scientific – Biosciences (Waltham, MA, USA)
ERα (human) HC-20 (sc-543) rabbit polyclonal	Santa Cruz Biotechnology Inc. (Dallas, TX, USA)
GR (human) E-20X (sc-1003) rabbit polyclonal	Santa Cruz Biotechnology Inc. (Dallas, TX, USA)
FoxA1(human) ab23738 rabbit polyclonal	Abcam (Cambridge, MA, USA)
PR (human) H-190X (sc-7208) rabbit polyclonal	Santa Cruz Biotechnology Inc. (Dallas, TX, USA)
RNA polymerase II (human) ab5131 rabbit polyclonal	Abcam (Cambridge, MA, USA)
Peroxidase-AffiniPure Goat-anti-Rabbit IgG (H+L)	Jackson Immuno Research Laboratories (West Grove, PA, USA)

Magnetic Beads	Company
Dynabeads M-280 sheep anti mouse IgG	Noves (Oslo, Norway)
Dynabeads M-280 sheep anti rabbit IgG	Noves (Oslo, Norway)

2.1.5   Oligonucleotide primers.

All oligonucleotide primers have been purchased from Eurofins MWG Operon (Huntsville, AL, USA).

Primers	Sequence 5'-3'
MYC Forward	GGCTCACCCTTGCTGATGCT

MYC Reverse	GCTCTGGGCACACACATTGG
TFF1 TSS Forward	CCTGGATTAAGGTCAGGTTGGA
TFF1 TSS Reverse	TCTTGGCTGAGGGATCTGAGA
PER1 Forward	CATCATGTTCTCTTGGCTGGTGG
PER1 Reverse	AGGACGGCTGTCGTTTTGTTG

2.1.6   Software.

Software	Company
Acapella High Content Imaging and Analysis Software	PerkinElmer (Waltham, MA, USA)
CFX Manager Software 3.0	Bio-Rad (Hercules, CA, USA)
CorelDrawX5	Corel Inc. (Menlo Park, CA, USA)
DAVID	National Cancer Institute at (Frederick, MD, USA)
DeSeq	European Molecular Biology Laboratory (Heidelberg, Germany)
Hypergeometric Optimization of Motif Enrichment (Homer)	University of California (SD, USA)
Multiple Experiment Viewer (MeV)	Dana-Farber Cancer Institute (Boston, MA, USA)
NanoDrop ND 1000 3.3	Nanodrop Technologies (Wilmington, DE, USA)
RStudio	Rstudio Inc. (Boston, MA, USA)

R version 3.0.2	Institute for Statistics and Mathematics (Vienna University of Economics and Business, Vienna, Austria)

2.2 Buffers and Solutions

All buffers and solution are prepared using autoclaved reverse osmosis (RO) H_2O and stored at room temperature unless otherwise state.

Calcium Chloride ($CaCl_2$)

23.47g $CaCl_2$, 100mL nuclease free H_2O

ChIP lysis buffer

10mM EDTA, 0.5% SDS, 50mM Tris-HCl pH 8.0, H_2O

ChIP master mix

702uL ChIP lysis buffer, 11uL 0.5M EDTA pH 8.0, 222uL 5M NaCL, 27.5uL proteinase K, 55uL 1M Tris-HCl pH 7.5

Prepare the buffer the day required.

Elution buffer

55mM EDTA, 300mM NaCl, 0.5% SDS, 10mM Tris-HCl pH 8.0

Store at 4ºC for up to two months.

Freezing mix

10% DMSO, 20% FBS, 70% RMPI medium or DMEM medium

Store at 4ºC.

Glycine 20X

9.38g Glycine, 50mL PBS

High salt immuno complex buffer

2mM EDTA, 500mM NaCl, 20mM Tris-HCl pH 8.0, 1% Triton x-100, 0.1% SDS, H_2O

Store at 4ºC for up to two months.

6X loading dye

0.0125g bromophenol blue, 3mL 100% glycerol, 0.0125g xylene cyanol FF, 7mL H_2O

Store at 4ºC.

LiCL immune complex buffer

1% deoxycholate, 1mM EDTA, 1% igepal CA-630, 0.25M LiCl, 10mM Tris-HCl pH 8.0, H_2O

Store at 4ºC for up to two months.

Low salt immune complex buffer

2mM EDTA, 150mM NaCl, 20mM Tris-HCl pH 8.0, 1% Triton x-100, 0.1% SDS, H_2O

Store at 4ºC for up to two months.

PBS containing 1X PI

50mL PBS, 500uL 100X PI

Prepared the buffer the day required.

Ponceau S stain

0.5% Acetic Acid, 0.1% Ponceau S, H_2O

RIPA Buffer

1mM EDTA, 0.5mM EGTA, 140mM NaCl, 0.1% SDS, 1% Triton x-100, 100mM Tris-HCl pH 8, H_2O

1X TAE

900mL of H_2O, 100mL of 10X TAE

0.1% TBS-T

1X TBS, 0.1% Tween20

1X TE buffer

1mM EDTA, 10mM Tris-HCl pH 8.0, H_2O

Stored at 4ºC for up to two months.

1X Tris Glycine Transfer Buffer

200mL of methanol, 800uL of 1X Tris Glycine Transfer buffer

2.3 Methods

2.3.1   Cell culture.

The MCF-7 breast cancer cell line is maintained in DMEM containing 4.5g/L of D-glucose and supplemented with 10% FBS, 2mM L-glutamine, 1mM sodium pyruvate, 1X non-essential amino acids, and 1% penicillin-streptomycin. The ZR-75-1 breast cancer cell line is maintained in RPMI 1640 medium containing 2mM L-glutamine and supplemented with 10% FBS, 1mM sodium pyruvate, 1X non-essential amino acids, and 1% penicillin-streptomycin. The T-47D breast cancer cell line is maintained in RPMI 1640 medium containing 2mM L-glutamine and supplemented with 10% FBS, 1mM sodium pyruvate, 1X non-essential amino acids, 0.2U/mL bovine insulin, and 1% penicillin-streptomycin. All cell line maintenance is performed using aseptic conditions in a biological class II safety cabinet. Cell lines are grown at 37ºC with 5% carbon dioxide (CO_2).

2.3.1.1 General cell maintenance

Every third day culture medium is removed and replaced with fresh culture medium. Alternatively when cells are at 80% confluence they are either repassaged or seeded for the required experiment. The medium is discarded and for a T225 culture flask 5mL of 1X PBS is used to wash the cells and remove any remaining FBS. PBS is removed and 5mL of trypsin-EDTA 0.25% (trypsin) is added, cells are incubated for 5 min at 37ºC to detach the cells. Fifteen mL of culture medium is added and the cell suspension is centrifuged at 1,500 revolutions per minute (rpm) for 5 min. The medium is removed and the cell

pellet is resuspended in the required fresh medium. Cells are repassaged in a new flask at the appropriate density. If cells are to be seeded for an experiment, the concentration is determined using a cell haemocytometer. The cell suspension is then diluted at the appropriate concentration and seeded in the tissue culture plates and medium as described in the appropriate method.

2.3.1.2 Cell freezing

Cells in a T225 flask are washed with PBS and 5mL of trypsin is added. The cells are incubated for 5 min at 37ºC to allow for detachment of the cells. 15mL of culture medium is added and the cell suspension is centrifuged at 1,500 rpm for 5 min. The medium is removed and the cell pellet is resuspended in 5mL of freezing mix. One mL aliquots are placed in a cryovial and then put in a freezing box containing isopropanol at -80ºC for 24 h. After 24 h the cryovials are placed in liquid nitrogen.

2.3.1.3 Cell thawing

The cryovials are thawed at 37ºC and 5mL of the required culture medium is added to the cell suspension. The cell suspension is centrifuged at 1,500 rpm for 5 min and cell medium removed. The cell pellet is resuspended in 6mL of media and seeded in to a T25 culture flask.

2.3.1.4 Mycoplasma detection

Cells are routinely tested for mycoplasma contamination using the Lonza MycoAlert mycoplasma detection kit LT07-218 (Lonza, Basel, Switzerland). 1mL of culture media from a flask of cells grown in antibiotic free conditions is centrifuged at 1,500 rpm for 5 min. Fifty uL of supernatant is placed in a 96 well

plate and 50uL of MycoAlert reagent is added to the sample. Analysis is performed on the Victor ^{TM} x4 2030 MultiReader (PerkinElmer, Waltham, MA, USA) at a 1 second (sec) integrated reading and the result is recorded as Reading A. Fifty uL of MycoAlert substrate is added to the sample and incubated at room temperature for 10 min. The sample is read on the luminometer again and the result recorded as Reading B. A ratio is calculated as *Reading B/Reading A*. A negative result is a ratio < 1.0 and a positive result a ratio > 1.0.

2.3.1.5 Preparation of steroid stocks

All steroid powder is dissolved in 100% ethanol to a concentration of 10^{-2} M and further diluted in 100% ethanol to a concentration of 10^{-4} M. Both concentrations are stored at -20ºC. When cells are treated with steroids, the 10^{-4} M stock is added to the medium at a 1:1000 dilution to result in a 100nM concentration of steroid treatment.

2.3.2   Immunoblot

2.3.2.1 Preparation of lysates

Cells are placed on to ice, the media is removed and the cells are washed with ice cold PBS and collected with trypsin. The cell suspension is centrifuged at 1,500 rpm for 5 min and a cell pellet collects. 100uL (MCF-7 and T-47D cells) or 200uL (ZR-75-1 cells) is added to the cell pellets. The cell lysates is centrifuged at 10,000 rpm for 10 min at 4ºC and the cell supernatant is transferred to a new microcentrifuge tube. A Bradford protein assay is utilised to determine the protein concentration of each sample. Bradford assays are performed by adding 2uL of sample to 800uL of H_2O. For standards 0, 0.5, 1, 2, 6, and 10uL of 2ng/uL of BSA is used. 200uL of protein assay dye reagent is add to each sample. Using

a spectrometer at a wavelength of 595 nm, the absorbance of the samples is measured.

2.3.2.2 Immunoblotting

The protein samples are prepared in 4X protein load dye (NuPAGE LDS sample Buffer 4X) (Invitrogen) and denatured at 95ºC for 5 mins. The samples are added to the specific lanes of a NuPAGE 3-8% TAE gel (Invitrogen) and the HiMark Pre-Stained HMW protein standard (Invitrogen) is added to one lane per gel. The proteins are electrophoresed in 1X NuPAGE Tris-Acetate SDS Running Buffer (Invitrogen) at 150V for approximately 1.5 h. Under wet transfer condition in a Criterion Blotter (Bio-Rad), the proteins are transferred to a Immun-Blot LF PVDF membrane (Bio-Rad) which is soaked in 100% methanol for 5 mins in cold 1X Tris Glycine Transfer Buffer at 400mA for approximately 1.5 h. For transfer, the gel and membrane are stacked between Extra Thick Blot Paper (Bio-Rad). To determine efficient protein transfer, the membrane was stained in Ponceau stain and then membrane was the washed in 0.1% TBS-T. The membranes are blocked in 3% skim milk powder in 0.1% TBS-T for 1 hr at room temperature, followed by incubation with the appropriate primary antibody overnight at 4ºC. After incubation, the membrane is washed 3 times for 10 min each wash in 0.1% TBS-T and then incubated in the appropriate HRP-conjugated secondary antibody for 2 h and washed 3 times for 10 min in 0.1% TBS-T. All primary and secondary antibodies were diluted in 3% skim milk powder in 0.1% TBS-T. Detection of bound antibody is performed using Super Signal West Pico Chemiluminescent Substrate as per the manufacturer's instructions (Thermo Scientific) and visualised using the Bio-Rad ChemiDoc MP imaging system.

2.3.3 Cellular growth curves.

Cells are harvested and plated in 96-well Matrical glass bottom plates (MGB096-1-2-LG-BC) and treated with the corresponding hormone treatment as per the required experiment. After either 0 h, 24 h, 48 h, or 72 h cells are fixed with 4% paraformaldehyde for 15 mins. Cells are then washed 3 times with 200uL of PBS. Nuclei are then stained with Hoescht at a concentration of 1:5000 for 15 mins and wells are washed again 3 times with 200uL of PBS. Plates are imaged using the Perkin Elmer Opera imaging system. Images are analysed and cell counts are determined using Acapella. Three biological replicates are conducted per treatment per cell line. Eight wells per treatment per cell line are analysed for each biological replicate and 12 images are take per well.

2.3.4 Chromatin immunoprecipitation Assay (ChIP).

2.3.4.1 Formaldehyde cross-linking and harvesting of cells

After cells are treated with steroid, 675uL of 37% formaldehyde is added to each 150mm tissue culture plate for 10 min in a 37ºC hybridisation incubator. After 10 min 1.5mL of 20X glycine is added to each plate and left to incubate for 10 min at room temperature. Medium is removed and each tissue culture plate is washed with ice cold PBS twice and 4mL of PBS containing 1X PI is added to each plate. Cells are scrapped and three plates are evenly distributed into two 15ml tubes. Cell suspension is centrifuged at 2,000 rpm at 4ºC for 5 min, supernatant is aspirated and cell pellets are placed on ice.

2.3.4.2 Sonication of chromatin

The pellet is resuspended in 600uL of ChIP lysis buffer and 1X PI for 1 h on ice. Samples are placed in 15mL sonication tubes and sonicated at the optimised cycle condition for each cell line using the Bioruptor 300 (Diagenode Inc, Denville, NJ, USA). Samples are centrifuged at 14000 rpm at 4ºC for 10 min and supernatant collected containing chromatin.

2.3.4.3 Quantification of chromatin

The samples are left on ice and a 15ul aliquot of sample is added to 185uL of ChIP master mix. The reaction is placed at 65ºC for 1.5 h to de crosslink and the sample chromatin concentration is measured using the NanoDrop spectrophotometer ND 1000 (NanoDrop Technologies, Wilmington, DE, USA). De-crosslinked samples are mixed with 6X loading dye and electrophoresed on 1% agarose TAE gel in 1X TAE buffer to determine that the sonication of chromatin is approximately 300 bp. Agarose gels contained 1ug/mL of GelRed nucleic acid stain and a 1kb DNA ladder is utilised. The DNA is electrophoresed through the 1X TAE gel at 100 volts (V) for 1 h and then visualised with ultraviolet (UV) light using the Bio-Rad ChemiDoc MP imaging system. Remaining samples on ice are diluted at least 5 fold in ChIP dilution buffer with 1X PI to a final concentration of 100ug of chromatin per mL.

2.3.4.4 Linking of antibodies to magnetic beads

Eighty uL of appropriate Dynabeads as per required antibody are aliquoted in 2mL tubes and washed twice with 1mL of PBS to pre clear. Between each wash the tubes are rotated for 5 min at room temperature and placed on a magnetic rack for 1 min to remove supernatant. 1mL of low salt buffer is added to each aliquot followed by the appropriate antibody. The tubes are then rotated for 6 h at 4ºC.

2.3.4.5 Immunoprecipitation

Eighty uL of appropriate Dynabeads as per antibody per sample are washed with PBS as described in section 2.3.3.4. Once supernatant is removed 2mL of sample is added to the beads and the sample is rotated for 2 h at 4ºC. The tubes are placed on a magnetic rack for 1 min along with the tubes containing the antibody. The supernatant from the tubes containing antibody is discarded and the sample is removed from the original tubes and placed in the appropriate tube containing beads with antibody now attached. Before the sample is added to the beads with antibody attached, 100uL aliquot is stored at 4ºC for the input. Tubes are rotated overnight at 4ºC. Samples are then placed on a magnetic rack for 1 min and supernatant removed. The Dynabeads are then placed in 1mL of wash buffer followed by 15 min rotation at 4ºC and tubes are then placed in a magnetic rack for 1 min. Supernatant is removed and the next wash buffer is added. Wash buffers are as follows; low salt immune complex, high salt immune complex, LiCl immune complex, and 1X TE. After the final wash buffer is removed 400uL of elution buffer is added to the beads. 300uL of elution buffer is added to the 100uL aliquot stored over night at 4ºC designated for input. Five uL of proteinase K is added to all samples including input and they are placed overnight at 65ºC.

2.3.4.6 Phenol chloroform precipitation

400uL of phenol-chloroform-isoamyl alcohol is added to each sample and centrifuged at 14,000 rpm for 10 min at room temperature. The top aqueous layer is transferred to a new tube and 4ug of glycogen is added to each sample. 1mL of ice cold 100% ethanol is added to each sample and incubated at -20ºC for 30 min. The samples are then centrifuged at 14,000 rpm for 30 min at 4ºC and the

supernatant is removed. The pellet is washed in 500uL of 70% ethanol and samples further centrifuged at 14,000 rpm for 20 min at 4ºC. The supernatant is removed and the pellets left to air dry for 2 h. The samples are resuspended in 10uL of nuclease free H_2O and stored at -20ºC.

2.3.4.7 Quantitative polymerase chain reaction (qPCR)

To determine efficient protein binding to chromatin qPCR is utilised. Samples are diluted 1:10 using nuclease free H_2O and an input sample is serially diluted 1:4, 1:16, and 1:64 for a standard curve. Quantifiable-PCR is performed using a 25uL reaction mix of 12.5uL of iQ SYBR green super mix, 1uL of forward primer, 1mL of reverse primer, 8.5uL of nuclease free H_2O, and 2uL of sample template. Quantifiable-PCR reaction is performed on a CFX96 Real-Time system C1000 touch thermal cycler under the following cycling conditions: 95ºC for 2 min followed by 40 cycles of 95ºC for 15 sec and 60ºC for 1 min, and a melt curve performed from 65ºC to 95ºC at 0.5ºC increments per 5 sec. Data is calculated as enrichment over input.

2.3.4.8 High-throughput sequencing

Ten uL of each sample is sent to the National Cancer Institute Advanced Technology Program Sequencing Facility for sequencing services. The samples are then assembled into libraries for sequencing. The Illumina Solexa genome analyser platform is used to generate sequence reads (36-mer). Unique tags are then aligned to the human reference genome (UCSC Hg19 assembly).

2.3.5   Bioinformatic processing of high-throughput sequencing data.

Hotspots and peaks are called using previously described methods (Baek, Sung et al. 2012). Briefly, peaks are determined using a hotspot detection algorithm. This determines the enrichment of tags in a 250 bp target window relative to a 200 kb surrounding window by using a model based on the binomial distribution. Each tag is extended to be 150 bp and a 250 bp target window centred and the extended tag is assigned a *z* score. A hotspot is defined as a continuous cluster of 250 bp windows whose *z* scores are nominally significant (> 2). A final z-score is calculated on candidate hotspots and peaks for each data set based on a 0% false discovery rate (FDR). Before calling hotspots and peaks, the repeat sequences are eliminated by filtering out sequence reads which overlap satellites, long interspersed repetitive elements (LINE), and short tandem repeats (STR). Replicate concordants are then calculated between replicates (performed by Songjoon Baek, NCI, LRBGE).

For RNA PolII analysis Homer has been used to annotate RNA PolII binding across the gene bodies for each treatment group and each replicate utilising RefSeq defined genes. Changes in RNA PolII binding across gene bodies were determined using DeSeq.

For comparison of different ChIP-seq data sets, regions are considered to overlap if they shared at least 1 bp. To construct heat maps, peaks unique to the hormone treatments are identified. Using these, a list of unique chromosomal positions is generated by removing overlapping peaks from the samples providing a list of unique peaks. Supervised clustering of the peaks is conducted tagging each unique peak for presence or absence of binding in each experiment and ordering them according to these tags across the samples. Using Homer, the total number

Chapter 2 – Materials and Methods
Page 47

of sequence reads under the peaks for each ChIP-seq sample are extracted and corrected for the total number of reads in the sample (reads under peak/ 10M total reads). MeV is used to generate heat map images.

For scatter plots and box plots, Homer is used to retrieve the total number of sequence reads under the peaks for each cluster. Plots are graphed and Pearson correlations and p values are calculated using the statistical program R. The p values are calculated using the Kolmogorov-Smirnov test. Factor binding distribution, motif distribution, and motif analysis is constructed using Homer.

2.3.6   Statistical Analysis.

Statistical analysis is performed where indicated utilising R software.

Chapter 3

Treatment of Human Breast Cancer Cells with Differing Hormones Affects Cellular Growth Rates and RNA Polymerase II Activation at Specific Genes.

It has been well established that by pro-proliferative mechanisms, ER and PR can drive breast cancer tumourgenesis upon activation by their respective hormones. ER is found to be expressed in approximately 55-80% of breast cancers, whereas PR is expressed in approximately 45-82% of cases (McGuire 1978, Rosa, Caldeira et al. 2008). PR is a well characterised estrogen regulated gene (Nardulli, Greene et al. 1988, Read, Snider et al. 1988, Wei, Krett et al. 1988), and is assessed together with ER by immunohistochemistry to predict the response of breast cancer to current endocrine therapies (Creighton, Kent Osborne et al. 2009). The prognostic value of PR expression is attributed to its dependence on estrogen activity, with the absence of PR assumed to reflect non-functional ER (Cui, Schiff et al. 2005).

It is now becoming apparent that GR is involved in breast cancer progression and development (Vaidya, Baldassarre et al. 2010, Vilasco, Communal et al. 2011). More specifically, it has been observed that GR mRNA levels are higher in the stroma of breast tissue, suggesting a potential role for GR in stromal and epithelial tumour interactions (Smith, Lea et al. 2007). In addition, GR has also been shown to have direct clinical implications. In grade 3 tumours, GR was found to be over expressed when compared with grade 1 and 2 tumours as well as normal breast tissue (Smith, Lea et al. 2003). Further, it has been demonstrated that high levels of GR are associated with a significantly better prognosis in ER positive breast cancers compared with ER negative cancers. In addition, these patients with ER negative breast cancers have a shorter relapse-free survival

Chapter 3 – Treatment of Human Breast Cancer Cells with Differing Hormones
Affects Cellular Growth Rates and RNA Pol II Activation at Specific Genes
Page 50

period and have been shown to have increased activation of EMT, cell adhesion, and cell survival (Pan, Kocherginsky et al. 2011). It has also been shown that increased stress levels in women, resulting in an increase in cortisol levels, have a potential to promote the development of breast cancer (Antonova and Mueller 2008).

It has been long understood that E2 and P4 have a proliferative effect on breast cancer cells. This was demonstrated over 100 years ago when the removal of the ovaries resulted in a suppression of breast cancer (Beatson 1983). More recently it has been shown in MCF-7, ZR-75-1, and T-47D (Table 3.1) breast cancer cells that a subset of synthetic progestins has limited to no effect on cell proliferation. However, when in combination with E2, the effects observed are a significant decrease in proliferation compared with E2 alone (Hissom and Moore 1987, Moore, Hagley et al. 1988, Gill, Tilley et al. 1991, van der Burg, Kalkhoven et al. 1992). This suggests that PR has the ability to antagonise the ER response. In addition, the effect of Dex on E2 proliferation has also been described. It has been shown that while Dex alone has less than a 2-fold effect on proliferation compared to unstimulated cells, Dex in combination with E2 has a repressive effect on the E2 alone mediated response. This suggests that, to some extent, ligand activated GR can inhibit the E2 mediated response (Zhou, Bouillard et al. 1989, Karmakar, Jin et al. 2013). However, despite the small increase in proliferation observed with Dex in these experiments, it has also been demonstrated that glucocorticoids can inhibit the growth of the ER positive cell lines MCF-7 and ZR-75-1 cells by blocking the G_0/G_1 growth phase (Lippman, Bolan et al. 1976, Hundertmark, Buhler et al. 1997). Together these studies

provide evidence to indicate the potential for SR crosstalk in cell proliferative responses.

What is also becoming apparent is the combined effect of Dex and E2 on gene transcription. It has been demonstrated that Dex and E2 can modulate the expression of proinflammatory genes (Cvoro, Yuan et al. 2011). In addition, it has also been shown that corticosteroids can reverse the effects of E2 on a small set of E2 regulated genes in human leiomyoma cells (Whirledge, Dixon et al. 2012). More specifically, a recent study investigated the effect of Dex on the E2 mediated expression of *pS2* and *Cyclin D*, two known E2 regulated genes in MCF-7 cells. It was shown, that while Dex alone had no significant affect on transcription compared to unstimulated samples, Dex in combination with E2 inhibited the increase observed in transcription with E2 alone (Karmakar, Jin et al. 2013). This suggests that Dex has the ability to alter the E2 transcriptional response at some genes. Further, the effects of Dex and E2 have also been previously investigated via expression microarray analysis providing a genome-wide response. It was shown that Dex and E2 in combination can affect expression of a subset of genes which differs from what was observed by the single treatment. These genes that were found to be associated with changes by dual treatment, were also associated with dual changes in either ER and GR binding within 20 kb of the genes TSS (Miranda, Voss et al. 2013). This study, however, was performed in a mouse mammary cell line engineered to express GR and ER. To provide a more direct effect of Dex and E2 on gene transcription, these experiments need to be performed in a more representative breast cancer cell model.

We know that ER binds to over 10,000 sites across the genome. This promotes the recruitment of coregulators and regulates the binding of RNA polymerase II (RNA PolII) transcription machinery (Acevedo and Kraus 2004, Cheung and Kraus 2010). Tiled microarrays have been commonly used to assess the global analysis of hormone-regulated gene expression (Cheung and Kraus 2010). In addition there have been multiple gene expression studies in MCF-7 cells profiling E2 regulated genes (Charpentier, Bednarek et al. 2000, Coser, Chesnes et al. 2003, Frasor, Danes et al. 2003, Carroll, Liu et al. 2005, Rae, Johnson et al. 2005, Kininis, Chen et al. 2007, Lin, Vega et al. 2007, Stender, Frasor et al. 2007). However, the number of E2 regulated genes in these studies ranged from 100-1500. This demonstrates there is some discrepancy among the studies and suggests that microarray analysis may not be the most ideal platform to test gene regulation. This may be in part due to mRNA levels not entirely reflecting gene activity as they are subject to degradation and further regulation. In addition, mature mRNA requires longer treatment times to allow for accumulation of transcripts. This can allow for the accumulation of transcripts from primary target genes which can lead to secondary transcriptional effects (Hah, Danko et al. 2011). It has been shown that promoters of many genes are preloaded with RNA PolII, referred to as promoter proximal enrichment of RNA PolII. This suggests that control of elongation in addition to RNA PolII recruitment to promoters has an important function in the activation of genes (Muse, Gilchrist et al. 2007, Core, Waterfall et al. 2008). This provides evidence to indicate that assessing RNA PolII binding maybe an ideal tool for determining gene transcription, especially due to being able to identify rapid changes upon hormone induction.

Chapter 3 – Treatment of Human Breast Cancer Cells with Differing Hormones
Affects Cellular Growth Rates and RNA Pol II Activation at Specific Genes
Page 53

Studies show that GR plays a potential role in breast cancer progression; however, the direct effects of Dex on transcription in breast cancer cells, is unknown. We know that Dex and E2 in combination can alter gene transcription compared to the effects observed by the single hormone alone as shown by microarray analysis in an artificial system (Miranda, Voss et al. 2013). Nevertheless, the early effects of Dex and E2 in combination on RNA PolII binding have not been assessed and are still unclear. The aim of this study is to assess the effects of dual hormones on proliferation in differing breast cancer cell lines. In addition, the effects of Dex and E2 in MCF-7 breast cancer cells on RNA PolII binding genome-wide is determined. This will allow us to further understand the potential role for GR and ER crosstalk in breast cancer cells and further establish the effects of dual treatment on gene transcription at an early response.

3.2 Methods

3.2.1 Cell seeding.

MCF-7, ZR-75-1 and T-47D cells are routinely maintained as described in chapter 2, section 2.3.1.1. Once the cells reach 80% confluence and are ready to be repassaged or seeded, they are harvested and the cell's concentration is calculated using a cell haemocytometer. The media utilised for MCF-7 cells is phenol red free DMEM containing 4.5g/L D-glucose supplemented with 10% CSS, 1mM sodium pyruvate, 1X non-essential amino acids, 0.2U/mL bovine insulin, and 1% penicillin-streptomycin. The media utilised for ZR-75-1 and T-47D cells is phenol red free RPMI 1640 medium that contains 2mM L-glutamine

and is supplemented with 10% CSS, 1mM sodium pyruvate, 1X non-essential amino acids, 0.2U/mL bovine insulin, and 1% penicillin-streptomycin.

3.2.2 Immunoblot.

The MCF-7, ZR-75-1, and T-47D cells are seeded at a concentration of 5×10^3 cells per mL in 100 mm cell culture plate in 10 mL of media. The cells are left untreated and after 72 h are lysed with RIPA buffer and immunoblot analysis performed as described in chapter 2, section 2.3.6. GR, ER, PR, and FoxA1 are detected in the cell lysates by immunoblotting with GR (E-20X; 1:1000), ERα (HC-20; 1:500), PR (H-190X 1:500), FoxA1 (ab23738; 1:500). Goat anti-rabbit HRP-conjugated secondary antibody is used at a concentration of 1:10,000.

3.2.3 Cellular growth curves.

Cell growth curves are performed as described in chapter 2, section 2.3.5. More specifically, MCF-7 and T-47D cells are seeded at a concentration of 2×10^4 cells per mL and ZR-75-1 cells at 3×10^4 per mL in a 96-well Matrical glass bottom plate at 100uL per well. Cells are treated by overlaying 100uL of either 100nM Dex, 100nM E2, 100nM Dex + E2, 100nM P4, 100nM P4 + E2, or left untreated for either 0, 24, 48, or 72 h. Upon paraformaldehyde fixation nuclei are stained with Hoescht. Cells are imaged utilising the Perkin Elmer Opera imaging system.

3.2.4 ChIP-seq.

MCF-7 cells are seeded at 8×10^6 cells per mL in a 150 mm cell culture plate in 30 mL of media. After 48 h, cells are treated with either 100nM of Dex, 100nM E2, 100nM Dex + E2, or left untreated. To achieve the desired concentration of

100nM, 30uL of 1mM stock solution of the appropriate hormone is added directly to the 150mm cell culture plate containing the medium. The ChIP-seq experiments are performed as described in chapter 2, section 2.3.2. More specifically, once the MCF-7 cells have been treated with the hormones for 30 mins, the cells are cross-linked with formaldehyde and removed from the plates via scrapping. The cell suspension is centrifuged at 2,000 rpm and a cell pellet is collected. The cell pellet is then resuspended in 600uL of ChIP lysis buffer, which contains 1X PI, and sonication is performed in 15mL sonication tubes. The sonication conditions are 15 cycles for 15 sec on, 30 sec off, at 4ºC. After sonication is complete, the DNA is quantified and samples are diluted 5 fold in ChIP dilution buffer and 1X PI to a final concentration of 100ug of chromatin per mL. For samples treated with 100nM Dex, 100nM Dex + E2, and left untreated, GR antibody is prepared. Seven ug/uL of GR (E-20X) antibody is linked to 80uL of Dynabeads (M-280) sheep anti-rabbit IgG. For samples treated with 100nM E2, 100nM Dex + E2, and untreated, ER antibody is prepared. Then 1.4 ug/uL of ERα (HC-20) antibody and 5 ug/uL of ER (Ab-10) antibody is linked to 40uL of Dynabeads (M-280) sheep anti-rabbit IgG and 40uL of Dynabeads (M-280) sheep anti-mouse IgG. For samples treated with 100nM Dex, 100nM E2, 100nM Dex + E2, and untreated, RNA PolII antibody is prepared. Four ug/uL of RNA PolII (ab5131) antibody is linked to 80uL of Dynabeads (M-280) sheep anti-rabbit IgG. Next 100uL of each sample is removed and stored at 4ºC overnight and utilised as the no antibody control referred to as input. Each sample is incubated with the appropriate antibody/Dynabead complex overnight. After the overnight incubation, the complex is washed with the appropriate wash buffers. The samples are eluted from the Dynabeads and DNA extraction is performed using

phenol-chloroform-isoamyl. Each sample pellet is suspended in 10uL of nuclease free H_2O. Each experiment is repeated four times resulting in four biological replicates. To determine efficient protein binding qPCR analysis is utilised at known sites. For all ER ChIP experiments *MYC* forward and reverse primers are utilised (Miranda, Voss et al. 2013). For all GR ChIP experiment's *PER1* forward and reverse primers are utilised. For all RNA PolII experiment's TFF1_TSS forward and reverse primers were used (Kininis, Chen et al. 2007). Two biological replicates are pooled for each sample resulting in two technical replicates per sample set submitted to the National Cancer Institute Advanced Technology Program Sequencing Facility for sequencing services.

3.2.5 Bioinformatic analysis.

The Illumina HiSeq genome analyser platform has been used to generate sequence reads (36-mer) and unique tags have been aligned to the human reference genome (UCSC hg19 assembly). Homer has been used to determine the tag density across each gene body for each sample replicate. DeSeq has been used to determine statistically relevant changes in RNA PolII binding across treatment groups for each gene. RNA PolII binding is considered statistically different if the fold difference between the sample sets is 2-fold and the pval < 0.05. Differentially expressed genes for each treatment group compared to the untreated sample set have been determined. Venn diagrams have been created by comparing the differentially expressed genes for each group with the other treatment samples. Volcano plots have been created by determining genes that are differentially expressed in the Dex + E2 treatment samples compared to either the Dex or E2 treated samples. The statistical program R has been used to

generate the volcano plots. For GR and ER ChIP-seq, hotspots, regions of enriched tags, have been called using previously described methods with minor modifications (Baek, Sung et al. 2012). The values for the tag densities have been normalised to 10 million reads to adjust for differences in the depth of sequencing between samples. The data sets have been adjusted by subtracting tags found in the input. Hotspots have been called using a 0% FDR. A tag density threshold of 30 (1 standard deviation of the maximum tag density) has been applied. Replicate concordants have been calculated between replicates.

3.3 Results

3.3.1 <u>Immunoblot analysis determines steady state protein levels in MCF-7, ZR-75-1 and T-47D breast cancer cells.</u>

Unstimulated MCF-7, ZR-75-1, and T-47D cells, the three most commonly studied E2 responsive breast cancer cells (Lacroix and Leclercq 2004), have been tested for the expression of GR, ER, PR, and FoxA1 steady state protein levels (Figure 3.1 A-D). In ZR-75-1 cells it seems that GR is expressed at a slightly higher level compared with MCF-7 cells. T-47D cells express relatively low levels of GR, ER, and FoxA1, however, they have very high expression levels of PR compared with the other two cells lines. Further there is relatively low levels of PR in MCF-7 cells. These findings are in line with previous studies investigating mRNA expression levels of GR, ER, and PR in the three cell lines (Vienonen, Miettinen et al. 2003). This further indicates that the current cell lines used in this thesis are suitable for investigating the SRs mechanism in a variety of

different breast cancer cell line models in regards to SRs and FoxA1 expression levels.

3.3.2 Dual treatment can shift the proliferative effects of E2 alone in MCF-7, ZR-75-1, and T-47D breast cancer cells.

To assess the proliferative effects of hormone treatment on MCF-7, ZR-75-1, and T-47D cells, cell growth has been calculated after 0, 24, 48, and 72 h in cells treated with either 100nM of Dex, E2, P4, Dex + E2, P4 + E2, or left untreated (Figure 3.2 A-C). There is a general finding that over the course of three days, cell proliferation in all treatment groups increases. Treatment of all cells with E2 alone demonstrates the highest level of cell proliferation with Dex and P4 alone, having very little effect when compared with untreated cells. In addition, the dual combination of either Dex + E2 or P4 + E2 results in a inhibition of the proliferative response observed with E2. While this data does not demonstrate statistical significants it highlights a trend toward a change in proliferation. This confirms previous studies that have investigated cell proliferation in a dual setting (Hissom and Moore 1987, Moore, Hagley et al. 1988, Zhou, Bouillard et al. 1989, Gill, Tilley et al. 1991, van der Burg, Kalkhoven et al. 1992, Karmakar, Jin et al. 2013). More specific, it also demonstrates that the natural hormone, P4, functions as observed with synthetic progestins on breast cancer cell proliferation, and that the dual effects of Dex + E2 are also present in all three cell lines. This confirms that hormones in a dual setting have the ability to function differently compared to the single treatment. Further, this also suggests that one hormone has the ability to alter the proliferative response of another.

3.3.3 Validation of GR, ER and RNA PolII binding in MCF-7 breast cancer cells.

To further investigate the effects of dual hormones on SRs binding and transcriptional response, ER, GR, and RNA PolII binding patterns have been mapped genome-wide in MCF-7 cells. ER has been mapped after stimulation with either E2, Dex + E2, or left untreated, GR has been mapped after stimulation of Dex, Dex + E2, or left untreated, and RNA PolII has been mapped after treatment with Dex, E2, Dex + E2, or left untreated. In addition ER binding has been mapped after Dex stimulation and GR binding mapped after E2 stimulation (data not shown). Analysis has identified there are no ER peaks specific to Dex treatment and GR peaks specific to E2 treatment.

To determine if optimal protein binding to the DNA has been achieved in all four biological replicates, qPCR analysis has been utilised at known GR, ER, and RNA PolII binding sites (Kininis, Chen et al. 2007, Miranda, Voss et al. 2013). In MCF-7 cells treated with E2, Dex + E2, and left untreated, ER binding is increased at the *MYC* site in the E2 and Dex + E2 treatment groups compared with untreated samples (Figure 3.3A). Primers at a *PER1* site, which has previously been shown to be hypersensitive and contain a GRE and PRE motif, has been designed to assess GR binding. GR binding is increased at the *PER1* site when cells are treated with Dex and the co-treatment of Dex + E2 (Figure 3.3B). In MCF-7 cells treated with either Dex, E2, Dex + E2, or left untreated, RNA PolII binding is increased at the TFF1-TTS site in the E2 and Dex + E2 treatment groups (Figure 3.3C). This qPCR analysis confirms that efficient protein binding to DNA has been achieved via ChIP experiments, and the samples are suitable for sequencing.

3.3.4 Co-treatment of MCF-7 human breast cancer cells with Dex and E2 induces changes in RNA PolII binding genome-wide.

To further investigate the effect of Dex and E2 in a dual treatment setting on MCF-7 cells, RNA PolII binding genome-wide has been assessed upon stimulation of cells with either Dex, E2, Dex + E2, or left untreated for 30 mins. This has allowed us to assess the transcriptional response upon dual activation of GR and ER as an early event. Analysis of RNA PolII binding across whole genes reveal a total of 108 upregulated genes and 30 downregulated genes in the different treatment groups compared to untreated cells (Figure 3.4A-B). Of particular interest to this study, are the 35 genes upregulated and unique to E2 treatment, and the 13 genes upregulated and unique to Dex treatment.

Upon the addition of the dual treatments, the expression of these genes are no longer upregulated, and 18 new genes are now over expressed by 2-fold or more and are unique to Dex + E2. This finding is not as defined in the genes that are down regulated.

Pathway analysis has been performed utilising the computational program, The Database for Annotation, Visualisation and Integrated Discovery (DAVID) on all genes that are affected by either the gain or loss of the dual treatment (Figure 3.5). It was demonstrated that of the 91 genes, there were 40 pathways with a number of these genes found to be significantly involved, using an integrated pathway analysis of all available databases. There are a subset of genes involved in androgen and estrogen metabolism, pregnancy, and regulation of receptor cycling. However, of particular interest are the genes found to be involved in ovarian

carcinoma with a fold enrichment of approximately 190. This pathway is the most significantly enriched and suggests that a subset of genes regulated by dual treatment are highly involved in this cancer pathway, which is known to be driven by sex hormones.

To look further into the effects of the dual hormone treatment and the possible influence it has on genes also regulated by the single hormone treatment, the effect of E2 on Dex regulated genes and conversely the effect of Dex on E2 regulated genes has been investigated. Firstly, it is shown that when E2 treated samples are compared to samples treated with both Dex and E2, the majority of genes are unaffected by the addition of Dex treatment. However there are still 34 genes that are specific to the dual treatment and are not regulated by Dex alone, and 11 genes specific to Dex treatment (Figure 3.6A). Further, this same general finding has been observed for all genes regulated by Dex, demonstrating the majority of these genes are unaffected by the addition of E2 to Dex treated cells. However, there are a subset of genes (168) whose expression changes upon the addition of E2 to Dex treatments and a subset 19 that are specific to E2 treatment (Figure 3.6B). Overall these findings suggest that the dual treatment of Dex and E2 has a unique ability to regulate the transcriptional response in MCF-7 cells by either inhibiting the regulation of some genes and by regulating genes previously unaffected by the single hormone treatment.

Chapter 3 – Treatment of Human Breast Cancer Cells with Differing Hormones
Affects Cellular Growth Rates and RNA Pol II Activation at Specific Genes
Page 62

3.3.5 Stimulation of GR binding genome-wide upon the single and dual hormone treatments in MCF-7 human breast cancer cells correlates to the regulation of genes.

To investigate the GR and ER binding landscape and how that correlates to gene regulation under dual activation, GR and ER binding has been assessed genome-wide in MCF-7 cells after treatment with either Dex, E2, Dex + E2, or left untreated. Genes shown to be unique to either Dex, E2, or Dex + E2 compared with untreated sample identified in section 3.3.4 have been assessed for GR and ER binding sites 5000 bp on either side of the TSS of the genes. Genes demonstrated to be regulated by Dex treatment alone, show an increase in GR binding activated by Dex treatment and an overall inhibition of GR binding upon the dual treatment (Figure 3.7A). Conversely, in genes uniquely regulated by the dual treatment of Dex + E2, there is an overall increase in GR binding in the dual treatment compared with the Dex alone treatment, although GR binding is lost at some sites upon the dual hormone treatment (Figure 3.7B). Of specific interest, are the changes in GR binding with Dex alone, compared with Dex + E2, near genes regulated by E2 alone (Figure 3.7C). It is important to note that the correlation between GR binding and gene regulation isn't as prominent with ER binding. Overall, these findings suggest that the gene changes observed between the single and dual treatments appear to correlate to GR and ER binding. This provides evidence to further assess GR and ER binding patterns genome-wide upon dual activation.

It is becoming apparent that the dual activation of SRs can have differing effects on breast cancer cellular mechanisms, compared with the response observed with single receptor activation. Investigations into Dex and E2 treatment at a gene transcriptional level by microarray analysis has previously been performed in an engineered mouse mammary cell line (Miranda, Voss et al. 2013). These studies demonstrated that the combination of Dex and E2 can alter a subset of genes, and that dual activation correlates with binding patterns for ER and GR within 20 kb of the gene TSS. This shows that GR and ER crosstalk affects gene transcription. However, these studies did not allow for the identification of early changes in transcriptional response due to the fact that microarrays were used. In addition, the studies performed by Miranda *et al*. were in a mouse mammary cell line engineered to over express GR and ER. Utilising a cell model that is more representative of human breast cancer and expresses more relative levels of SRs, will allow us to begin to determine the early effects of GR and ER signalling on breast cancer cell transcriptional responses.

Genome-wide investigations of RNA Pol II binding in MCF-7 cells have allowed for the determination of early responses to hormone treatments on gene transcription. The majority of genes are regulated by the single treatment; however, there is a unique subset of genes whose expression levels are either increased or decreased in dual hormone setting. These changes in gene expression indicate that upon early induction of GR and ER there is a direct effect on gene regulation by the assessment of RNA PolII binding. This confirms previous studies that have been performed at a single gene level, and by

microarray analysis, demonstrating that Dex can alter the E2 driven response (Karmakar, Jin et al. 2013, Miranda, Voss et al. 2013). This suggests that the dual activation of GR and ER has the ability to shape the RNA PolII recruitment to DNA and change the response observed in a single hormone setting. This change in gene regulation and the ability of GR to affect the E2 gene regulation response has the ability to effect breast cancer progression.

The important role that GR plays in breast cancer progression is becoming apparent. Studies show that patients with high GR levels have significantly better outcomes if they have ER positive breast cancer than ER negative breast cancer, and that women with GR positive/ER negative cancers have a shorter relapse free survival compared with ER positive patients (Pan, Kocherginsky et al. 2011). This suggests that GR and ER have the ability to function together. GR appears to have negative effects on breast cancer alone. It has been shown that in the absence of ER, high levels of GR in breast cancer can promote EMT activation, cell adhesion, and cell survival (Pan, Kocherginsky et al. 2011). This suggests that ER may be playing a protective role toward the negative effects of GR on breast cancer development. This could also occur at a gene transcription level, as this chapter demonstrates there is a subset of Dex-responsive genes lost upon the addition of E2. Currently, in the clinic, ER expression is inhibited in breast cancers that are driven by E2 with endocrine therapies (Ali and Coombes 2002). However, recent studies suggest that in the absence of a functional ER, GR may have negative effects.

In conclusion, this chapter demonstrates that in multiple breast cancer cell lines, dual activation of SRs can have differing affects on cellular responses compared

with single receptor signalling. Further, in MCF-7 cells, it has been shown that the combination of Dex + E2 can reshape the E2 and Dex transcriptional response. In addition, this response can shift to a Dex only mediated regulation in the absence of ER signalling. This has the potential to have negative effects on breast cancer, and suggests that GR expression also needs to be considered when clinicians are tailoring treatment plans for breast cancer. Specifically, ER inhibition can have the potential to reshape the GR response. GR signalling alone has been shown to influence breast cancer survival, and this may be through a shift in Dex gene regulation that is observed in the absence of ER.

Chapter 3 – Treatment of Human Breast Cancer Cells with Differing Hormones
Affects Cellular Growth Rates and RNA Pol II Activation at Specific Genes
Page 66

Cell line	Cell Type	Disease	Tissue Type	Molecular subtype
MCF-7 (passage 1-23)	epithelial	adenocarcinoma	derived from the metastatic site (pleural effusion) (Soule, Vazguez et al. 1973)	Luminal A (Neve, Chin et al. 2006, Mackay, Tamber et al. 2009)
ZR-75-1 (passage 1-21)	epithelial	ductal carcinoma	derived from the metastatic site (ascites) (Engel, Young et al. 1978)	Luminal B (Neve, Chin et al. 2006, Mackay, Tamber et al. 2009)
T-47D (passage 1-22)	epithelial	ductal carcinoma	derived from the metastatic site (pleural effusion) (Keydar, Chen et al. 1979)	Luminal A (Neve, Chin et al. 2006, Mackay, Tamber et al. 2009)

Table 3.1: Table summary of breast cancer cell lines. Table represents the clinical characteristics of each cell line utilised in this study.
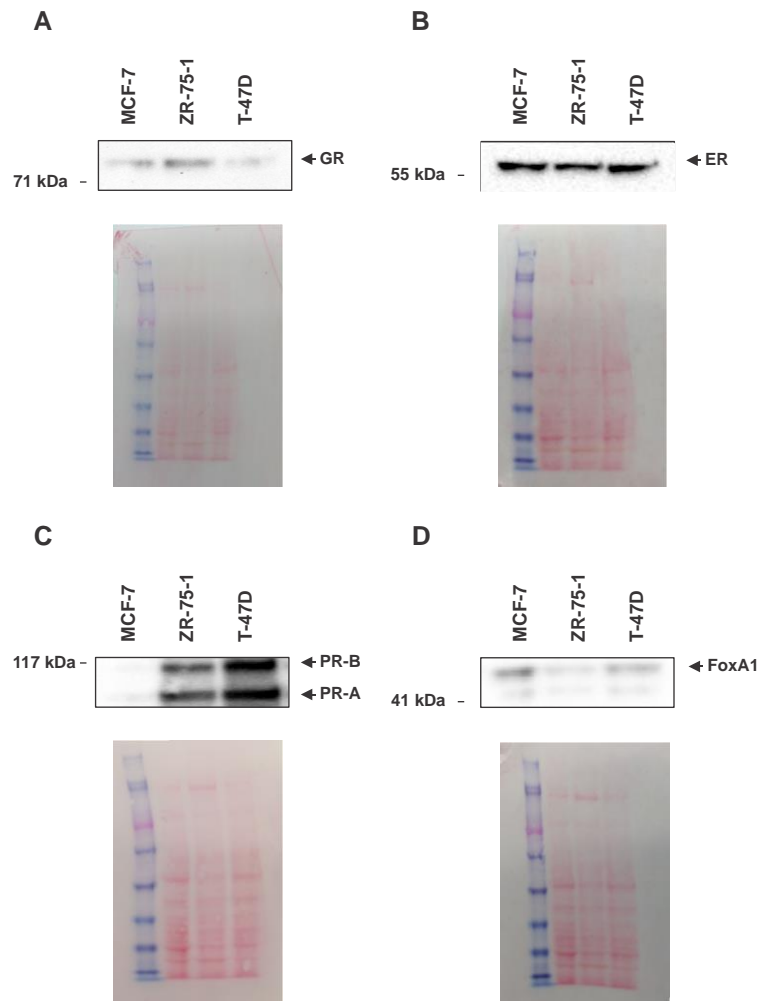
Figure 3.1: Immunoblot analysis of GR, ER, PR, and FoxA1 steady state protein levels in breast cancer cells. **A.** Steady state protein levels of GR in untreated MCF7, ZR-75-1, and T-47D breast cancer cells. Ponceau staining of membrane has been used to demonstrate equal loading of samples. **B.** Steady state protein levels of ER in untreated MCF7, ZR-75-1, and T-47D breast cancer cells. Ponceau staining of membrane has been used to demonstrate equal loading of samples. **C.** Steady state protein levels of PR in untreated MCF7, ZR-75-1, and T-47D breast cancer cells. Bands for isoforms A and B has been detected. Ponceau staining of membrane has been used to demonstrate equal loading of samples. **D.** Steady state protein levels of FoxA1 in untreated MCF7, ZR-75-1, and T-47D breast cancer cells. Ponceau staining of membrane has been used to demonstrate equal loading of samples. Each protein has been detected on separate membrane.
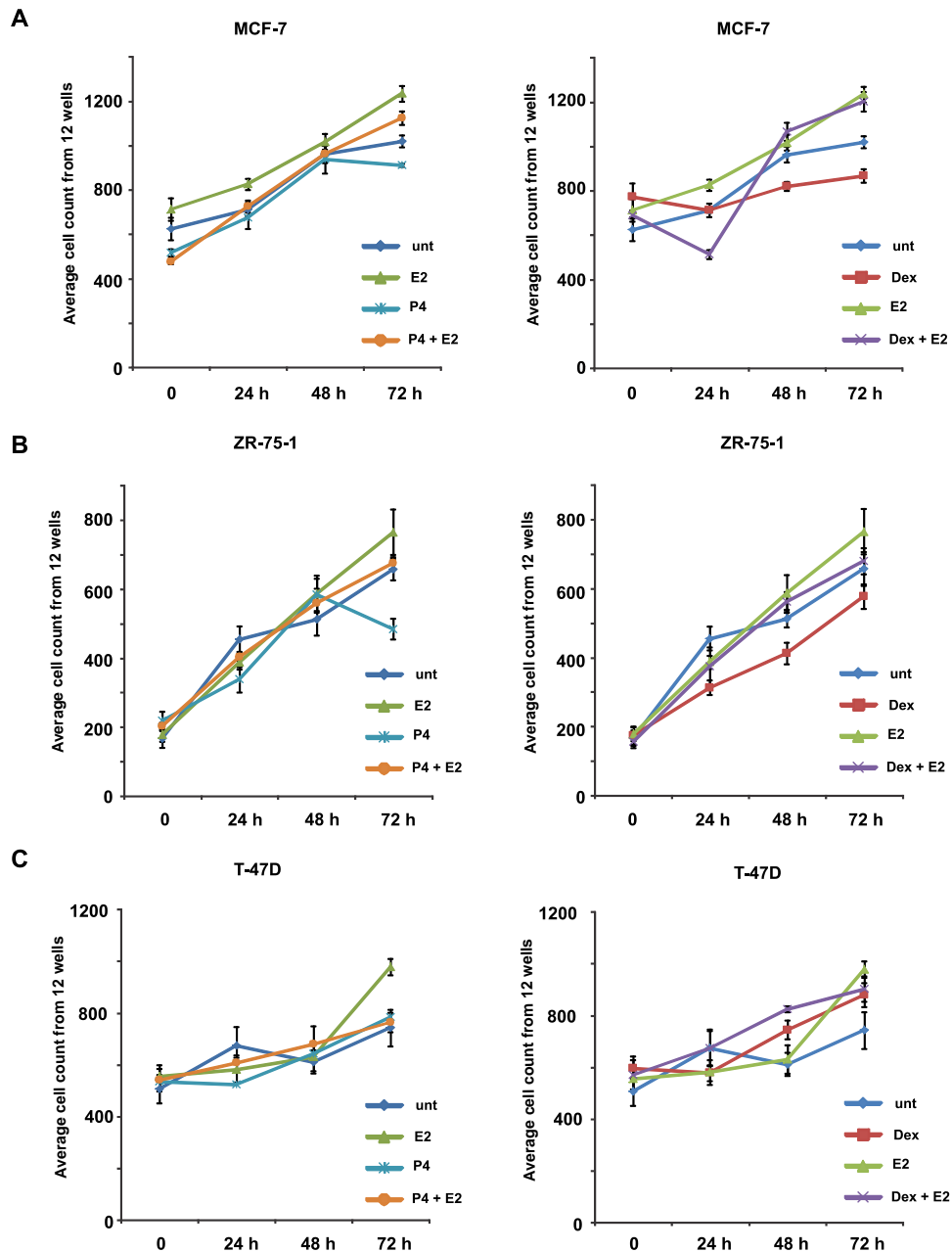
Figure 3.2: Cell proliferation assay of hormone treated MCF-7, ZR-75-1, and T-47D cells. MCF-7, ZR-75-1, and T-47D breast cancer cells have been treated with either 100nM Dex, 100nM E2, 100nM P4, 100nM Dex + E2, 100nM P4 + E2, or left untreated for 0h, 24h, 48h, or 72h. **A.** Results demonstrate MCF-7 breast cancer cell count after hormone treatment. Graph separated to represent 100nM P4, 100nM E2, 100nM P4 + E2 or untreated samples together and 100nM Dex, 100nM E2, 100nM Dex + E2 or untreated samples. Error bars represent to standard error of the mean of biological replicates.

Chapter 3 – Treatment of Human Breast Cancer Cells with Differing Hormones
Affects Cellular Growth Rates and RNA Pol II Activation at Specific Genes
Page 69
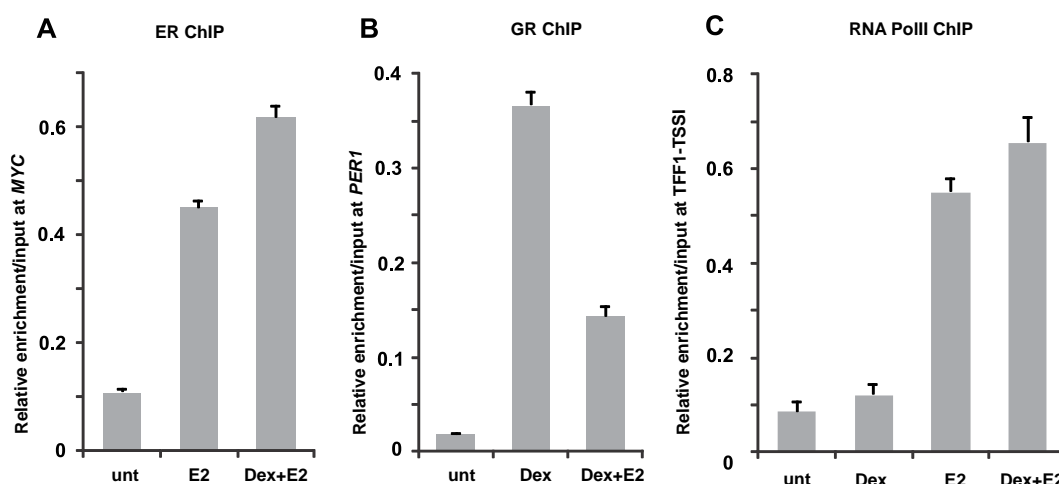
Figure 3.3: Analysis of ER, GR, and RNA PolII binding confirms sufficient enrichment for ChIP-seq. A. Quantitative-PCR shows that ER binding is increased at a *MYC* site in MCF-7 breast cancer cells treated with either 100nM of E2 or 100nM of Dex and E2. Data presented as relative enrichment over input. Results demonstrate that ER ChIP samples are suitable for sequencing. Figure is a representative example of one biological replicate. Error bars represent technical replicates. **B.** Quantitative-PCR shows that GR binding is increased at a *PER1* site in MCF-7 breast cancer cells treated with either 100nM of Dex or 100nM of Dex and E2. Data presented as relative enrichment over input. Results demonstrate that GR ChIP samples are suitable for sequencing. Figure is a representative example of one biological replicate. Error bars represent technical replicates. **C.** Quantitative-PCR shows that RNA PolII binding is increased at a TFF1-TSS site in MCF-7 breast cancer cells treated with either 100nM of E2 or 100nM Dex and E2 compared with untreated or 100nM Dex samples. Data presented as relative enrichment over input. Results demonstrate that RNA PolII ChIP samples are suitable for sequencing. Error bars represent technical replicates.

A   **Increase in RNA PolII Binding**

B   **Decrease in RNA PolII Binding**
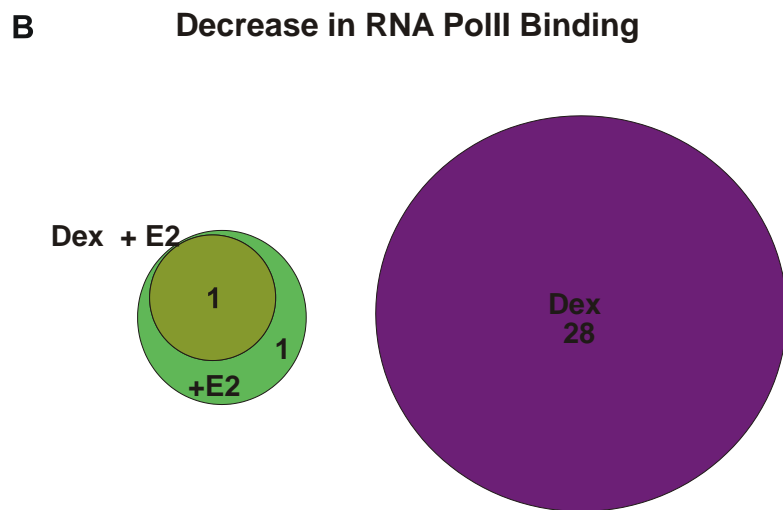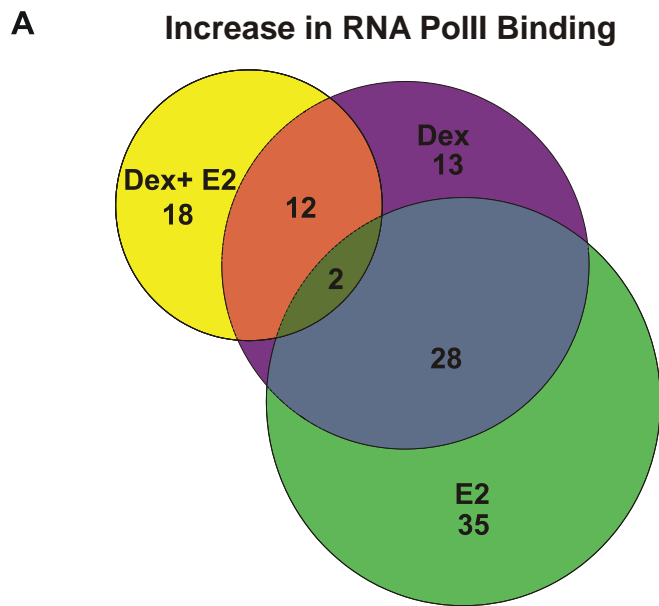
Figure 3.4: Changes in RNA PolII binding in hormone treated MCF-7 breast cancer cells. **A.** Venn diagram represents RNA PollII binding sites that are increased when treated with either 100nM Dex, 100nM E2, or 100nM Dex and E2 when compared with untreated cells. **B.** Venn diagram represents RNA PolII binding sites that are decreased when treated with either 100nM Dex, 100nM E2, or 100nM Dex and E2 when compared with untreated cells. Changes in binding is considered statistically significant if the fold change is ≥ 2 and has a pval < 0.05 using DeSeq.

Chapter 3 – Treatment of Human Breast Cancer Cells with Differing Hormones
Affects Cellular Growth Rates and RNA Pol II Activation at Specific Genes
Page 71
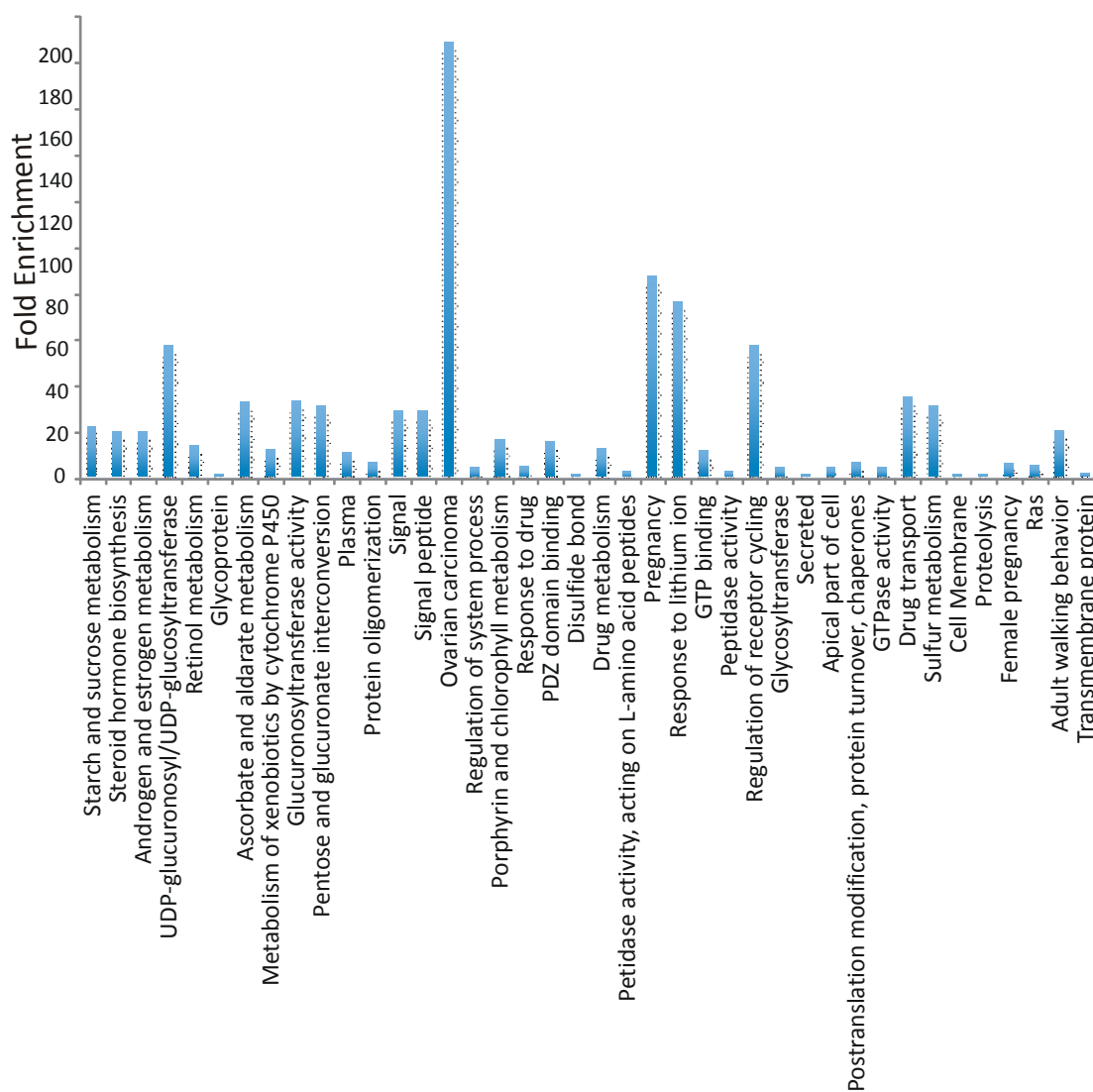
Figure 3.5: Pathway analysis on all RNA PolII binding sites at genes gained or lost by the dual treatment of Dex and E2 in MCF-7 breast cancer cells. Pathways analysis on genes gained or lost by the dual hormone treatment of Dex and E2 has been performed using DAVID. Forty pathways have been found to be significantly involved with identified genes.

Chapter 3 – Treatment of Human Breast Cancer Cells with Differing Hormones
Affects Cellular Growth Rates and RNA Pol II Activation at Specific Genes
Page 72
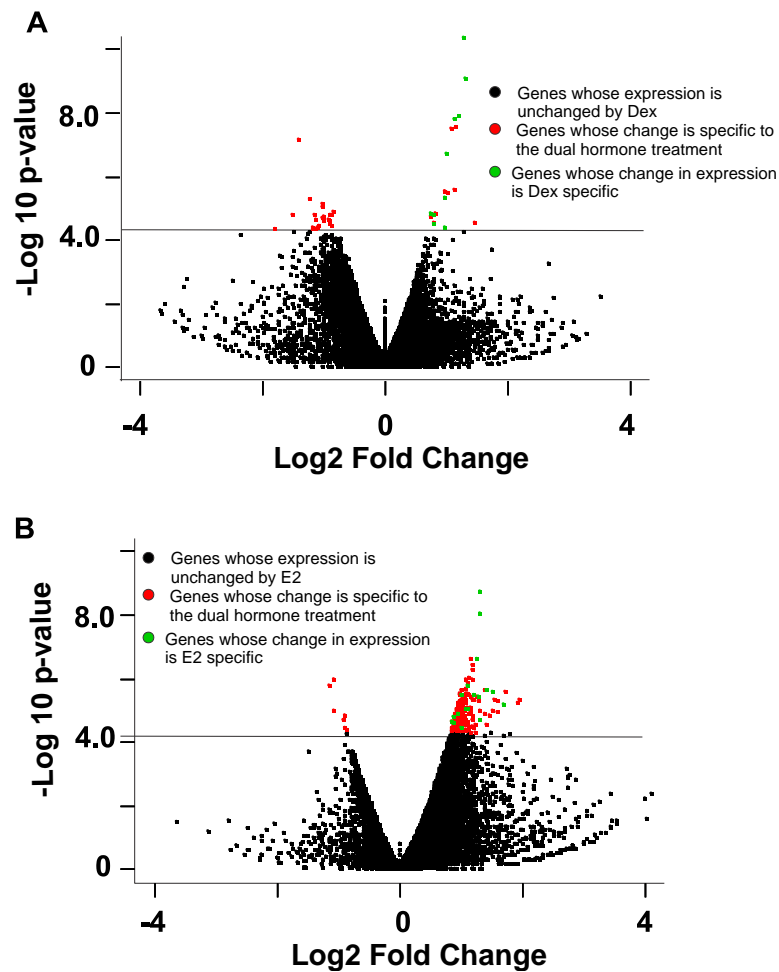
Figure 3.6: Effect of dual hormone treatment of Dex and E2 on RNA PolII binding in MCF-7 breast cancer cells. A. Volcano plot comparing RNA PolII binding in Dex + E2 treated MCF-7 breast cancer cells versus E2 treated cells. **B.** Volcano plot comparing RNA PolII binding in Dex + E2 treated MCF-7 breast cancer cells versus Dex treated cells. Significant changes have been determined using a fold change ≥ 2 and a pval < 0.05 using DeSeq.
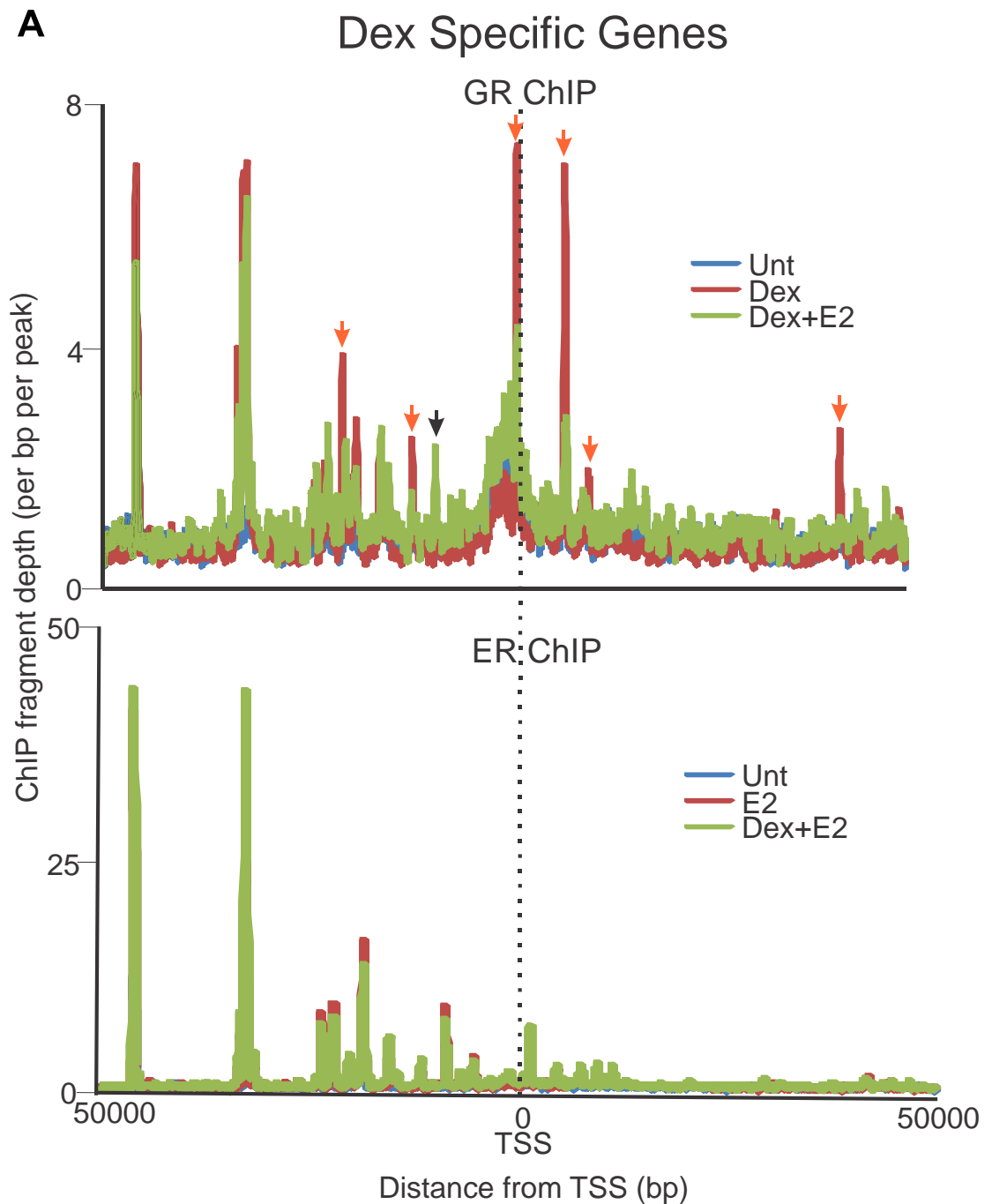
Figure 3.7: Changes in SR binding near TSS of genes that expression is effected by dual hormone treatment of Dex and E2 in MCF-7 breast cancer cells. A. Histogram represents changes in GR binding (top) and ER binding (bottom) at genes significantly regulated by 100nM of Dex. Dual hormone treatment of 100nM Dex + E2 inhibits Dex regulation of these genes. Orange arrows represent SR binding sites lost upon dual hormone treatment. Black arrows represent SR binding gained by dual hormone treatment.

Chapter 3 – Treatment of Human Breast Cancer Cells with Differing Hormones
Affects Cellular Growth Rates and RNA Pol II Activation at Specific Genes
Page 74

B

Dex + E2 Specific Genes
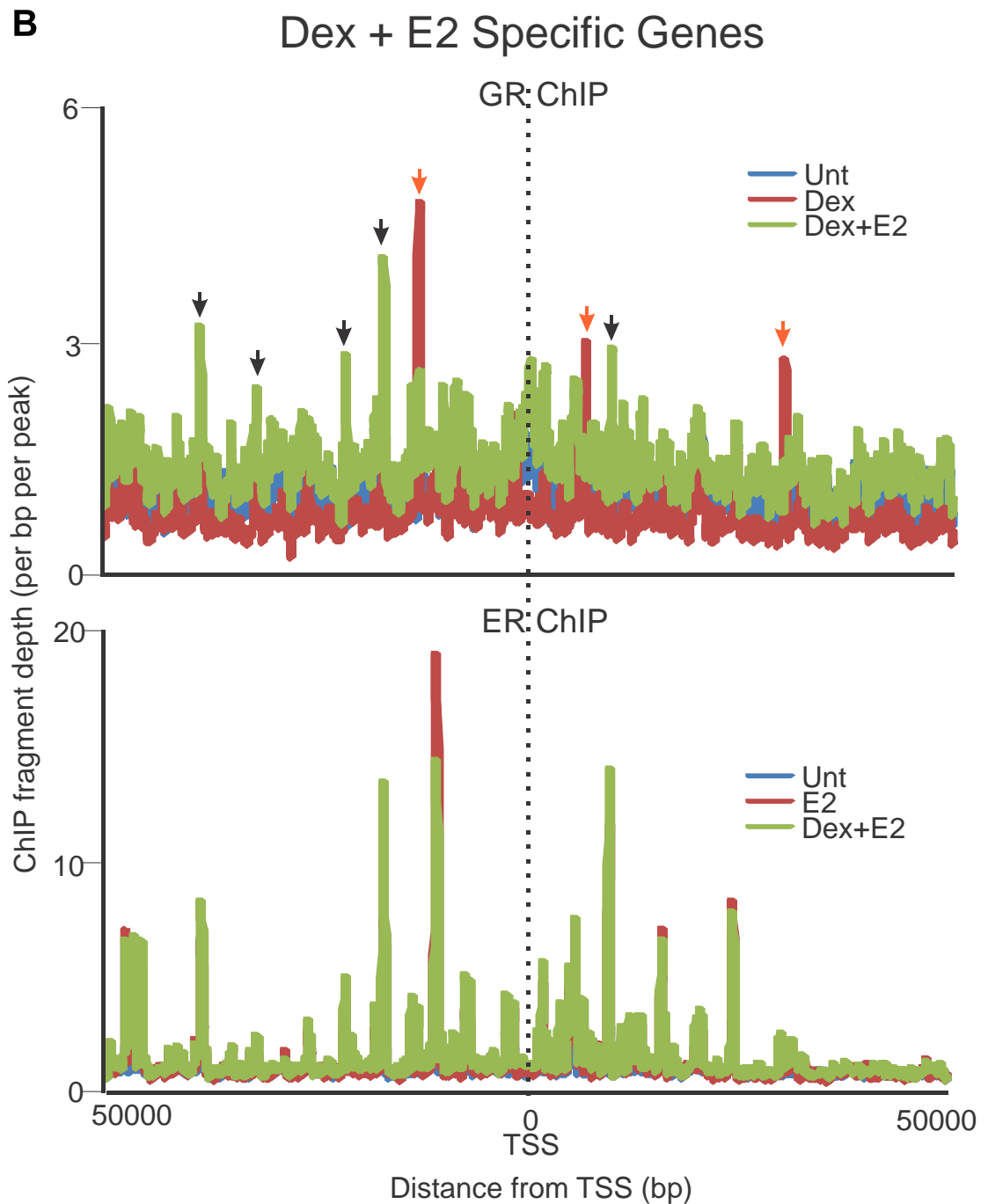
Figure 3.7: Changes in SR binding near TSS of genes that expression is effected by dual hormone treatment of Dex and E2 in MCF-7 breast cancer cells. B. Histogram represents changes in GR binding (top) and ER binding (bottom) at genes significantly regulated by 100nM of Dex + E2. Single treatment of either Dex or E2 treatment does not regulate these genes. Orange arrows represent SR binding sites lost upon dual hormone treatment. Black arrows represent SR binding gained by dual hormone treatment.

Chapter 3 – Treatment of Human Breast Cancer Cells with Differing Hormones
Affects Cellular Growth Rates and RNA Pol II Activation at Specific Genes
Page 75

C

E2 Specific Genes
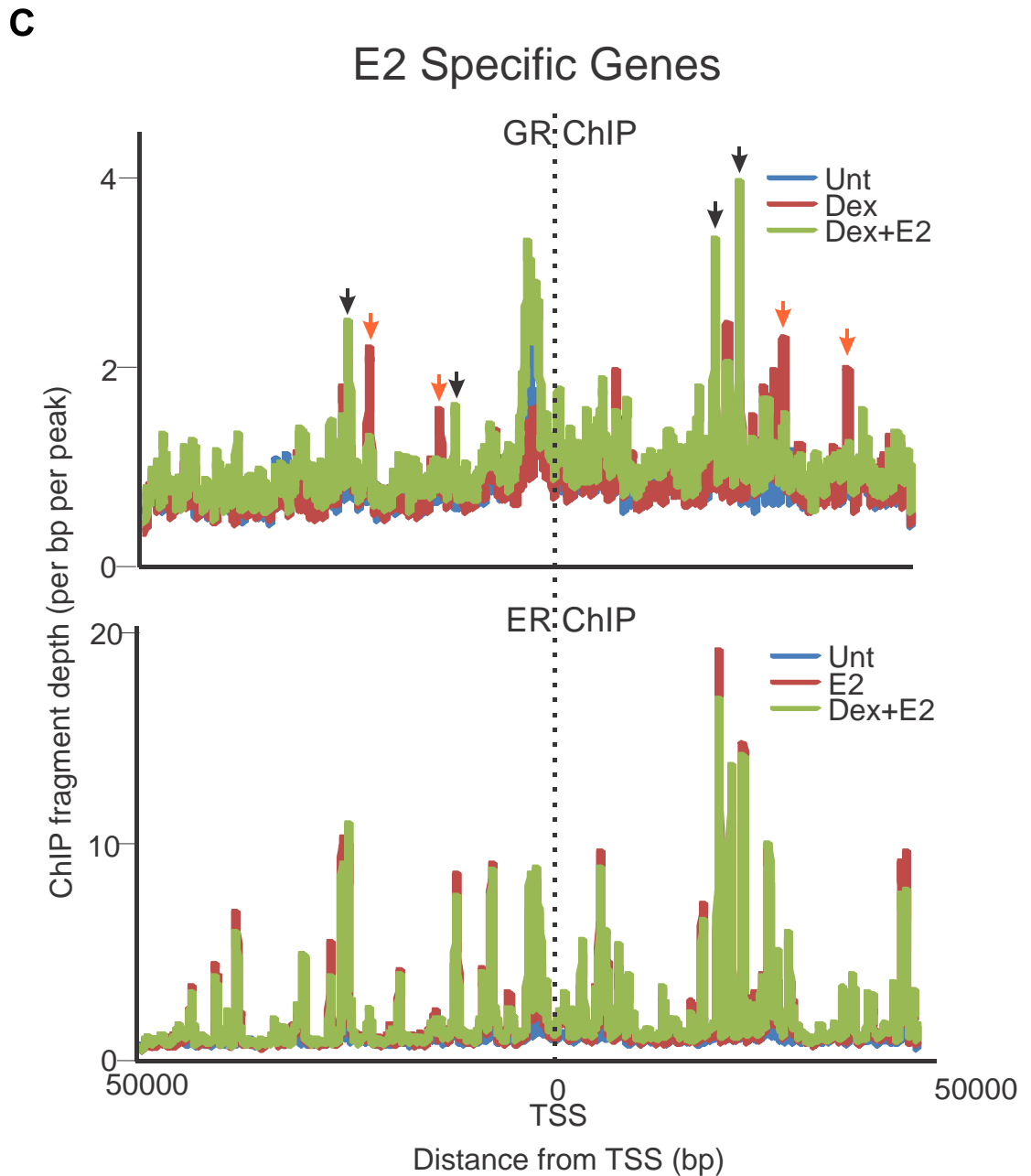
Figure 3.7: Changes in SR binding near TSS of genes that expression is effected by dual hormone treatment of Dex and E2 in MCF-7 breast cancer cells. C. Histogram represents changes in GR binding (top) and ER binding (bottom) at genes significantly regulated by 100nM of E2. Dual hormone treatment of 100nM Dex + E2 inhibits E2 regulation of these genes. Orange arrows represent SR binding sites lost upon dual hormone treatment. Black arrows represent SR binding gained by dual hormone treatment.

Chapter 4

GR, ER, and PR Interplay in MCF-7 Human

Breast Cancer Cells

4.1 Introduction

As demonstrated in chapter 3, combinatorial treatment of cells with hormones can have differing effects on the transcriptional responses and growth rate of breast cancer cells. This suggests that hormones in a dual setting can alter the cellular response compared with a single hormone treatment. Genome-wide investigations provide important information and contribute to our understanding of SR functions; however, the majority of those studies are performed in an environment where only one receptor is activated at a given time. This is not representative of a biological setting, since physiologically, multiple SRs are activated due to cells being exposed to multiple hormones. Little investigation has gone into further understanding the crosstalk of SRs in breast cancer; however, it is becoming apparent that co-activation of multiple SRs can affect each other's function and responses at a cellular level.

Early studies, investigating ER binding patterns after activation with E2 in MCF-7 cells utilising ChIP-chip to a single chromosome, have surprisingly revealed that ER binds distal to gene TSS and not promoter regions as previously thought (Carroll, Liu et al. 2005). These findings were later confirmed using genome-wide analysis via ChIP-seq (Carroll, Meyer et al. 2006, Welboren, van Driel et al. 2009). While investigations into the mechanisms of ER binding have been intensively studied, a lack of understanding in PR and GR genomic interactions in breast cancer cells is apparent. Utilising the T-47D breast cancer cells and AB32 cells, a stable PR expressing clone of the MCF-10A immortalised normal breast cancer cell line, demonstrates that upon stimulation with a synthetic progestin, ORG2058, PR binding genome-wide correlates with transcriptional responses.

However, there is little overlap between the binding of PR sites in both cell lines. A PR binding sequence has been identified in each individual cell line, in addition to known cofactor binding motifs, including FoxA1 for T-47D cells, and NF1 and AP-1 for AB32 cells (Clarke and Graham 2012). A recent study has demonstrated, in a T-47D breast cancer cell model (Truss, Bartsch et al. 1995), that the majority of PR sites are near progestin induced genes, generally around enhancers. There is also a global correlation between the effect of hormones on gene expression and the number of PR binding sites (Ballare, Castellano et al. 2013). While global characterisation of GR binding sites via genome-wide ChIP-seq is well established (Reddy, Pauli et al. 2009, John, Sabo et al. 2011), mapping of GR in breast cancer cells is limited. A recent study evaluated GR binding and changes in gene expression upon treatment of a premalignant breast cancer cell line that does not express ER with Dex (Moran, Gray et al. 2000). These studies led to the discovery that GR activation is an important aspect in epithelial-to-mesenchymal transition (EMT) pathways in MCF10A-MYC cells (Pan, Kocherginsky et al. 2011).

SR binding patterns have been reported to be cell specific, with different binding patterns observed across the genome in different cell types, suggesting a specific TF binding pattern is indeed unique to a particular biological state or disease (Lefterova, Steger et al. 2010, John, Sabo et al. 2011). Studies have shown that chromatin accessibility is a critical regulator to this cell specific TF occupancy. It has long been understood that GR is able to induce chromatin remodelling *de novo* in a hormone dependent fashion via the recruitment of chromatin remodelling complexes, such as Swi/Snf (Fryer and Archer 1998). Genome-wide DHS-seq has shown that *de novo* induction of chromatin accessibility is not the

predominant feature of GR activation, and that most GR binding occurs at accessible pre-programmed chromatin sites (John, Sabo et al. 2011). In mouse mammary cells, > 70% of GR binding sites are associated with pre-programmed open chromatin, whereas approximately 20% are found at de novo remodelled sites induced by hormone (John, Sabo et al. 2011). The global association of GR to pre-programmed chromatin was also observed in pituitary cells, human lung epithelial cells, and mouse liver (John, Sabo et al. 2008, Reddy, Gertz et al. 2012, Grontved, John et al. 2013). Studies into the mechanisms dictating ER binding are somewhat controversial. It has been shown that ER binding events demonstrate the same pattern as GR, with approximately 70% of events being associated with pre-programmed chromatin and 20% being found at *de novo* remodelled sites induced by E2 (Gertz, Savic et al. 2013). However, FAIRE analysis has shown that ER sites shared by FoxA1 (approximately 50%) were found to be associated with closed chromatin, whereas ER binding events that were not shared with FoxA1 were nucleosome depleted and open (Hurtado, Holmes et al. 2011). In addition, another study claimed that the majority of ER binding occurs at pre-programmed sites, and there is also a smaller subset of sites induced in MCF-7 cells. It has; however, been suggested that the increase in accessibility is not associated with hormone-dependent nucleosome depletion (He, Meyer et al. 2012).

While SRs preferentially bind to regulatory elements that are pre-programmed, it is exhibited that some of these regions have an increase in accessibility following receptor binding. The increase in accessibility is due to the recruitment of chromatin modifiers to these sites, upon activation of the receptor. However, the

specific mechanisms that result in the opening of chromatin upon receptor binding are unclear.

It is demonstrated that PR binds to pre-programmed chromatin sites flanked by nucleosomes, that undergo H1 and H2A/H2B dimer removal, following PR binding (Ballare, Castellano et al. 2013). It is further suggested that when ER binds to sites flanked by histones marked with H3K4me3 can undergo acetylation of H3K9, which has the ability to increase chromatin access upon ER binding (Foulds, Feng et al. 2013). It is also illustrated that, upon activation, GR can recruit chromatin remodellers to specific binding sites, which cause an increase in DHS accessibility and allows for the binding of other TFs at these sites. This has also been shown to assist in binding other TFs, such as AP-1 and ER (Voss, Schiltz et al. 2011, Miranda, Voss et al. 2013).

Current SR genome-wide investigations are eliminating the specific role each receptor plays on the genomic localisation of other TFs. More specifically, the effects of SR crosstalk on genomic mapping, the distribution of SRs, and the ability of SRs to alter chromatin access for another SR are inadequately investigated. Studies in our laboratory and others are beginning to investigate SR crosstalk at a genome-wide level and how dual signalling can alter the genomic distribution of SRs. ChIP coupled with transcriptional studies in ZR-75-1 breast cancer cells, illustrates crosstalk between ER and AR (Need, Selth et al. 2012). Need *et al*. demonstrates that dual treatment of cells with E2 and DHT affected 26% of E2 regulated genes and 15% of DHT regulated genes. Further, this study shows that dual treatment has the ability to either enhance or inhibit ER and AR binding at three specific sites common to both receptors. However, the dual

treatment did not result in a total loss of binding of either receptor. This indicates a possible role for crosstalk between ER and AR at a site-specific level (Need, Selth et al. 2012). Consequently, these studies need to be further investigated genome-wide in order to obtain a complete picture of how ER and AR interact in breast cancer cells.

Recently, GR and ER genome-wide crosstalk studies have demonstrated that SRs can dictate the binding of other nuclear receptors via a DynaLoad mechanism (Figure 4.1). Here, an SR that has access to the chromatin can bind and recruit chromatin-remodelling proteins, resulting in reprogramming of the chromatin structure. This in turn allows access of other SRs to these previously inaccessible sites (Voss, Schiltz et al. 2011, Miranda, Voss et al. 2013). In a mouse mammary cell line, this mechanism was first demonstrated utilising a mutated ER (ER pBox) that binds to a GRE in the MMTV array. These studies show that binding GR to a GRE does not compete with the binding state of ER pBox to the same GRE sites; however, it demonstrates that activation of GR to the GRE in the MMTV array results in an increase in chromatin accessibility. This, in turn, allows for the binding of ER pBox to this exact site. This indicates that although GR and ER pBox recognise the same binding sequence, ER pBox is not capable of binding to these sites within specific chromatin localisation without the activation of GR. This may be due to differences in co-factor recruitment by GR and ER pBox (Voss, Schiltz et al. 2011). This finding was further investigated in a mouse mammary cell line engineered to overexpress GR and ER. It was observed genome-wide that ER and GR can influence each other's binding at specific sites via the proposed DynaLoad mechanism. Upon co-activation of both receptors, the chromatin landscape is remodelled, resulting in a global shift of

their binding patterns. Specifically, activation of GR allows the selective access of ER to a subset of binding sites by facilitating an open chromatin structure at these response elements. The binding of ER to these sites is found to be dependent on AP-1, which suggests that ER is brought to these newly remodelled sites through a tethering mechanism with AP-1. It was also observed that upon ER activation, chromatin structure changed at a subset of GR binding sites allowing access of these sites to GR (Miranda, Voss et al. 2013). This provided further evidence to suggest that DynaLoad can occur between two receptors and is a dynamic exchange; however, this study was performed in an engineered cell system (Miranda, Voss et al. 2013) and doesn't represent a direct model of breast cancer.

In MCF-7 breast cancer cells it has been previously demonstrated that GR can bind to three ER binding sites in the presence of Dex + E2, whereas the single treatment of Dex does not facilitate binding (Karmakar, Jin et al. 2013). This provides more evidence to indicate the DynaLoad mechanism can function between different SRs, with one having the ability to reprogram chromatin, allowing another to bind.

While the notion that dual activation of specific SRs can result in distribution of binding sites has begun to be investigated, the role of DynaLoad in a breast cancer setting is largely still unknown. Although there are specific binding clusters for GR and ER under the single and dual setting in an engineered mouse model system, this phenomenon has not been extended into breast cancer cells. Further, the role of ER and PR dual activation has not been explored despite the fact that ER and PR play a dominant role in breast cancer progression and survival as

previously described. In chapter 3, it has been illustrated that the combinations of P4/E2 and Dex/E2 can have an altered effect on breast cancer cell proliferation. In addition, RNA PolII binding is altered in the dual treatment setting of Dex and E2 compared with the single treatments alone. This confirms previous findings and provides evidence that further studies of SR crosstalk genome-wide in a breast cancer model are warranted. In this chapter, I aim to determine if dual activation of GR and ER results in a subset of unique binding clusters across the genome and establish a role for DynaLoad in MCF-7 breast cancer cells. MCF-7 cells were selected as the model system, due to the large amount of publically available genome-wide data sets. The goal is to overlay the data generated in this chapter with these other data sets in hopes to gain insight into the mechanism behind the crosstalk between SRs. In addition, I aim to identify if the dual activation of PR and ER can alter the genomic response of both receptors resulting in unique subsets of binding modules in the same cell model. This chapter will further develop our current understanding of SR action in breast cancer, resulting in an increased knowledge of SRs crosstalk.

4.2 Methods

4.2.1 Preparation of cells for ChIP-seq.

4.2.1.1 Seeding of cells.

Cells were maintained as described in chapter 2, section 2.3.1.1. When the cells reacted 80% confluence and were ready to be repassaged or seeded, they were harvested and their concentration was calculated utilising a cell haemocytometer. MCF-7 human breast cancer cells were seeded in 150 mm cell culture plates in 30

mL of culture medium at a concentration of 8 x 10^6 cells per mL. The media utilised for the ChIP experiments was phenol red free DMEM containing 4.5g/L D-glucose supplemented with 10% CSS, 1mM sodium pyruvate, 1X non-essential amino acids, 0.2U/mL bovine insulin, and 1% penicillin-streptomycin. Every individual treatment group required the use of three cell culture plates.

4.2.1.2 Hormone treatment of cells.

Cells were plated and left to adhere for 48 h before treatment with hormone. Cells were treated with either 100nM Dex, 100nM E2, 100nM Dex + E2, 100nM P4, 100nM P4 + E2, or untreated for 30 mins. To achieve the desired concentration of 100nM, 30uL of 1mM stock solution of the appropriate hormone was added directly to the 150mm cell culture plate containing the medium.

4.2.2 ChIP-seq.

The ChIP-seq experiments were performed as described in chapter 2, section 2.3.2. More specifically, once the MCF-7 cells had been treated with the hormones for 30 mins, the cells were cross-linked with formaldehyde and removed from the plates via scrapping. The cell suspension was centrifuged at 2,000 rpm and a cell pellet was collected. The cell pellet was resuspended in 600uL of ChIP lysis buffer which contained 1X PI, and sonication was performed in 15mL sonication tubes. The sonication conditions were 15 cycles for 15 sec on, 30 sec off, at 4ºC. After sonication was complete, the DNA was quantified and samples were diluted 5 fold in ChIP dilution buffer and 1X PI to a final concentration of 100ug of chromatin per mL. For samples treated with 100nM Dex, 100nM Dex + E2, and untreated, GR antibody was prepared. Seven ug/uL of GR (E-20X) antibody was linked to 80uL of Dynabeads (M-280) sheep anti-

rabbit IgG. For samples treated with 100nM E2, 100nM Dex + E2, 100nM P4 + E2, and untreated, ER antibody was prepared. 1.4 ug/uL of ERα (HC-20) antibody and 5 ug/uL of ER (Ab-10) antibody was linked to 40uL of Dynabeads (M-280) sheep anti-rabbit IgG and 40uL of Dynabeads (M-280) sheep anti-mouse IgG. For samples treated with 100nM P4, 100nM P4 + E2, and untreated, PR antibody was prepared. Five ug/uL of PR (H-190X) antibody was linked to 80uL of Dynabeads (M-280) sheep anti rabbit IgG. 100uL of each sample was removed and stored at 4ºC overnight and utilised as the no antibody control referred to as input. Each sample was incubated with the appropriate antibody/Dynabead complex overnight. After the overnight incubation, the complex was washed with the appropriate wash buffers. The samples were eluted from the Dynabeads and DNA extraction was performed using phenol-chloroform-isoamyl. Each sample pellet was suspended in 10uL of nuclease free H_2O. Each experiment was repeated four times resulting in four biological replicates. To determine efficient protein binding qPCR analysis was utilised at known sites. For all ER ChIP experiments *MYC* forward and reverse primers were utilised (Miranda, Voss et al. 2013). For all GR and PR ChIP experiment's *PER1* forward and reverse primers were utilised. Two biological replicates were pooled for each sample, resulting in two technical replicates per sample set submitted to the National Cancer Institute Advanced Technology Program Sequencing Facility for sequencing services.

4.2.3 Bioinformatic analysis.

The Illumina HiSeq genome analyzer platform has been used to generate sequence reads (36-mer) and unique tags have been aligned to the human

reference genome (UCSC hg19 assembly). Hotspots, regions of enriched tags, have been called using previously described methods with minor modifications (Baek, Sung et al. 2012). The values for the tag densities have been normalized to 10 million reads to adjust for differences in the depth of sequencing between samples. The data sets have been adjusted by subtracting tags found in the input. Hotspots have been called using a 0% FDR. A tag density threshold of 30 has been applied to all sample sets except PR ChIP-seq. Due to the overall lower tag density values, the tag threshold for PR samples has been set at 7, which represents the mode for this sample set. Replicate concordants have been calculated between replicates. For comparison of GR, ER, and PR data sets, regions are considered to overlap if they shared at least 1 bp. Peaks unique to the hormone treatments are then identified. Using these peaks, a list of unique chromosomal positions has been created by removing overlapping peaks from the samples being compared (GR-ChIP +Dex, GR-ChIP +Dex + E2, ER-ChIP +E2, ER-ChIP +Dex + E2; PR-ChIP +P4, PR-ChIP +P4 + E2, ER-ChIP +E2, ER-ChIP +P4 + E2; ER-ChIP +untreated, ER-ChIP +E2). This has provided a list of 13,211 unique peaks for the ER and GR comparisons, 6817 unique peaks for the ER untreated and ER +E2 comparison, and 856 for the PR and ER comparisions. Supervised clustering of the peaks has been conducted tagging each unique peak for presence or absence of binding in the experiments and ordering them according to these tags across the samples. Using Homer, the total number of sequence reads under the peaks for each ChIP-seq sample has been extracted and corrected for the total number of reads in the sample (reads under peak/ 10M total reads) so that a heat map can be generated utilising MeV software. For box plots, Homer has been used to retrieve the total number of sequence reads for The

Encyclopedia of DNA Elements (ENCODE) data under the peaks for each module analysed. Plots have been graphed using the statistical program R. De novo motif analysis has been conducted using Homer (Heinz, Benner et al. 2010).

<div style="border:1px solid black; text-align:center;">

4.3   Results

</div>

4.3.1 <u>Validation of PR and ER binding in MCF-7 human breast cancer cells.</u>

To assess the cellular binding patterns of PR genome-wide in MCF-7 cells, ChIP-seq experiments are performed after activation of the receptors under differing hormone treatments. Cells are treated with either 100nM of P2, E2, P4 + E2, or untreated for 30 min and PR and ER ChIP-seq is performed. To determine if optimal protein binding to the DNA has been achieved in all four biological replicates, qPCR analysis is utilised at known GR, ER, and PR binding sites (Miranda, Voss et al. 2013).

In MCF-7 cells treated with E2, P4 + E2, and untreated, ER binding is increased at the *MYC* site in the E2 and P4 + E2 treatment groups (Figure 4.2A). Primers at a *PER1* site, which has previously been shown to be hypersensitive and contain a GRE and PRE motif, has been designed to assess PR binding. PR binding is increased at the *PER1* site when cells are treated with P4 and P4 + E2 (Figure 4.2B). This qPCR analysis confirms that efficient protein binding to DNA is achieved via ChIP experiments, and the samples are suitable for sequencing.

4.3.2 <u>Co-treatment of MCF-7 human breast cancer cells with Dex and E2 induces changes in the GR and ER binding landscapes genome-wide.</u>

To investigate the GR and ER binding landscape under dual activation, GR and ER binding under the stimulation of either Dex, E2, or the combination of both treatments has been assessed (chapter 3). Analysis of GR ChIP-seq data reveals 5151 binding sites in total, of which 831 are found to be in common with either Dex alone or the combination of Dex + E2. Interestingly, there is a unique subset of GR binding sites (121) that are gained in the combination treatment and are therefore not present when ER is not activated. Further, there is a very large subset of 4199 sites that are observed in the single treatment of cells with Dex. Binding of GR at these sites is inhibited upon introducing E2 to the cells (Figure 4.3A). Identical analysis of ER binding sites in cells treated with E2 compared with the dual treatment of Dex + E2 revealed very similar findings to GR binding patterns demonstrating there is a global re-distribution of ER binding under differing hormone conditions. Analysis of ER ChIP-seq mapped a total of 7083 ER binding sites, of which 6650 are found to be active in either the single or dual treatment. There is a unique set of ER binding sites (374) that are gained with the dual treatment and 59 sites that are unique to the single treatment of E2. Binding of ER at these sites are inhibited if Dex is present (Figure 4.3B). Together this suggests that GR and ER have the ability to alter the genomic response of one another at a DNA binding level. The effects observed by mapping GR and ER with the single and dual treatments demonstrated at specific genomic regions utilising UCSC browser shots (Kent, Sugnet et al. 2002) (Figure 4.4A-D). These results confirm that the previously described crosstalk model also occurs in a breast cancer cell line and may therefore be important for breast cancer development.

Supervised clustering analysis has been performed to determine overall binding patterns for GR under untreated, Dex, and Dex + E2 stimulation, and ER under untreated, E2, and Dex + E2. Analysis demonstrates that there are 11 unique binding clusters for GR and ER in MCF-7 cells (Figure 4.5). Cluster 1 contains binding sites that are found to be in common with GR and ER in both the single and dual treatments (344 peaks). Cluster 7 (4847 peaks) and 8 (439 peaks) represent the ER and GR classical binding sites. The term classical demonstrates binding of the receptor with both the single and dual treatments. In the ER classical cluster binding occurred only in the E2 and Dex + E2 treatment groups; however, in the GR classical cluster, ER also binds at these sites in the untreated, E2 and Dex + E2 groups. The clusters that are of specific interest represent the DynaLoad mechanism at clusters 2, 5, and 6. Cluster 2 (48 peaks) demonstrates binding sites where ER recruitment is dependent in GR activation. This mechanism is termed ER DynaLoad. Cluster 5 (84 peaks) and cluster 6 (36 peaks) both represent GR binding elements where GR binding is contingent on ER stimulation by E2. This phenomenon is referred to as GR DynaLoad and has been separated into two unique clusters. Cluster 5 demonstrates GR binding in the dual treatment group of Dex + E2, including ER binding in the E2 and Dex + E2 treatments. However, Cluster 6 is a unique cluster representing GR DynaLoad where, in addition to the binding patterns observed in cluster 5, ER binding also occurs in the untreated group as seen in the GR classical cluster. This suggests there are some low basal active levels of ER at some of the GR binding clusters. However, it is noteworthy to mention that although ER can bind to these sites in the absence of hormone, GR can only bind once ER is activated. This suggests that ER is not fully functional at these sites until the cells undergo treatment with

E2. Lastly, cluster 3 (134 peaks) represents ER gained sites only observed in the Dex + E2 group and not overlapping with GR binding, and cluster 4 (192 peaks) contains GR binding sites that occur in the Dex only group and doesn't overlap with any ER binding sites. It is possible that long-range interactions play a role at these sites.

Most surprisingly, is the massive inhibition of GR binding across the genome upon the addition of E2. Cluster 9 (1368) and 10 (2859) represent sites where GR binding is inhibited upon dual treatment. In cluster 9 ER binding overlaps at these sites in the E2 and Dex + E2 groups, and at cluster 10 ER binding in the untreated, Dex, and Dex + E2 group. Cluster 11 describes ER lost sites where ER binding is inhibited upon dual treatment. These sites do not overlap with GR binding, suggesting the ER and GR are not directly competing for binding at these sites and other mechanisms may be involved such as squelching.

Genomic localisation analysis of all binding patterns revealed that the majority of all binding sites (40-70%) in each cluster fall within intron and intergenic regions. Cluster 6, which represents GR DynaLoad with ER in the untreated group has approximately 10% of sites in the promoter regions which is the highest number of sites found in this region compared with any of the other cluster groups (Figure 4.6).

4.3.3 Motif analysis of GR and ER binding modules.

To determine if specific motifs were overrepresented within each cluster, *de novo* motif analysis was performed utilising Homer (Figure 4.7A). Cluster 2, representing ER DynaLoad, has a high prevalence for a GRE and AP-1 binding motif. Despite ER binding at these sites, an ERE binding motif was not

identified. This finding supports a previous study, which showed that activation of GR in a mouse mammary cell line allows for the selective access of ER to a subset of binding sites. ER binding to these sites was found to be dependent on AP-1 via a tethering mechanism (Miranda, Voss et al. 2013). Similarly, clusters 5 and 6 representing GR DynaLoad, contain an ERE as the top motif. The GRE motif is not present in these clusters, suggesting that GR may not be recruited to these sites through direct binding with the DNA. Cluster 9 and 10, representing lost GR binding sites, contain a FoxA1 binding motif as the highest identified sequence. This suggests that loss of GR may be through a FoxA1 mediated mechanism at these sites, upon ER activation. Since both ER and GR have been shown to interact with FoxA1, it is possible that the inhibition of GR at these sites is due to the squelching of FoxA1 by ER. *De novo* motif analysis was performed on all other GR and ER cluster and presented in appendix 1A.

To further investigate the presence of the GRE and AP-1 binding motif identified at ER DynaLoad (cluster 2) binding sites, finding individual motif occurrences (FIMO) analysis has been utilised (Grant, Bailey et al. 2011), to investigate the distribution of sequences within binding clusters. Comparison of cluster 2, ER DynaLoad sites, with cluster 7, ER classical sites, reveal that there is a higher occurrence of GRE and AP-1 motifs in cluster 2, with a higher prevalence of ERE motifs in cluster 7 (Figure 4.6B). This further supports the model that ER DynaLoad may occur via a GR and AP-1 mechanism as previously described.

4.3.4 <u>Changes in DHS upon E2 treatment correlates with GR DynaLoad (ENCODE data).</u>

Genome-wide DHS-seq analysis allows us to determine the accessibility of chromatin thereby to DNase I. This can be used to measure how accessible a binding sites is to a TF. ENCODE project has mapped regions of transcription, TF association, chromatin structure, and histone modifications in the human genome (Consortium, Bernstein et al. 2012). Included in the analysis is DHS-seq in MCF-7 breast cancer cells, treated with 100nM E2 or left untreated for 60 mins (Thurman, Rynes et al. 2012). Utilising this data, the changes in DHS upon E2 treatment have been analysed. Further, a cross analysis with the 11 GR and ER cluster binding patterns have been performed. This analysis identified that there is an increase in DHS upon stimulation of cells with E2 at GR DynaLoad binding sites (Figure 4.8). This also suggests that at these GR DynaLoad sites, ER recruits chromatin modifiers upon activation. This leads to an increase in the accessibility of these sites, thereby allowing for the binding of GR. No significant changes were observed in the other binding modules where ER activation effects GR binding upon E2 stimulation. This indicates that changes in GR binding at these sites is through other mechanisms. DHS-seq data for MCF-7 cells treated with Dex is currently not available. Therefore, changes in chromatin structure at ER DynaLoad sites could not be assessed. However, Miranda *et al.* observed that ER DynaLoad by GR was accompanied by changes of accessibility at these sites upon treatment of the artificial cell line with Dex (Miranda, Voss et al. 2013).

4.3.5 Comparison of GR and ER clusters with ENCODE histone modification data.

As described in section 4.3.3, ENCODE has performed a variety of genome-wide sequencing analysis, that includes ChIP-seq of histone modifications in

unstimulated MCF-7 breast cancer cells (Consortium, Bernstein et al. 2012). All 11 GR and ER binding clusters has been compared with the genomic profiles for H3K4me3, H3K36me3, and H3K27ac, histone marks associated with active chromatin, p300, a histone acetyltransferase, H3K9me3, and H3K27me3 marks associated with repressed chromatin. This has been performed to determine if there were any histone marks associated with specific binding clusters (Figure 4.9A). We determined that there is a high level of the H3K4me3, H3K36me3, and H3K27ac histone marks at all ER binding clusters and low levels of the H3K9me3 and H3K27me3 histone marks. The p300 protein is highly present at all ER binding modules except cluster 10 where GR binding is inhibited by the dual hormone treatment and ER remains bound to these sites. Further analysis of this data utilising ER binding intensities in each cluster demonstrates a unique trend where histone marks associated with active chromatin mimic the binding intensity of ER at each specific cluster in the E2 alone and Dex + E2 treatment groups (Figure 4.9B). An identical analysis for GR binding intensities showed no specific correlation (Figure 4.9C). This suggests that while there may not be one specific histone modification associated with a specific cluster, active histone marks may be correlated to ER binding intensities in a cell setting. In addition ENCODE has assessed multiple TF binding patterns in unstimulated MCF-7 cells; however, no correlation was observed between GR/ER binding clusters and TF binding patterns (data not shown).

4.3.6 Association of ER genome-wide in untreated versus E2 samples.

It has previously been shown that ER has the ability to function in an unligand state (Takai, Matsumura et al. 2014). In addition, the genome-wide binding

patterns have very recently been mapped in MCF-7 cells and it was shown that unligand ER contributed to the transcriptional response of genes that are functionally related to cellular proliferation and development (Caizzi, Ferrero et al. 2014). It has been identified in section 4.3.2, that there is a subset of clusters (6, 8, 10) where ER is also bound in the untreated samples. This finding was not observed in previous studies by Miranda *et al.* (Miranda, Voss et al. 2013). To begin to investigate the rationale behind the presence of ER in the untreated samples, supervised clustering analysis has been performed on all the ER binding sites identified in the untreated and E2 samples. Two clusters were identified, cluster 1, containing 5416 binding sites unique to E2 alone, and cluster 2, containing 1398 binding sites common to untreated and E2. A third cluster containing ER sites in the untreated alone was not identified. Interestingly, the binding intensity of ER was stronger in the E2 and untreated overlap samples compared to the sites present only upon E2 stimulation (Figure 4.10A). FIMO analysis has been utilised to investigate the distribution of sequences between the two clusters (Figure 4.10B). It has been revealed that there is a 20% higher prevalence for a FoxA1 motif in cluster 2 compared with cluster 1 indicating FoxA1 may be more involved in the ER recruitment at sites active in untreated and E2 samples compared with E2 alone.

DHS-seq ENCODE data (Thurman, Rynes et al. 2012), utilised in section 4.3.4, has been overlapped with the two ER binding clusters to assess any possible changes in DHS between the two ER binding groups. There appears to be more DHS accessibility in sites where ER is found in the untreated samples when compared with ER E2 only sites (Figure 4.11A). However, there is no observed change in DHS upon stimulation of cells with E2 at either cluster (Figure 4.11B).

This suggests that the increase in accessibility at cluster 2 sites may allow for ER binding in the absence of hormone. Lastly, the ENCODE histone modification data (Consortium, Bernstein et al. 2012) utilised in section 4.3.5 for the three histone modifications associated with active chromatin and p300 has been crossed with the two individual ER binding clusters. There appears to be no differences in the levels of H3K4me3, H3K36me3, H3K27ac, and p300 at these clusters, suggesting that they are not responsible for the differences in ER binding between the 2 clusters (Figure 4.12).

4.3.7 Co-treatment of MCF-7 breast cancer cells with P4 and E2 induces an altered ER and PR binding landscape genome-wide.

To further investigate the proposed model of SR crosstalk in MCF-7 cells, I aim to determine if re-distribution of receptor binding observed with the co-activation of GR and ER also occurs when both PR and ER are stimulated. To assess this, PR and ER ChIP-seq genome-wide has been performed in cells treated with P4 or E2 respectively, or the dual treatment of P4 + E2. Analysis of the PR ChIP-seq data set has resulted in a lower number of PR (856) peaks mapped compared to the ER peaks (4489). This may be due to the low levels of PR expression in MCF-7 cells, due to the experimental conditions. It is known that PR is regulated by E2 and that treatment of MCF-7 cells with E2 increase PR gene expression (Nardulli, Greene et al. 1988, Read, Snider et al. 1988, Wei, Krett et al. 1988). Of the mappable PR peaks, there are 676 peaks common to either the single or dual treatment and 170 sites are unique to the single treatment of P4 alone. These sites are lost when E2 is added to the cells in combination with P4. There are only 10 PR binding sites that are gained upon the dual treatment of cells. While this

number is low there is still a possibility that ER, at very select sites, is playing a role in the addition of new PR binding sites (Figure 4.13A).

Analysis of ER ChIP-seq in cells stimulated with E2 or P4 + E2 has shown that 3613 ER binding sites are common with either treatment condition, with 102 sites unique to the E2 alone. These sites are lost when P4 is added in combination with E2. There are 774 sites that are indeed gained upon the dual treatment of cells (Figure 4.13B). This suggests that PR could be playing a role in ER re-distribution of binding at specific sites as has previously been described for GR. Representative examples of lost and gained PR and ER binding sites at genomic regions is presented utilising UCSC browser shots (Kent, Sugnet et al. 2002) (Figure 4.14A-D). To further determine if there is any specific crosstalk between PR and ER, supervised clustering analysis has been performed, to look at specific overlap of each receptor under the differing hormone conditions (Figure 4.15). Six different binding modules have been identified. Cluster 1 (67 peaks) represents PR and ER sites that are common to both treatment combinations; however, neither receptor binds in the untreated group. In cluster 2 (750 peaks), ER binding sites are gained upon the dual treatment; however, there appears to be a small level of ER binding only in the E2 samples. There is no PR binding detected at these sites. This suggests that while the addition of P4 enhances binding at these sites, PR may not be playing a direct role and long range interactions may be involved. Clusters 3 and 4 represent PR and ER classical binding sites respectively. While cluster 3 demonstrates classical PR binding with the single and dual treatments at 483 peaks, ER also binds at these sites in the untreated, E2, and P4 + E2 samples. These findings are similar to what was observed in section 4.3.2 with GR binding in MCF-7 cells in the classical cluster

8. Cluster 4 (3536 peaks) demonstrates the standard pattern of classical ER binding where ER is mapped in the E2 and P4 + E2 treatment groups, whereas cluster 5 demonstrates ER lost sites (102 peaks). These sites are similar to cluster 2 since there is only a decrease in binding from the E2 compared with the P4 + E2 treatments. While P4 appears to play a role in altering the binding pattern of ER at these binding elements, these sites do not appear to overlap with PR binding. Cluster 6 (161 peaks) demonstrates PR lost sites upon the dual hormone treatment. PR binds only with P4 treatment and these sites are lost with the addition of E2. ER binding overlaps at these sites in the E2 and P4 + E2 groups, suggesting that ER activation plays a direct role in dictating PR binding at these sites.

As mentioned earlier, in the PR classical cluster 3, ER binding is also present in the untreated, E2, and P4 + E2 treatment. This finding is also observed in the GR classical cluster 8 in section 4.3.2. It is known that PR can respond to corticoid steroids and bind to GREs, which does make investigating SR crosstalk difficult in cells where both receptors are expressed (Ham, Thomson et al. 1988, Issar, Sahasranaman et al. 2006). Further, it is interesting that ER binding is observed in both of these clusters in all treatment groups including the untreated cells. To elucidate the possibility that the sites identified in the GR and PR classical clusters are not in fact the same receptor, a cross analysis of sites identified in the GR and ER cluster 8 with the sites from the PR and ER cluster 3 has been performed (Figure 4.16). The analysis demonstrates that while there are 121 sites in common between both receptors, there are also sites unique to PR and GR. This suggests that these sites are different, and are not PR being activated by Dex,

and GR is not being activated by P4. It also confirms that the antibodies used for the ChIP assays do not cross react.

While a shift in PR and ER binding patterns under dual activation, the total number of sites mapped was low with particular respect to PR. While previous studies have mapped PR binding genome-wide, it has been performed in a breast cancer cell line model that expressed high PR levels, T-47D breast cancer cells (Clarke and Graham 2012, Ballare, Castellano et al. 2013). In addition, PR is an E2 stimulated gene (Nardulli, Greene et al. 1988, Read, Snider et al. 1988, Wei, Krett et al. 1988). The low levels of PR mapped in MCF-7 cells is most likely due to experimental conditions and either needs to be investigated in another cell line model, or the cells need to be primed with a long term E2 treatment to upregulated PR levels.

4.3.8 Motif analysis of PR and ER binding modules.

To determine if there are any specific binding sequences at the individual ER/PR binding clusters, *de novo* motif analysis was performed utilising the Homer software (Figure 4.17). Surprisingly, cluster 2, which represents ER gained sites by the addition of P4, does not contain an ERE or PRE motif. However, an AP1 and a FoxA1 binding motif are the most prevalent sequences within this cluster. This suggests that both FoxA1 and AP-1 may play a potential role in ER recruitment at these sites. Clusters 3 and 4 represent classical PR and ER binding sites respectively and both contain their conical binding motif, as well as a FoxA1 binding motif. *De novo* motif analysis was performed on all clusters and is presented in appendix 1B.

Investigations into GR and ER crosstalk by genome-wide ChIP-Seq under stimulation of single and dual treatments have previously been performed in a mouse mammary cell line engineered to overexpress GR and ER. Miranda *et al*. revealed that there is a global redistribution of GR and ER binding sites, which demonstrates a gain or loss of receptor binding in the genome upon the activation of both receptors (Miranda, Voss et al. 2013). The authors have proposed a DynaLoad model showing that co-activation of both receptors results in the remodelling of the chromatin landscape and a shift in GR and ER binding across the genome. In this model, the activation of GR allows ER to access a subset of binding sites by facilitating the opening of chromatin structure at these specific ER binding sites. The recruitment of ER to these sites has also been shown to be dependent on AP-1, suggesting that ER is brought to these sites through a tethering mechanism with AP-1. The data presented in this chapter extends on previous studies and provides further insight into the molecular crosstalk between GR and ER in cancer cells. Using a highly estrogenic cell line (Lacroix and Leclercq 2004), which provides a model that is more representative of breast cancer, and making use of the publically available data (ENCODE) (Consortium, Bernstein et al. 2012), has allowed further investigation into the mechanisms driving GR and ER crosstalk in breast cancer cells.

Genome-wide analysis of ER and GR binding in the MCF-7 breast cancer cell line shows that a GR and ER Dynaload mechanism also exists in these cells. Similarly to previous studies, ER Dynaload sites were found to contain an AP-1 motif (Miranda, Voss et al. 2013). This indicates that ER may be recruited to

these sites through interactions with AP-1, confirming the proposed model. Most surprisingly, is the discovery of a very high number of GR sites that are lost upon activation of ER and is in contrast to the findings of Miranda *et al*., where only a very small subset of GR binding sites are lost upon stimulation of cells with E2 (Miranda, Voss et al. 2013). In addition, the GR binding sites that are lost in the MCF-7 cells overlap with ER binding sites. Conversely, Miranda *et al*. show no overlap between the lost GR sites and ER binding (Miranda, Voss et al. 2013). The differences observed are perhaps due to the previous studies being conducted in an engineered cell line, which is not as estrogen centric at the MCF-7 cells.

Recently, a study has demonstrated that GR and ER pBox (a mutant ER protein that recognises GREs instead of EREs) do not compete for binding at binding elements across the genome, due to the rapid on and off rates of the receptors at these sites (Voss, Schiltz et al. 2011). This suggests that the loss of GR binding observed upon E2 treatment in MCF-7 cells is not due to competitive binding, although ER and GR are binding at the same sites. In addition, it has been shown in this chapter that there are no changes in DHS at these sites upon activation of ER and that these sites are not pre-marked by specific histone modifications. This suggests that other mechanisms must be involved in regulating the response of GR at these sites upon stimulation of cells with E2. It has recently been shown that peptidylarginine deiminase (PAD), an enzyme that converts arginine and methylarginine residues to citrulline, is recruited to ER binding sites in MCF-7 cells upon stimulation, resulting in the citullination of H3R26 at these binding elements. This results in chromatin decondensation associated with gene transcription (Zhang, Bolt et al. 2012). It would be of particular interest to further investigate if the ER association with citrullination of H3R26 is involved in

inhibiting GR at these sites as a potential mechanism for the loss of GR binding upon activation of ER.

It is also possible that upon activation, ER is involved in squelching factors from GR that are needed for the recruitment of GR to these sites. Previous studies have shown that co-activation of ER and PR inhibits the transcription of a PR activated reporter gene. However, no evidence was found to indicate that ER interacted with PR or the reporter construct (Meyer, Gronemeyer et al. 1989). Voss *et al.* also demonstrated that co-activation of ER and GR resulted in a decrease in GR binding within a MMTV reporter construct, even though ER does not bind to this construct (Voss, Schiltz et al. 2011). This provides further evidence to suggest that squelching is a probable mechanism. Chapter 3 shows that the levels of ER in MCF-7 cells are high compared to GR levels, making it possible that activation of ER can deplete a pool of important factors needed by GR. In addition, it has been illustrated that the lost GR binding sites contain a FoxA1 motif. FoxA1 has been shown to be an important factor that facilitates the binding of SRs to DNA (Bernardo and Keri 2012). Therefore, it is possible that the loss of GR binding at these sites is due to ER and GR competing for access to FoxA1.

The massive reduction of GR binding upon ER activation can result in drastic consequences in breast cancer progression. It has recently been shown that high levels of GR are associated with a significantly better prognosis in ER positive breast cancer compared with ER negative cancers (Pan, Kocherginsky et al. 2011). Patients expressing high levels of GR are associated with a significantly better prognosis in ER positive breast cancers compared with ER negative cancers (Pan, Kocherginsky et al. 2011). ER negative cancer patients with high levels of

GR are also correlated with a shorter relapse-free period (Pan, Kocherginsky et al. 2011). Furthermore, in patients with ER negative breast cancer and high levels of GR, an increase in EMT activation, cell adhesion, and cell survival is observed (Pan, Kocherginsky et al. 2011). This suggests that ER has the ability to inhibit the potential negative transcription effects of GR by inhibiting GR binding. Currently, ER positive cancers are generally treated with endocrine therapies, including the antiestrogen tamoxifen (Ali and Coombes 2002). My current data suggests that inhibition of ER can allow GR to bind to sites normally not accessible to GR in an ER positive environment. Therefore, clinicians should consider determining the GR expression in patients in order to assess whether ablating ER function could have a negative effect through GR activities. Glucocorticoids have also been used in clinical oncology and are sometimes used as part of the endocrine therapy regimen for treatment of breast cancer (Rubens, Tinson et al. 1988, Walsh and Avashia 1992). This could also potentially have detrimental effects on breast cancer progression especially in the presence of a nonfunctional ER or ER negative breast cancer.

In conclusion, this chapter has provided valuable insight into the role of GR and ER in a breast cancer cell model. Previous findings have been validated, providing stronger evidence that GR and ER can dictate one another's binding patterns. Further, it has been shown that ER has the potential to influence GR's cellular activity by inhibiting it's binding to numerous sites within the genome. This new finding suggests that in an estrogenic cell line, ER plays a strong role in modulating GR's function, which can have consequences for disease outcome and relapse-free survival rates. In addition, it provides further evidence that GR plays

a functional role in breast cancer and that in the absence of ER signalling, it may have negative effects on breast cancer outcomes.
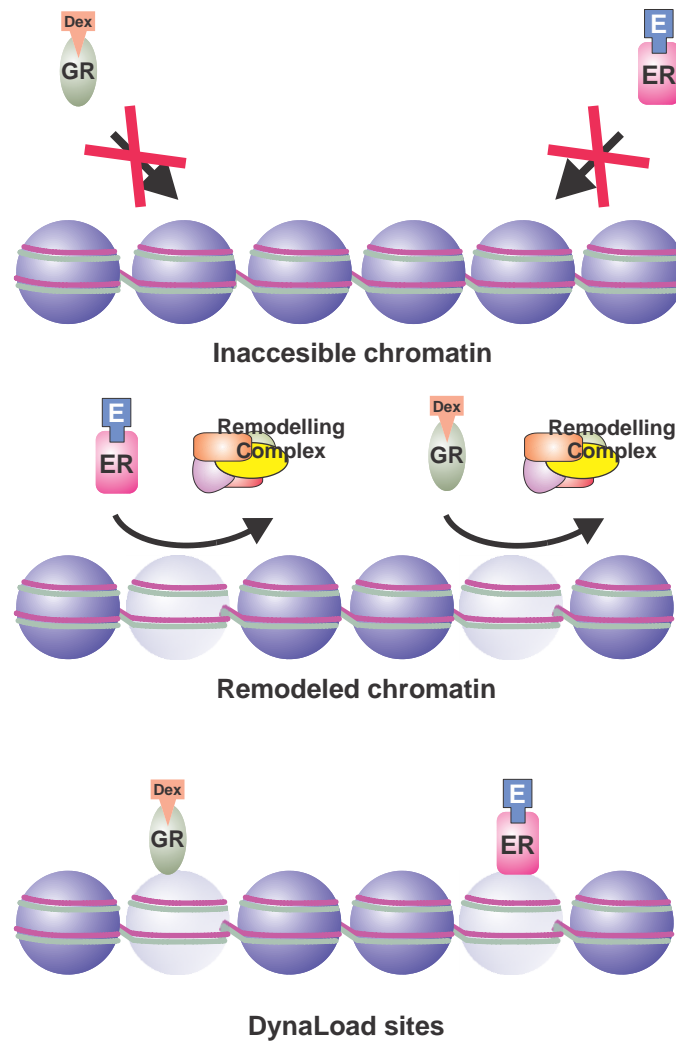
Figure 4.1: Diagram of GR and ER DynaLoad. GR and ER can dictate the binding of each other at specific sites in the genome. One receptor with access to the chromatin can bind and recruit chromatin-remodelling proteins. This induces reprogramming of the chromatin structure allowing the other receptor to bind to the previously inaccessible site.

A

ER ChIP

B
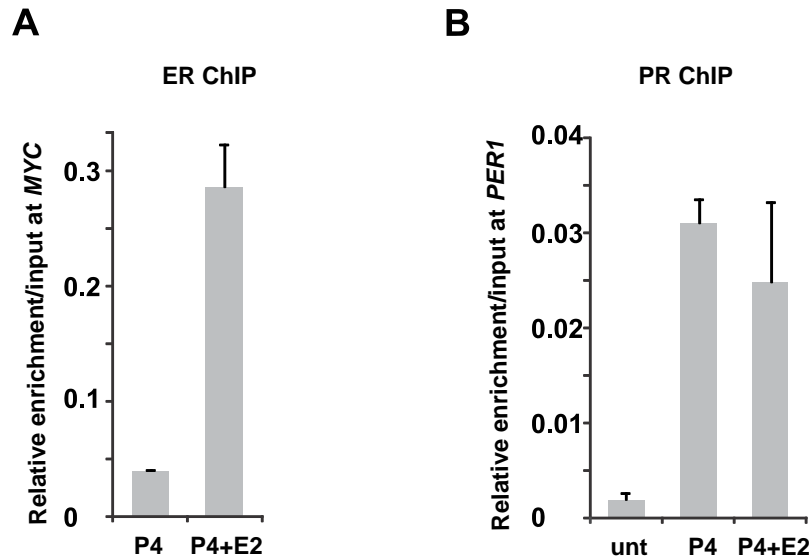
PR ChIP

Figure 4.2: Analysis of ER and PR binding confirms sufficient enrichment for ChIP-seq. A. Quantitative-PCR shows that ER binding is increased at a *MYC* site in MCF-7 breast cancer cells treated with 100nM of P4 and E2 compared with 100nM of P4 alone. Data presented as relative enrichment over input. Results demonstrate that ER ChIP samples are suitable for sequencing. Figure is a representative example of one biological replicate. Error bars represent technical replicates. **B.** Quantitative-PCR shows that PR binding is increased at a *PER1* site in MCF-7 breast cancer cells treated with either 100nM of P4 or 100nM of P4 and E2 compared to untreated cells. Data presented as relative enrichment over input. Results demonstrate that PR ChIP samples are suitable for sequencing. Figure is a representative example of one biological replicate. Error bars represent technical replicates.
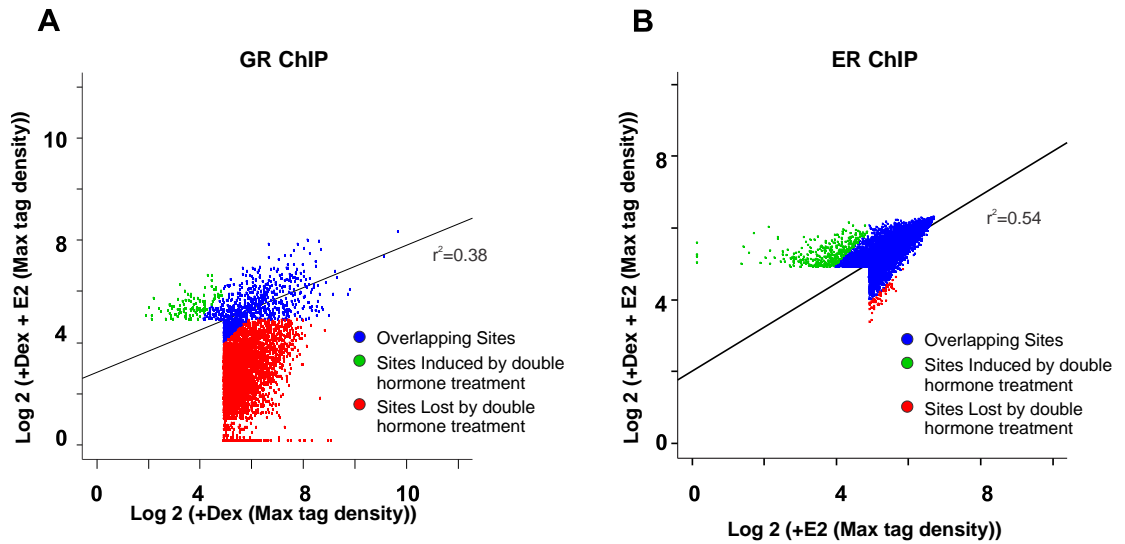
Figure 4.3: Changes in the GR and ER binding landscape upon Dex and E2 dual hormone treatment in MCF-7 human breast cancer cells. **A**. Global changes in GR binding patterns upon dual treatment of cells. Binding patterns of GR have been determined by ChIP-seq after treatment with either Dex or Dex + E2. Scatterplot represents the global changes in GR binding between Dex and Dex + E2. The sites shown to be either gained or lost by the dual hormone treatment have at least a 2-fold change in tag density. **B**. Global changes in ER binding patterns upon dual treatment of cells. Binding patterns of ER have been determined by ChIP-seq after treatment with either E2 or Dex + E2. Scatterplot represents the global changes in ER binding between E2 and Dex + E2. The sites shown to be either gained or lost by the dual hormone treatment have at least a 2-fold change in tag density.

Figure 4.4: Examples of the effects of dual treatment on ER and GR binding.
Examples of GR binding in MCF-7 breast cancer cells treated with either 100nM of Dex, E2, Dex + E2 or left untreated. GR ChIP-seq has been performed after 30 min of hormone treatment. **A.** A genomic region demonstrating gained GR binding upon dual activation of GR and ER (UCSC browser shot). The black arrow illustrates a GR gained site. **B.** A genomic region demonstrating lost GR binding upon dual activation of GR and ER (UCSC browser shot). The black arrow illustrates a GR lost site.

Figure 4.4: Examples of the effects of dual treatment on ER and GR binding. Examples of ER binding in MCF-7 breast cancer cells treated with either 100nM of Dex, E2, Dex + E2 or left untreated. ER ChIP-seq has been performed after 30 min of hormone treatment. **C.** A genomic region demonstrating gained ER binding upon dual activation of GR and ER (UCSC browser shot). The black arrow illustrates a ER gained site. **D.** A genomic region demonstrating lost ER binding upon dual activation of GR and ER (UCSC browser shot). The black arrow illustrates a ER lost site.
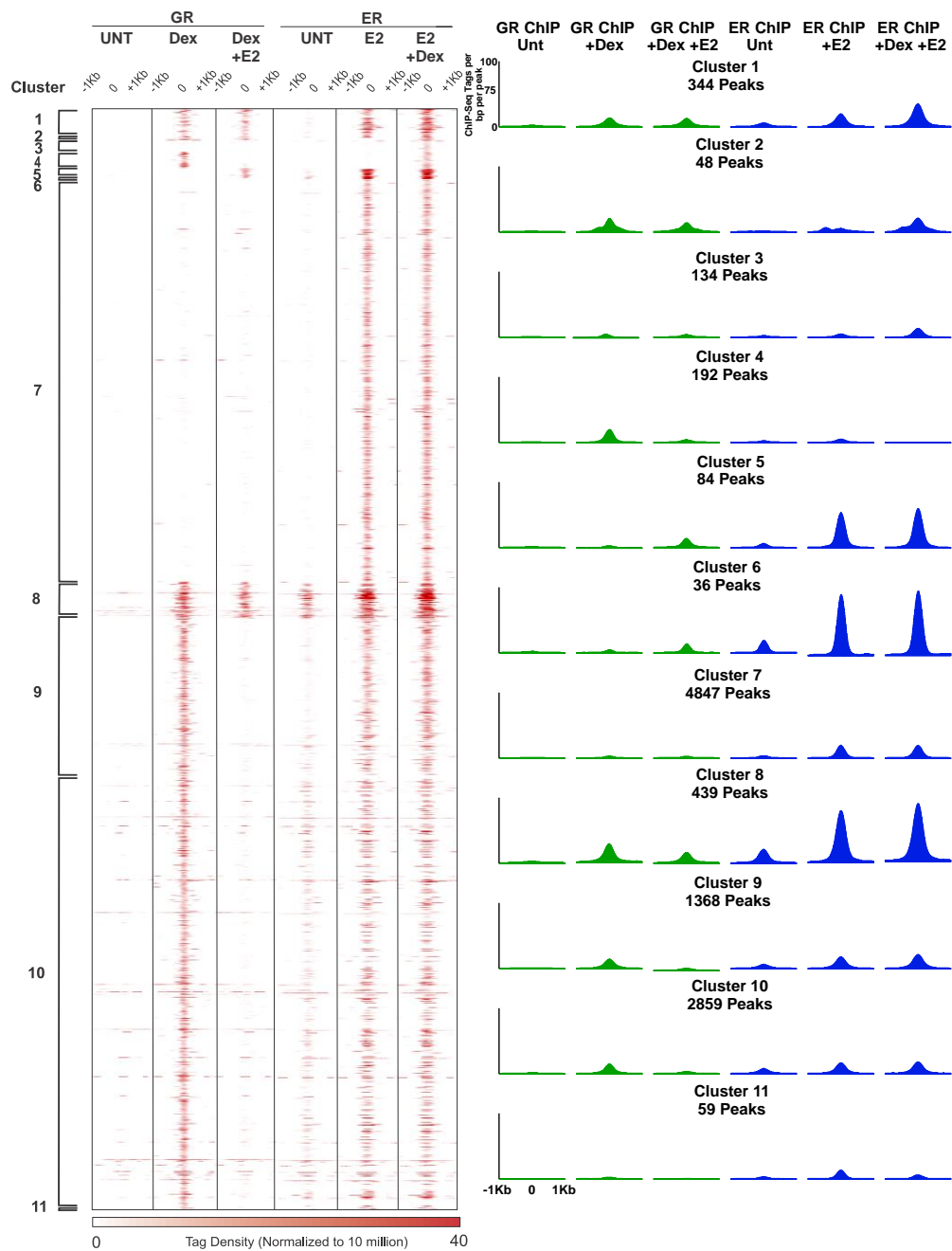
Figure 4.5: Specific GR and ER binding modules. Supervised clustering analysis of 6817 peaks identified by GR and ER ChIP-seq in MCF-7 breast cancer cells treated with either 100nM of Dex, E2, or Dex and E2. Heatmap analysis portrays the number of reads per 10^6 sequences as well as the position of the reads within 2 kb of ChIP-seq peak. Untreated samples are included in the analysis. Eleven different binding clusters have been identified which are notated by the brackets. Histograms represent the overall GR and ER binding intensities in each cluster for the various treatments within a 2 kb interval of the ChIP-seq peaks.
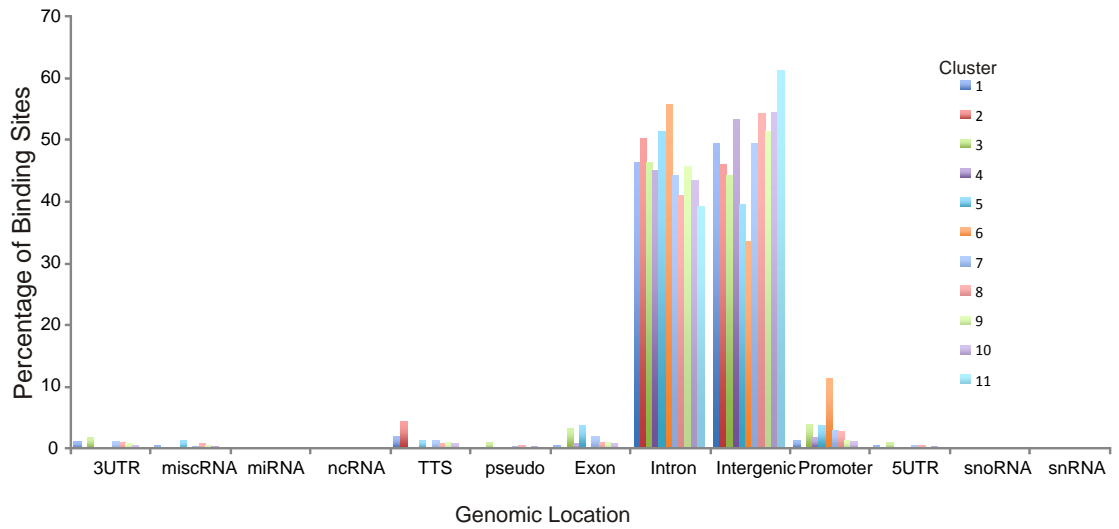
Figure 4.6: Genomic location of GR and ER binding clusters in MCF-7 breast cancer cells. Comparison of the genome-wide distribution of GR and ER binding patterns among the 11 identified clusters. Data presented as a percentage of binding sites from each cluster located in the individual genomic locations.

A

B
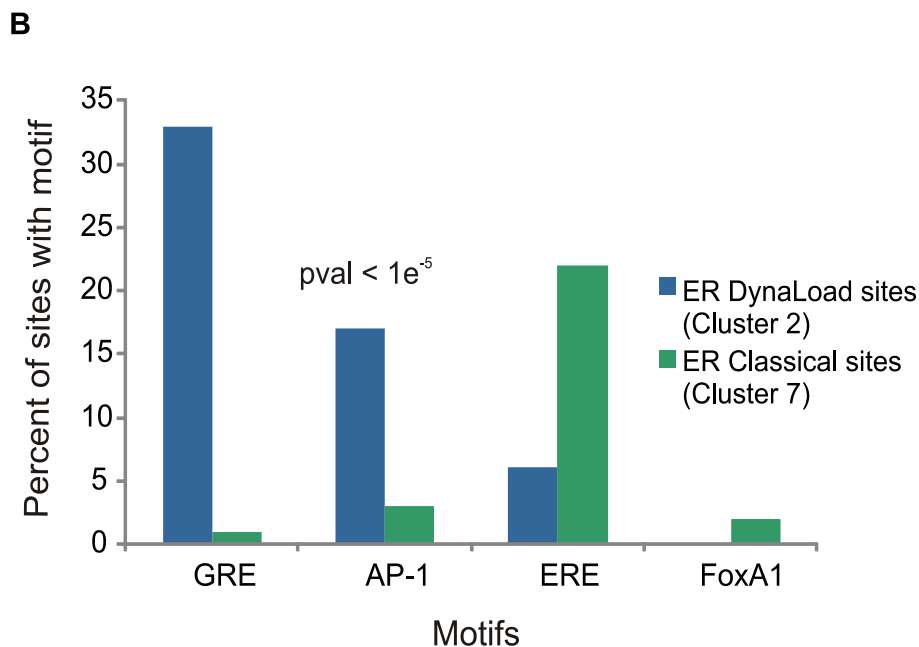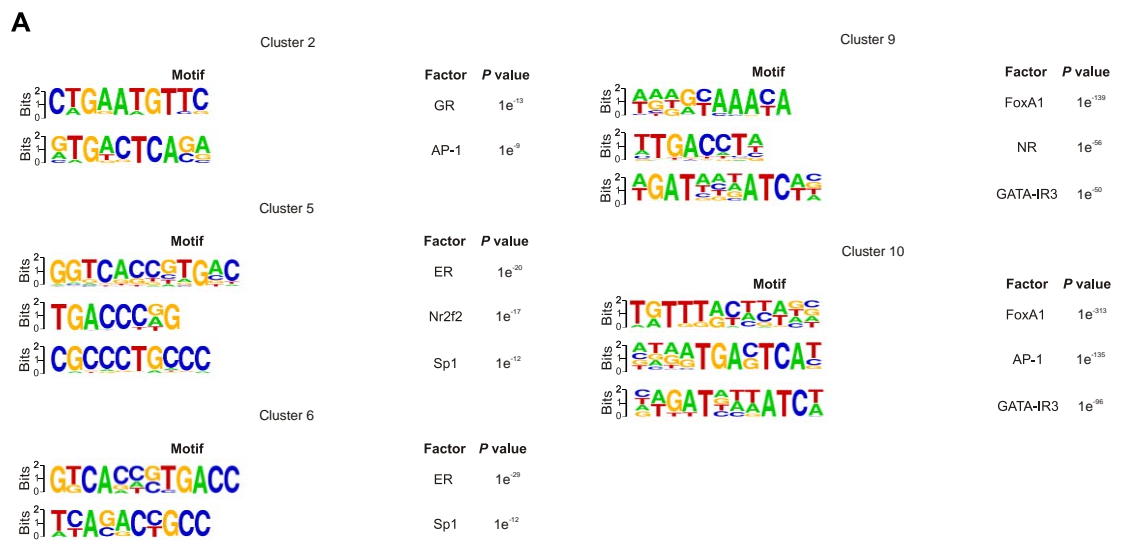
Figure 4.7: Motif analysis of GR and ER binding clusters. **A.** *De novo* motif analysis has been conducted on ER/GR DynaLoad sites and GR lost sites. The data represents the top three most highly enriched motifs determined by Homer. **B.** The distribution of GRE, AP-1, ERE, and FoxA1 motifs within the ER DynaLoad and the ER classical clusters has been determined using FIMO analysis. The results are reported as the percentage of sites containing the motif with pval $< 1e^{-5}$.

DHS (unt vs E2)

		1	2	3	4	5	6	7	8	9	10	11
	Unt	-	-	-	-	-	+	-	+	-	+	-
ER	E2	+	-	-	-	+	+	+	+	+	+	+
	Dex + E2	+	+	+	-	+	+	+	+	+	+	-
	Unt	-	-	-	-	-	-	-	-	-	-	-
GR	Dex	+	+	-	+	-	-	-	+	+	+	-
	Dex + E2	+	+	-	-	+	+	-	+	-	-	-
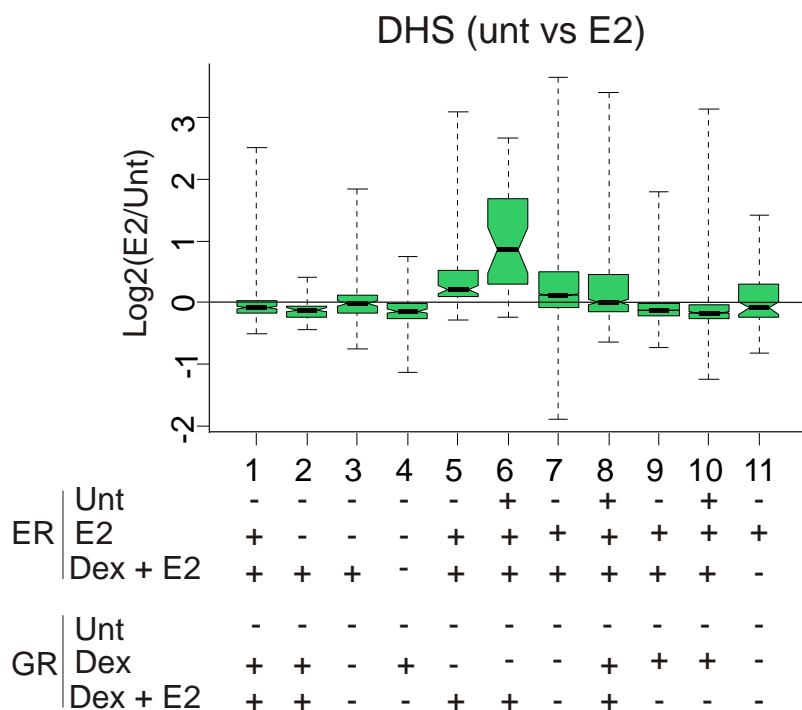
Figure 4.8: Analysis of DHS sites as an indicator of chromatin accessibility at the 11 ER and GR binding clusters utilising ENCODE data. The changes in E2 stimulated DHS in MCF-7 breast cancer cells (ENCODE) has been determined for each ER and GR binding module. Box plot shows the fold change in E2 stimulated DHS as a Log2 value. Each box correlates to the individual cluster label on the x-axis.
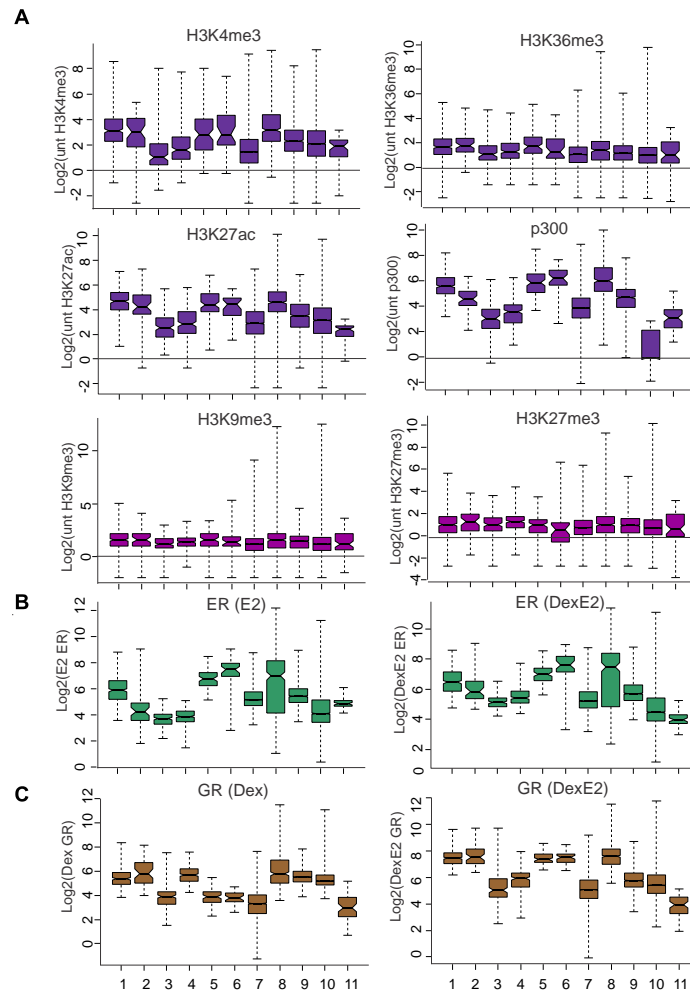
Figure 4.9: Histone modifications at ER and GR binding clusters correlate with ER binding intensities. A. The presence of histone modifications (H3K4me3, H3K36me3, H3K27ac, H3K9me3, and H3K27me3 and p300 in unstimulated MCF-7 breast cancer cells (ENCODE) has been determined for the ER and GR binding clusters.   The data is presented as box plots which demonstrate overall levels of each histone modification or factor binding at each cluster and is presented as Log2. Each box plot correlates to the individual cluster labelled on the x-axis. **B.** ER binding intensities at each ER and GR binding cluster for E2 treated MCF-7 breast cancer cells (left) and Dex + E2 treated cells (right). Binding intensity is plotted as a Log2 and each box correlates to the individual cluster labelled on the x-axis. **C.** GR binding intensities at each ER and GR binding cluster in Dex treated MCF-7 breast cancer cells (left) and Dex + E2 treated cells (right). Binding intensity is plotted as a Log2 and each box correlates to the individual cluster labelled on the x-axis.
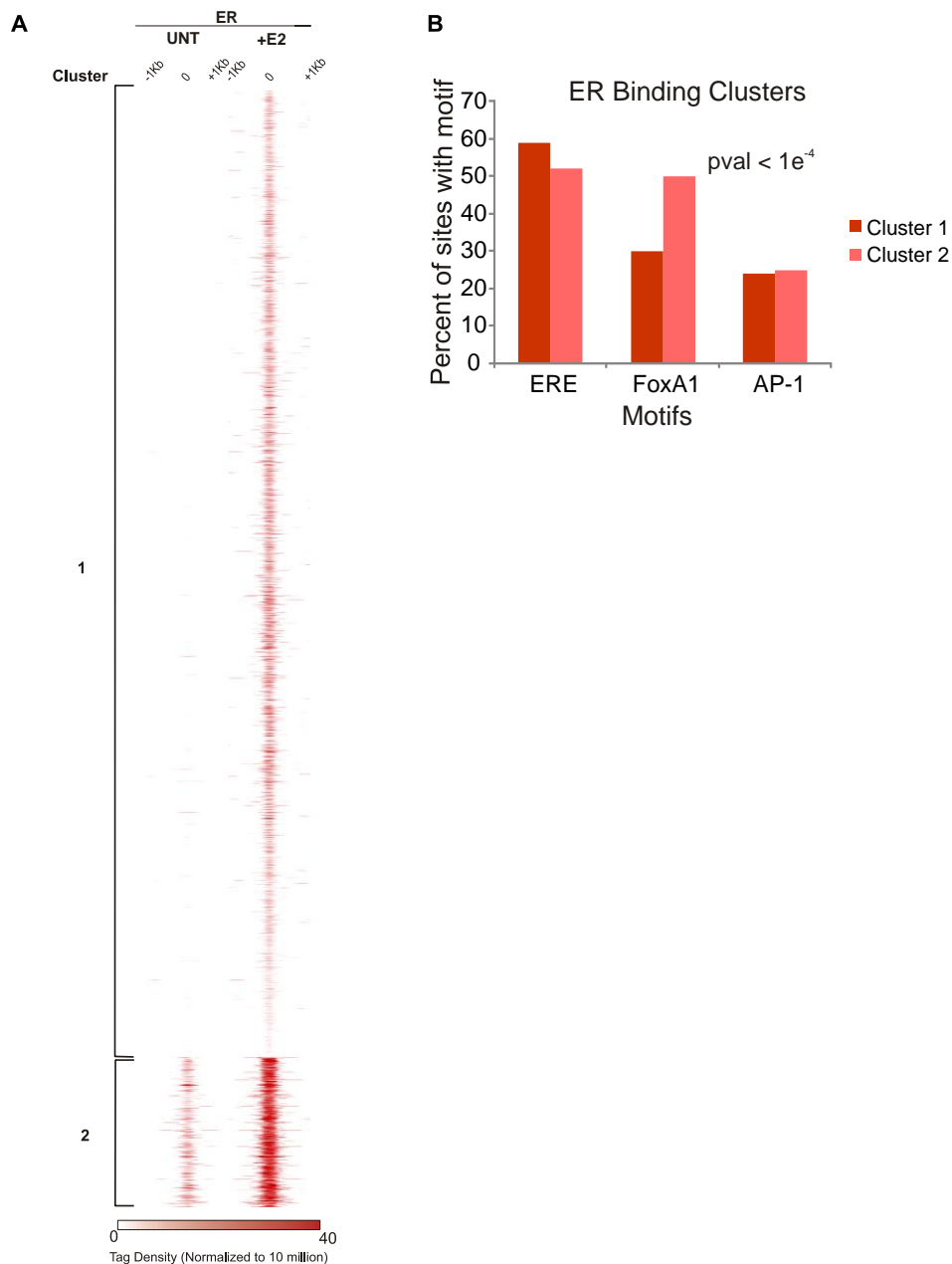
Figure 4.10: Analysis of ER binding patterns in untreated and E2 stimulated MCF-7 breast cancer cells. A. Supervised clustering analysis on all ER binding sites identified in untreated and E2 stimulated cells. Heatmap analysis portrays the number of reads per 10^6 sequences as well as the position of the reads with in 2 kb of ChIP-seq peaks. Two different binding clusters have been identified and are notated by the brackets. **B.** The distribution of ERE, FoxA1, and AP-1 motifs within the two ER binding clusters has been determined using FIMO analysis. The results are reported as the percentage of sites containing the motif with pval < $1e^{-4}$.
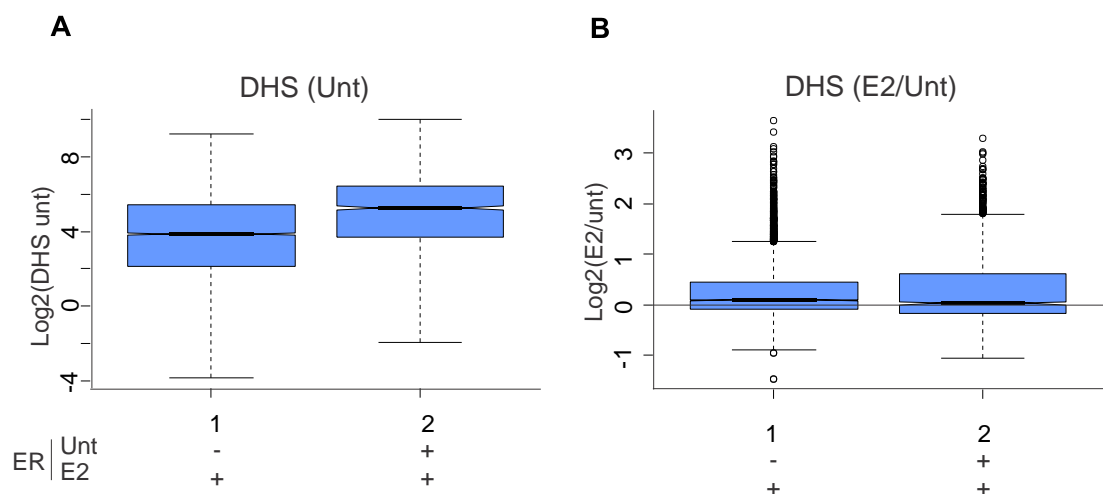
Figure 4.11: Analysis of DHS sites as an indicator of chromatin accessibility at ER binding sites. A. Chromatin accessibility patterns identified in untreated MCF-7 breast cancer cells (ENCODE) has been determined for the ER binding patterns identified in the untreated or E2 stimulated binding clusters. Box plots represent the DHS changes in unstimulated cells presented as Log2. Each box correlates to the individual clusters and is labelled on the x-axis. **B.** Changes in chromatin accessibility patterns between E2 stimulated MCF-7 breast cancer cells and untreated cells (ENCODE) has been determined for the ER binding clusters identified in untreated or E2 stimulated cells. Box plots demonstrate the changes DHS upon E2 stimulation and is presented as Log2. Each box correlates to the individual cluster label on the x-axis.
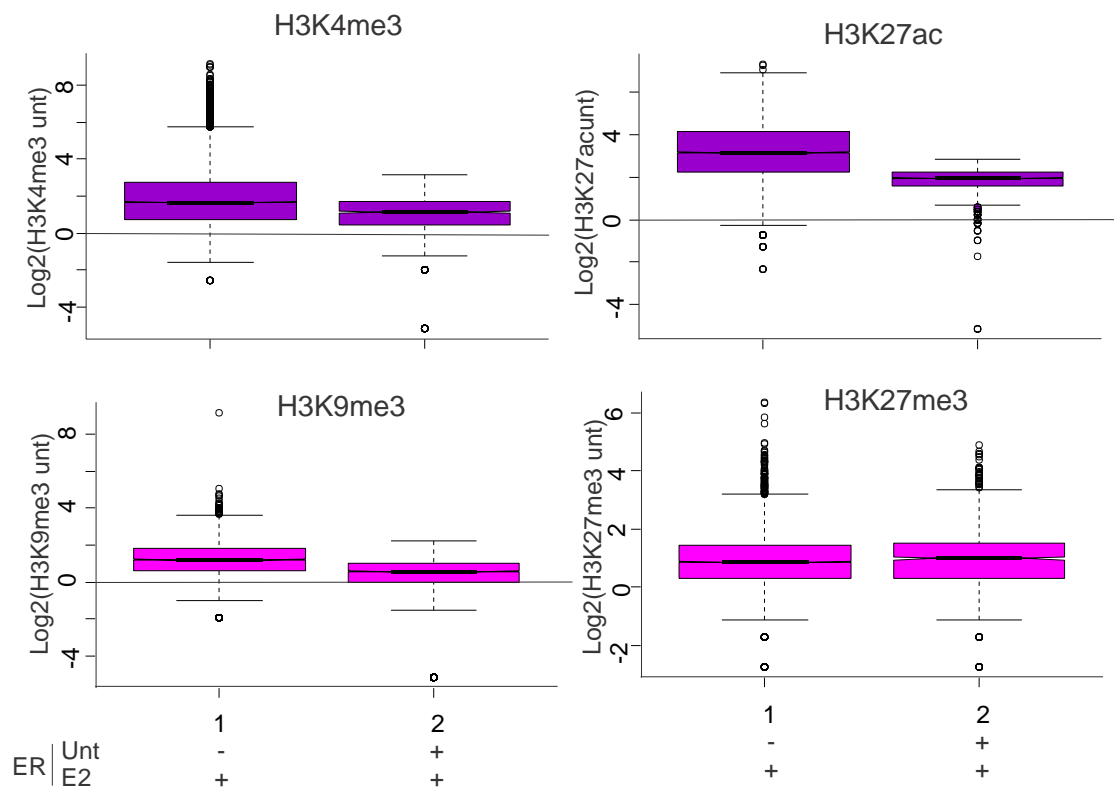
Figure 4.12: The presence of histone modifications at ER binding sites in untreated and E2 stimulated cells. Differences in H3K4me3, H3K27ac, H3K9me3, and H3K27me3 levels in unstimulated MCF-7 breast cancer cells (ENCODE) between the ER binding clusters have been determined. Box plots demonstrate overall levels at each module and are presented as Log2. Each box correlates to the individual module labelled on the x-axis.
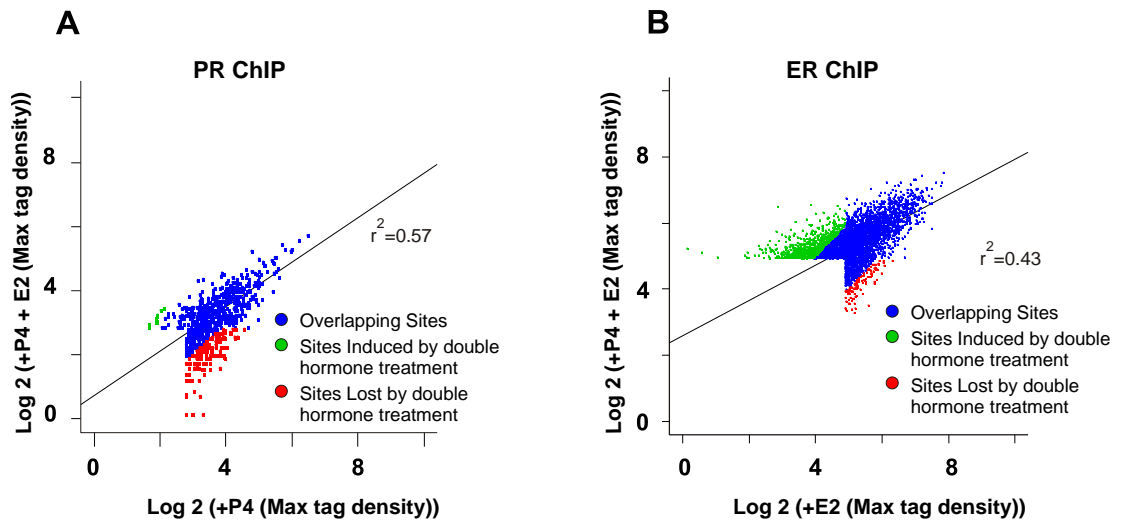
Figure 4.13: Changes in the PR and ER binding landscape upon P4 and E2 dual hormone treatment in MCF-7 human breast cancer cells. **A**. Global changes in PR binding patterns upon dual treatment of cells. Binding patterns of PR have been determined by ChIP-seq after treatment with either P4 or P4 + E2. Scatterplot represents the global changes in PR binding between P4 and P4 + E2. The sites shown to be either gained or lost by the dual hormone treatment have at least a 2-fold change in tag density. **B**. Global changes in ER binding patterns upon dual treatment of cells. Binding patterns of ER have been determined by ChIP-seq after treatment with either E2 or P4 + E2. Scatterplot represents the global changes in ER binding between P4 and Dex + E2. The sites shown to be either gained or lost by the dual hormone treatment have at least a 2-fold change in tag density.
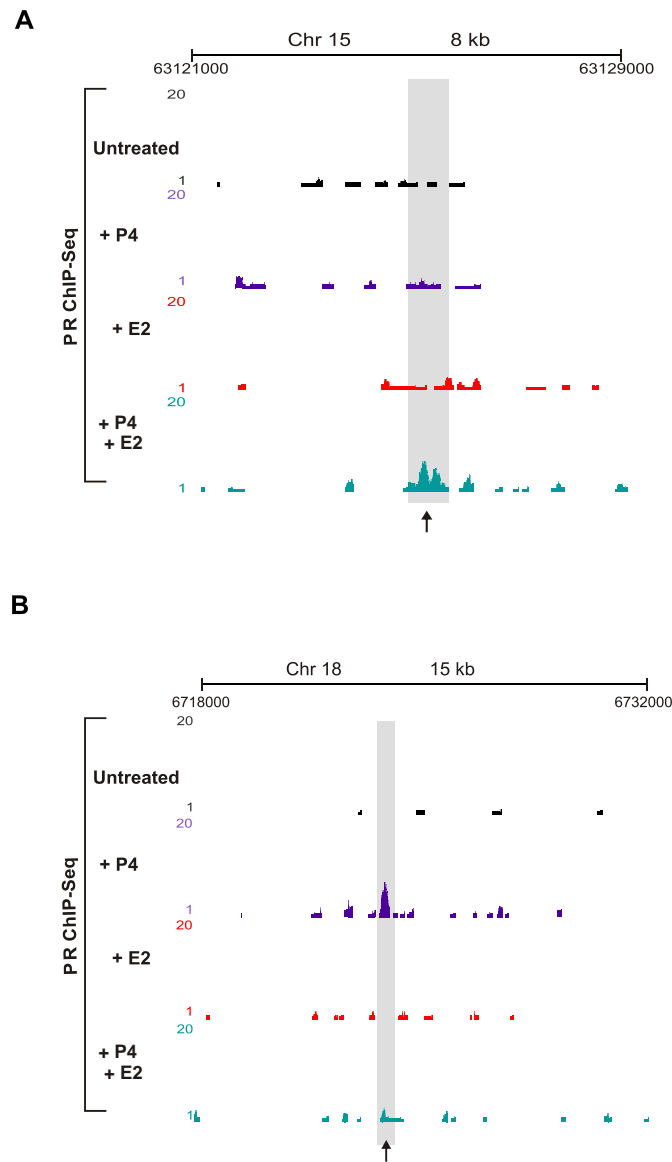
Figure 4.14: Examples of the effects of dual treatment on PR and ER binding. Examples of PR binding in MCF-7 breast cancer cells treated with either 100nM of P4, E2, P4 + E2 or left untreated. PR ChIP-seq has been performed after 30 min of hormone treatment. **A.** A genomic region demonstrating gained PR binding upon dual activation of PR and ER (UCSC browser shot). The black arrow illustrates a PR gained site. **B.** A genomic region demonstrating lost PR binding upon dual activation of PR and ER (UCSC browser shot). The black arrow illustrates a GR lost site.

Figure 4.14: Examples of the effects of dual treatment on PR and ER binding. Examples of ER binding in MCF-7 breast cancer cells treated with either 100nM of P4, E2, P4 + E2 or left untreated. ER ChIP-seq has been performed after 30 min of hormone treatment. **C.** A genomic region demonstrating gained ER binding upon dual activation of PR and ER (UCSC browser shot). The black arrow illustrates a ER gained site. **D.** A genomic region demonstrating lost ER binding upon dual activation of PR and ER (UCSC browser shot). The black arrow illustrates a ER lost site.
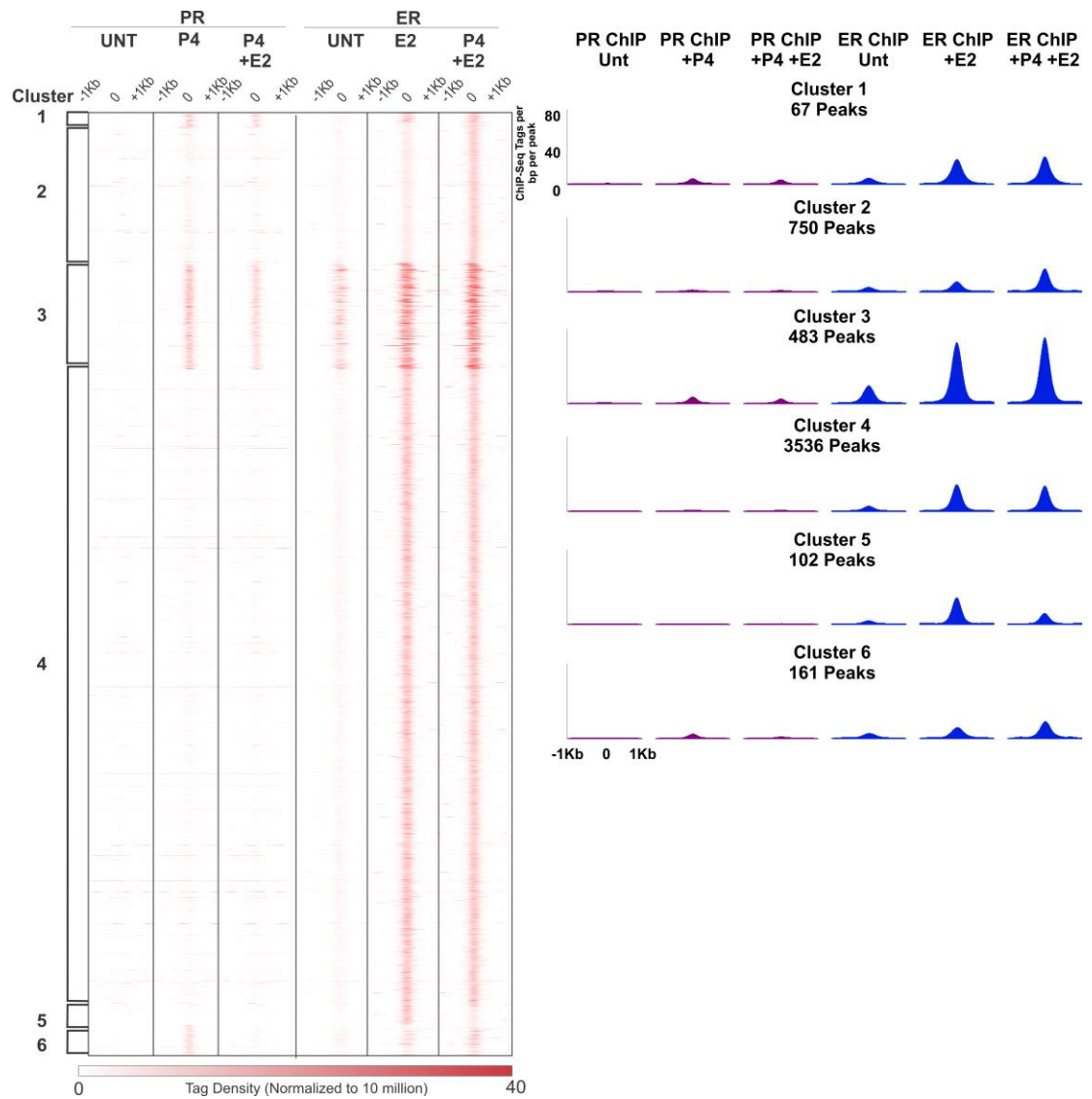
Figure 4.15: Specific GR and ER binding modules. Supervised clustering analysis of 856 peaks identified by PR and ER ChIP-seq in MCF-7 breast cancer cells treated with either 100nM of P4, E2, or P4 and E2. Heatmap portrays the number of reads per 10^6 sequences as well as the position of the reads within 2 kb of ChIP-seq peaks. Untreated samples are included in the analysis. Six different binding clusters have been identified and are notated by the brackets. The histograms demonstrate the overall binding intensities for PR and ER within each cluster.
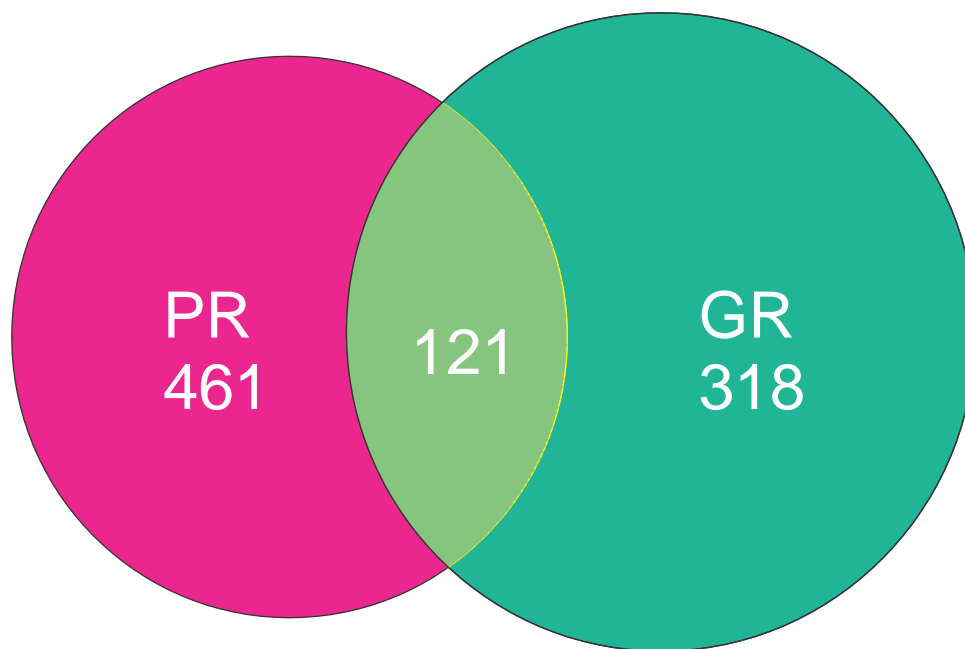
Figure 4.16: Cross analysis of PR and GR classical binding sites. Comparison of PR binding sites identified in MCF-7 breast cancer cells treated with either 100nM P4 or 100nM P4 + E2 with GR binding sites identified in MCF-7 breast cancer cells treated with either 100nM of Dex or 100nM Dex + E2. One hundred and twenty one sites are in common with PR and GR. Four hundred and sixty one are unique to PR and 318 to GR.

Cluster 2

Motif	Factor	P value
	Ap1	$1e^{-107}$
	FoxA1	$1e^{-61}$
	Nr2f2	$1e^{-45}$

Cluster 3

Motif	Factor	P value
	PR	$1e^{-100}$
	FoxA1	$1e^{-71}$
	ER	$1e^{-34}$

Cluster 4

Motif	Factor	P value
	ER	$1e^{-537}$
	NR	$1e^{-298}$
	FoxA1	$1e^{-241}$
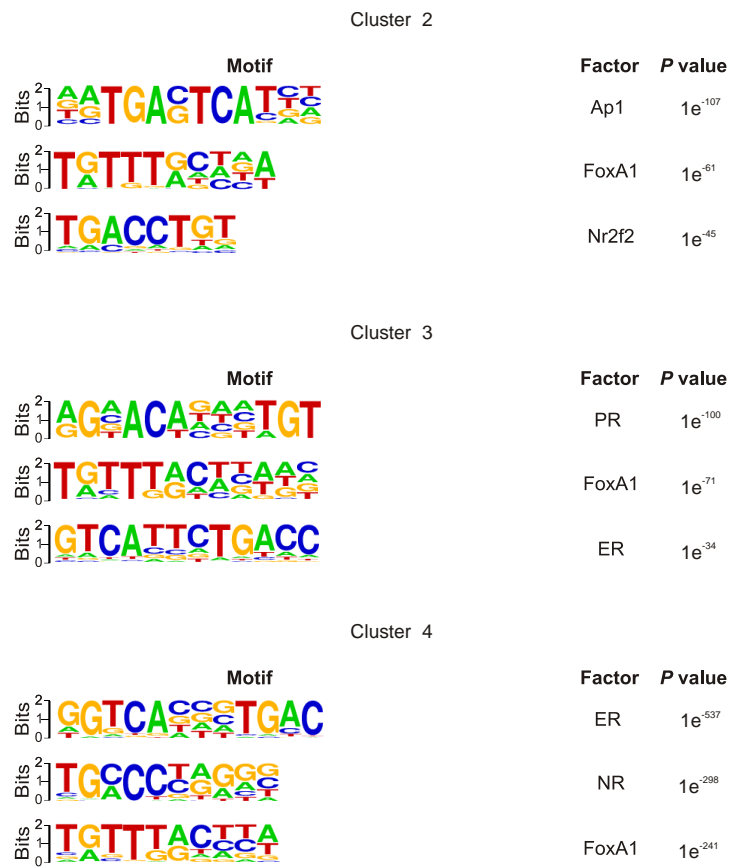
Figure 4.17: Motif analysis of PR and ER binding clusters. *De novo* motif analysis has been conducted on ER gained sites and PR and ER classical sites. The data represents the top three most highly enriched motifs determined by Homer.

Chapter 5

Molecular Crosstalk Between the Pioneer Factor FoxA1 with Either GR, ER, or PR in MCF-7 Human Breast Cancer Cells.

Pioneer factors have been described as a class of proteins that are a critical transcription apparatus during development, and more recently in cancer biology (Zaret and Carroll 2011). FoxA1 plays an important role in facilitating the binding of SRs in a number of disease settings (Bernardo and Keri 2012), specifically, ER and AR in breast and prostate cancer cells, respectively. FoxA1 proteins have been shown to interact with compact chromatin, modulating chromatin structure and binding to DNA as an early event. Upon chromatin binding, FoxA1 can induce nucleosomal rearrangement which can in turn result in an increase in the accessibility of DNA binding elements. This results in the recruitment of other transcriptional regulators and SRs, and specifically in the initiation of transcriptional processes (Cirillo, McPherson et al. 1998, Eeckhoute, Lupien et al. 2009, Hurtado, Holmes et al. 2011, He, Meyer et al. 2012). It has been suggested that pioneer factors, in particular FoxA1, limit the requirement of other factors at chromatin, allowing the interaction between FoxA1 and the chromatin to be quick, thereby facilitating rapid transcriptional responses (Hah, Danko et al. 2011). Early studies show that SRs bind to DNA and regulate their target genes from a distance in breast and prostate cancer cells (Carroll, Liu et al. 2005, Carroll, Meyer et al. 2006, Lin, Vega et al. 2007, Wang, Li et al. 2009). These studies also demonstrate that there was an enrichment of the FoxA1 binding motif in close proximity to approximately half of the ER binding sites that span chromosome 21 and 22 in MCF-7 breast cancer cells (Carroll, Liu et al. 2005). Further, it was shown in MCF-7 cells that FoxA1 binding sites overlap

with approximately 50% of ER binding sites (Carroll, Liu et al. 2005, Lupien, Eeckhoute et al. 2008), and that FoxA1 was required for almost all ER binding events (Carroll, Liu et al. 2005, Laganiere, Deblois et al. 2005). These findings were later confirmed via genome-wide analysis, demonstrating that over half of ER binding sites are also bound by FoxA1, and that FoxA1 is a required component of E2 mediated gene regulation and cell proliferation in MCF-7 breast cancer cells (Laganiere, Deblois et al. 2005, Carroll, Meyer et al. 2006, Lin, Vega et al. 2007, Charn, Liu et al. 2010, Hurtado, Holmes et al. 2011). In addition, in MCF-7 cells, FoxA1 binding correlates with RNA PolII and H4 acetylation at ER regulated genes (Eeckhoute, Carroll et al. 2006). Importantly, it is documented that FoxA1 interactions with DNA are not influenced by E2 stimulation (Lupien, Eeckhoute et al. 2008, Hurtado, Holmes et al. 2011). Further, at a clinical level, FoxA1 is functionally required in breast cancer progression in ER positive breast cancers, and is being utilised as a marker to identify luminal type breast cancer (Yamaguchi, Ito et al. 2008). As mentioned earlier, pioneer factors can interact with closed chromatin, which facilitates the access of other TFs. By FAIRE analysis, it has been described that the inhibition of FoxA1 results in a decrease in the level of accessible chromatin genome-wide, inhibiting ER binding to some sites (Eeckhoute, Lupien et al. 2009, Hurtado, Holmes et al. 2011). In addition, FoxA1 binding at accessible chromatin is also associated with increased H3K9ac, decreased H3K9me1 and me2, and an increase in H3K4me2 (Eeckhoute, Lupien et al. 2009). These results support a role for FoxA1 to function as a pioneer factor modulating the chromatin structure for ER binding, resulting in regulation of ER target genes.

While investigation into the interaction of FoxA1 and ER in breast cancer cells have been studied in depth, investigations into the role FoxA1 plays in GR and PR function are beginning to emerge. Utilising the mouse mammary tumour virus long terminal repeat (MMTV LTR), it has shown that FoxA1 has the ability to mediate chromatin remodelling as previously described. GR is then recruited to the DNA and an increase in hormone induced MMTV transcription occurs (Belikov, Astrand et al. 2009). In the same system it was further demonstrated that at very low synthetic corticoid levels, FoxA1 binding to DNA was increased compared with GR. This suggests that both factors have the ability to alter chromatin state in a concomitant mechanism (Belikov, Holmqvist et al. 2012). In VCaP prostate cancer cells, a subset of unique GR binding events do not appear to have a conical GRE sequence, but contain a FoxA-like cis element (Sahu, Laakso et al. 2013). While the genome-wide investigations into PR in breast cancer cells have been limited, they demonstrate that upon activation with progestin, a high percentage of PR binding sites contain a FoxA1 binding motif suggesting an interaction between the two proteins in T-47D cells (Clarke and Graham 2012).

To date, it seems apparent that the interplay between ER and FoxA1 is driven in a FoxA1 centric manner; however, there is evidence to suggest it may extend beyond the ability of FoxA1 to control ER activity. While it has been shown that there are FoxA1 binding motifs in ER target genes (Carroll, Liu et al. 2005), it has also been demonstrated that FoxA1 is an E2 induced ER target gene (Laganiere, Deblois et al. 2005). This provides evidence that suggests ER may regulate FoxA1, to a certain degree. In addition to these findings, an early study provided evidence to submit that GR can modulate FoxA1 activity. It was shown, *in vivo*,

that FoxA1 could bind to two GR responsive units of the rat tyrosine aminotransferase gene. It was also shown that FoxA1 binding to this site was in fact GR dependent, and occurred upon GR dependent disruption of nucleosomal structure. This suggests a DynaLoad model of transcriptional activation by GR, where GR binds to the sequence and recruits chromatin remodellers to the sites. GR is then removed from the sites leaving the binding element now accessible to FoxA1 (Rigaud, Roux et al. 1991).

What is becoming apparent is the notion that TF recruitment to DNA is a dynamic process, with multiple factors influencing this. Further, we are now beginning to discover that multiple TFs can influence the recruitment of one another to DNA binding elements. Previous studies show that FoxA1 acts as a pioneer factor for SR recruitment and binding to chromatin. However, a few studies have recently suggested that SRs can in fact influence FoxA1 functions. In chapter 4, it has been demonstrated that GR and ER can dictate one another's binding at specific sites via a DynaLoad mechanism. I aim to determine if activated GR, ER, and PR have the ability to shape the FoxA1 response in breast cancer cells. This will allow for further understanding of the role of FoxA1 in breast cancer and the interactions between pioneer factors and SRs.

5.2 Methods

5.2.1 Preparation of cells for ChIP-seq

5.2.1.1 Seeding of cells.

Cells are routinely maintained as described in chapter 2, section 2.3.1.1. Once they reach 80% confluence and are ready to be repassaged or seeded, they are harvested and the cell concentration is calculated, using a cell haemocytometer. MCF-7 cells are seeded at a concentration of 8 x 10^6 cells per mL in 150 mm cell culture plates in 30mL of media. Media utilised for the ChIP-seq experiments is phenol red free DMEM containing 4.5g/L D-glucose supplemented with 10% CSS, 1mM sodium pyruvate, 1X non-essential amino acids, 0.2U/mL bovine insulin, and 1% penicillin-streptomycin. Three plates per treatment group are used and cells are left to grow for 48 h before treatment with hormone.

5.2.1.2 Hormone treatment of cells.

After 48 h of growth, cells are treated with 30uL of 1mM of either Dex, E2, P4, or left untreated to equate to a final concentration of 100nM. Hormone is added directly to the media the cells are being maintained in for 30 min.

5.2.2 <u>ChIP-seq.</u>

The ChIP experiments in this chapter are performed as described in chapter 2, section 2.3.2. Specific details about experiment conditions are as follows. Each plate is formaldehyde cross-linked and then the cells are scaped, removed from the plates, and a cell pellet for each treatment is collected. The pellets are resuspended with 600uL of ChIP lysis buffer containing 1X PI. The resuspended material is sonicated in 15mL sonication tubes. The sonication conditions for each sample are 15 cycles for 15 sec on, 30 sec off at 4º C. Upon completion of sonication the DNA is quantified and samples are diluted 5 fold in ChIP dilution buffer and 1X PI to a final concentration of 100ug of chromatin per mL.

Antibody preparation for each sample is performed with 7 ug/uL of FoxA1 (ab23738) antibody linked to 80uL of Dynabeads (M-280) sheep anti-rabbit IgG. A 100uL aliquot of each sample is removed and stored at 4ºC for the input negative antibody control. The complex is washed with the appropriate buffers and the sample is eluted from the Dynabeads, and a phenol-chloroform-isoamyl extraction is performed. Each pellet is diluted in 10uL of nuclease free H_2O. This experiment is repeated four times to generate four biological replicates. To determine efficient protein binding qPCR was utilised at the *MYC* site as previously published (Hurtado, Holmes et al. 2011). Two biological replicates are pooled to equate to two technical replicates per sample set and submitted to the National Cancer Institute Advance Technology Program Sequence Facility for sequencing services.

5.2.3 <u>Bioinformatic analysis.</u>

The Illumina HiSeq genome analyzer platform has been used to generate sequence reads (36-mer) and unique tags have been aligned to the human reference genome (UCSC hg19 assembly). Hotspots, regions of enriched tags, have been called using previously described methods with minor modifications (Baek, Sung et al. 2012). The values for the tag densities have been normalized to 10 million reads to adjust for differences in the depth of sequencing between samples. The data sets have been adjusted by subtracting tags found in the input. Hotspots have been called using a 0% FDR. A tag density threshold of 30 (1 standard deviation of the maximum tag density) has been applied except for FoxA1 ChIP-seq P4 treated samples. Due to the overall lower tag density values, the tag threshold for FoxA1 ChIP-seq P4 treated samples has been set at 7, which

represents the mode for this sample set. Replicate concordants have been calculated between replicates. For comparison of GR and ER data sets, regions were considered to overlap if they shared at least 1 bp. Peaks unique to the hormone treatments are then identified. FoxA1 sites common to the untreated and hormone treated samples have been removed from the list. Using these peaks, a list of unique chromosomal positions has been created by removing overlapping peaks from the samples being compared (GR-ChIP +Dex, FoxA1-ChIP untreated, FoxA1-ChIP + Dex; ER-ChIP + E2, FOXA1-ChIP untreated, FOXA1-ChIP + E2; PR-ChIP + P4, FoxA1-ChIP untreared, FoxA1-ChIP + P4). This provides a list of 1217 unique peaks for the ER and FoxA1 comparisons, 643 unique peaks for the GR and FoxA1 comparison, and 2799 unique peaks for the PR and FoxA1 comparison. Supervised clustering of the peaks has been conducted tagging each unique peak for presence or absence of binding in the experiments and ordering them according to these tags across the samples. Using Homer, the total number of sequence reads under the peaks for each ChIP-seq sample has been extracted and corrected for the total number of reads in the sample (reads under peak/ 10M total reads) so that a heat map could be generated. Heatmap is generated using MeV software program. For box plots, Homer has been used to retrieve the total number of sequence reads for the ENCODE data under the peaks for each module analyzed. Plots have been graphed using the statistical program R. De novo motif analysis has been conducted using Homer (Heinz, Benner et al. 2010).

5.3.1 Validation of FoxA1 binding in MCF-7 human breast cancer cell.

To assess the genome-wide binding patterns of FoxA1, ChIP-seq has been performed after treatment with either Dex, E2, P4, or left untreated for 30 min. To ensure there is sufficient binding of the FoxA1 protein to DNA before samples are submitted for sequencing, qPCR analysis has been performed and primers for the *MYC* site have been utilised. It has been demonstrated in all four biological replicates that there is binding of FoxA1 at the *MYC* site under all treatment conditions. Cells treated with either Dex, E2, or left untreated demonstrates FoxA1 binding at the *MYC* sites (Figure 5.1A). Cells treated with P4 and compared to cells treated with P4 + E2 demonstrate FoxA1 binding at the *MYC* site (Figure 5.1B). This site does not appear to be specific to one treatment group; however, it provides enough information to demonstrate binding of the protein to DNA. This indicates that samples treated with either Dex, E2, P4 or left untreated are suitable for sequencing.

5.3.2 Investigation of GR and FoxA1 crosstalk in MCF-7 human breast cancer cells.

Genome-wide analysis of FoxA1 ChIP-seq has been performed in the untreated and Dex samples to investigate the role of activated GR on FoxA1 binding. Data analysis reveals a total of 18,785 FoxA1 binding sites. Of these binding sites, 18,142 are found to occur in both the untreated and Dex treated samples, and 72 are unique to the untreated group and are lost when cells are stimulated with Dex.

Of particular interest is a subset of 571 FoxA1 sites that are gained in the Dex treatment group (Figure 5.2). These data suggests there is a role for activated GR to modulate the FoxA1 response at a subset of sites genome-wide. To further assess if GR is playing a specific role in the recruitment of FoxA1 to specific sites within the genome, supervised clustering analysis has been performed with the FoxA1 sites unique to Dex or untreated along with the GR Dex ChIP-seq data analysed in chapter 4 (Figure 5.3). Four specific clusters are established, not including FoxA1 binding sites that are common in both the untreated and Dex treatment samples (FoxA1 classical binding sites).

Cluster 1 (236 peaks) represents FoxA1 gained sites with Dex treatment and overlap with GR binding sites. This cluster is of specific interest since it provides evidence that activated GR may recruit FoxA1 to specific sites through a DynaLoad mechanism. Surprisingly, cluster 2 (335 peaks) represented FoxA1 binding sites with Dex treatment that do not overlap with GR binding sites, suggesting there are other TFs and/or long-range interactions involved in FoxA1 recruitment. Cluster 3 (16 peaks) represents lost FoxA1 sites only present in the untreated group and overlap with GR sites. Cluster 4 also contains FoxA1 lost sites (56 peaks); however, these peaks do not overlap with GR binding sites. This also suggests that other TFs or long-range interactions are potentially involved in FoxA1 recruitment at these specific sites. The effects observed at clusters 1, 2, and 4 are demonstrated at specific genomic regions utilising UCSC browser shots (Kent, Sugnet et al. 2002) (Figure 5.4A-C).

5.3.3 Motif analysis of FoxA1 and GR binding clusters in MCF-7 human breast cancer cells.

To further assess the specific binding regions in each module, including FoxA1 classical binding sites, *de novo* motif analysis was performed utilising Homer software. Due to the very low numbers of FoxA1 peaks in cluster 3 and 4, motif analysis does not demonstrate any significant results. The FoxA1 classical sites contain a FoxA1 and AP-1 motif. However, FoxA1 binding sites which represent DynaLoad mechanism (cluster 1), contain a GRE and AP-1 binding sequence. This provides evidence to suggest that GR and perhaps AP-1 are playing a role in FoxA1 binding at these specific sites through a FoxA1 DynaLoad mechanism. In addition, FoxA1 binding sites which are gained with Dex treatment and do not overlap with GR binding (cluster 2) contain FoxA1 and AP-1 binding sequences (Figure 5.5). This suggests that AP-1 may be playing a role in the Dex activation of FoxA1 sites in the absence of GR binding.

5.3.4 Activation of ER affects a subset of FoxA1 binding events in MCF-7 human breast cancer cells.

Analysis of FoxA1 ChIP-seq under the stimulation of E2, compared with untreated, reveal a total number of 20,287 binding sites. Of this number, 19,068 are found to be in common when cells are stimulated with E2 or left untreated. Interestingly, there are 1095 binding sites that are gained in cells treated with E2. Further, there are 124 binding sites that are lost in the presence of E2 (Figure 5.6). This demonstrates there are subsets of FoxA1 binding sites that are unique to the E2 treatment, suggesting ER can dictate FoxA1 binding at a subset of sites, which

is contrary to previously published results. To further investigate the finding that activation of ER affects FoxA1, supervised clustering has been performed integrating ER E2 ChIP-seq data from chapter 4 with the FoxA1 binding sites unique to untreated or E2 treated samples (Figure 5.7). This clustering reveals three unique binding modules. Cluster 1 (122 peaks) represents FoxA1 sites that are lost upon E2 treatment and do not overlap with ER binding sites. These results are similar to what is observed in chapter 4 for GR and ER, and provides evidence that factors can inhibit the binding of one another through mechanisms other than direct competition. Cluster 2 (625 peaks) demonstrates FoxA1 sites that are gained by E2 treatment, but do not overlap with ER binding sites. Again, these results are in concordance with the GR and ER crosstalk data in chapter 4. The lack of overlap with ER sites suggest that FoxA1 binding at these sites is either through long-range interactions or are perhaps sites where ER has a fast resonance time and therefore cannot be cross-linked to these sites. Lastly, cluster 3 represents unique sites whereby FoxA1 binding is gained with E2 treatment only and overlaps with ER binding sites (470 peaks). This demonstrates that ER activation plays a role in FoxA1 DynaLoad resulting in a specific subset of new FoxA1 binding sites found with E2 treatment alone. This suggests that FoxA1 is not a pioneer factor in the classical sense such that its sole role is to prime the binding landscape for other TFs. It is important to note that FoxA1 peaks that are common to untreated and ER (FoxA1 classical binding sites) are at 19,068 and data was not included to the clustering analysis. Genomic location analysis revealed the majority of binding sites at each cluster, including FoxA1 classical binding sites, were found to be in intron and intergenic regions. Interestingly,

30% of sites in cluster 1, sites lost by E2 treatment, are found to be in promoter regions (Figure 5.8).

5.3.5 Motif analysis of FoxA1 and ER binding clusters in MCF-7 human breast cancer cells.

To further assess whether other factors may be involved in FoxA1's response to E2 treatment, *de novo* motif analysis was performed utilising Homer software on the different FoxA1 binding modules. FoxA1 classical binding sites contain a FoxA2, Arid5a, and AP-1 as the top three recognition sequences. The FoxA1 gained sites (cluster 2) that do not overlap with ER contain FoxA1 and AP-1 binding sequences as the top motifs. Surprisingly, these are the same motifs found in the FoxA1 sites gained with Dex treatment and do not overlap with GR binding sites (section 5.3.3, chapter 5). FoxA1 sites gained with E2 and overlapping with ER binding (cluster 3) interestingly contain an ERE and AP-1 binding motif, which is in contrast to the FoxA1 classical binding sites. This provides further evidence to suggest that ER and perhaps AP-1 are playing a role in FoxA1 recruitment at these specific sites by E2 activation through a FoxA1 DynaLoad mechanism. This also suggests that there may be FoxA1 and AP-1 interactions (Figure 5.9). *De novo* motif analysis of cluster 1 can be found in appendix 1C.

5.3.6 FoxA1 and ER cluster comparison with DHS-seq data (ENCODE).

To further evaluate the chromatin state at the specific FoxA1/ER binding modules, MCF-7 DHS-seq ENCODE data is utilised (Consortium, Bernstein et al. 2012, Thurman, Rynes et al. 2012). Cross analysis with FoxA1 classical binding

sites and the three FoxA1 and ER clusters demonstrates an increase in E2 stimulated DHS at cluster 3 sites compared with the other FoxA1 clusters identified (Figure 5.10A). This suggests that FoxA1 binding to these sites are dependent on ER activation and recruitment of chromatin remodellers to these sites. This finding is demonstrated at genomic regions utilising UCSC browser screen shots incorporating FoxA1 untreated and E2 ChIP-seq, ER E2 ChIP-seq and untreated, and E2 DHS-seq (Kent, Sugnet et al. 2002) (Figure 5.10B-C).

5.3.7 <u>Comparison of FoxA1 and ER clusters with histone modification sequencing data (ENCODE).</u>

As described in chapter 4, ENCODE also performed genome-wide sequencing of histone modifications in untreated MCF-7 cells (Consortium, Bernstein et al. 2012). The FoxA1 classical binding sites and the three clusters with genomic profiles were compared for histone marks associated with active chromatin, the p300 enzyme, and histone marks associated with repressed chromatin (Figure 5.11). Interestingly, there does appear to be higher levels of H3K4me3 at binding sites where FoxA1 is lost upon E2 treatment, when compared to the other binding modules. In addition, there are slightly lower levels of H3K4me3, H3K27ac, and p300 at FoxA1 binding sites that are induced by E2 but do not overlap with ER binding sites. There are no differences observed in the inactive marks H3K9me3 and H3K27me3 between the binding modules.

5.3.8 Comparison of FoxA1 and ER clusters with TF sequencing data (ENCODE).

The ENCODE project also mapped regions of TF association to DNA in MCF-7 cells (Consortium, Bernstein et al. 2012). Therefore, cross analysis of the three FoxA1 ER clusters including the FoxA1 classical binding sites with CCCTC-binding factor (CTCF), v-myc avian myelocytomatosis viral oncogene homolog (MYC), jun D proto-oncogene (JunD), and CCAAT/enhancer binding protein (C/EBP) data sets has been conducted (Figure 5.12). The changes in CTCF binding in the untreated data set and the E2 versus untreated data set has also been assessed. At binding sites where FoxA1 is lost upon treatment of cells with E2 (cluster 1), there is a higher level of CTCF binding in untreated cells compared to the other binding modules. In addition, there is an increase in CTCF levels at these sites upon E2 stimulation. Previous studies have shown that CTCF can inhibit FoxA1 binding at specific sites (Hurtado, Holmes et al. 2011). Therefore, it is possible that CTCF is somehow playing a role in dictating FoxA1 binding at elements within cluster 1. Further MYC occupancy in the untreated, and untreated versus E2 data sets has been compared. While there appears to be more of MYC binding at cluster 1 in the untreated samples, there is no increase in MYC binding at these sites upon treatment with E2. Furthermore, there appears to be no differences in JunD and C/EBP binding at the clusters.

5.3.9 An increase in FoxA1 binding is associated with ER binding at untreated and E2 samples.

In chapter 4, the ER binding events that occur in the untreated and E2 samples versuss the E2 alone samples has been investigated. To further determine if there is a factor distinguishing the two clusters, all FoxA1 sites identified in the untreated samples have been compared with ER binding sites present only with E2 treatment (cluster 1), and ER binding sites present in both untreated and E2 treated cells (cluster 2). The data demonstrates that there is an increase in FoxA1 binding at ER sites that occur in both the untreated and E2 groups, compared with the E2 treatment alone (Figure 5.13). This may be a potential reason as to why there is ER binding in the untreated samples at these specific sites. However, very recently published data shows that the knockdown of ER affects FoxA1 binding at specific sites in untreated cells (Caizzi, Ferrero et al. 2014). This suggests that in untreated cells, unliganded ER recruits FoxA1 to certain sites within the genome.

5.3.10 Activated PR does not appear to alter FoxA1 genome-wide in MCF-7 human breast cancer cells.

Changes in FoxA1 binding upon stimulation with P4 has been assessed to determine if PR plays a significant role in FoxA1 recruitment to specific sites. Analysis reveals a total of 9984 binding sites, of which 7185 are found to be in common to both untreated and P4. There are 1646 sites found to be activated in only the untreated group and are deemed lost by P4 treatment. Further, there are 1153 sites gained via P4 and are unique to that single hormone treatment (Figure 5.14). This suggests that when PR is activated by P4, a unique subset of FoxA1 sites are gained demonstrating a potential FoxA1 DynaLoad. To investigate this notion, supervised clustering has been conducted on the P4 stimulated PR ChIP-

seq data from chapter 4 and the FoxA1 sites identified to be unique to untreated or P4 (Figure 5.15). Analysis reveals only two clusters with no correlation to PR binding. Cluster 1 (1640 peaks) demonstrates FoxA1 sites unique to untreated, and cluster 2 represents FoxA1 gained sites with P4 (1153 sites). This suggests that while there are subsets of FoxA1 sites gained via P4, PR does not appear to play a direct role at these specific sites. *De novo* motif analysis has been performed on the data including the FoxA1 sites common to untreated and P4 treated samples (FoxA1 classical binding sites), omitted from supervised clustering analysis, utilising Homer software. As expected, the FoxA1 classical binding sites have a FoxA1 motif as the most highly enriched sequence. Cluster 2 representing gained sites by P4, contain a FoxA1 and AP-1 as the most highly enriched binding motifs (Figure 5.16). Motif analysis from cluster 1 can be found in appendix 1D. While there is a subset of FoxA1 sites that are modulated by P4 treatment, there is no direct correlation observed with PR binding at these sites. It has been illustrated in chapter 4 that the number of PR sites mapped is relatively low compared with GR and ER, with the suggestion that experimental condition could have affected this. PR binding sites have been mapped genome-wide in T-47D cells (Clarke and Graham 2012, Ballare, Castellano et al. 2013) which express higher levels of PR compared with MCF-7 cells and the affect of PR on FoxA1 binding should be further investigated in this cell model.

5.4 Discussion

FoxA1 has been well established as a pioneer factor for SR recruitment to specific sites across the genome (Bernardo and Keri 2012). Importantly, the interaction

between FoxA1 and ER has been shown to be a prominent factor in breast cancer development (Yamaguchi, Ito et al. 2008). However, the molecular interplay between ER and FoxA1 is not fully understood. Previous studies demonstrate that FoxA1 is required for ER recruitment at a majority of sites, and that 50% of ER binding sites overlap with FoxA1 sites in MCF-7 cells (Carroll, Liu et al. 2005, Lupien, Eeckhoute et al. 2008, Hurtado, Holmes et al. 2011). Furthermore, these previous studies have shown that, upon inhibition of ER, no changes in FoxA1 binding are observed (Lupien, Eeckhoute et al. 2008, Hurtado, Holmes et al. 2011). These results suggest that FoxA1 is a pioneer factor which establishes the binding landscape for ER and that ER plays no role in FoxA1 binding. However, these studies have either focused on a small number of binding locations or they have compared FoxA1 binding only between unstimulated cells and cells treated with an ER down-regulator (Lupien, Eeckhoute et al. 2008, Hurtado, Holmes et al. 2011). This chapter reveals that when unstimulated cells are compared with cells treated with E2, the binding landscape of FoxA1 is altered. ChIP-seq in the absence and presence of E2 shows that activation of ER can inhibit FoxA1 binding at specific binding elements and can recruit FoxA1 to other sites through a DynaLoad mechanism. This confirms that the activation of ER can dictate FoxA1 binding across the genome. Recent studies certifying these findings show that FoxA1 recruitment is dependent on stimulation of cells with E2 at 29% of sites where both ER and FoxA1 bind, although no mechanism was determined (Kong, Li et al. 2011). In addition, it has been shown that upon knockdown of ER, FoxA1 binding is lost at unstimulated ER binding sites (Caizzi, Ferrero et al. 2014). This chapter also demonstrated that there are a subset of FoxA1 sites gained upon Dex stimulation and overlap with GR sites. It

has previously been demonstrated that GR can modulate FoxA1 binding at specific GREs within the GR responsive units of the rat tyrosine aminotransferase gene. This enhanced binding of FoxA1 occurs upon a GR dependent disruption of nucleosomal structure (Rigaud, Roux et al. 1991). These findings reveal that the molecular interactions between ER, GR, and FoxA1 are far more complicated than previously thought, and further, the findings suggest that FoxA1 is not a "pioneer factor" in the classical sense, whose sole function is to bind to closed chromatin and establish the binding landscape for other factors.

Previous studies have shown that TFs can dictate on another's binding through a Dynaload mechanism (Voss, Schiltz et al. 2011, Miranda, Voss et al. 2013). AP-1 has been shown to modulate GR's binding, and GR can assist AP-1's binding using this mechanism (Voss, Schiltz et al. 2011). In addition, it has been demonstrated that STAT3 and CEBPB can recruit GR through a similar mechanism (Siersbaek, Nielsen et al. 2011, Langlais, Couture et al. 2012). Chapter 4 and previous studies established that the activation of both ER and GR causes binding of the receptors to novel sites across the genome (Voss, Schiltz et al. 2011, Miranda, Voss et al. 2013). These studies suggest that any TF may have the potential to bind chromatin and recruit remodellers to make the sites more "open" in configuration, allowing for the induction of binding of other TFs to these sites. This chapter shows ER and GR can also induce the recruitment of FoxA1 to specific sites, in addition to regulating the binding of ER and GR at other sites. This indicates that there may not be a set of "pioneer" factors, but that every factor can potentially affect the binding landscape of other TFs depending on the chromatin context.

In addition to recruiting FoxA1 to a subset of sites, activation of ER also causes a loss of FoxA1 binding at some sites. At FoxA1 sites lost upon E2 treatment there is an increase in CTCF binding in untreated and E2 stimulated samples compared to other FoxA1 binding sites. It has been previously reported that approximately 80% of FoxA1 and ER sites found to be in common contain binding of CTCF in MCF-7 cells, and these sites are enriched around E2 regulated genes. Additionally, silencing of CTCF in MCF-7 and ZR-75-1 breast cancer cells results in increases in FoxA1 binding. The increase in FoxA1 binding that is observed in MCF-7 cells upon knockdown of CTCF is at sites that have been previously observed only in the ZR-75-1 cells. Furthermore, increases in H3K4me1 are observed at these sites upon the silencing of CTCF (Hurtado, Holmes et al. 2011). This provides evidence that CTCF can modulate FoxA1 binding. In my studies, the FoxA1 sites lost upon E2 treatment do not overlap with ER binding. My findings, in addition to previous studies (Hurtado, Holmes et al. 2011), suggest that while E2 can influence FoxA1 binding, it may not be a direct interaction with ER due to the lack of ER binding at these sites. Conversely, the loss of FoxA1 binding may be by a CTCF mechanism that is activated by E2 treatment.

Although much progress has been made in understanding the role of chromatin structure on TF binding across the genome, these recent studies have shown that TF recruitment is a complex process and that there are still many avenues which are not clearly understood. The studies in this chapter have shown that our classical understanding of pioneer factors is not the full story. It is now apparent

that multiple TFs have the capability of binding to "closed" chromatin sites and recruit chromatin remodellers depending on the chromatin context.

A   FoxA1 ChIP

B   FoxA1 ChIP
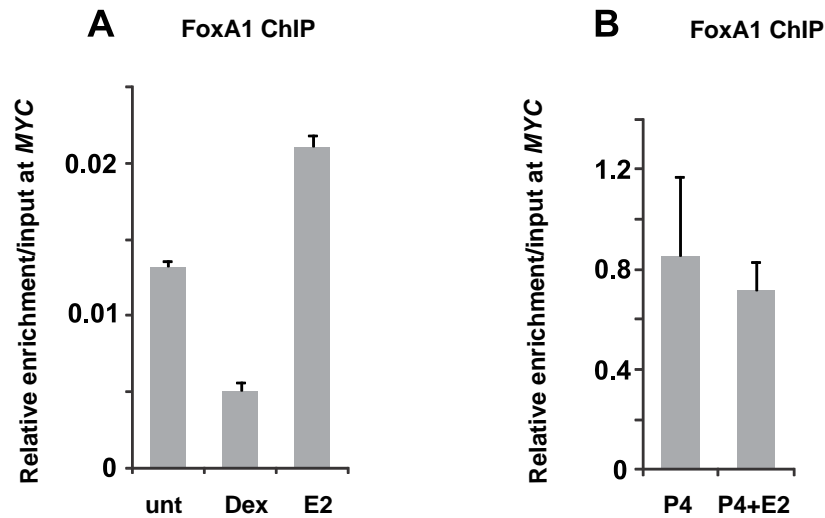
Figure 5.1: **Analysis of FoxA1 binding confirms sufficient enrichment for ChIP-seq. A.** Quantitative-PCR shows FoxA1 binding at a *MYC* site in MCF-7 breast cancer cells treated with either 100nM of Dex, 100nM E2, or left untreated. Data presented as relative enrichment over input. Results demonstrate that FoxA1 ChIP samples are suitable for sequencing. Figure is a representative example of one biological replicate. Error bars represent technical replicates. **B.** Quantitative-PCR shows FoxA1 binding at a *MYC* site in MCF-7 breast cancer cells treated with either 100nM of P4 or 100nM of P4 and E2. Data presented as relative enrichment over input. Results demonstrate that FoxA1 ChIP samples treated with 100nM P4 are suitable for sequencing. Figure is a representative example of one biological replicate. Error bars represent technical replicates.

Chapter 5 – Molecular Crosstalk Between the Pioneer Factor FoxA1 with Either
GR, ER, or PR in MCF-7 Human Breast Cancer Cells.
Page 145

FoxA1 ChIP

$r^2=0.82$

- Overlapping Sites
- Sites Induced by Dex hormone treatment
- Sites Lost by Dex hormone treatment

Log 2 (+Dex (Max tag density))

Log 2 (+untreated (Max tag density))
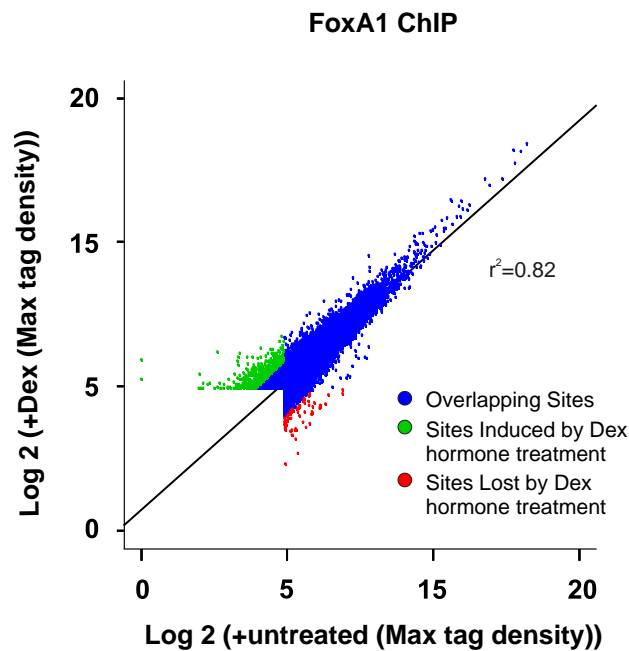
Figure 5.2: Changes in the FoxA1 binding landscape upon Dex hormone treatment in MCF-7 human breast cancer cells. Global changes in FoxA1 binding patterns upon 100nM Dex treatment of cells compared with untreated cells. Binding patterns of FoxA1 have been determined by ChIP-seq after treatment with either Dex or left untreated. Scatterplot represents the global changes in FoxA1 binding between Dex and untreated cells. The sites shown to be either gained or lost by Dex hormone treatment have at least a 2-fold change in tag density.
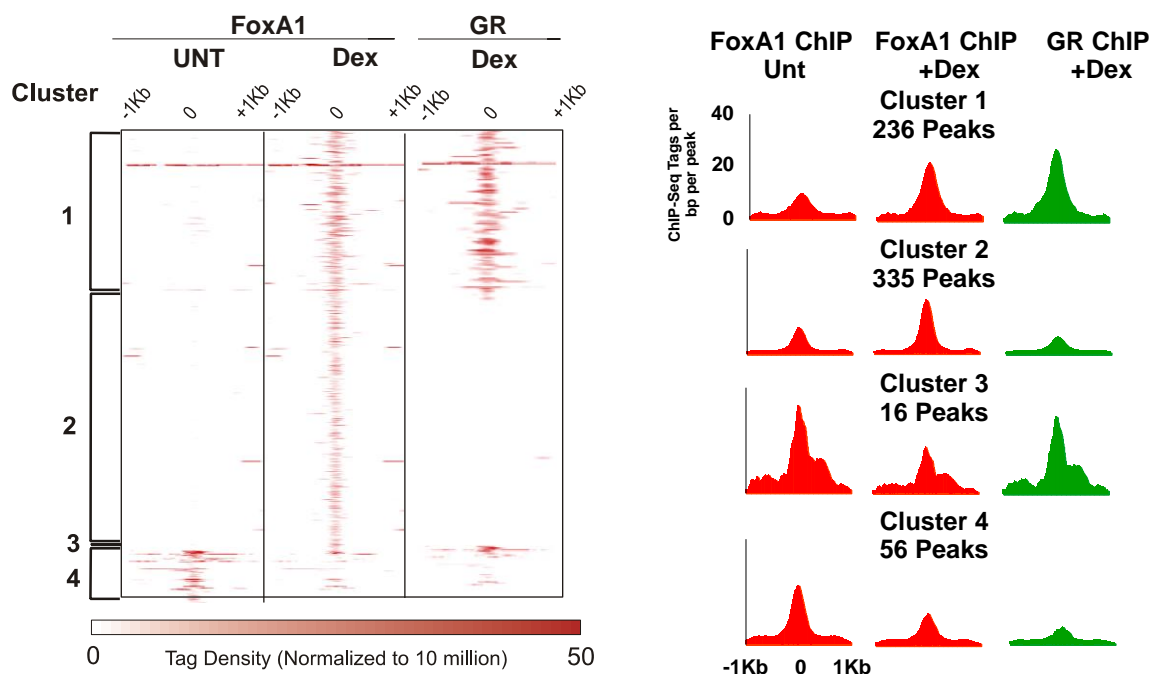
Figure 5.3: Specific FoxA1 and GR binding modules. Supervised clustering analysis of 643 peaks identified by FoxA1 and GR ChIP-seq in MCF-7 breast cancer cells treated with either 100nM Dex or left untreated. Heatmap analysis portrays the number of reads per 10^6 sequences as well as the position of the reads within 2 kb of ChIP-seq peak. Four different binding clusters have been identified which are notated by the brackets. Histograms represent the overall FoxA1 and GR binding intensities in each cluster for the various treatments within a 2 kb interval of the ChIP-seq peaks.
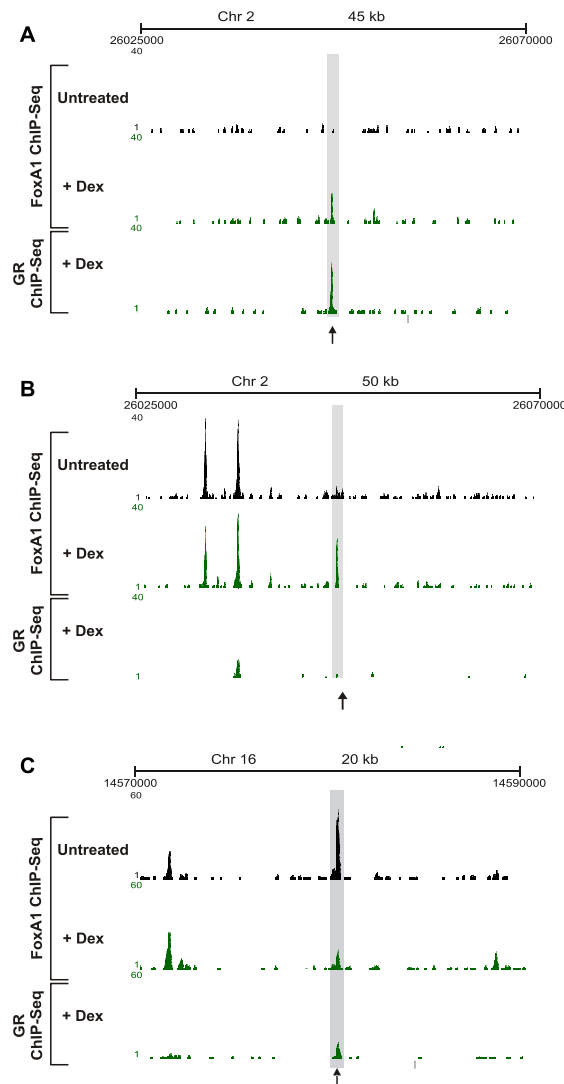
Figure 5.4: Examples of the effects of Dex treatment on FoxA1 binding.
Examples of FoxA1 binding in MCF-7 breast cancer cells treated with either
100nM of Dex or left untreated. FoxA1 ChIP-seq has been performed after 30
min of hormone treatment. **A.** A genomic region demonstrating gained FoxA1
binding upon Dex treatment which overlaps with GR binding (cluster 1: FoxA1
DynaLoad) (UCSC browser shot). The black arrow illustrates a FoxA1 gained
site. **B.** A genomic region demonstrating gained FoxA1 binding upon Dex
treatment which does not overlaps with GR binding (cluster 2) (UCSC browser
shot). The black arrow illustrates a FoxA1 gained site. **C.** A genomic region
demonstrating lost FoxA1 binding upon Dex treatment which does not overlaps
with GR binding (cluster 4) (UCSC browser shot). The black arrow illustrates a
FoxA1 lost site.

*Chapter 5 – Molecular Crosstalk Between the Pioneer Factor FoxA1 with Either
GR, ER, or PR in MCF-7 Human Breast Cancer Cells.*
Page 148

FoxA1 classical binding sites.

Motif	Factor	*P* value
	FoxA1	$1e^{-3784}$
	AP1	$1e^{-484}$
	Arid5A	$1e^{-475}$

Cluster 1

Motif	Factor	*P* value
	GR	$1e^{-26}$
	AP1	$1e^{-23}$
	FoxP1	$1e^{-19}$

Cluster 2

Motif	Factor	*P* value
	FoxA1	$1e^{-73}$
	AP1	$1e^{-47}$
	FoxA2	$1e^{-16}$
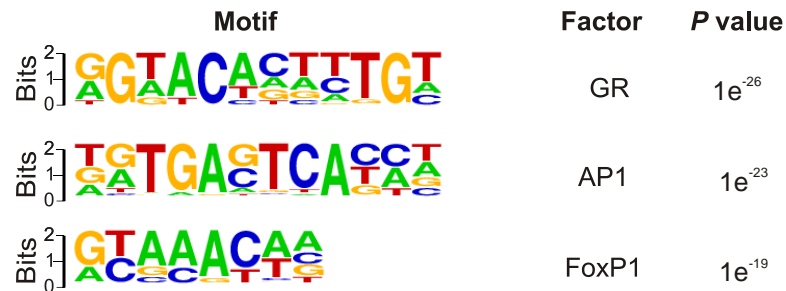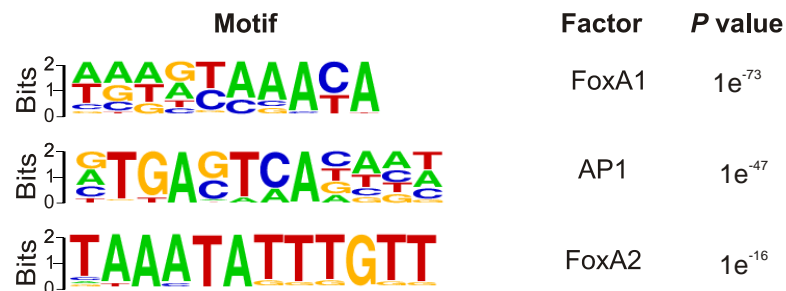
Figure 5.5: Motif analysis of FoxA1 and ER binding clusters. *De novo* motif analysis has been conducted on FoxA1 classical binding sites, cluster 1, and cluster 2. The data represents the top three most highly enriched motifs determined by Homer.

FOXA1 ChIP

$r^2 = 0.77$

- ● Overlapping Sites
- ● Sites Induced by E2 treatment
- ● Sites Lost by E2 treatment

y-axis: Log 2 (+ E2 (Max tag density))

x-axis: Log 2 (+ untreated (Max tag density))
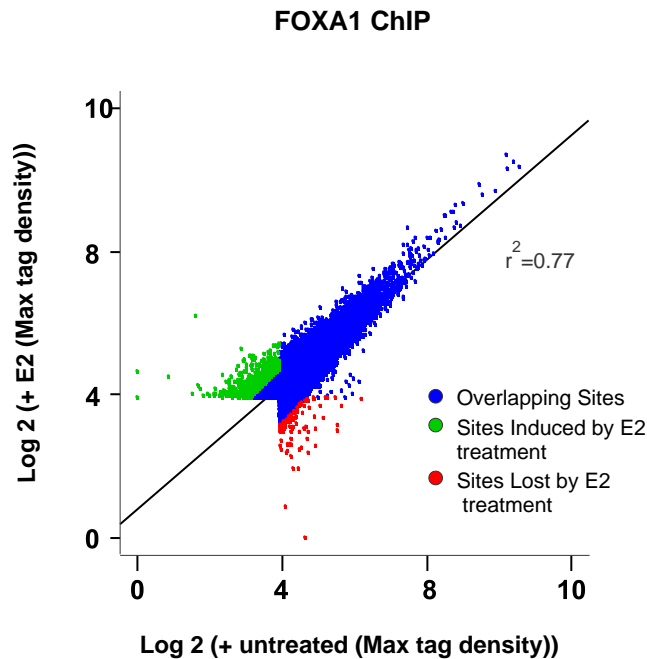
Figure 5.6: Changes in the FoxA1 binding landscape upon E2 hormone treatment in MCF-7 human breast cancer cells. Global changes in FoxA1 binding patterns upon 100nM E2 treatment of cells compared with untreated cells. Binding patterns of FoxA1 have been determined by ChIP-seq after treatment with either E2 or left untreated. Scatterplot represents the global changes in FoxA1 binding between E2 and untreated cells. The sites shown to be either gained or lost by E2 hormone treatment have at least a 2-fold change in tag density.
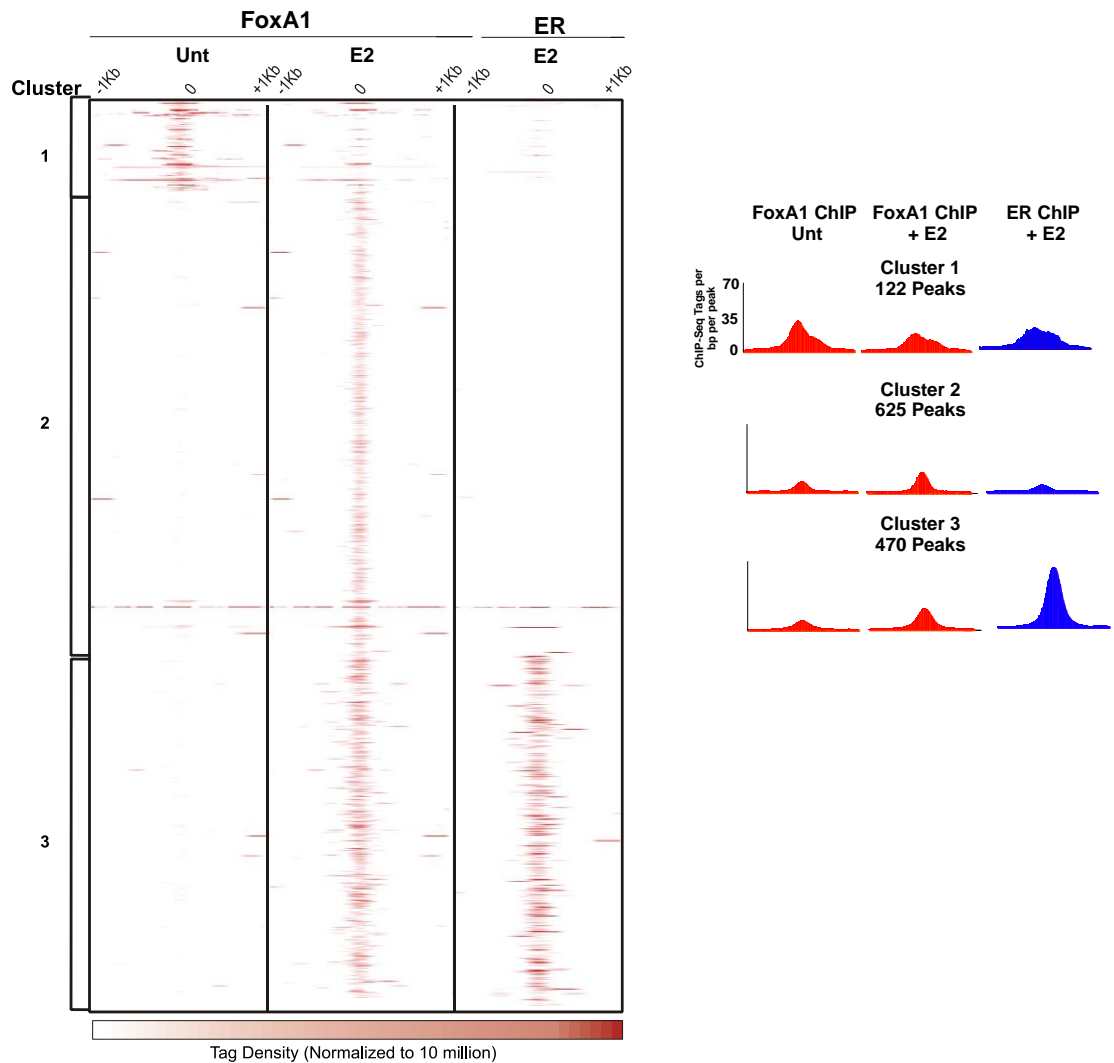
Figure 5.7: Specific FoxA1 and ER binding modules. Supervised clustering analysis of 1217 peaks identified by FoxA1 and ER ChIP-seq in MCF-7 breast cancer cells treated with either 100nM E2 or left untreated. Heatmap analysis portrays the number of reads per 10^6 sequences as well as the position of the reads within 2 kb of ChIP-seq peak. Three different binding clusters have been identified which are notated by the brackets. Histograms represent the overall FoxA1 and ER binding intensities in each cluster for the various treatments within a 2 kb interval of the ChIP-seq peaks.
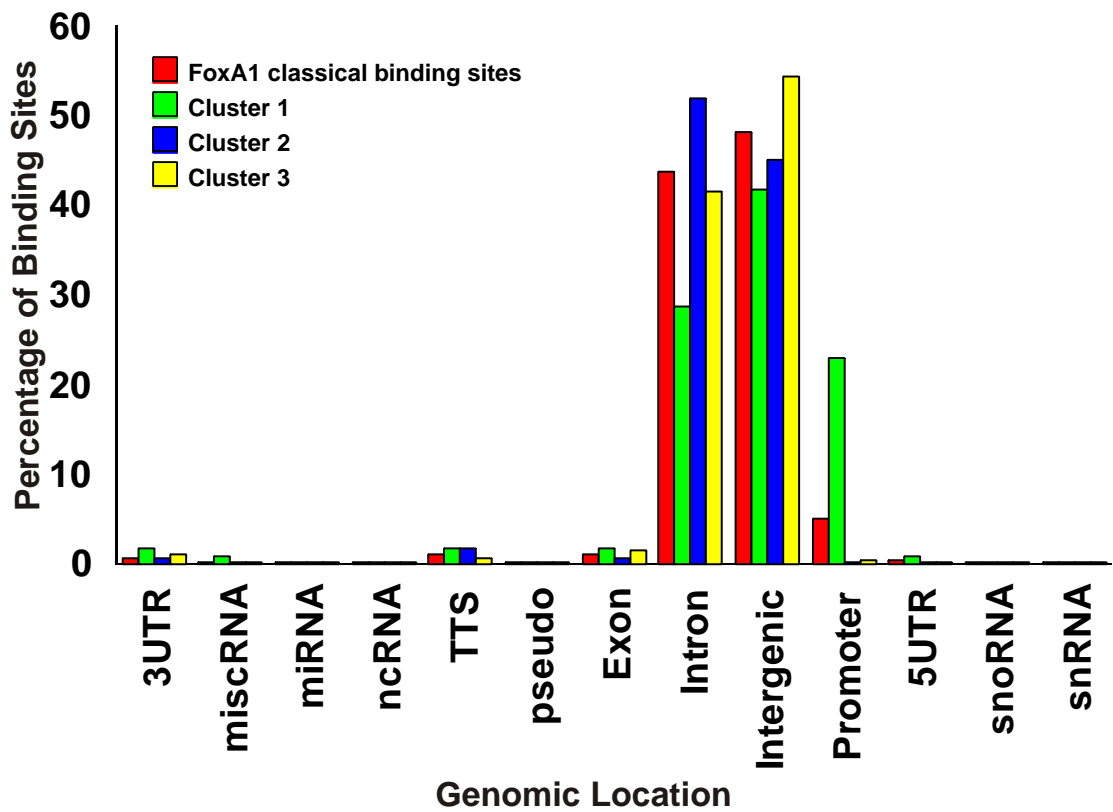
Figure 5.8: Genomic location of FoxA1 and ER binding clusters in MCF-7 breast cancer cells. Comparison of the genome-wide distribution of FoxA1 and ER binding patterns among the three identified clusters including FoxA1 classical sites. Data presented as a percentage of binding sites from each cluster located in the individual genomic locations.

FoxA1 classical binding sites

Motif	Factor	*P* value
	FOXA2	$1e^{-3613}$
	Arid5a	$1e^{-506}$
	AP1	$1e^{-449}$

Cluster 2

Motif	Factor	*P* value
	FOXA1	$1e^{-100}$
	AP1	$1e^{-46}$
	Six1	$1e^{-15}$

Cluster 3

Motif	Factor	*P* value
	ERE	$1e^{-105}$
	AP1	$1e^{-28}$
	Foxo1	$1e^{-22}$

Figure 5.9: Motif analysis of FoxA1 and ER binding clusters. *De novo* motif analysis has been conducted on FoxA1 classical binding sites, cluster 2 (gained sites), and cluster 3 (DynaLoad sites). The data represents the top three most highly enriched motifs determined by Homer.

A E2 vs Unt DHS

FoxA1	Unt	+	+	-	-
	E2	+	-	+	+
ER	E2	-/+	-	-	+

B Chr 2   15 kb

C Chr15   15 kb
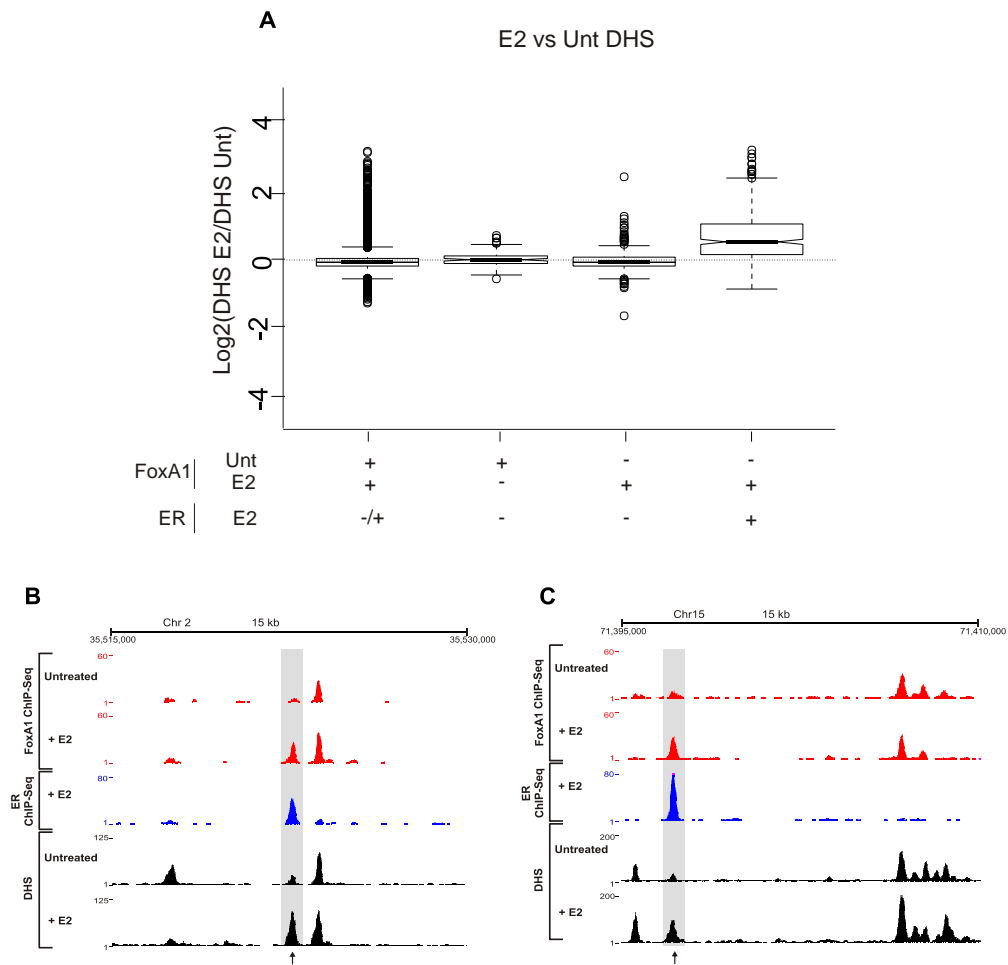
Figure 5.10: Analysis of DHS sites as an indicator of chromatin accessibility at the three FoxA1 and ER binding clusters utilising ENCODE data. A. The changes in E2 stimulated DHS in MCF-7 breast cancer cells (ENCODE) has been determined for each FoxA1 binding module including FoxA1 classical sites. Box plot shows the fold change in E2 stimulated DHS as a Log2 value. Each box correlates to the individual cluster label on the x-axis. **B-C.** Examples of FoxA1 DynaLoad binding in MCF-7 breast cancer cells treated with either 100nM of E2 or left untreated, correlated with ER binding in 100nM E2 treated cells, and DHS in either 100nM E2 treated cells or left untreated. Two genomic regions demonstrate FoxA1 DynaLoad upon E2 treatment which overlaps with ER binding and increased DHS with E2 treatment (UCSC browser shot). The black arrow illustrates a FoxA1 DynaLoad site.
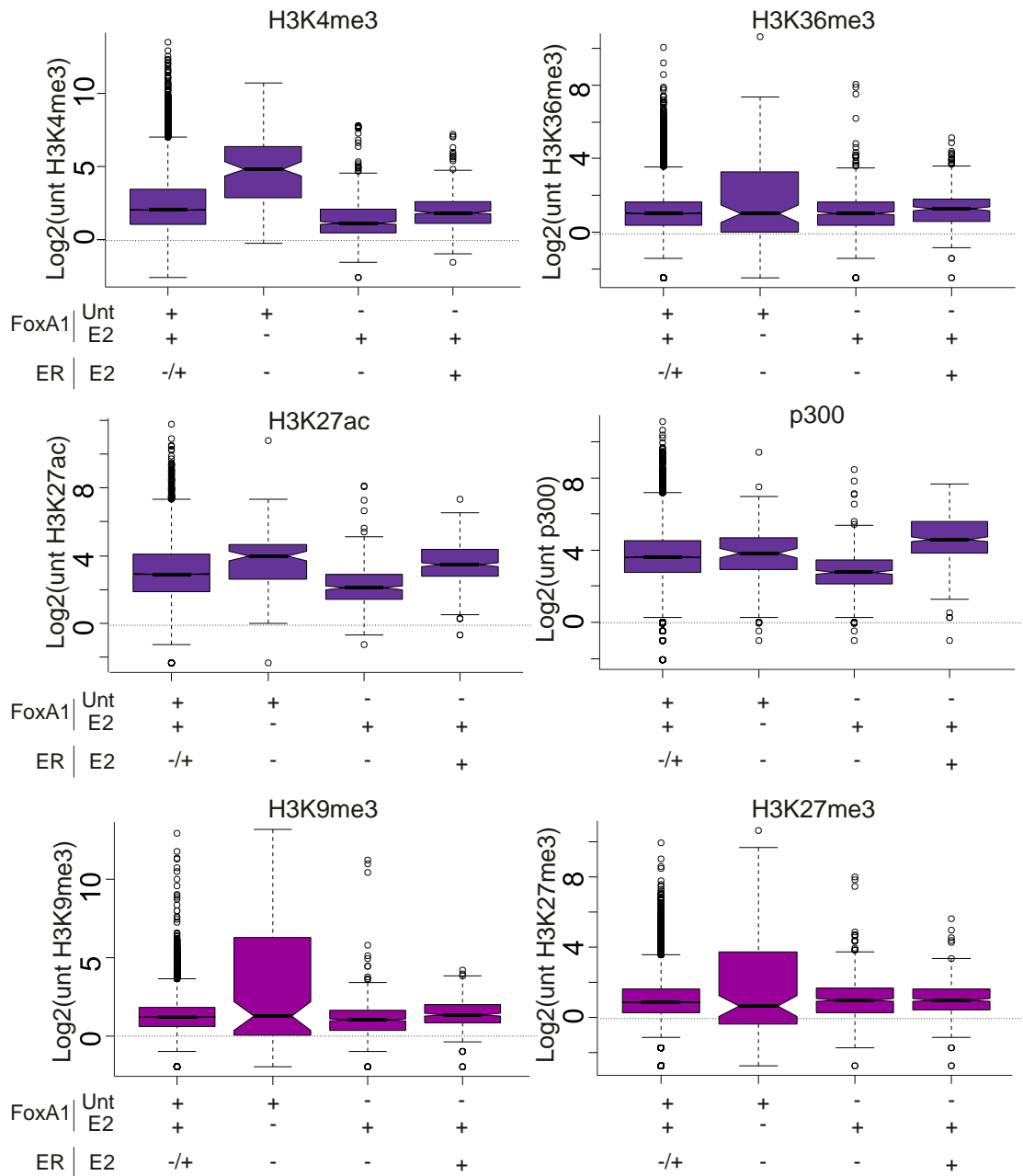
Figure 5.11: Histone modifications at FoxA1 and ER binding clusters. The presence of histone modifications (H3K4me3, H3K36me3, H3K27ac, H3K9me3, and H3K27me3) and p300 in unstimulated MCF-7 breast cancer cells (ENCODE) has been determined for the FoxA1 and ER binding clusters including FoxA1 classical binding sites. The data is presented as box plots which demonstrate overall levels of each histone modification or factor binding at each cluster and is presented as Log2. Each box plot correlates to the individual cluster labelled on the x-axis
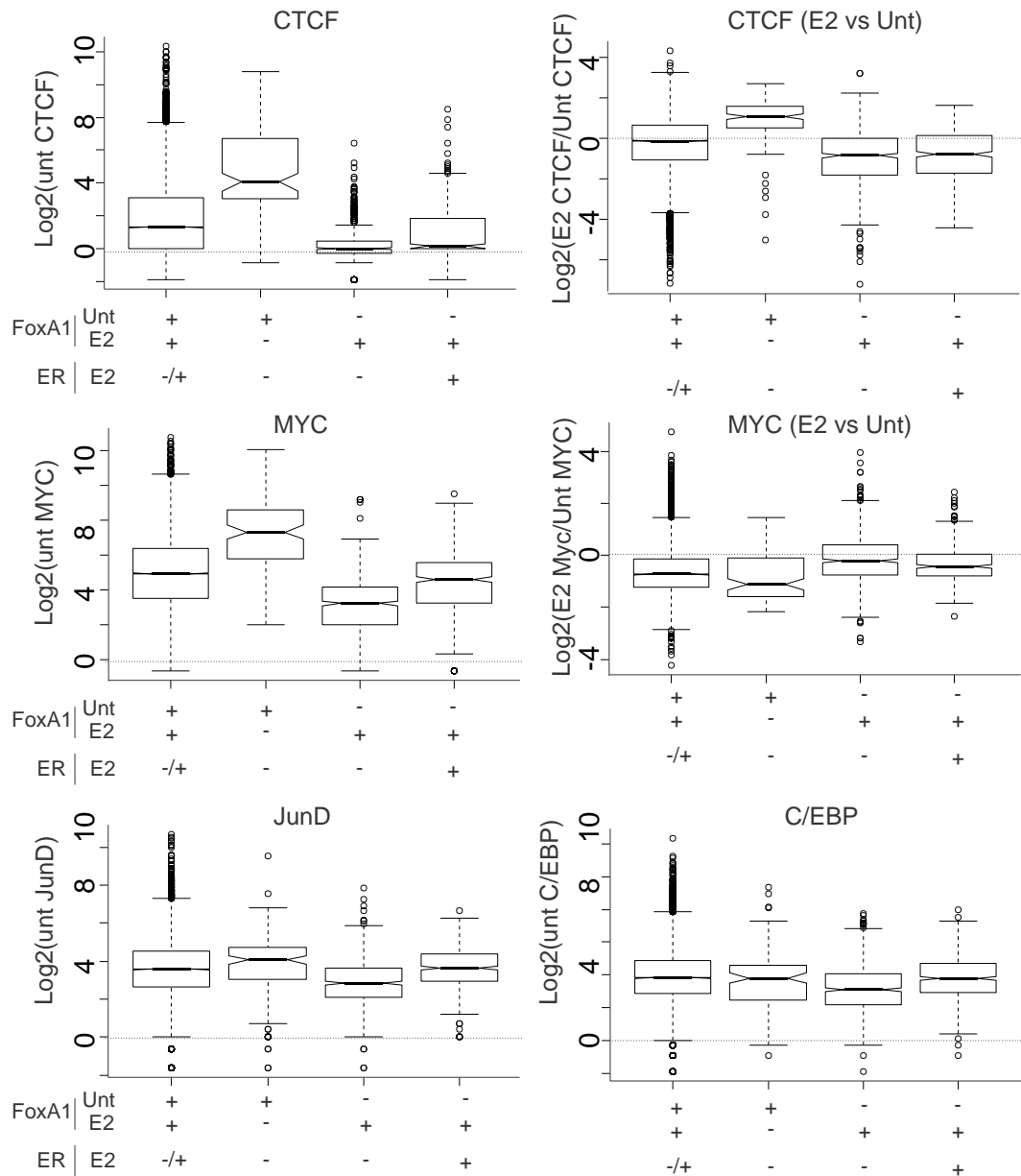
Figure 5.12: Transcription factor association at FoxA1 and ER binding clusters. The presence of transcription factors (CTCF, MYC, JunD, and C/EBP) in MCF-7 breast cancer cells (ENCODE) has been determined for the FoxA1 and ER binding clusters including FoxA1 classical binding sites. CTCF and MYC association has been determined in unstimulated cells and E2 treated cells. JunD and C/EBP association has been determined in unstimulated cells. The data is presented as box plots which demonstrate overall levels of each transcription factor binding at each cluster and is presented as Log2. Each box plot correlates to the individual cluster labelled on the x-axis.
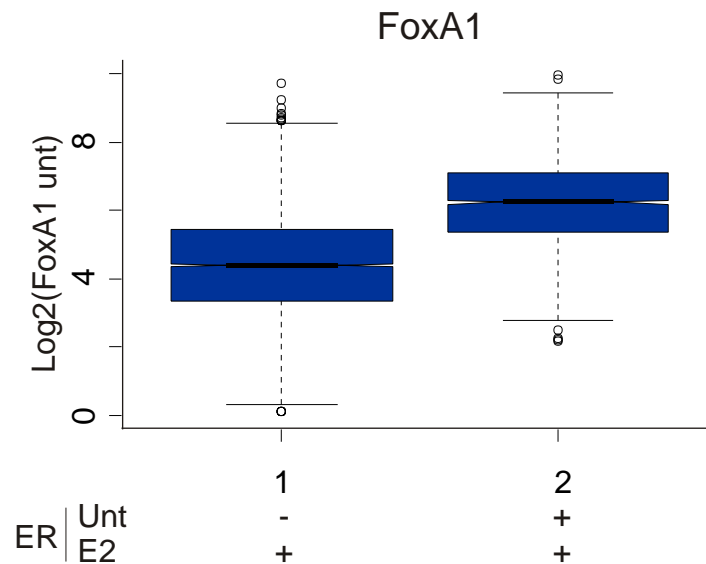
Figure 5.13: The presence of FoxA1 binding at ER binding sites in untreated and E2 stimulated cells. The presence of FoxA1 binding at the two ER binding clusters identified with either E2 treated or untreated MCF-7 breast cancer cells (chapter 4) has been determined. Box plots demonstrate overall levels at each module and are presented as Log2. Each box correlates to the individual module labelled on the x-axis.

Chapter 5 – Molecular Crosstalk Between the Pioneer Factor FoxA1 with Either
GR, ER, or PR in MCF-7 Human Breast Cancer Cells.
Page 157

FoxA1 ChIP
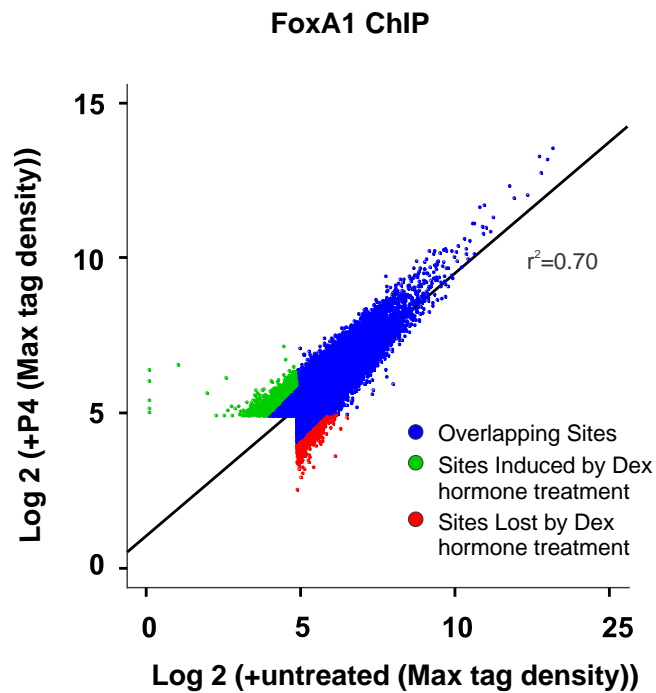
Figure 5.14: Changes in the FoxA1 binding landscape upon P4 hormone treatment in MCF-7 human breast cancer cells. Global changes in FoxA1 binding patterns upon 100nM P4 treatment of cells compared with untreated cells. Binding patterns of FoxA1 have been determined by ChIP-seq after treatment with either P4 or left untreated. Scatterplot represents the global changes in FoxA1 binding between P4 and untreated cells. The sites shown to be either gained or lost by P4 hormone treatment have at least a 2-fold change in tag density.

Chapter 5 – Molecular Crosstalk Between the Pioneer Factor FoxA1 with Either
GR, ER, or PR in MCF-7 Human Breast Cancer Cells.
Page 158
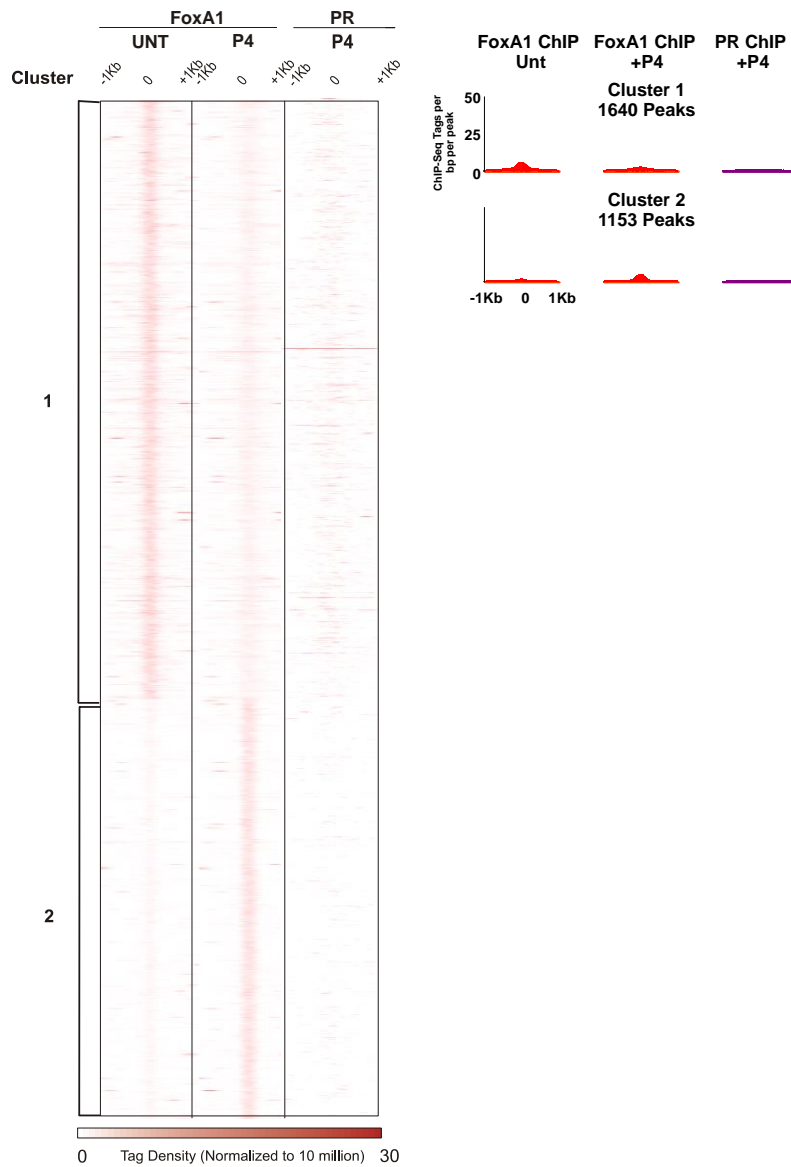
Figure 5.15: Specific FoxA1 and PR binding modules. Supervised clustering analysis of 2799 peaks identified by FoxA1 and PR ChIP-seq in MCF-7 breast cancer cells treated with either 100nM P4 or left untreated. Heatmap analysis portrays the number of reads per 10^6 sequences as well as the position of the reads within 2 kb of ChIP-seq peak. Two different binding clusters have been identified which are notated by the brackets. Histograms represent the overall FoxA1 and PR binding intensities in each cluster for the various treatments within a 2 kb interval of the ChIP-seq peaks.

FoxA1 classical binding sites

Motif	Factor	*P* value
	FoxA1	1e^{-725}
	Myb	1e^{-234}
	Boris	1e^{-217}

Cluster 2

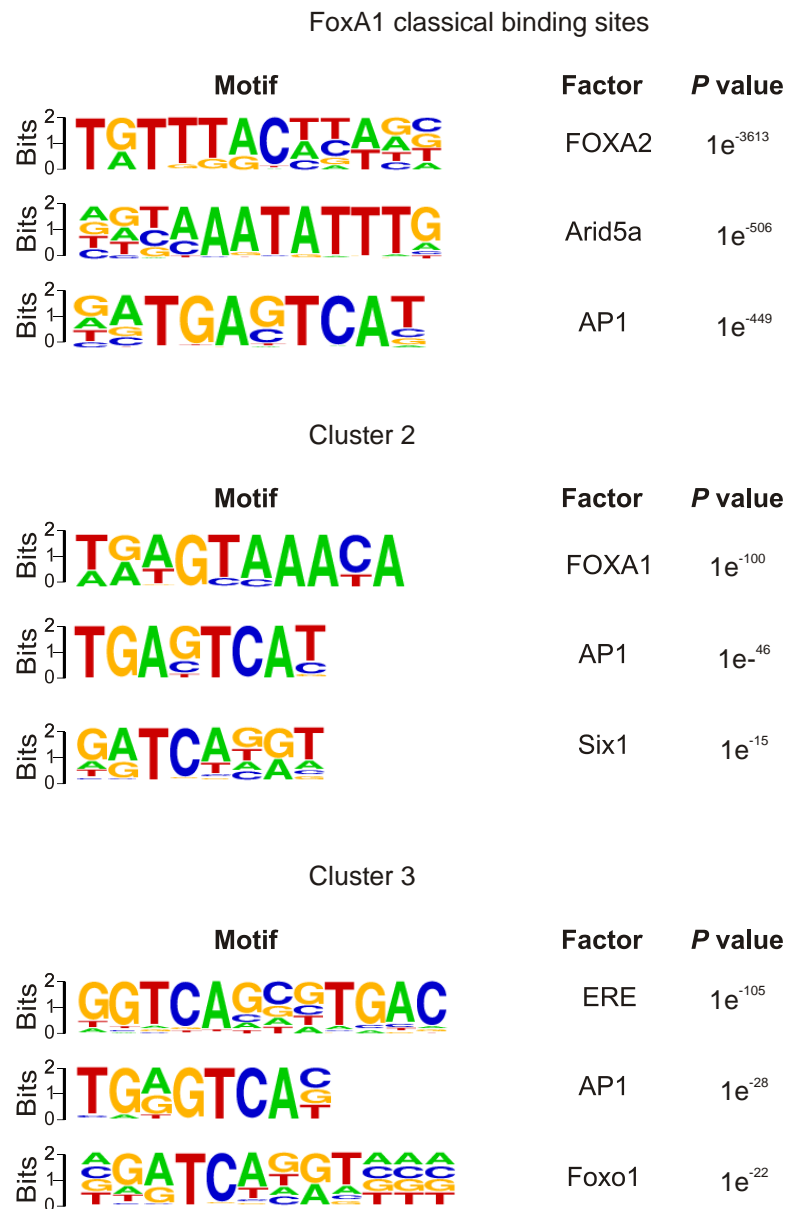| Motif	Factor	*P* value
	FoxA1	1e^{-237}
	Ap1	1e^{-57}
	Gata-IR4	1e^{-37}
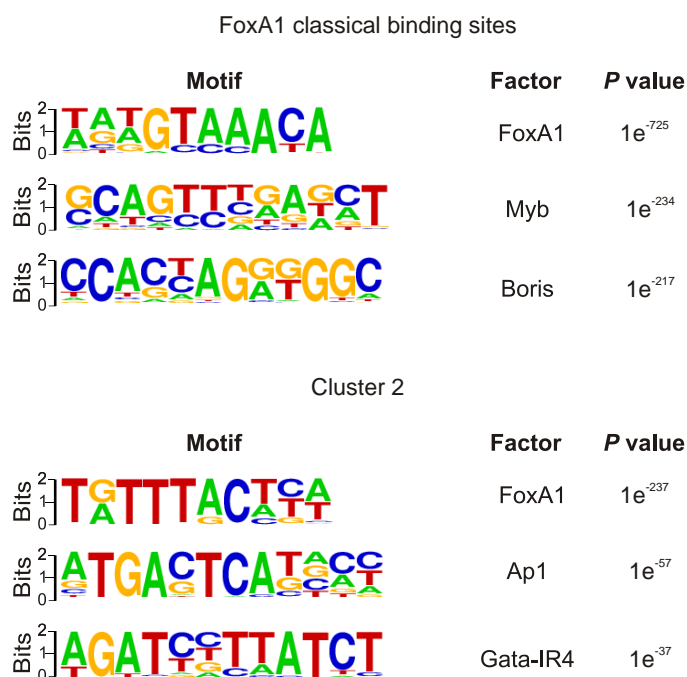
Figure 5.16: Motif analysis of FoxA1 and PR binding clusters. *De novo* motif analysis has been conducted on FoxA1 classical binding sites and cluster 2 (gained sites). The data represents the top three most highly enriched motifs determined by Homer.

Chapter 6

GR, ER, and FoxA1 Interplay in ZR-75-1 and

T-47D Human Breast Cancer Cells

6.1 Introduction

The preceding chapters of this thesis have affirmed that binding of GR, ER, and FoxA1 to DNA can be induced by a DynaLoad mechanism. Chapter 4 revealed that there is a unique subset of GR binding sites which are only accessible to GR binding upon activation of ER. These sites surprisingly lack a GRE motif. Additionally, there is a subset of ER binding sites demonstrating that ER is only recruited to these sites after GR activation. This work validates findings previously described in this laboratory in an artificially engineered system (Miranda, Voss et al. 2013). To complement these findings, chapter 5 has shown that a number of FoxA1 binding sites in MCF-7 cells are reliant on the activation of either GR, ER, or to a less extent PR. Therefore, to gain a better understanding of these dynamic TF systems in breast cancer, the next objective of this thesis is to determine if the findings in previous chapters are a general observation in breast cancer cells, or are specific to a single cell line. To fully gain an in depth understanding of the molecular interplay between GR, ER, and FoxA1 these studies have been repeated in ZR-75-1 and T-47D human breast cancer cells.

It is becoming clear that studies into breast cancer mechanisms need to be carried out in multiple cell line models. Breast cancer is not a single cell disease state. It is known that breast cancer is a collection of cellular settings that have differing histopathology, genetics, genomic variation, abilities to progress at differing rates, and different metastatic potential. In addition, breast cancers can originate from either the ducts of the breast, termed ductal carcinoma, or the lobules, called lobular carcinoma (Hayes 1993). Ductal carcinoma is the most common form of

breast cancer, with there being two subtypes, either ductal carcinoma *in situ* (DCIS) or invasive ductal carcinoma (IDC).

DCIS is neoplastic lesions confined to the ducts, whereas IDC contains cancerous cells that have breached the basement membrane and are infiltrating. Lobular carcinoma also exists in two forms; lobular carcinoma *in situ* (LCIS), which is localised to the lobules, or invasive lobular carcinoma (ILC), which is where the cells have metastasised from the lobules. However, both LCIS and ILC account for a very small percentage of all breast cancers (Hayes 1993). In addition to originating from various sections of the breast, breast cancers can also vary in the expression patterns of receptors. Therefore, in order to fully understand the role of crosstalk between SR in breast cancer development multiple types of cancers and cells should be studied.

Clinically to date, protein expression levels for ER, PR, and human epidermal growth factor receptor 2 (Her2) are the primary markers used to detect what treatment options should be administered to breast cancer patients. Breast cancer tumours can be characterised into three main groups; ER-positive, Her2-amplified, and triple negative, which do not express any of the current biomarkers utilised. Of all breast cancers, up to 70% express ER and PR associating them with a better overall survival (Bardou, Arpino et al. 2003). In addition, tumours that contain high Her2 levels are associated with worse outcomes (Slamon, Clark et al. 1987). More recently, molecular testing has begun to be utilised in the clinic. This has provided further means into detecting tumour aggressiveness, risk of relapse, and better treatment strategies. Comprehensive analysis has allowed the identification of five unique breast cancer molecular subtypes; Luminal A,

Luminal B, Her2 enriched, Basal-like, and Claudin-low (Perou, Jeffrey et al. 1999, Perou, Sorlie et al. 2000, Sorlie, Perou et al. 2001, Network 2012). Luminal A tumours commonly express high levels of ER and PR, whereas Luminal B has high levels of ER and lower PR expression levels. In this extensive study nearly 75% of all tumours were identified as being either Luminal A or Luminal B. They appear to have the most heterogeneity and the least prominent molecular markers. Her2 enriched tumours are generally driven by the amplification of Her2 locus, PR-negative and either ER positive or negative. The Basal-like tumours rarely expressed ER, PR, and Her2 and are driven by phosphatidylinositide 3-kinase pathway mutation (Network 2012). More recently, the claudin-low subtype was described as not expressing ER, PR, or Her2 but differs from basal-like as there is downregulation of claudin-3, claudin-4, and low expression of the proliferation marker Ki67 (Sorlie, Perou et al. 2001). These studies demonstrate that the expression levels of factors are important for breast cancer outcomes and for identifying individual treatment options for patients. Therefore, it is important to understand how receptors interact with one another in various types of breast cancers. The transcriptional profiling of breast cancer cell lines has enabled the classification of cell lines into the different categories. It is now known that MCF-7 and T-47D human breast cancer cell lines represent a model of Luminal A type and ZR-75-1 human breast cancer cells represent Luminal B cancers (Neve, Chin et al. 2006, Mackay, Tamber et al. 2009). MCF-7, ZR-75-1, and T-47D cell lines are all derived from carcinomas of ductal origin (Soule, Vazguez et al. 1973, Engel, Young et al. 1978, Keydar, Chen et al. 1979). By comparing SR crosstalk in these cell lines we can begin to understand how crosstalk plays a role in breast cancer progression.

Therefore, the aim of this chapter is to determine if there are similar DNA binding signatures among different breast cancer models, and if GR and ER DynaLoad is specific to one cell line model or is found throughout different representative breast cancer cells. In addition, I have aimed to determine if the effect of SR activation on FoxA1 binding patterns is specific to one type of ER positive cancer or observed in multiple models. This will provide a more detailed understanding in SRs and TFs in breast cancer cells and allow us the possibility to further characterise breast cancer cell types by SR and TF action.

<div style="border:1px solid black; text-align:center;">

6.2 Methods

</div>

6.2.1 <u>Preparation of cells for ChIP-seq.</u>

6.2.1.1 Seeding of cells.

Cells are maintained as described in chapter 2, section 2.3.1.1. Once cells react 80% confluence they are harvested and their concentration is calculated using a cell haemocytometer. ZR-75-1 and T-47D human breast cancer cells are seeded in phenol red free RPMI 1640 medium that contains 2mM L-glutamine and supplemented with 10% CSS, 1mM sodium pyruvate, 1X non-essential amino acids, 0.2U/mL bovine insulin, and 1% penicillin-streptomycin. The ZR-75-1 cells are seeded at a concentration of 1.5×10^7 cells per mL and the T-47D cells at 8×10^6 cells per mL. Both cell lines are seeded in 150mm cell culture plate at 30mL of media per plate with three plates per treatment required. Cells are left for 48 h before treatment with hormone.

6.2.1.2 Hormone treatment of cells.

After 48 h of cell growth, ZR-75-1 and T-47D cells are treated with either 100nM Dex, 100nM E2, 100nM of Dex + E2, or left untreated for 30 min. To achieve the desired concentration of 100nM, 30uL of 1mM stock solution of the appropriate hormone is added directly to the 150mm cell culture plate containing the medium.

6.2.2 <u>ChIP-seq.</u>

ChIP-seq experiments have been performed as described in chapter 2, section 2.3.2. Specifically, after the ZR-75-1 and T-47D cells are treated with hormone and each 150 mm plate is cross-linked with formaldehyde, cells are scrapped and a cell pellet is collected. The cell pellets are resuspended in 600uL of ChIP lysis buffer containing 1X PI and sonication is performed. The sonication condition for both ZR-75-1 and T-47D cells is 15 cycles for 15 sec on, 30 sec off, at 4º C. All sonication is performed in 15mL sonication tubes. After the DNA is quantified, samples are diluted 5 fold in ChIP dilution buffer and 1X PI to a final concentration of 100ug of chromatin per mL. For each ZR-75-1 and T-47D ChIP sample antibody preparation is performed as follows. Seven ug/uL of GR (E-20X) antibody is linked to 80uL of Dynabeads (M-280) sheep anti-rabbit IgG in the untreated, Dex and Dex + E2 samples. 1.4 ug/uL of ERα (HC-20) antibody and 5 ug/uL of ER (Ab-10) antibody is linked to 40uL of Dynabeads (M-280) sheep anti-rabbit IgG and 40uL of Dynabeads (M-280) sheep anti-mouse IgG in the untreated, E2 and Dex + E2 samples. Seven ug/uL of FoxA1 (ab23738) antibody linked to 80uL of Dynabeads (M-280) sheep anti-rabbit IgG in the untreated, Dex and E2 samples. One hundred uL of each sample is removed and

stored at 4ºC for the no antibody control input. The samples are incubated with the antibody/Dynabead complex overnight and the complex is washed with the appropriate buffers. The samples are eluted from the Dynabeads and a phenol-chloroform-isoamyl extraction is performed. Each sample pellet is suspended in 10uL of nuclease free H_2O. For each cell line the ChIP experiment is repeated four times resulting in four biological replicates. To determine efficient protein binding to chromatin qPCR is utilised. For ZR-75-1 cells, *MYC* forward and reverse primers are utilised for ER and FoxA1 binding (Hurtado, Holmes et al. 2011, Miranda, Voss et al. 2013) and *PER1* forward and reverse primers are utilised for GR binding. Currently, there are no known GR, ER, and FoxA1 binding sites in T-47D breast cancer cells. However, GR did demonstrate binding to the *PER1* site in the T-47D cell line. Two biological replicates for each ChIP experiment are pooled resulting in two replicates per sample set, and submitted to the National Cancer Institute Advanced Technology Program Sequencing Facility for sequencing services.

6.2.3 <u>Bioinformatic analysis.</u>

The Illumina HiSeq genome analyser platform has been used to generate sequence reads (36-mer) and unique tags have been aligned to the human reference genome (UCSC hg19 assembly). Hotspots, regions of enriched tags, have been called using previously described methods with minor modifications (Baek, Sung et al. 2012). The values for the tag densities have been normalised to 10 million reads to adjust for differences in the depth of sequencing between samples. The data sets have been adjusted by subtracting tags found in the input. Hotspots have been called using a 0% FDR. A tag density threshold of 30 has

been applied to all sample sets except for FoxA1 ChIP-seq in T-47D cells. Due to the overall lower tag density values, the tag threshold FoxA1 ChIP-seq in T-47D cells has been set at 12, which represents the mode for this sample set. Replicate concordants have been calculated between replicates. For comparison of GR, ER, and FoxA1 data sets, regions were considered to overlap if they shared at least 1 bp. Peaks unique to the hormone treatments are then identified. Using these peaks, a list of unique chromosomal positions has been created by removing overlapping peaks from the samples being compared (GR-ChIP +Dex, GR-ChIP +Dex + E2, ER-ChIP +E2, ER-ChIP +Dex + E2; GR-ChIP +Dex, FoxA1-ChIP untreated, FoxA1-ChIP +Dex; ER-ChIP +E2, FoxA1-ChIP untreated, FoxA1-ChIP +E2). Supervised clustering of the peaks has been conducted tagging each unique peak for presence or absence of binding in the experiments and ordering them according to these tags across the samples. Using Homer, the total number of sequence reads under the peaks for each ChIP-seq sample has been extracted and corrected for the total number of reads in the sample (reads under peak/ 10M total reads) so that a heat map could be generated utilising MeV.

Binding modules have been compared between cell lines by looking for overlapping peaks using Homer (Heinz, Benner et al. 2010). For box plots, Homer has been used to retrieve the total number of sequence reads for the ENCODE data under the peaks for each module analysed. Plots have been graphed using the statistical program R. The distribution of H3K27ac and the motif distribution have been constructed using Homer (Heinz, Benner et al. 2010). *De novo* motif analysis has been conducted using Homer (Heinz, Benner et al. 2010). Frequency of finding an ERE, GRE, FoxA1, or AP-1 binding site

within different binding modules have been determined using FIMO. Results are reported as the number of motif occurrences per number of binding sites within a cluster (pval of $< 1e^{-5}$).

<div style="border:1px solid black; text-align:center">

6.3 Results

</div>

6.3.1 <u>Validation of GR, ER, and FoxA1 binding in ZR-75-1 and T-47D human breast cancer cell ChIP samples.</u>

ChIP-seq experiments have been performed to assess the binding patterns genome-wide of GR, ER, and FoxA1 in ZR-75-1 and T-47D breast cancer cells under differing hormone treatments. For GR binding, cells have been stimulated with 100nM of either Dex, Dex + E2, or left untreated. For ER binding, cells have been stimulated with 100nM of either E2, Dex + E2, or left untreated. For FoxA1 binding, cells have been stimulated with either 100nM of Dex, E2, or left untreated. To ensure efficient binding of GR, ER, and FoxA1 in all ZR-75-1 ChIP samples qPCR analyses are performed using primers designed to protein binding sites that have been previously shown to bind these factors in MCF-7 cells. In ZR-75-1 cells GR binding is increased at the *PER1* site when treated with Dex and Dex + E2 compared to untreated cells (Figure 6.1A). In ZR-75-1 cells treated with E2, ER binding at the *MYC* site is increased compared with other treatments groups (Figure 6.1B) In ZR-75-1 cells FoxA1 binding at the *MYC* site is present in all treatment groups (Figure 6.1C).

In T-47D cells, GR binding is present at the *PER1* site in the Dex and Dex + E2 samples (Figure 6.2A), and FoxA1 binding is present in all treatment groups at

the *MYC* site (Figure 6.2B). However, ER did not bind the *MYC* site as shown for MCF-7 and ZR-75-1 cells. This data indicates that the ChIP experiment has resulted in efficient GR and FoxA1 binding suitable for sequencing. Upon performing sequencing, the ChIP-seq data reveals that there is still efficient binding of ER across the genome in T-47D breast cancer cells.

6.3.2 <u>Co-treatment of ZR-75-1 human breast cancer cells with Dex and E2 induces changes in the GR and ER binding landscape genome-wide.</u>

To investigate if the mechanisms observed in MCF-7 cells are unique to that cell line, or are also found to be widespread among other breast cancer cell models, GR and ER binding events have been mapped in ZR-75-1 cells. The cells are stimulated with either Dex, E2, Dex + E2, or left untreated. Analysis of GR ChIP-seq samples, upon stimulation with Dex and Dex + E2, reveal a total of 8894 binding sites. While 7021 sites are common to the single and dual treatments, only 142 are found in the single Dex treatment and 1731 are gained in the dual treatment conditions (Figure 6.3A). Analysis of the ER ChIP-seq data upon E2 and Dex + E2 treatment reveal a total of 5288 sites. Of these total sites 4979 are found to be in common with both treatments. 6 sites are found to be unique to the single treatment of E2; however, 303 are gained upon the addition of Dex (Figure 6.3B).

To further investigate the overall change in GR and ER binding patterns, supervised clustering analysis has been performed for GR and ER incorporating the untreated, single, and dual treatment samples. This analysis reveals ten unique binding modules (Figure 6.4). Cluster 1 represents GR and ER binding

sites common to all hormone treatment groups (255 peaks). Clusters 6 (6628 peaks) and 8 (4347 peaks) represent the classical GR and ER binding sites respectively. However, as previously observed in MCF-7 cells, there is also ER binding in the untreated, E2, and Dex + E2 samples at the GR classical binding sites. In chapter 4, three DynaLoad clusters are in MCF-7 cells. This mechanism is also observed here in ZR-75-1 cells at three clusters. Cluster 2 (140 peaks) demonstrates ER binding sites only in the presence of Dex + E2 and overlaps with GR binding in the single and dual treatments representing ER DynaLoad. Clusters 5 and 7 both demonstrate GR DynaLoad upon the addition of E2 and much like in MCF-7 cells (chapter 4), there are two separate clusters. Cluster 5 (1336 peaks) represents GR gained sites with Dex + E2 only and overlaps with ER binding at the untreated, E2, and Dex + E2 samples. Cluster 7 (370 peaks) closely matches cluster 5; however, ER does not bind at these sites in the untreated samples.

Cluster 3 (26 peaks) denotes ER and GR binding only in the dual treatment group and cluster 4 (138 peaks) demonstrates ER sites that are gained with the Dex + E2 treatment but do not overlap with GR binding. Cluster 9 (6 peaks) and cluster 10 (143 peaks) demonstrates a lost in ER or GR binding with the dual treatment. Cluster 10 is GR lost sites that overlap with ER binding in the untreated, E2, and Dex + E2 groups. These findings are different in comparison to what is observed in the MCF-7 cells in chapter 4. The MCF-7 cells demonstrate a larger decrease in GR binding suggesting receptor levels could play an important role. MCF-7 cells contain higher levels of ER. These higher levels have the potential to squelch more GR co-factors thereby inhibiting GR binding at more sites.

Genomic localisation analysis of all cluster patterns revealed that the majority (40-80%) of binding patterns for each cluster fall in intron and intergenic regions (Figure 6.5).

6.3.3 <u>Motif analysis of GR and ER binding clusters in ZR-75-1 human breast cancer cells.</u>

In order to determine the prevalent binding sequences within the GR and ER clusters, *de novo* motif analysis was performed utilising Homer software (Figure 6.6). At ER DynaLoad sites there is a high prevalence for GRE, FoxA2, and GATA3 binding sequences. Similar to the ER DynaLoad sites in MCF-7 cells, there is no ERE found at these sites. In addition, at GR DynaLoad with the presence of ER binding in the untreated samples, there is an ERE binding motif as the most commonly observed sequence. These sites do not contain a GRE motif. Analysis of cluster 7 sites, which also represent GR DyanLoad with ER binding only in the E2 and Dex + E2 samples, reveal there is only a nuclear receptor class binding sequence. GR classical binding elements contain a GRE and FoxA1 motif sequence, and ER classical binding sites contain an ERE and FoxA1 motif, as has been previously observed. For GR lost sites, the only motif of statistical significance is a FoxA1 sequence. Motif modules have not been identified for clusters 3 and 9, and analysis for clusters 1 and 4 can be found in appendix 1E.

6.3.4 <u>Co-treatment of T-47D human breast cancer cells with Dex and E2 induces changes in the GR and ER binding landscape genome-wide.</u>

GR and ER binding patterns were mapped in T-47D breast cancer cell lines to further investigate the notion of ER and GR DynaLoad in breast cancer cells.

This cell line has lower GR and ER steady state protein levels than MCF-7 and ZR-75-1 cells (chapter 3). Investigation of GR binding patterns treated with Dex versus Dex + E2 revealed a total of 841. 492 sites are found to be in common with both the single and dual treatments with 10 sites being specific to Dex and lost with the addition of E2. There are also 339 sites gained with the addition of E2 and are unique to the dual treatment (Figure 6.7A). In addition, ER ChIP-seq analyses reveal similar binding distribution patterns with a total of 2302 sites mapped. Of these sites, 2221 are in common with the single and dual treatments and 23 sites are unique to E2 alone and lost upon the addition of Dex. Further, 58 sites are unique to the dual treatment of Dex + E2 (Figure 6.7B). Together this represents a lower number in GR and ER binding sites than previously observed for the MCF-7 and ZR-75-1 cell lines. However, both analyses suggest there is still a possible GR and ER DynaLoad in this cell model.

Supervised clustering has been performed as previously described and identified 9 unique clusters; however, the peaks are relatively low compared to the other cell lines utilised in this study (Figure 6.8). Cluster 1 (14 peaks) represents GR and ER binding in both the single and dual treatments. Cluster 7 (2195) represents the classical ER binding sites under E2 and Dex + E2 stimulation. The classical GR binding sites are represented in cluster 5 (46 peaks) and as previously observed in the other two cell lines these sites do overlap with ER binding sites in the untreated, E2, and Dex + E2 samples. Cluster 2 (13 peaks) represents ER DynaLoad sites with ER binding only in the Dex + E2 samples. ER binding at these sites overlaps with GR binding. Again, as previously identified in the two other cell models, there are two clusters that represent GR DynaLoad sites.

Cluster 4 (326 peaks) demonstrates GR binding in the Dex + E2 samples only. These sites overlap with ER binding found in the untreated, E2, and Dex + E2 samples. Cluster 6 (12 peaks) demonstrates GR binding with Dex + E2 only and overlaps with ER binding at the E2 and Dex + E2 samples only. Cluster 3 (43 peaks) denotes ER and GR binding in the dual treatments. Clusters 8 and 9 represent ER and GR binding that decreases with the dual treatment respectively. The major finding in MCF-7 cells (chapter 4) was the massive inhibition on GR binding upon E2 stimulation. This is not observed in T-47D cells. The majority of peaks from all clusters are spread among the intron and intergenic regions. Of interest, approximately 90% of cluster 9 is located in the intergenic region and the remaining 10% in the introns (Figure 6.9).

6.3.5 <u>Motif analysis of GR and ER binding clusters in T-47D human breast cancer cells.</u>

To further rationalise the DynaLoad mechanism and also identify what binding recognition elements are present at the different clusters, *de novo* motif analysis has been performed utilising Homer software. However, due to the low number of peaks identified in each cluster, *de novo* analysis did not provide any significant motifs. Therefore each cluster has been screened for enrichment of known motifs (Figure 6.10). ER DynaLoad sites (cluster 2) show a high prevalence for GRE. Clusters 4 and 6, which represent GR DynaLoad sites, both contain either SR motifs or an ERE and FoxA1 motif. GR classical binding sites (cluster 5) contained a GRE as the top known motif, and cluster 7 (ER classical binding sites) contains an ERE as the top known motif. Motif analysis performed on the remaining clusters can be found in appendix 1F. While *de novo* analysis

cannot be performed, this analysis still provides evidence that the motifs present at the DynaLoad sites are similar in all three cell lines.

6.3.6 Investigation of GR and ER clusters identified in MCF-7, ZR-75-1, and T-47D breast cancer cell lines.

Due to the observation that ER and GR DynaLoad is a general finding among breast cancer cells, further investigation of this mechanism has been conducted. Cross analysis between the DynaLoad binding sites in each cell line has been done in order to determine if there is any commonality between these binding elements. Very little crossover is observed between the ER DynaLoad sites in all three cell lines (Figure 6.11A). To further investigate the binding modules in all three cell lines, FIMO analysis is utilised at a P value of $< 1e^{-5}$ to investigate the overall percentage of GRE, AP-1, ERE, and FoxA1 binding motifs at the ER DynaLoad sites (Figure 6.11B). As previously described in this thesis, each of these clusters contains a GRE as the top motif. No prevalence of an ERE or FoxA1 is found at these sites in any of the three cell lines. Further, an AP-1 motif is identified in MCF-7 cells, supporting previous studies that indicate ER is recruited to a subset of sites tethered to AP-1 upon activation of GR (Miranda, Voss et al. 2013). However, this motif had no significance at the ER DynaLoad sites in ZR-75-1 and T-47D cells upon motif analysis. Analysis of specific motifs in all three cell lines demonstrate that approximately 60% of MCF-7 sites in this cluster contain a GRE, compared with approximately 45% and 80% in ZR-75-1 and T-47D cells, respectively. This reveals that GRE is a prevalent binding sequence at these sites in all three cell lines. Interestingly, approximately 45% of sites in the MCF-7 cells and 20% of ZR-75-1 cells contain an AP-1 motif. It is

possible that other factors may be important for ER recruitment to these sites in these cell lines. While it has been demonstrated that AP-1 is required to tether ER to DynaLoad sites, the lack of the AP-1 binding sequence in ZR-75-1 and T-47D cells may be due to limited availability of AP-1 in these cells. As expected at these sites, there is a limited representation of ERE and FoxA1 binding modules. Overall, this provides strong evidence suggesting that GR is binding at ER DynaLoad sites and is involved in the recruitment of ER. The lack of an ERE suggests that ER is not recruited to these sites by a direct interaction with the DNA.

In order to understand why there is very little overlap between the ER DynaLoad sites across the three cell lines, the question as to why ER does not bind to the sites identified in the T-47D and ZR-75-1 cells in the MCF-7 cells has been assessed. The ER DynaLoad sites identified in the three cell lines have been separately analysed for the presence of histone modifications in untreated MCF-7 cells. The analysis shows that the ER DynaLoad sites present in MCF-7 cells contain high levels of acetylation at lysine 27 in histone H3. In contrast, sites identified in T-47D and ZR-751 cells have very low levels of acetylation in the MCF-7 cells (Figure 6.12). Further analysis shows that the acetylated histones flank the MCF-7 DynaLoad binding sites, and that there is very little difference in DHS between the sites that ER binds to in the MCF-7 cells versus the binding positions identified in the T-47D and ZR-75-1 cells (Figure 6.13). This suggests that the sites in the MCF-7 cells that recruit ER through a DynaLoad mechanism are pre-marked with H3K27ac. Therefore, ER does not bind to the sites identified in the T-47D and ZR-75-1 cells in the MCF-7 cells due to the lack of histone

acetylation at these sites. The occupancy of FoxA1, GATA3, CTCF, and MYC has also been assessed in untreated MCF-7 cells. However, no differences in binding is observed for these factors between the DynaLoad sites identified in the MCF-7 cells and the sites found in the T-47D and ZR-75-1 cell lines (Figure 6.14).

Further, a cross analysis of the GR DynaLoad clusters reveals very little crossover between cell lines (Figure 6.15A-B). However, the ZR-75-1 cells contained approximately 80% more sites in these clusters, compared with the MCF-7 and T-47D cells combined. Since the ZR-75-1 cells do contain higher levels of GR, this suggests that expression levels can affect the distribution of binding patterns. To understand the mechanism that specifically tags the binding elements in MCF-7 for GR DynaLoading the two clusters have been combined and histone modifications for the sites identified in the three cell lines have been individually assessed in untreated MCF-7 cells. No differences in H3K4me3, H3K27ac, H3K9me3, or H3K27me3 are observed between the three different clusters of sites (Figure 6.16A); however, GR DynaLoad sites found in MCF-7 cells contain higher levels of CTCF compared to the binding elements that have been identified in the T-47D and ZR-75-1 cells (Figure 6.16B). This suggests that CTCF may play a role in recruiting GR to the DynaLoad sites in MCF-7 cells. CTCF binding is lower at the GR DynaLoad sites identified in T-47D and ZR-75-1, suggesting that GR does not bind to these sites in MCF-7 cells due to the low levels of CTCF found at these sites.

Due to the very high level of GR lost sites in the MCF-7 cells, cross analysis of these clusters in the three cell lines has been conducted. Consequently, in MCF-7

cells, two clusters are identified. The cluster with no ER binding in the untreated samples (cluster 9) is not observed in the ZR-75-1 and T-47D cells. Therefore, the two GR lost clusters in MCF-7 cells are combined and compared with the GR lost sites identified in ZR-75-1 and T-47D cells (Figure 6.17). Again, as previously observed, there was very little crossover with only 21 sites in common between MCF-7 cells and ZR-75-1 cells. There are 95% more binding sites in MCF-7 cells compared with ZR-75-1 and T-47D cells combined, suggesting that this mechanism is more prevalent in the MCF-7 cells. Since GR levels are lower in MCF-7 cells, ER is able to more efficiently inhibit GR binding.

6.3.7 <u>Activated GR alters the FoxA1 genomic response in ZR-75-1 human breast cancer cells.</u>

To further investigate the findings in chapter 5 that show activated GR can redistribute FoxA1 binding patterns, FoxA1 ChIP-seq in ZR-75-1 breast cancer cells under Dex and untreated conditions has been performed. There are a total of 27,398 FoxA1 binding sites, with 27,060 common to both untreated and Dex. There are 61 sites specific to the unstimulated cells, and 277 gained in the presence of Dex (Figure 6.18). To further determine if GR is playing a role in the observed FoxA1 sites gained by the stimulation of cells with Dex, supervised clustering analysis has been performed (Figure 6.19A). Analysis of the FoxA1 binding elements that are unique to either untreated cells or cells that are stimulated with Dex compared with GR Dex ChIP-seq revealed three specific clusters. Cluster 1 (62 peaks) shows FoxA1 gained sites that are activated by Dex but do not overlap with GR binding. Cluster 2 (215 peaks) represents FoxA1 gained sites that do overlap with GR binding, suggesting these sites are FoxA1

DynaLoad sites. In MCF-7 cells, with lower GR levels, this effect is not as prominent. Cluster 3 (60 peaks) contains sites that are lost with Dex treatment and do not overlap with GR. In order to understand what is unique about the FoxA1 DynaLoad sites in cluster 2, *de novo* motif analysis at all cluster data sets has been performed (Figure 6.19B). Cluster 2 contains a GRE as the most highly enriched binding motif at these sites. This suggests FoxA1 may not be recruited by direct interactions with DNA at these DynaLoad sites. The other observed clusters do not contain a GRE, but do have a FoxA1 motif. This provides further evidence that GR can reshape the FoxA1 landscape at a subset of sites and may play an important role in breast cancer. Motif analysis of FoxA1 classical binding sites excluded from the supervised clustering, cluster 1, and cluster 3 are found in appendix 1G.

6.3.8 <u>Activated ER can alter the FoxA1 genomic response in ZR-75-1 human breast cancer cells.</u>

To determine if the findings in chapter 5, demonstrating that activated ER can alter the FoxA1 binding landscape in MCF-7 cells, correlates to other breast cancer cells FoxA1 ChIP-seq in E2 and untreated ZR-75-1 cells has been performed. Analysis reveals a total of 27,218 sites mapped, with 25,178 common to the untreated and E2 groups. 1,342 sites are found only in the untreated group and upon E2 stimulation 698 sites are gained (Figure 6.20). In total, this is a higher number of affected FoxA1 binding sites than is observed in MCF-7 cells. Utilising the ER ChIP-seq data from E2 stimulated ZR-75-1 cells, supervised clustering analysis has been performed to determine if there is a correlation between FoxA1 and ER binding at specific sites (Figure 6.21A). Omitting FoxA1

sites common to the untreated and E2 stimulated group (FoxA1 classical binding sites), there are four unique clusters identified. Cluster 1 (14 peaks) represents FoxA1 sites gained upon E2 treatment that don't overlap with ER binding sites. Cluster 2 (682 peaks) contains FoxA1 sites gained upon E2 stimulation that overlap with ER binding sites, demonstrating FoxA1 DynaLoad. The number of DynaLoad sites observed in the ZR-75-1 cells is higher than what is observed at the same cluster in MCF-7 cells (chapter 4). Cluster 3 (14 peaks) contains FoxA1 sites lost by E2 treatment that overlap with ER binding. Lastly, cluster 4 (1326 peaks) represents FoxA1 binding sites lost upon E2 treatment that do not overlap with ER binding. Binding events in this cluster suggest long-range interactions with ER may be playing a role at these sites. It is important to note that this cluster is not observed in MCF-7 cells (chapter 4). To determine specific binding motifs at each cluster including FoxA1 classical binding sites, *de novo* motif analysis has been utilised using Homer software (Figure 6.21B). FoxA1 DynaLoad sites contain an ERE motif as the most prevalent motif. Sites in this cluster lack a FoxA1 motif. These results suggest that FoxA1 is not recruited to DynaLoad sites through direct DNA binding with DNA. This is in accordance with what is observed at other DynaLoad sites. Due to the low number of peaks in cluster 3, a motif of statistical significance was not observed. Motif analysis for FoxA1 classical binding sites, cluster 1, and cluster 4 can be found in appendix 1H.

6.3.9 FoxA1 binding patterns genome-wide are altered by activate GR and ER in T-47D human breast cancer cells.

To further investigate the notion that activated ER, and to a lesser extent activated GR, can alter the FoxA1 genomic response in breast cancer cells, FoxA1 ChIP-seq has been performed in T-47D breast cancer cells under stimulation of Dex, E2, or left untreated. Analysis of FoxA1 binding in untreated cells compared with Dex treated cells reveals 27,787 total binding sites. Of that total, 26,252 are found to be in common with untreated and Dex treated cells and 982 are unique to the untreated samples and are lost upon Dex treatment. Further, 548 are gained when Dex is added to the cells and are specific to that treatment group (Figure 6.22A). Analysis of FoxA1 ChIP-seq data in cells stimulated with E2 or left untreated reveal a very similar pattern with a total number of 27,806 peaks. 26,489 sites are found to be common, with 751 sites specific to the untreated cells, and are lost upon addition of E2. 566 sites are gained in the presence of E2 and are unique to that treatment group (Figure 6.22B). To determine if GR and ER have a specific role in FoxA1 binding, supervised clustering analysis has been performed on each individual data set as previously described. Analysis of FoxA1 sites unique to untreated and Dex only compared with GR sites activated with Dex reveals four individual clusters. Cluster 1 represents FoxA1 DynaLoad sites; however, this cluster only contains 14 peaks. The majority of FoxA1 sites induced by Dex treatment do not overlap with GR binding in this cell line (cluster 2; 534 peaks). Cluster 3 (63 peaks) and cluster 4 (919 peaks) represent FoxA1 binding sites that are lost upon GR activation (Figure 6.23).

Further analysis of FoxA1 binding sites unique to either the untreated or E2 treated cells has been crossed with ER binding sites activated by E2 treatment. There are four clusters identified in this analysis. Cluster 1 (182 peaks) represents FoxA1 binding sites upon E2 treatment that overlap with ER sites. While cluster 2 contains gained sites that do not correspond with ER binding. Clusters 3 (4 peaks) and 4 (747 peaks) represent FoxA1 binding sites that are lost upon E2 treatment (Figure 6.24). These findings show that activated ER can reshape the FoxA1 binding patterns in T-47D cells. Motif analysis has been performed for all FoxA1/GR and FoxA1/ER clusters (Figure 6.25A-B). The analysis has shown that the T-47D cells have a similar motif distribution across the binding modules as the MCF-7 and ZR-75-1 cells. Together this suggests hormones can modulate a FoxA1 response and provides evidence to indicate FoxA1, GR, and ER levels play a prominent role in modulating a response.

6.3.10 <u>Investigation of FoxA1 DynaLoad by ER activation in MCF-7, ZR-75-1, and T-47D human breast cancer cell lines.</u>

The results presented thus far show that there is a strong representation of FoxA1 DynaLoad binding sites upon activation of ER in all three cell lines. To further determine if there are any common sites in the FoxA1 DynaLoad between the three cells lines, a cross-analysis has been performed. The venn diagram demonstrates there are 70 sites in common between the MCF-7 and ZR-75-1 cells and 46 common between the T-47D and ZR-75-1 cells (Figure 6.26A). The ERE motif was the highest binding sequence identified at these binding sites, therefore, a FIMO motif analysis has been conducted to determine the percentage of the ERE motif sequences at these sites compared with FoxA1 in all three cell lines,

including the FoxA1 only sites identified in MCF-7 cells (Figure 6.26B). Using a pval of $< 1e^{-4}$ it is demonstrated that the majority of FoxA1 DynaLoad sites contain a strong ERE compared with the classical FoxA1 binding sites which have a low prevalence for an ERE. The classical FoxA1 binding sites contain a FoxA1 motif. The prevalence of this motif in the DynaLoad clusters is low. This provides strong evidence to suggest that ER is binding directly to the DNA at these FoxA1 DynaLoad sites and recruits FoxA1 to these sites. To identify factors that may pre-mark the FoxA1 DynaLoad sites, the presence of histone modifications, CTCF, GATA3, and MYC at the identified sites have been assessed in untreated MCF-7 cells. No differences are observed in H3K27ac, H3K4me3, H3K9me3, or H3K27me3 levels between the sites (data not shown). However, the FoxA1 DynaLoad sites found in MCF-7 cells have overall lower levels of CTCF in the untreated MCF-7 cells, compared with the sites observed in the ZR-75-1 and T-47D cells (Figure 6.27). This suggests that the higher levels of CTCF at these sites in the untreated MCF-7 cells may prevent ER from recruiting FoxA1 to these sites. Similar results are seen in chapter 5. The FoxA1 binding sites that are lost upon stimulation of MCF-7 cells with E2 have an increase in CTCF binding.

6.4   Discussion

It is known that in a physiological setting breast cancer is not a single disease state, but is comprised of multiple syndromes each distinguished by a set of individual factors. This highlights the importance of investigating the mechanisms of breast cancer in multiple breast cancer cell lines. In this chapter,

genome-wide investigation of ER, GR, and FoxA1 DynaLoad has been conducted in ZR-75-1 and T-47D breast cancer cell lines. This allows for the results obtained for the MCF-7 cells in chapter 4 to be compared to alternative breast cancer cell models which represent both the luminal B and luminal A breast cancers. The findings of this chapter provide further evidence supporting ER and GR's ability to redistribute each others binding patterns upon activation, and further establishes the role of activated ER in altering FoxA1's genomic response. In addition, this chapter provides strong evidence that in cell lines that highly express GR, activated GR can function to alter a unique subset of FoxA1 binding sites.

Genome-wide ChIP-seq analysis of GR and ER binding patterns in the ZR-75-1 and T-47D breast cancer cells reveals binding modules that are similar to those observed in the MCF-7 cells. However, in MCF-7 cells, there is a greater inhibition of GR binding upon ER activation compared to the other cell lines. This may be due to the high level of expression of ER and the low levels of GR found in the MCF-7 cells. Previous studies have shown that patients expressing high levels of GR are associated with a significantly better prognosis in ER positive breast cancers compared with ER negative cancers (Pan, Kocherginsky et al. 2011). This suggests that ER has the ability to inhibit the potential negative transcription effects of GR by inhibiting GR binding in some breast cancers. Therefore, it may be important for clinicians to consider the ER and GR levels before prescribing a treatment regime, since different breast cancer cells can respond differently to the various hormone treatments.

In addition to the inhibition of GR binding upon dual hormone treatment, all cell lines that have been examined show binding modules representing ER and GR DynaLoad. However, when the ER and GR DynaLoad sites are compared across the three cell lines, little overlap is observed. A recent study has shown that ER binding sites that are shared across breast cancer cell lines are characterized by high-affinity estrogen response elements and a lack of DNA methylation, whereas cell-specific sites correlate with the binding of other transcription factors to these sites and DNA methylation (Gertz, Savic et al. 2013). The previous results show that ER is recruited to one-third of the cell-specific sites through tethering with other transcription factors (Gertz, Savic et al. 2013). Motif analysis of the ER DynaLoad clusters reveals that all three cell lines lack an ERE at these sites, suggesting that ER is recruited to these cell-specific sites through tethering. Similarly, the GR DyanLoad modules are found to lack a GRE. It has recently been proposed that ER is recruited to ER DynaLoad sites through tethering with AP-1 in a mouse cell line (Miranda, Voss et al. 2013). However, the AP-1 motif is highly prevalent only in the MCF-7 cells and is absent in the other cell lines. This indicates that other cell specific factors are involved in the recruitment of ER to the DynaLoad sites in the ZR-75-1 and T-47D cells and provides an explanation for the low overlap in ER binding observed in the three cell lines.

In order to determine if the DynaLoad sites are pre-marked with histone modifications, various histone marks have been examined in the untreated MCF-7 cells. DynaLoad sites identified in MCF-7 cells have been compared to DynaLoad sites observed in T-47D or ZR-75-1 cells that are not found in mCF-7 cells. It is shown that DynaLoad sites present in the MCF-7 cells contain higher

levels of H3K27ac in untreated MCF-7 cells compared to sites specific to the other cell lines. This suggests that the H3K27ac marks DynaLoad "active" sites in the MCF-7 cells. Although the DynaLoad sites found in the T-47D and ZR-75-1 cells have the potential to bind ER in MCF-7 cells, ER is not recruited to these sites due to the lack of H3K27ac. It has previously been shown that H3K9ac and H3K14ac highly correlate with ER occupancy (Joseph, Orlov et al. 2010). However, this is the first time that H3K27ac has been associated with ER recruitment. Recent studies have shown that enhancers associated with lineage-specific genes lack H3K27ac in the progenitor cells, but gain this mark during differentiation (Creyghton, Cheng et al. 2010). Therefore, enhancers are classified into poised and active states based on the status of the H3K27 residue (Rada-Iglesias, Bajpai et al. 2011). Interestingly, no differences in H3K27ac are observed at the GR DynaLoad sites.

Although all three cell lines contain FoxA1 DynaLoad sites there is little overlap observed between the three cell lines. Consequently, in all cell lines tested, there is no FoxA1 motif at these sites. This suggests that FoxA1 is potentially recruited to these sites through a tethering mechanism that is similar to what is observed at the ER and GR DynaLoad sites. When histone modifications are compared between the sites found in the MCF-7 cells, and sites found only in the T-47D or ZR-75-1 cells, little difference is observed in untreated MCF-7 cells. However, ER activated DynaLoad sites present in the MCF-7 cells have lower CTCF binding in untreated MCF-7 cells compared to sites that are specific to the T-47D and ZR-75-1 cells. This suggests that the sites observed in the T-47D and ZR-75-1 cells are blocked by CTCF in the MCF-7 cells, thus preventing FoxA1

recruitment. It has previously been reported that CTCF works upstream of FoxA1 and establishes higher-order chromatin structures that demarcates the genomic structures response to estrogen (Zhang, Liang et al. 2010). These studies show that knockdown of CTCF results in a decrease in binding of FoxA1 at the TFF1 gene, which is in contrast to what is observed at the ER activated FoxA1 DynaLoad sites. However, the ER activated GR DynaLoad sites observed in MCF-7 cells have higher levels of CTCF binding in untreated MCF-7 cells compared to the sites specific in the T-47D or ZR-75-1 cells, suggesting that CTCF may be playing a different role at these various modules.

These studies show that ER, GR, and FoxA1 DynaLoad are general mechanisms that occur in multiple cell lines. However, the lack of overlap of these DynaLoad sites between cell lines suggests that the DynaLoad mechanism is far more complicated than has previously been thought. Activation of multiple receptors does reprogram the binding landscape for other receptors; however, the newly available sites are cell specific. This suggests that other factors in the cell are also involved in the process. This chapter shows that histone modifications along with other transcription factors expressed in the cell may affect which sites are available for DynaLoad in a specific cell. Evidence has also suggested that cell specific factors may recruit these proteins to the DynaLoad sites through tethering (Miranda, Voss et al. 2013). It is therefore going to become important to understand the role these other factors play in cancer progression, so that targeted therapies can be developed for breast cancer patients.
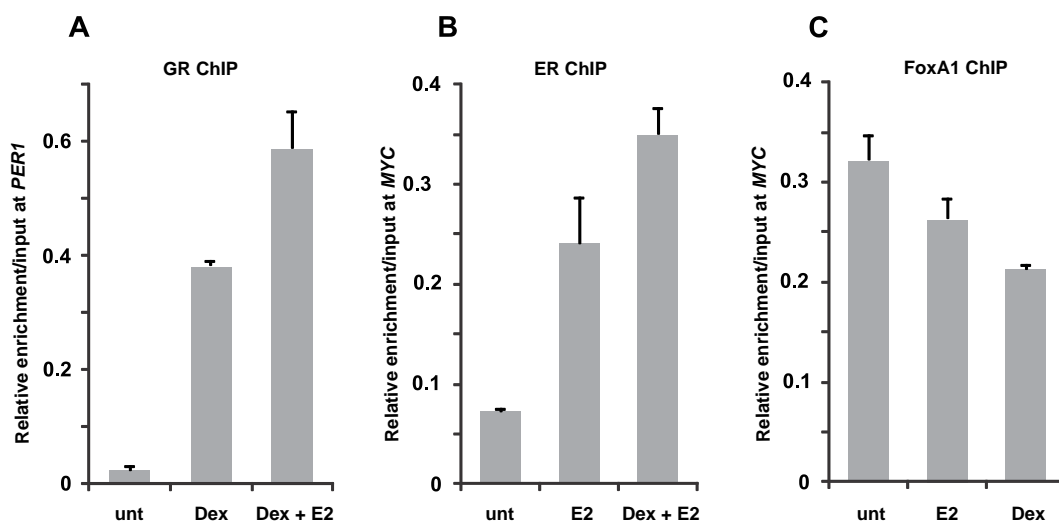
Figure 6.1: Analysis of GR, ER, and FoxA1 binding confirms sufficient enrichment for ChIP-seq. A. Quantitative-PCR shows that GR binding is increased at a *PER1* site in ZR-75-1 breast cancer cells treated with either 100nM of Dex or 100nM of Dex and E2. Data presented as relative enrichment over input. Results demonstrate that GR ChIP samples are suitable for sequencing. Figure is a representative example of one biological replicate. Error bars represent technical replicates. **B.** Quantitative-PCR shows that ER binding is increased at a *MYC* site in ZR-75-1 breast cancer cells treated with either 100nM of E2 or 100nM of Dex and E2. Data presented as relative enrichment over input. Results demonstrate that ER ChIP samples are suitable for sequencing. Figure is a representative example of one biological replicate. Error bars represent technical replicates. **C.** Quantitative-PCR shows that FoxA1 binding is increased at a *MYC* site in ZR-75-1 breast cancer cells treated with either 100nM of E2, 100nM Dex, or left untreated. Data presented as relative enrichment over input. Results demonstrate that FoxA1 ChIP samples are suitable for sequencing. Error bars represent technical replicates.

Figure 6.2: Analysis of GR and FoxA1 binding confirms sufficient enrichment for ChIP-seq. A. Quantitative-PCR shows that GR binding is increased at a *PER1* site in T-47D breast cancer cells treated with either 100nM of Dex or 100nM of Dex and E2. Data presented as relative enrichment over input. Results demonstrate that GR ChIP samples are suitable for sequencing. Figure is a representative example of one biological replicate. Error bars represent technical replicates. **B.** Quantitative-PCR shows that FoxA1 binding is increased at a *MYC* site in T-47D breast cancer cells treated with either 100nM of E2, 100nM Dex, or left untreated. Data presented as relative enrichment over input. Results demonstrate that FoxA1 ChIP samples are suitable for sequencing. Error bars represent technical replicates.

A

GR ChIP

Log 2 (+Dex + E2 (Max tag density)) vs Log 2 (+Dex (Max tag density))

$r^2=0.56$

- Overlapping Sites
- Sites Induced by double hormone treatment
- Sites Lost by double hormone treatment

B

ER ChIP

Log 2 (+Dex + E2 (Max tag density)) vs Log 2 (+E2 (Max tag density))

$r^2=0.64$

- Overlapping Sites
- Sites Induced by double hormone treatment
- Sites Lost by double hormone treatment
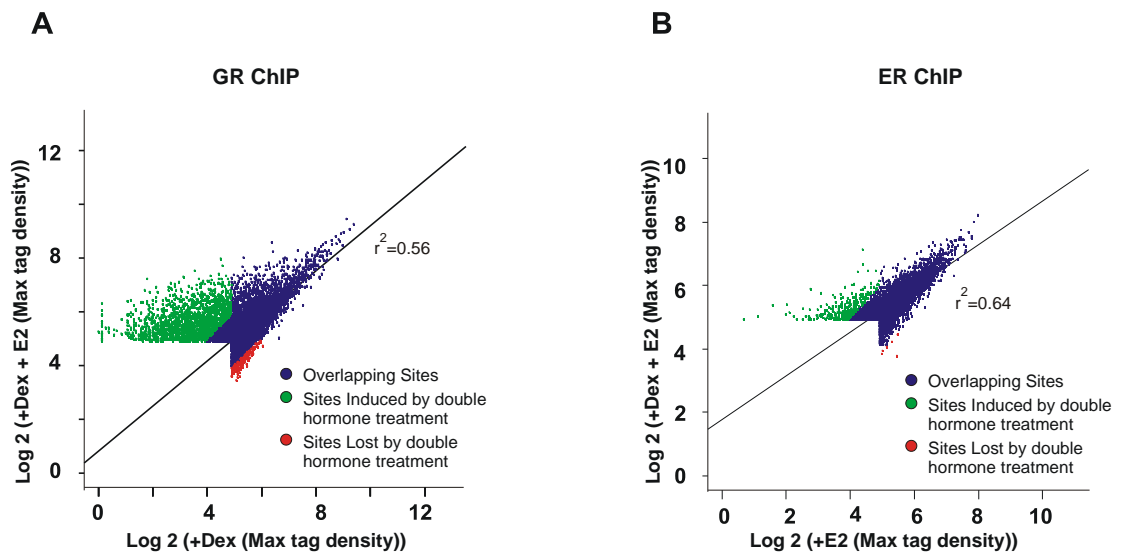
Figure 6.3: Changes in the GR and ER binding landscape upon Dex and E2 dual hormone treatment in ZR-75-1 human breast cancer cells. **A**. Global changes in GR binding patterns upon dual treatment of cells. Binding patterns of GR have been determined by ChIP-seq after treatment with either Dex or Dex + E2. Scatterplot represents the global changes in GR binding between Dex and Dex + E2. The sites shown to be either gained or lost by the dual hormone treatment have at least a 2-fold change in tag density. **B**. Global changes in ER binding patterns upon dual treatment of cells. Binding patterns of ER have been determined by ChIP-seq after treatment with either E2 or Dex + E2. Scatterplot represents the global changes in ER binding between E2 and Dex + E2. The sites shown to be either gained or lost by the dual hormone treatment have at least a 2-fold change in tag density.

Figure 6.4: Specific GR and ER binding modules. Supervised clustering analysis of 13,873 peaks identified by GR and ER ChIP-seq in ZR-75-1 breast cancer cells treated with either 100nM of Dex, E2, or Dex and E2. Heatmap analysis portrays the number of reads per 10^6 sequences as well as the position of the reads within 2 kb of ChIP-seq peak. Untreated samples are included in the analysis. Ten different binding clusters have been identified which are notated by the brackets. Histograms represent the overall GR and ER binding intensities in each cluster for the various treatments within a 2 kb interval of the ChIP-seq peaks.
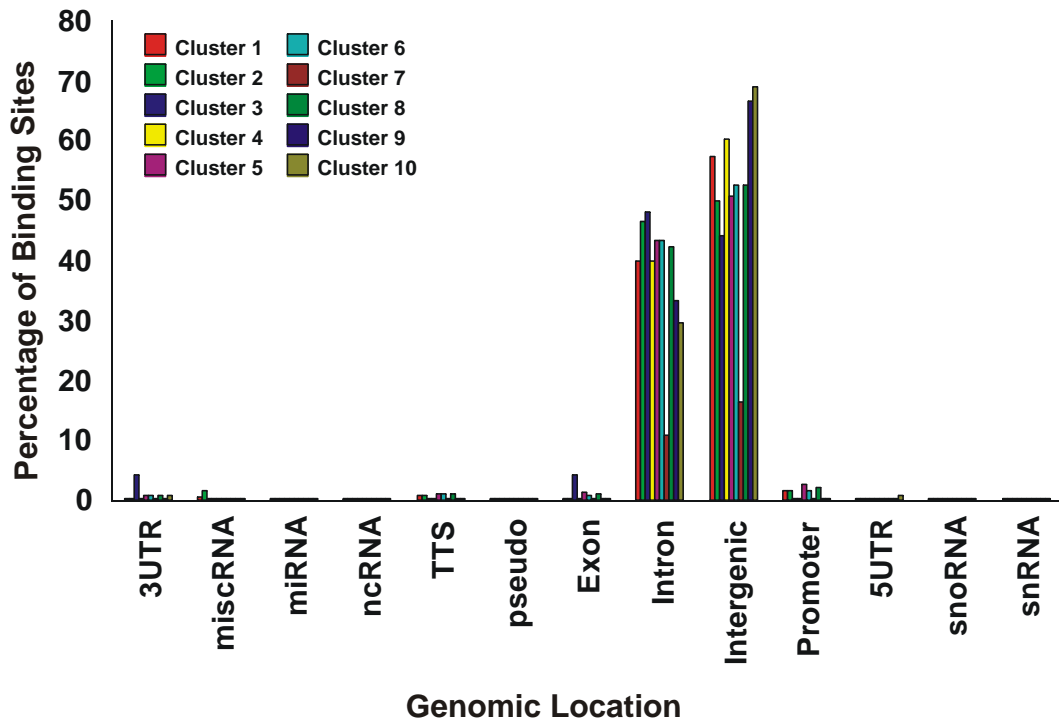
Figure 6.5: Genomic location of GR and ER binding clusters in ZR-75-1 breast cancer cells. Comparison of the genome-wide distribution of GR and ER binding patterns among the ten identified clusters. Data presented as a percentage of binding sites from each cluster located in the individual genomic locations.
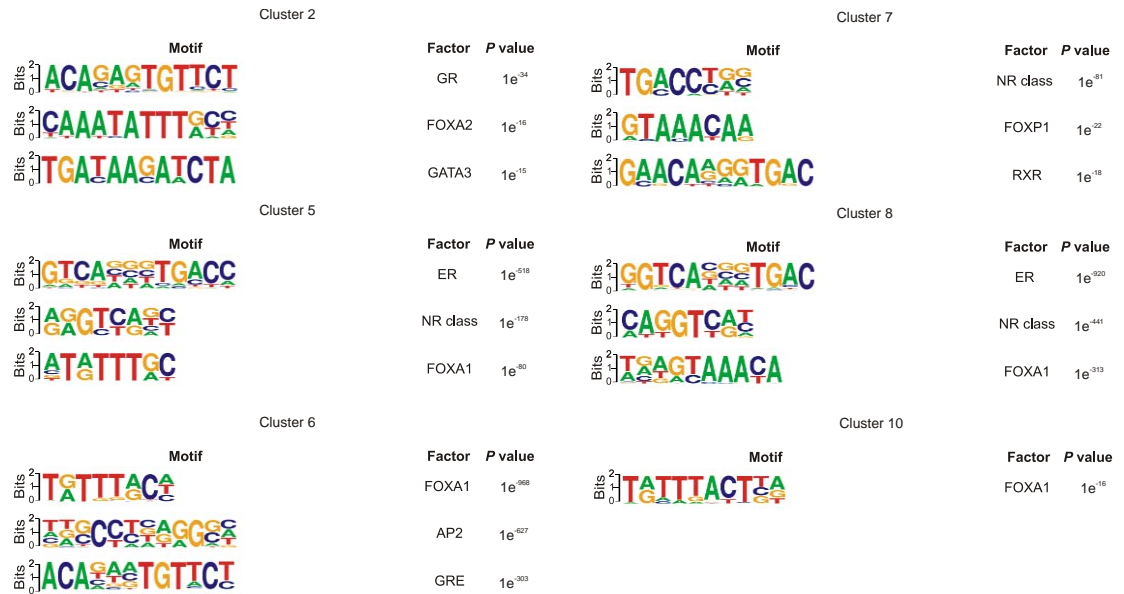
Figure 6.6: Motif analysis of GR and ER binding clusters. *De novo* motif analysis has been conducted on GR and ER DynaLoad sites, GR and ER classical sites, and GR lost sites. The data represents the top three most highly enriched motifs determined by Homer.
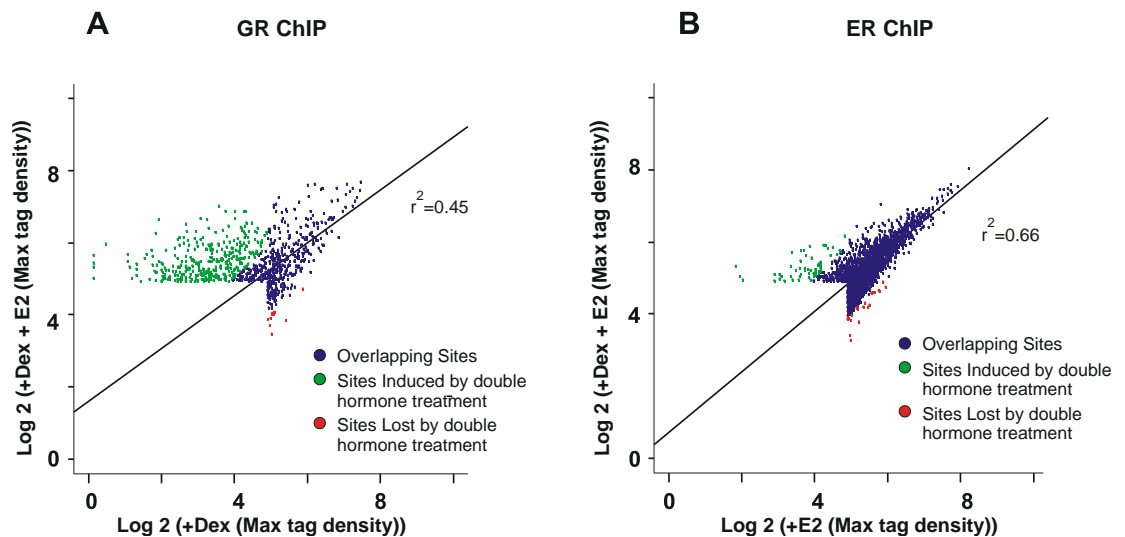
Figure 6.7: Changes in the GR and ER binding landscape upon Dex and E2 dual hormone treatment in T-47D human breast cancer cells. **A**. Global changes in GR binding patterns upon dual treatment of cells. Binding patterns of GR have been determined by ChIP-seq after treatment with either Dex or Dex + E2. Scatterplot represents the global changes in GR binding between Dex and Dex + E2. The sites shown to be either gained or lost by the dual hormone treatment have at least a 2-fold change in tag density. **B**. Global changes in ER binding patterns upon dual treatment of cells. Binding patterns of ER have been determined by ChIP-seq after treatment with either E2 or Dex + E2. Scatterplot represents the global changes in ER binding between E2 and Dex + E2. The sites shown to be either gained or lost by the dual hormone treatment have at least a 2-fold change in tag density.

Figure 6.8: Specific GR and ER binding modules. Supervised clustering analysis of 3143 peaks identified by GR and ER ChIP-seq in T-47D breast cancer cells treated with either 100nM of Dex, E2, or Dex and E2. Heatmap analysis portrays the number of reads per 10^6 sequences as well as the position of the reads within 2 kb of ChIP-seq peak. Untreated samples are included in the analysis. Nine different binding clusters have been identified which are notated by the brackets. Histograms represent the overall GR and ER binding intensities in each cluster for the various treatments within a 2 kb interval of the ChIP-seq peaks.
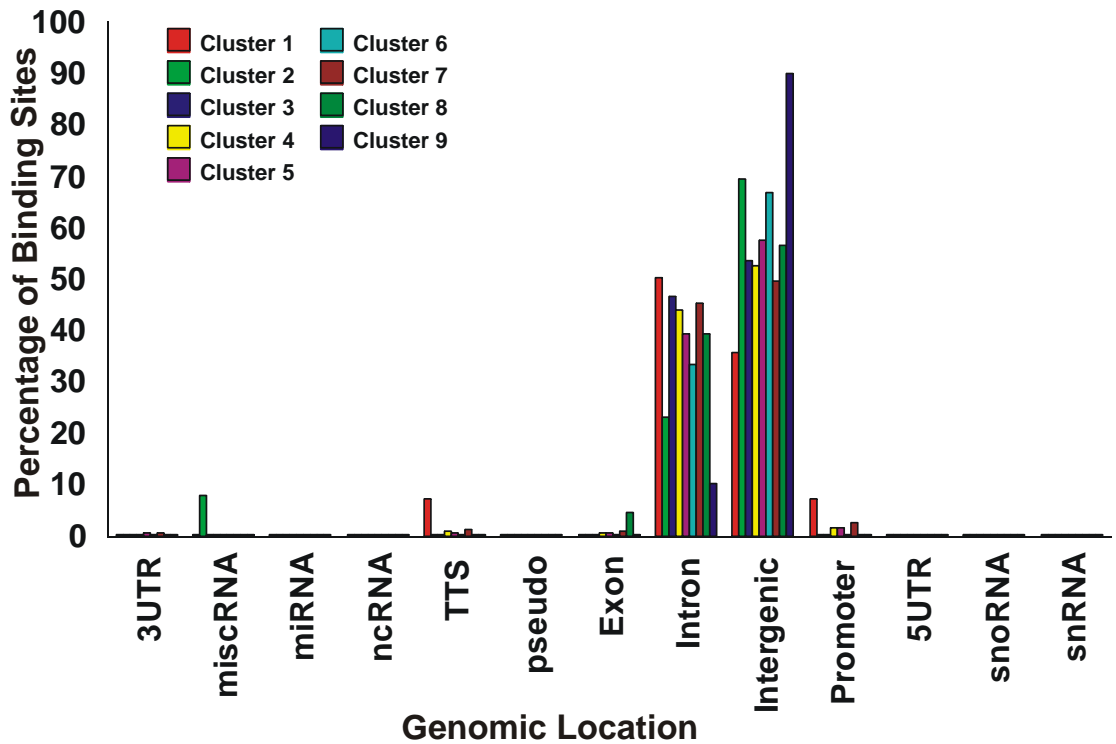
Figure 6.9: Genomic location of GR and ER binding clusters in T-47D breast cancer cells. Comparison of the genome-wide distribution of GR and ER binding patterns among the nine identified clusters. Data presented as a percentage of binding sites from each cluster located in the individual genomic locations.
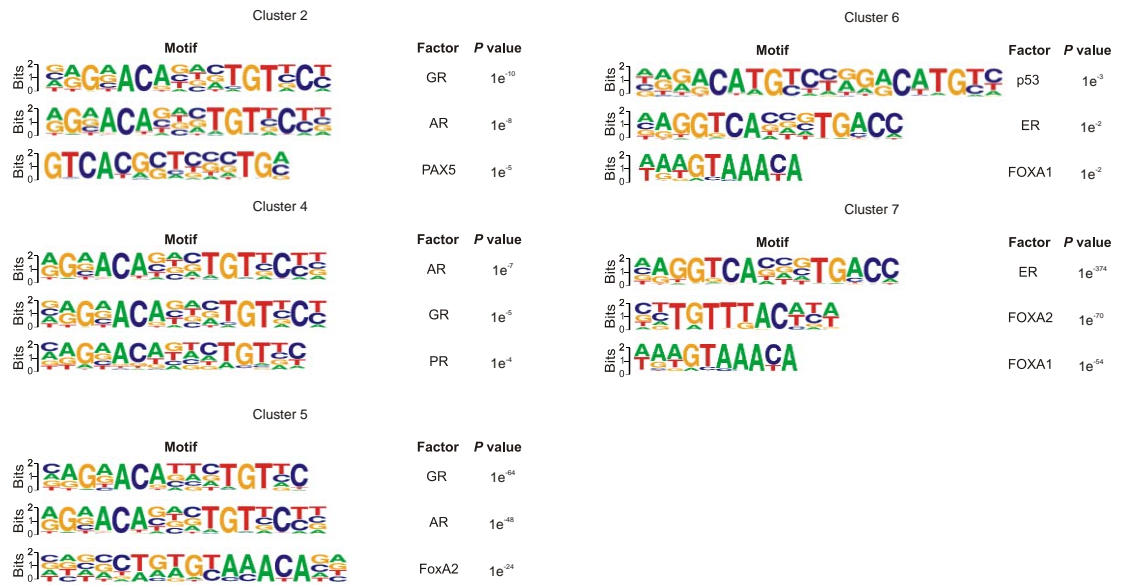
Figure 6.10: Motif analysis of GR and ER binding clusters. *De novo* motif analysis has been conducted on the GR and ER DynaLoad sites and the GR and ER classical sites. The data represents the top three most highly enriched motifs determined by Homer.
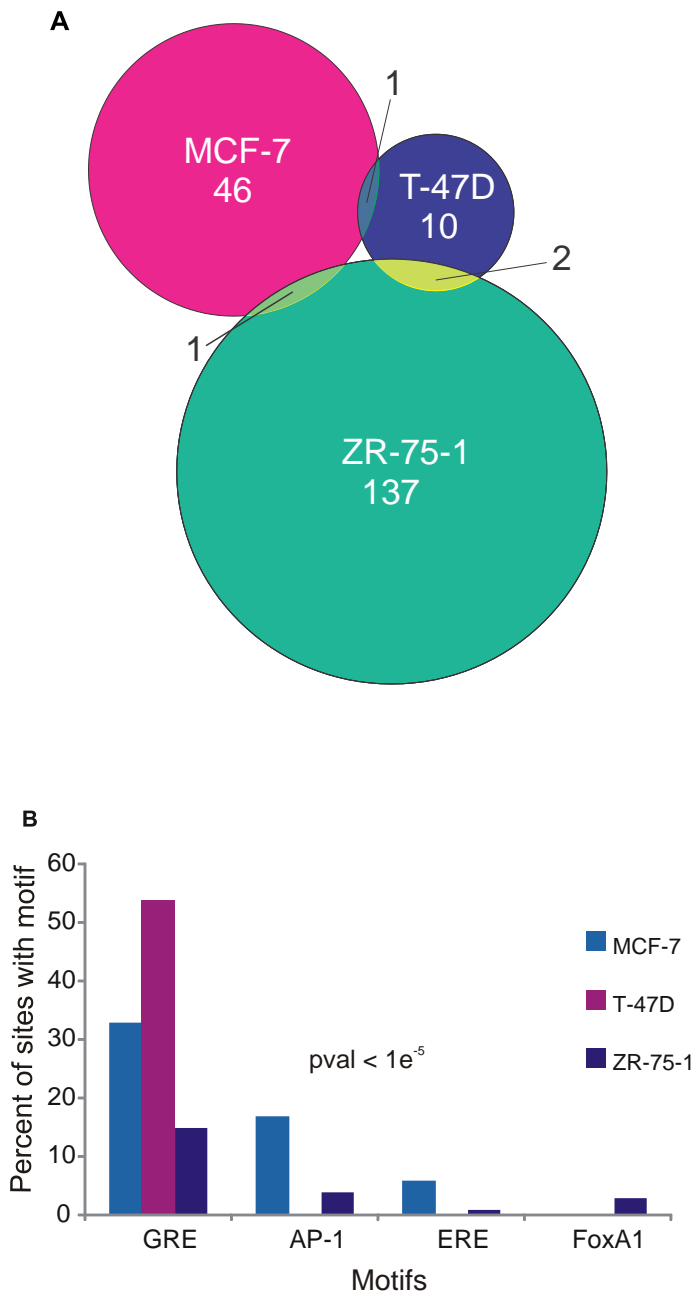
Figure 6.11: Cross analysis of ER DynaLoad sites in MCF-7, T-47D, and ZR-75-1 breast cancer cells. **A.** Comparison of ER DynaLoad site in three breast cancer cell lines. **B.** The distribution of GRE, AP-1, ERE, and FoxA1 motifs within the ER DynaLoad sites in MCF-7, T-47D, and ZR-75-1 breast cancer cells has been determined using FIMO analysis. The results are reported as the percentage of sites containing the motif with pval $< 1e^{-5}$.
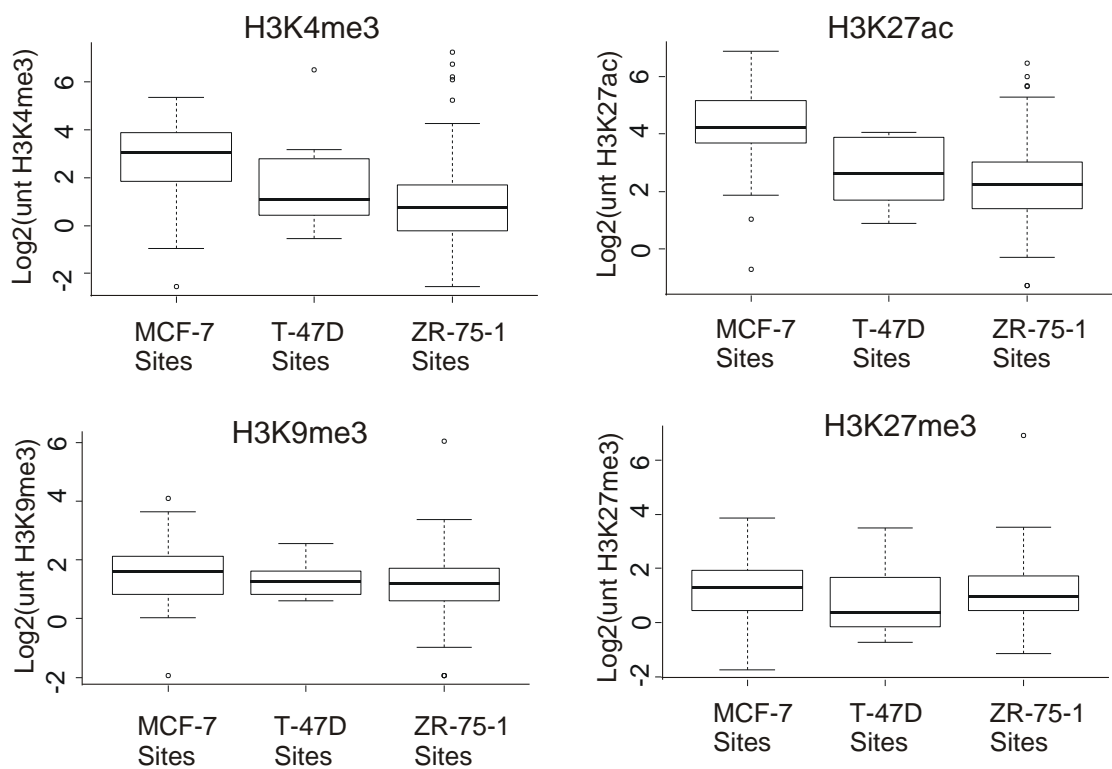
Figure 6.12: The presence of histone modifications in untreated MCF-7 cells at ER DynaLoad sites identified in MCF-7, T-47D and ZR-75-1 breast cancer cells. Differences in H3K4me3, H3K27ac, H3K9me3, and H3K27me3 levels in MCF-7 breast cancer cells between the ER DynaLoad sites identified in MCF-7, T-47D and ZR-75-1 breast cancer cells has been determined. Box plots demonstrate overall levels at each module and are presented as Log2. Each box correlates to the sites identified in each cell line labelled on the x-axis.
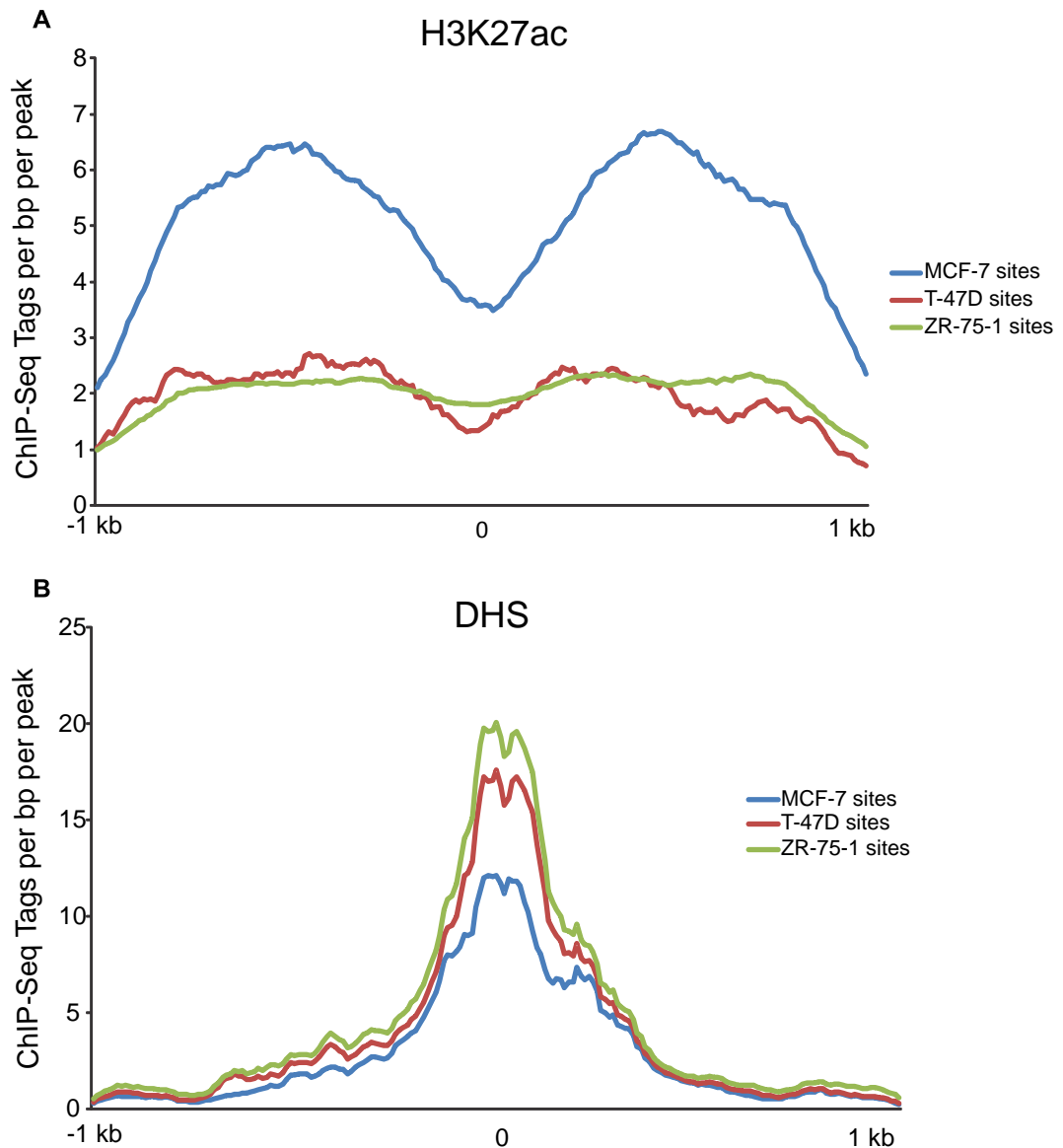
Figure 6.13:   The presence of H3K27ac and DHS in MCF-7 breast cancer cells at ER DynaLoad sites identified in MCF-7, T-47D and ZR-75-1 breast cancer cells.   A.   The distribution of H3K27ac in untreated MCF-7 cells at ER DynaLoad sites identified in MCF-7, T-47D, and ZR-75-1 breast cancer cells. H3K27ac levels within 2 kb of the DynaLoad sites have been determined.   **B.** DHS distribution in untreated MCF-7 cells at ER DynaLoad sites identified in MCF-7, T-47D and ZR-75-1 cells.   DHS is shown for a 2 kb range around the DynaLoad site.
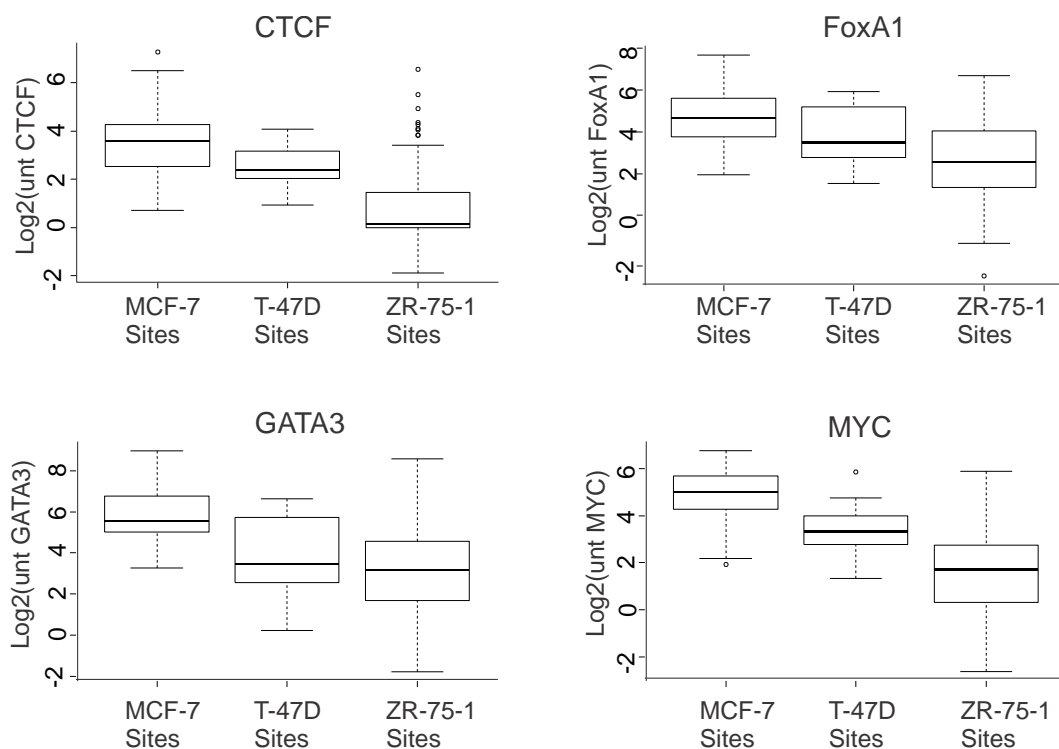
Figure 6.14: Transcription factor association in untreated MCF-7 breast cancer cells at ER DynaLoad sites identified in MCF-7, T-47D, and ZR-75-1 breast cancer cells. The presence of transcription factors (CTCF, FoxA1, GATA3, and MYC) in untreated MCF-7 breast cancer cells has been determined for ER DynaLoad sites identified in MCF-7, T-47D, and ZR-75-1 breast cancer cells. The data is presented as box plots which demonstrate overall levels of each transcription and is presented as Log2. Each box plot correlates to the sites identified in each cell line labelled on the x-axis.
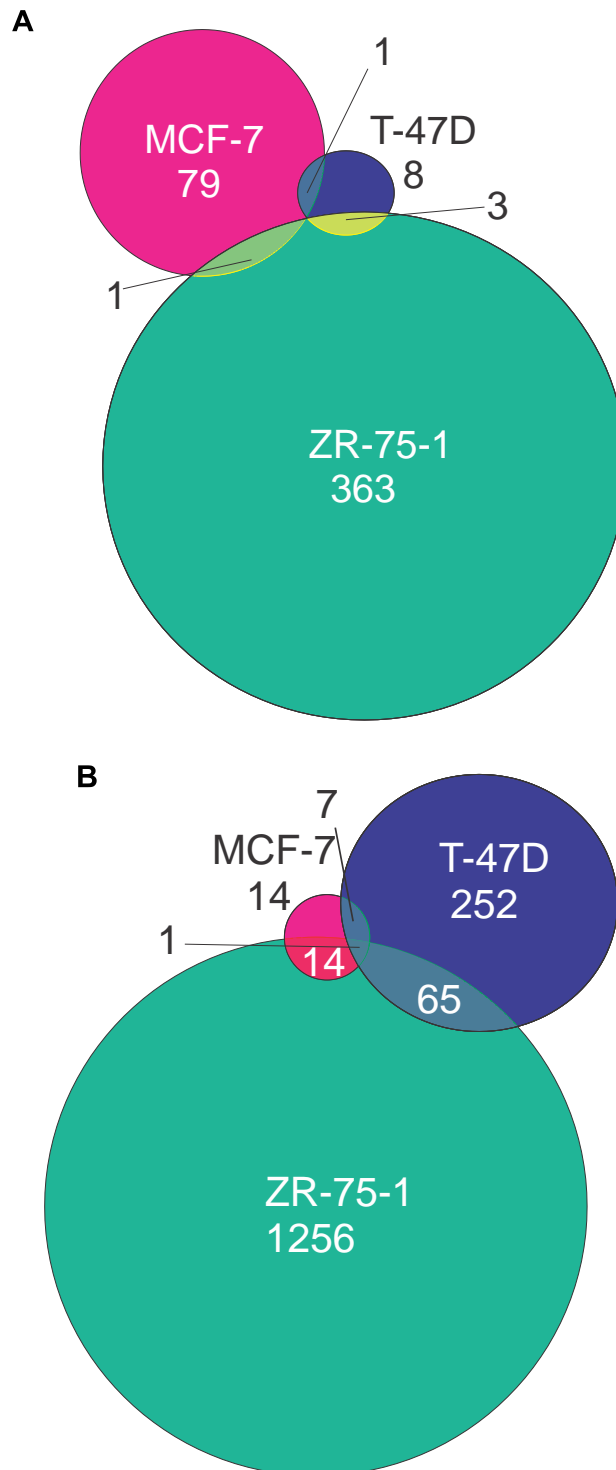
Figure 6.15: Cross analysis of GR DynaLoad sites in MCF-7, T-47D and ZR-75-1 breast cancer cells. A. Comparison of GR DynaLoad sites (no ER binding in untreated cells) in three breast cancer cell lines. **B.** Comparison of GR DynaLoad sites (ER binding in untreated cells) in three breast cancer cell lines.
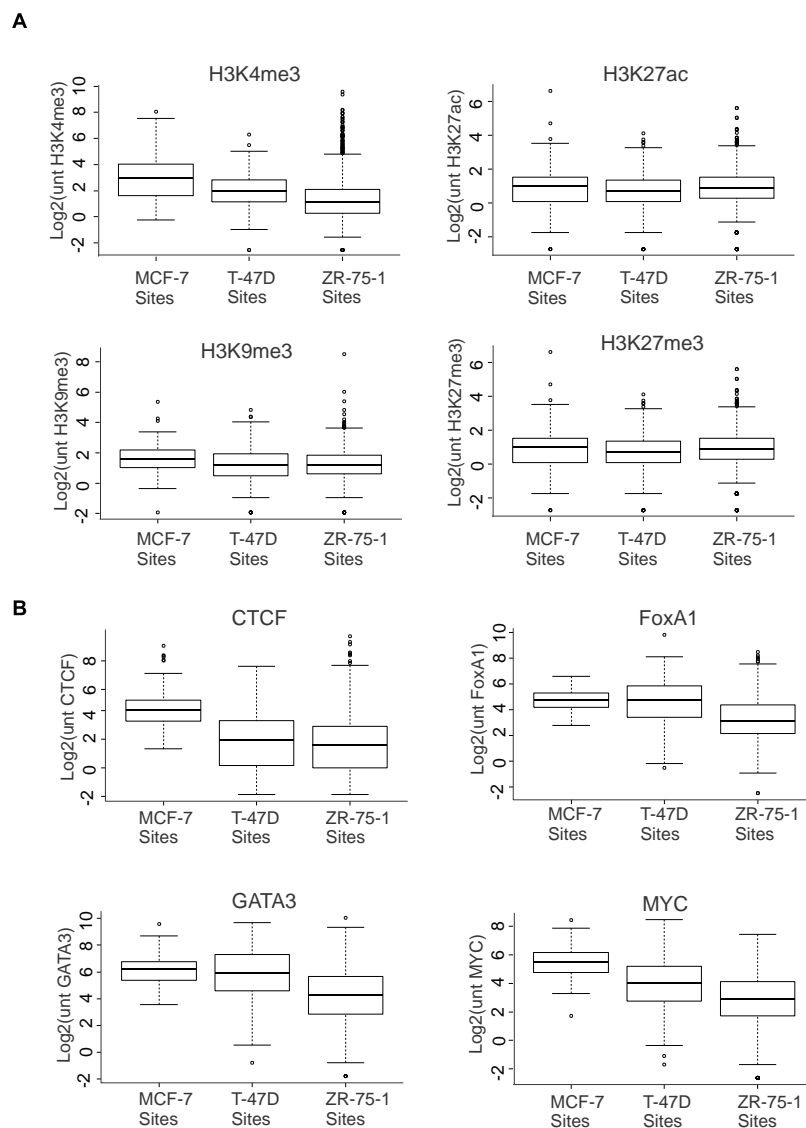
Figure 6.16: Histone modification and transcription factor association in untreated MCF-7 breast cancer cells at GR DynaLoad sites identified in MCF-7, T-47D, and ZR-75-1 breast cancer cells. A. The presence of histone modifications (H3K4me3, H3K27ac, H3K9me3, and H3K27me3) in untreated MCF-7 breast cancer cells has been determine for combined GR DynaLoad sites identified in MCF-7, T-47D, and ZR-75-1 breast cancer cells. **B.** The presence of transcription factors (CTCF, FoxA1, GATA3, and MYC) in MCF-7 breast cancer cells has been determined for combined GR DynaLoad sites identified in MCF-7, T-47D, and ZR-75-1 breast cancer cells. The data is presented as box plots which demonstrate overall levels of each histone mark or transcription factor binding and is presented as Log2. Each box plot correlates to the sites identified in each cell line labelled on the x-axis.
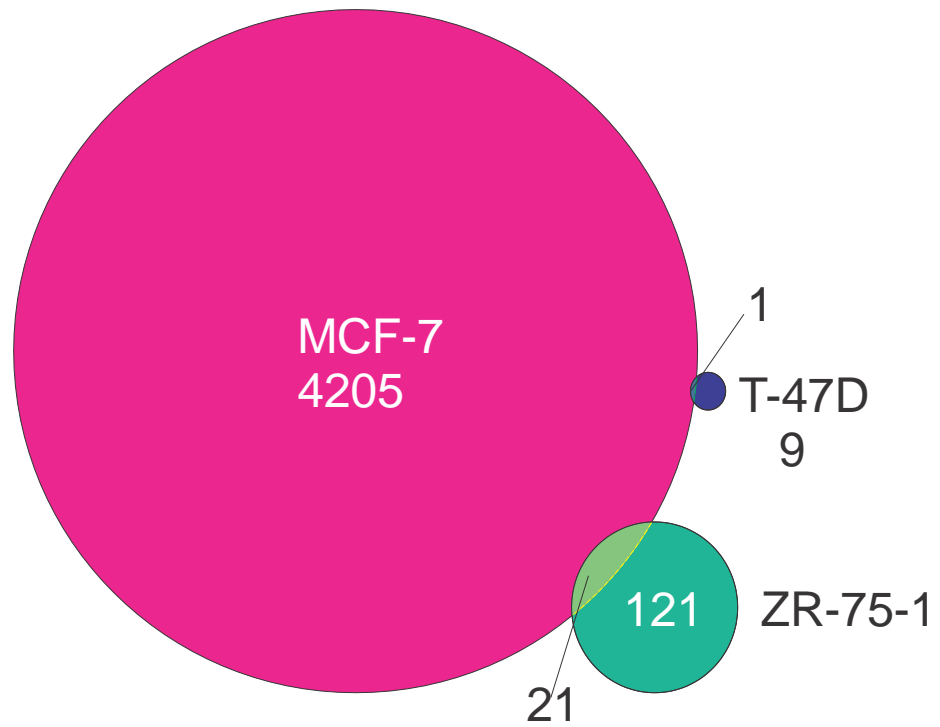
Figure 6.17: Cross analysis of GR lost sites in MCF-7, T-47D, and ZR-75-1 breast cancer cells. Comparison of GR lost sites in three breast cancer cell lines.

FoxA1 ChIP

r^2=0.88

Log 2 (+Dex(Max tag density))

● Overlapping Sites
● Sites Induced by Dex hormone treatment
● Sites Lost by Dex hormone treatment

Log 2 (+untreated (Max tag density))
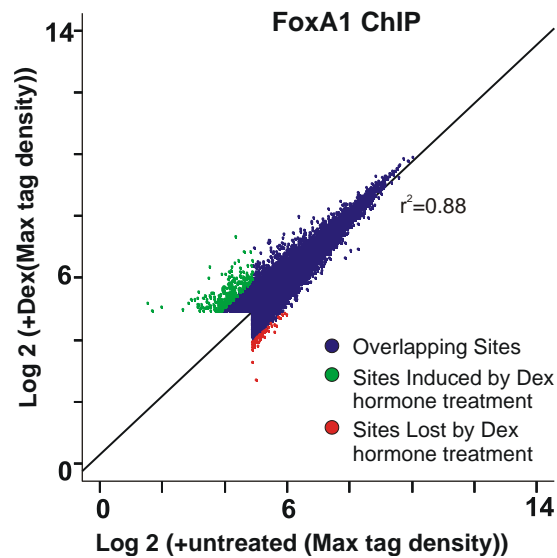
Figure 6.18: Changes in the FoxA1 binding landscape upon Dex hormone treatment in ZR-75-1 human breast cancer cells. Global changes in FoxA1 binding patterns upon 100nM Dex treatment of cells compared with untreated cells. Binding patterns of FoxA1 have been determined by ChIP-seq after treatment with either Dex or left untreated. Scatterplot represents the global changes in FoxA1 binding between Dex and untreated cells. The sites shown to be either gained or lost by Dex hormone treatment have at least a 2-fold change in tag density.
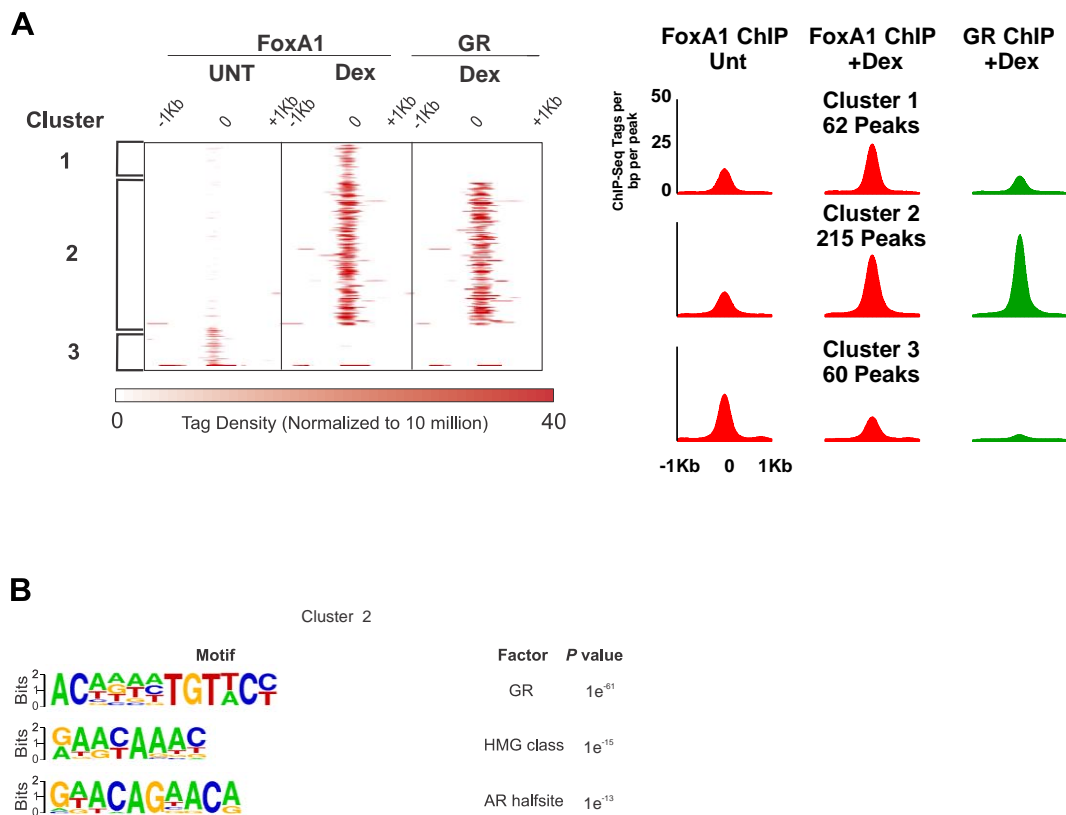
Figure 6.19: Specific FoxA1 and GR binding modules. **A.** Supervised clustering analysis of 328 peaks identified by FoxA1 and GR ChIP-seq in ZR-75-1 breast cancer cells treated with either 100nM Dex or left untreated. Heatmap analysis portrays the number of reads per 10^6 sequences as well as the position of the reads within 2 kb of ChIP-seq peak. Three different binding clusters have been identified which are notated by the brackets. Histograms represent the overall FoxA1 and GR binding intensities in each cluster for the various treatments within a 2 kb interval of the ChIP-seq peaks. **B.** *De novo* motif analysis has been conducted on the FoxA1 DynaLoad cluster. The data represents the top three most highly enriched motifs determined by Homer.
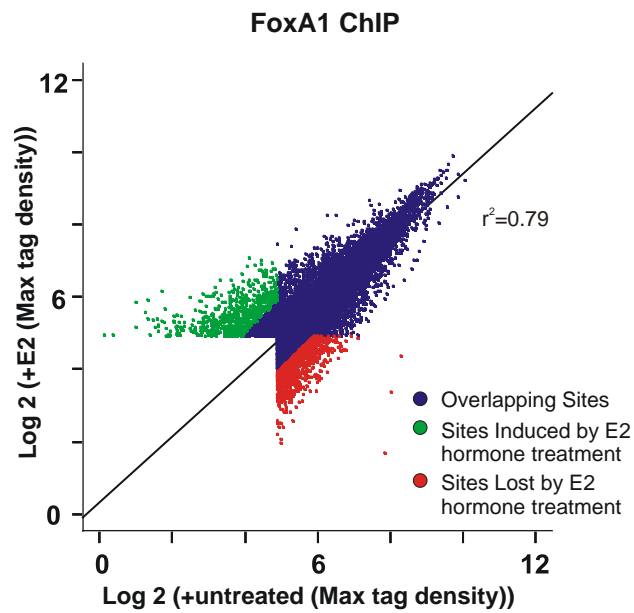
Figure 6.20: Changes in the FoxA1 binding landscape upon E2 hormone treatment in ZR-75-1 human breast cancer cells. Global changes in FoxA1 binding patterns upon 100nM E2 treatment of cells compared with untreated cells. Binding patterns of FoxA1 have been determined by ChIP-seq after treatment with either E2 or left untreated. Scatterplot represents the global changes in FoxA1 binding between E2 and untreated cells. The sites shown to be either gained or lost by E2 hormone treatment have at least a 2-fold change in tag density.
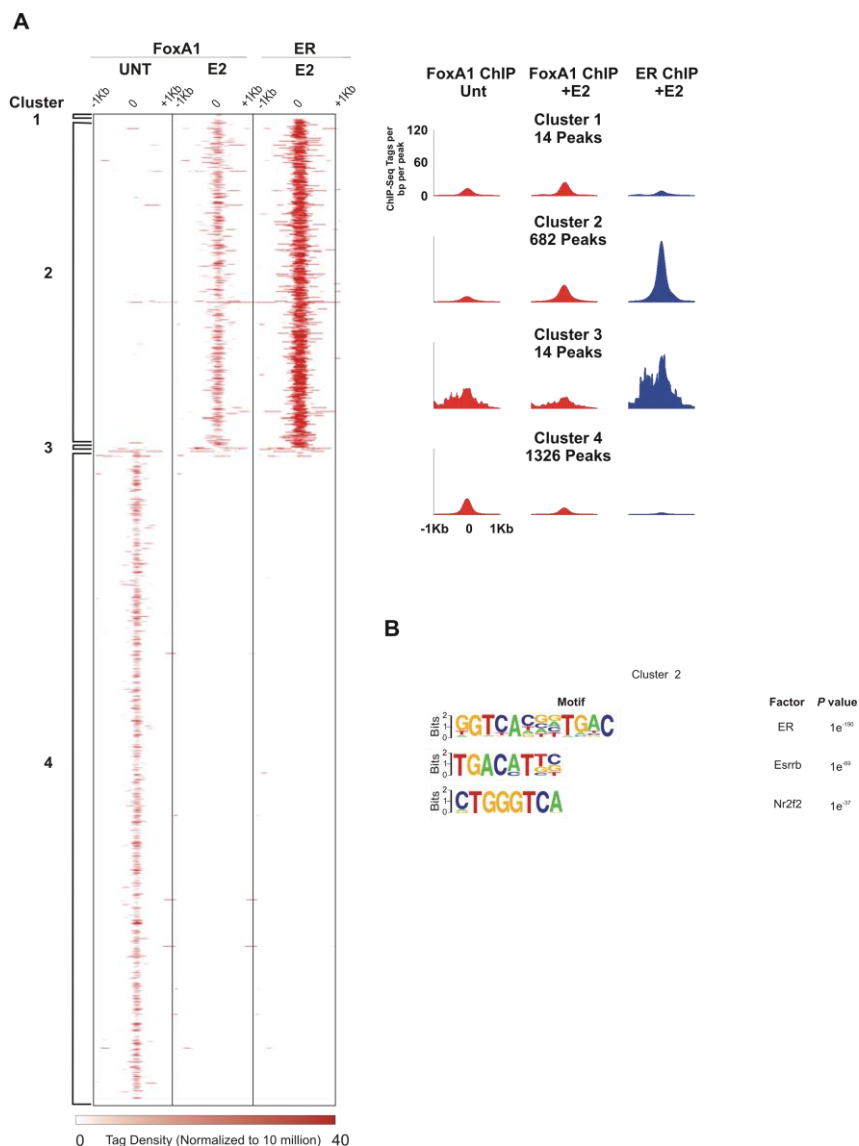
Figure 6.21: Specific FoxA1 and ER binding modules. **A.** Supervised clustering analysis of 2040 peaks identified by FoxA1 and ER ChIP-seq in ZR-75-1 breast cancer cells treated with either 100nM E2 or left untreated. Heatmap analysis portrays the number of reads per 10^6 sequences as well as the position of the reads within 2 kb of ChIP-seq peak. Three different binding clusters have been identified which are notated by the brackets. Histograms represent the overall FoxA1 and ER binding intensities in each cluster for the various treatments within a 2 kb interval of the ChIP-seq peaks. **B.** *De novo* motif analysis has been conducted on the FoxA1 DynaLoad cluster. The data represents the top three most highly enriched motifs determined by Homer.
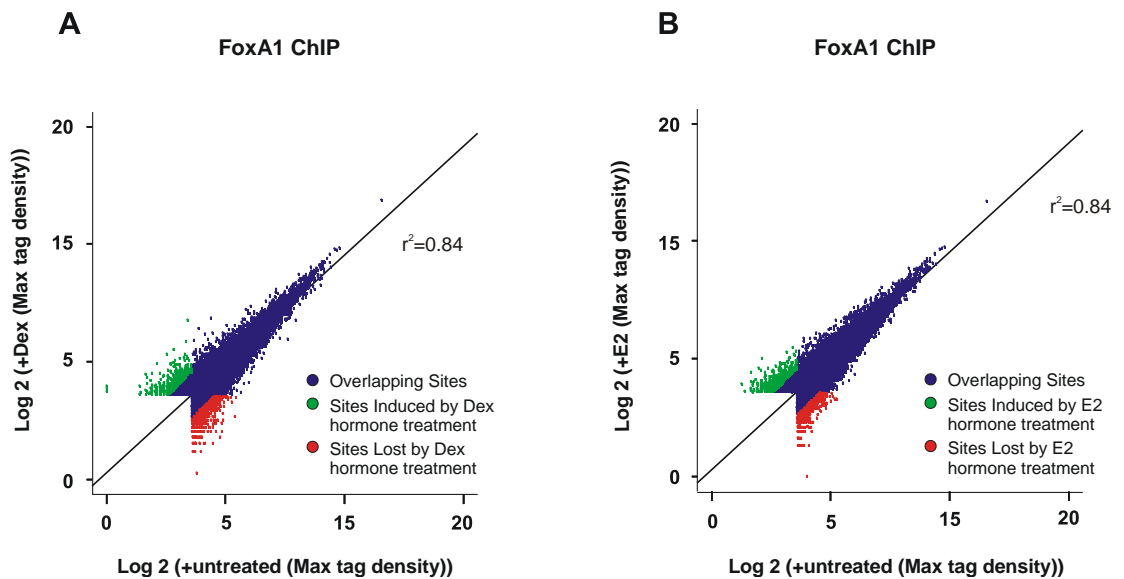
Figure 6.22: Changes in the FoxA1 binding landscape upon Dex and E2 hormone treatment in T-47D human breast cancer cells. **A**. Global changes in FoxA1 binding patterns upon 100nM Dex treatment of cells compared with untreated cells. Binding patterns of FoxA1 have been determined by ChIP-seq after treatment with either Dex or left untreated. Scatterplot represents the global changes in FoxA1 binding between Dex and untreated cells. The sites shown to be either gained or lost by Dex hormone treatment have at least a 2-fold change in tag density. **B**. Global changes in FoxA1 binding patterns upon 100nM E2 treatment of cells compared with untreated cells. Binding patterns of FoxA1 have been determined by ChIP-seq after treatment with either E2 or left untreated. Scatterplot represents the global changes in FoxA1 binding between E2 and untreated cells. The sites shown to be either gained or lost by E2 hormone treatment have at least a 2-fold change in tag density

Figure 6.23: Specific FoxA1 and GR binding modules. Supervised clustering analysis of 1530 peaks identified by FoxA1 and GR ChIP-seq in T-47D breast cancer cells treated with either 100nM Dex or left untreated. Heatmap analysis portrays the number of reads per 10^6 sequences as well as the position of the reads within 2 kb of ChIP-seq peak. Four different binding clusters have been identified which are notated by the brackets. Histograms represent the overall FoxA1 and GR binding intensities in each cluster for the various treatments within a 2 kb interval of the ChIP-seq peaks.
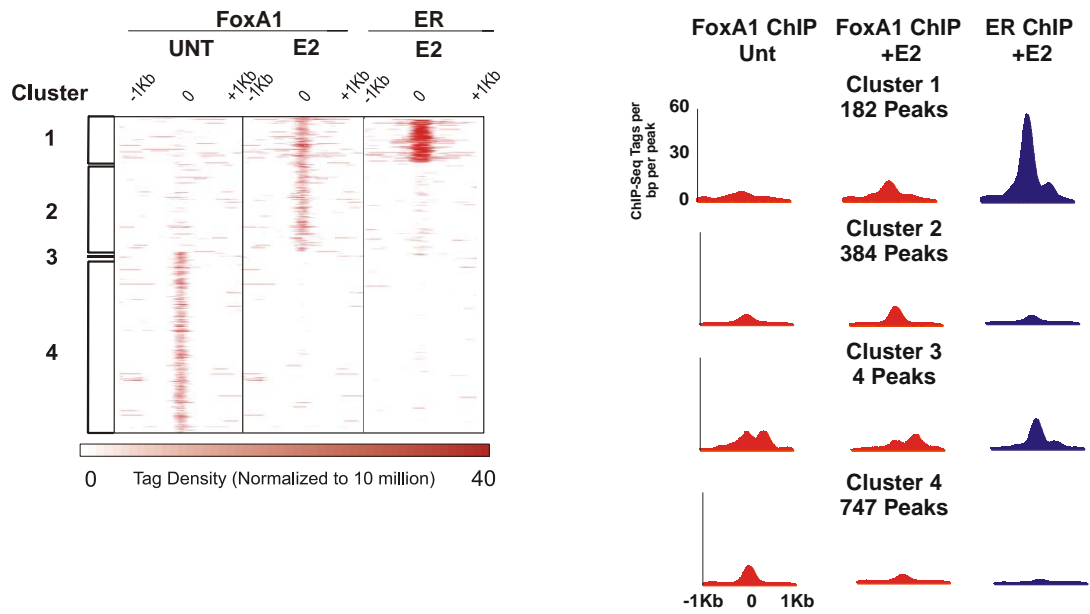
Figure 6.24: Specific FoxA1 and ER binding modules. Supervised clustering analysis of 1317 peaks identified by FoxA1 and ER ChIP-seq in T-47D breast cancer cells treated with either 100nM E2 or left untreated. Heatmap analysis portrays the number of reads per 10^6 sequences as well as the position of the reads within 2 kb of ChIP-seq peak. Four different binding clusters have been identified which are notated by the brackets. Histograms represent the overall FoxA1 and ER binding intensities in each cluster for the various treatments within a 2 kb interval of the ChIP-seq peaks.

A

FoxA1 classical binding sites

Motif	Factor	*P* value
	FoxA1	1e^{-5236}
	AP2	1e^{-310}
	Tead4	1e^{-252}

Cluster 2

Motif	Factor	*P* value
	FoxD1	1e^{-72}
	FoxA2	1e^{-22}
	GR	1e^{-17}

Cluster 3

Motif	Factor	*P* value
	ER	1e^{-32}
	NR4A2	1e^{-15}

Cluster 4

Motif	Factor	*P* value
	FoxA1	1e^{-151}
	FoxA2	1e^{-24}
	ER	1e^{-17}

B

FoxA1 classical binding sites

Motif	Factor	*P* value
	FoxA2	1e^{-5217}
	Arid5a	1e^{-797}
	Gata3	1e^{-289}

Cluster 1

Motif	Factor	*P* value
	ER	1e^{-55}
	AP2	1e^{-12}

Cluster 2

Motif	Factor	*P* value
	FoxP1	1e^{-55}
	Runx1	1e^{-13}
	Tead4	1e^{-12}

Cluster 4

Motif	Factor	*P* value
	FoxA2	1e^{-138}
	FoxI1	1e^{-16}
	Boris/CTCF	1e^{-16}

Figure 6.25: Motif analysis of FoxA1 binding clusters in T-47D breast cancer cells. **A.** *De novo* motif analysis has been conducted on FoxA1/GR binding clusters. The data represents the top three most highly enriched motifs determined by Homer. **B.** *De novo* motif analysis has been conducted on FoxA1/ER binding clusters. The data represents the top three most highly enriched motifs determined by Homer.
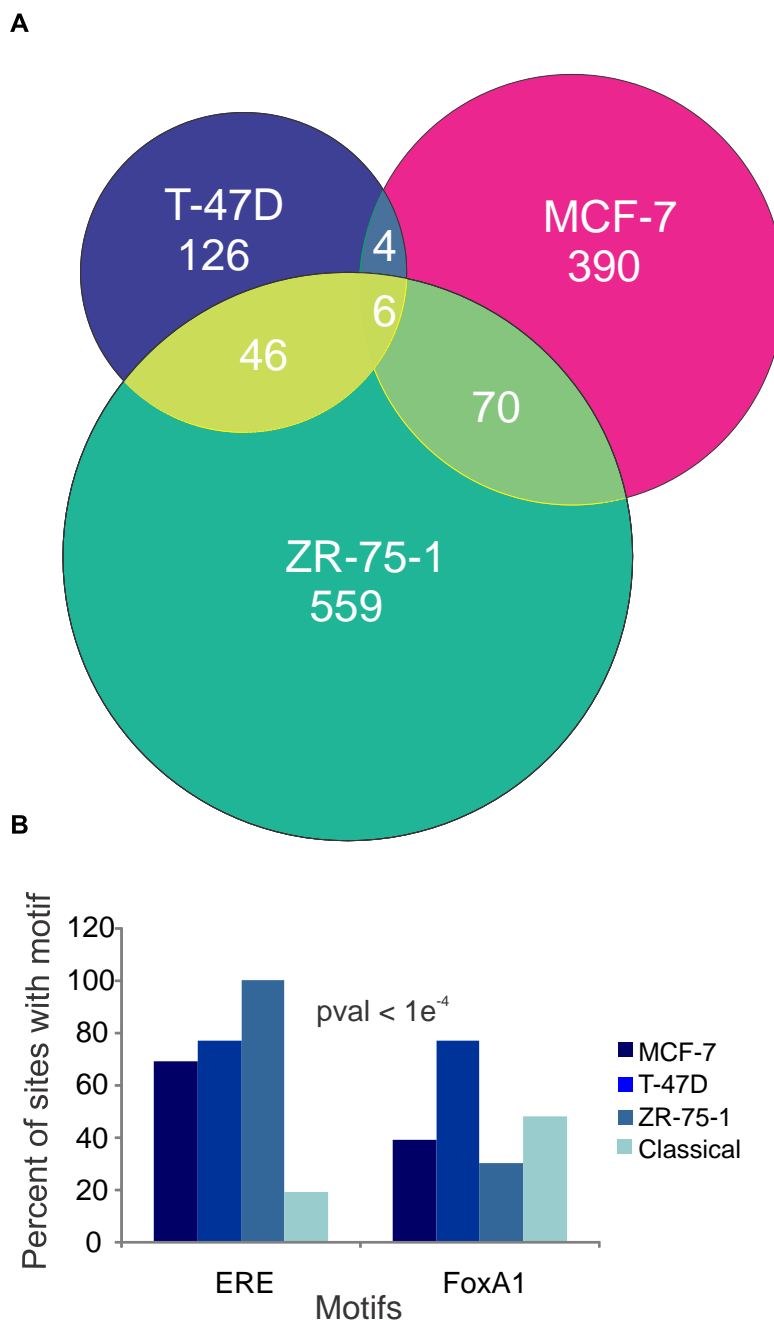
Figure 6.26: Cross analysis of FoxA1 DynaLoad sites upon E2 stimulation in MCF-7, T-47D, and ZR-75-1 breast cancer cells. A. Comparison of E2 activated FoxA1 DynaLoad site in three breast cancer cell lines. **B.** Enrichment of ERE and FoxA1 motifs within the E2 stimulated FoxA1 DynaLoad in MCF-7, T-47D, and ZR-75-1 breast cancer cells and the FoxA1 classical binding sites in MCF-7 breast cancer cells has been determined using FIMO analysis. The results are reported as the percentage of sites containing the motif with pval < 1e^{-4}.
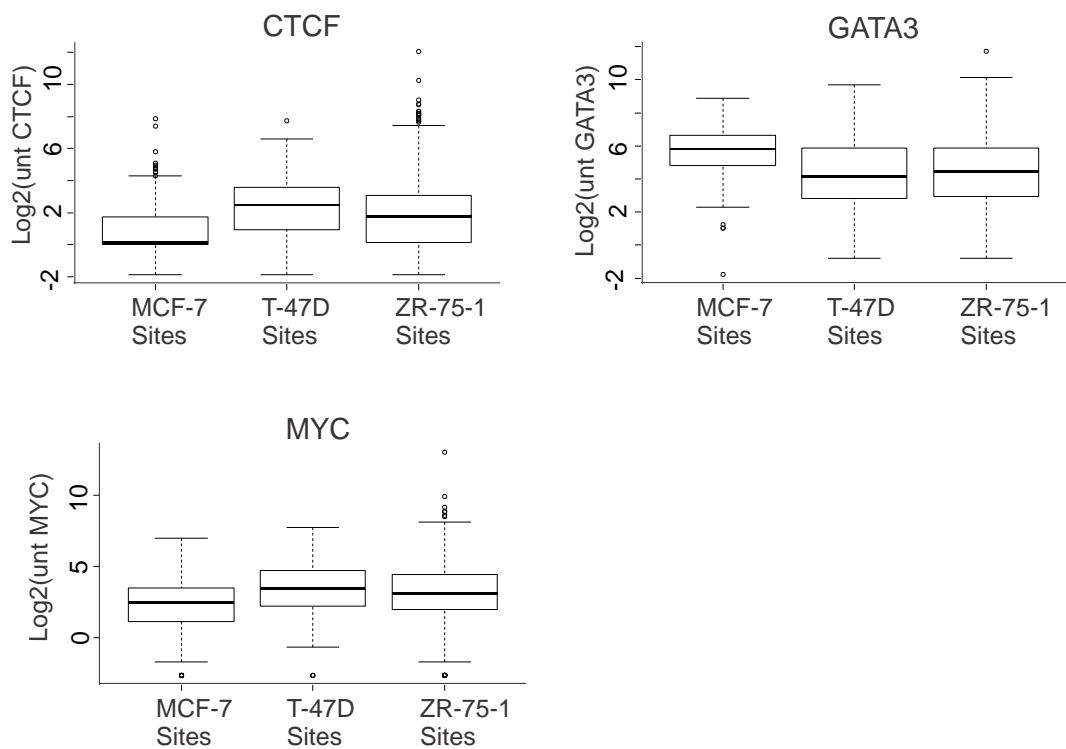
Figure 6.27: Transcription factor association in untreated MCF-7 breast cancer cells at E2 stimulated FoxA1 DynaLoad sites identified in MCF-7, T-47D, and ZR-75-1 breast cancer cells. The presence of transcription factors (CTCF, GATA3, and MYC) in untreated MCF-7 breast cancer cells has been determined for combined E2 stimulated FoxA1 DynaLoad sites identified in MCF-7, T-47D, and ZR-75-1 breast cancer cells. The data is presented as box plots which demonstrate overall levels of each transcription factor binding and is presented as Log2. Each box plot correlates to the sites identified in each cell line labelled on the x-axis.

Chapter 7

General Discussion

Estrogens and P4 play an important role in the development, growth, and maintenance of normal cells and breast cancer. What is now becoming more apparent is the potential involvement of glucocorticoids in breast cancer progression (Vaidya, Baldassarre et al. 2010, Vilasco, Communal et al. 2011). Investigations into ER binding in breast cancer cells has been extensive (Carroll, Liu et al. 2005, Carroll, Meyer et al. 2006, Welboren, van Driel et al. 2009); however, there is a lack of understanding in the molecular function of PR and GR. Previous studies have shown a role for GR and ER crosstalk in a mouse mammary cell line, engineered to overexpress GR and ER (Miranda, Voss et al. 2013). This study identified that dual activation of both receptors can reformat the chromatin landscape, allowing the receptors to bind to previously inaccessible sites. In addition, it is well known that the pioneer factor, FoxA1, is a required component to ER mediated responses in breast cancer cells (Carroll, Liu et al. 2005, Lupien, Eeckhoute et al. 2008, Hurtado, Holmes et al. 2011). However, there appears to be some controversy into whether activated ER can modulate the FoxA1 response. This thesis examined the outcomes of GR and ER crosstalk in multiple breast cancer cell lines with a particular emphasis on GR and ER DynaLoad. In addition, this thesis further explored the possibility of hormone regulation on the function of FoxA1 and the implications that it might have on the binding distribution patterns of FoxA1.

7.1 Major Findings of this Thesis

7.1.1 Dual activation of GR and ER alters the response of RNA PolII binding affecting gene transcriptional responses in MCF-7 human breast cancer cells.

The findings in chapter 3 of this thesis demonstrate that dual treatment of Dex and E2 alters the gene transcriptional response compared to the single activation of either receptor determined by RNA PolII binding. These findings are consistent with previous studies using either microarray analysis or studies conducted at a single gene level that suggest Dex and E2, in combination, can alter a subset of genes (Karmakar, Jin et al. 2013, Miranda, Voss et al. 2013). Specifically, it has been shown in this thesis that while the dual treatment does not seem to affect the majority of genes regulated by the single hormone treatment, there are unique subsets of genes gained or lost when both GR and ER are activated. In addition, there is a strong correlation between gene regulation and GR binding which corresponds to either the single or dual treatment. Together, this suggests that dual activation of GR and ER has the potential to reshape the RNA PolII response altering what is observed in the single hormone setting. These findings propose a role for GR and ER crosstalk in breast cancer cells, supporting previous findings indicating GR and ER can modulate each other's response in a dual hormone setting (Miranda, Voss et al. 2013). In women diagnosed with breast cancer, it has been identified that higher GR levels are associated with altered disease outcomes depending on ER expression (Pan, Kocherginsky et al. 2011). This suggests that GR and ER have a collaborative response in breast cancer, and that GR alone can have negative effects in the absence of a functional ER. The potential impact of disrupting the estrogen and glucocorticoid response is illustrated here by a significant change in gene transcriptional response. Due to the current use of endocrine disrupters that alter ER signalling in ER positive breast cancers (Ali and Coombes 2002), a better understanding of the potential consequence of GR and ER crosstalk in breast cancer is essential.

7.1.2 Activated GR and ER can modulate unique binding patterns in human MCF-7 breast cancer cells.

It has previously been reported in a mouse mammary cell line engineered to overexpress GR and ER, that the binding patterns of GR and ER can be redistributed by dual activation (Miranda, Voss et al. 2013). In particular, it has been shown that there are a unique subset of GR binding sites that are gained upon activation of ER, and conversely, there are ER binding sites that are acquired upon GR activation. This mechanism is termed DynaLoad, whereby one TF can bind to DNA and recruit chromatin remodelling complexes, which leads to an increase in DHS, and allows for another TF to bind to the site that was previously deemed inaccessible. The functional effect of this mechanism on a cell line that is more representative of an estrogenic breast cancer, MCF-7 cells, has been tested in chapter 4.

The findings in chapter 4 support the hypothesis that GR and ER dual activation can alter binding patterns in human breast cancer cells, with GR and ER DynaLoad identified in this cell model. What is most surprising is the discovery of a very high number of GR binding sites lost upon activation of ER, which is in contrast to findings observed by Miranda *et al*. Highlighted by immunoblot analysis in chapter 3, MCF-7 cells express higher levels of ER than GR, and this may be why the results seen in chapter 4 differ to what has been observed previously.

Further investigation into the possible mechanism behind the mass inhibition of GR binding upon ER activation in MCF-7 cells has revealed that there are no changes in DHS at these sites upon activation of ER. Further, these sites are not

pre-marked by specific histone modifications, indicating that other mechanisms must be involved in regulating the GR response at these sites. Previous studies have demonstrated that GR and ER pBox, a mutant ER protein that binds to GRE's, do not compete for binding as a result of the rapid on and off rates of the receptors at these sites (Voss, Schiltz et al. 2011). This suggests the loss of GR binding is not due to competition even though ER and GR are binding at the same sites. Further studies are required to determine the mechanism behind the loss of GR binding upon the activation of ER in MCF-7 breast cancer cells, although, the squelching of cofactors by ER may be a potential mechanism. It has been determined that high GR levels can have consequences on patients' outcome with ER negative cancer compared to ER positive cancers (Pan, Kocherginsky et al. 2011). Findings in chapter 3 and 4 have demonstrated together that ER can affect the GR response, suggesting that in an ER negative cell line, or in the presence of ER inhibition therapy, GR may have undesirable effects on breast cancer progression.

7.1.3 Activated GR and ER can alter the FoxA1 response genome-wide.

FoxA1 proteins, a class of pioneer factors, have been shown to interact with compact chromatin, modulate chromatin structure, and bind to DNA as an early event. This results in the recruitment of other transcriptional regulators and SRs, and the initiation of transcriptional processes (Cirillo, McPherson et al. 1998, Eeckhoute, Lupien et al. 2009, Hurtado, Holmes et al. 2011, He, Meyer et al. 2012). Particularly, it is well established that FoxA1 is required for almost all ER binding events and binds at over 50% of ER binding sites (Carroll, Liu et al. 2005, Lupien, Eeckhoute et al. 2008, Hurtado, Holmes et al. 2011). However,

there has been some controversy into whether activated ER can modulate a specific FoxA1 response. It has been reported on multiple occasions that ER does not alter the binding pattern of FoxA1 (Lupien, Eeckhoute et al. 2008, Hurtado, Holmes et al. 2011). Conversely, it has been recently reported that although no mechanism has been detected, at 29% of ER and FoxA1 shared sites, FoxA1 recruitment is dependent on E2 stimulations (Kong, Li et al. 2011). In addition, it has been shown that upon knockdown of ER, FoxA1 binding is lost at unstimulated ER binding sites (Caizzi, Ferrero et al. 2014). Findings in chapter 5 of this thesis have determined that in MCF-7 breast cancer cells there are a unique subset of FoxA1 binding sites that are lost or gained upon the stimulation of cells with E2. Furthermore, the gained sites are shown to be from a DynaLoad mechanism, with an increase in DHS, the presence of ER binding, and an ERE binding motif at these sites.

In addition to recruiting FoxA1 to a subset of sites, activation of ER also causes a loss of FoxA1 binding, which is correlated with an increase of CTCF binding at these sites. It has previously been reported, in MCF-7 cells, that there is an increase in CTCF binding at approximately 80% of FoxA1 and ER shared sites (Hurtado, Holmes et al. 2011), suggesting CTCF can modulate FoxA1 response.

In addition, it has been determined that activation of GR by Dex stimulation can also alter a subset of FoxA1 binding sites, by a DynaLoad mechanism. This supports a very early finding, whereby FoxA1 can bind to two GR responsive units *in vivo*, and that FoxA1 binding to this site is GR dependent. Activation of GR results in the disruption of nucleosomal structure at these two responsive units (Rigaud, Roux et al. 1991). Together, findings in this thesis have shed new light

into the current understanding of pioneer factors, indicating that multiple TF can function as a "pioneer" factor given the right chromatin landscape. In addition, we are providing new evidence to suggest that ER can alter the FoxA1 binding pattern, in potential collaboration with CTCF.

7.1.4 GR, ER, and FoxA1 crosstalk genome-wide is not cell specific and the varying degree of crosstalk is dependent on receptor levels.

Breast cancer is not a single disease state and it is known that breast cancer can function in a multitude of ways having differing histopathology, genomic variation, and metastatic potential. This deems it impossible to treat and detect all breast cancers in the same way. Therefore, it is becoming apparent that studies into the mechanism of breast cancer need to be carried out in multiple cell line models. Findings in chapter 6 have demonstrated that GR and ER crosstalk at the genomic level is observed in ZR-75-1 and T-47D breast cancer cells. However, this response occurs at varying degrees among all three cells lines. It has been shown in chapter 3 that while MCF-7 cells express the highest level of ER, ZR-75-1 cells express the highest level of GR, and T-47D cells have fairly low levels of both receptors. Nonetheless, GR and ER DynaLoad is active in all three cell lines. Of particular interest is the observation that the massive inhibition of GR binding upon E2 stimulation in MCF-7 cells is not as apparent in ZR-75-1 and T-47D cells. The results in chapter 6 are more consistent with previous findings (Miranda, Voss et al. 2013). This suggests that in a cell line with higher ER expression the GR genomic profile can be redistributed; however, in breast cancer cells with lower ER levels, GR is able to exert a more normal response. Taken together, the findings in this thesis suggest that ER is required to inhibit GR

responses that may promote cancer cell growth. When ER levels are decreased, GR has the ability to function in a potentially negative way. These findings indicate that the GR and ER expression should be tested in the clinic, and perhaps the GR expression needs to be considered before endocrine treatments are given to patients.

While an association has been observed between multiple cell lines, the specific binding sites are in fact cell line specific. However, this supports previous studies that have shown that ER binding patterns are generally unique between MCF-7, ZR-75-1, and T-47D cell lines (Hurtado, Holmes et al. 2011). More specifically, it has been recently shown that ER binding sites, that are cell line specific, do not contain an ERE (Gertz, Savic et al. 2013). This supports findings in chapter 6, that show ER DynaLoad sites that are unique in all three cell lines, do not contain an ERE.

It has recently been suggested that ER is recruited to ER DynaLoad sites through tethering with AP-1 in a mouse cell line (Miranda, Voss et al. 2013). What is interesting in this thesis is that the AP-1 motif is only prevalent in the MCF-7 cells and absent in ZR-75-1 and T-47D cells. This suggests that other cell specific factors are required for the recruitment of ER to the DynaLoad sites in ZR-75-1 and T-47D cells.

It has been determined that the ER DynaLoad sites identified in MCF-7 cells contain high levels of H3K27ac, in contrast, the ER DynaLoad sites identified in ZR-75-1 and T-47D cells, have very low levels of H3K27ac in the MCF-7 cells. This suggests H3K27ac marks active ER DynaLoad in MCF-7 cells. Previous studies have identified a correlation between H3K9ac and H3K14ac with ER

binding (Joseph, Orlov et al. 2010), but the association of H3K27ac is a new and novel finding.

It has also been determined in chapter 6 that FoxA1 DynaLoad is functional in multiple breast cancer cell lines. Contrary to previous studies indicating E2 does not regulate FoxA1 at a genome-wide level (Lupien, Eeckhoute et al. 2008, Hurtado, Holmes et al. 2011), this further supports the findings in chapter 5 where it is observed that Dex and E2 can modulate a FoxA1 response. Similar to what is observed for GR and ER binding across breast cancer cell lines, FoxA1 binding sites that are affected by the stimulation of cells with Dex or E2 have very little overlap between cell lines. This supports previous studies showing that FoxA1 binding patterns are specific for each cell line.

In this thesis, CTCF has also been shown to play a role in marking cell specific GR and FoxA1 DynaLoad. Previous studies have demonstrated that CTCF functions up stream of FoxA1 and that knockdown of CTCF results in a decrease in FoxA1 binding at the TFF1 gene (Zhang, Liang et al. 2010). This is contrary to findings in chapter 6, where FoxA1 DynaLoad sites, activated by ER in MCF-7 cells, have lower levels of CTCF binding compared to the sites identified in ZR-75-1 and T-47D cells. This suggests that FoxA1 cannot bind to the sites identified in the other cell lines in MCF-7 cells due the higher levels CTCF. This also supports findings in chapter 5 correlating an increase in CTCF binding at FoxA1 sites lost upon E2 treatment. In addition, at the GR DynaLoad sites identified in MCF-7 cells, there are higher levels of CTCF binding, compared with the sites identified in ZR-75-1 and T-47D cells.

Overall, this has demonstrated that activation of multiple receptors can reprogram the binding landscape for other receptors and TFs; however, these sites are highly cell line specific. In addition, histone modifications and other TF are involved in the DynaLoad mechanism.

7.2 Future Directions

7.2.1 Further investigation of GR, ER, and FoxA1 binding patterns in cancer cell lines.

A large subset of bioinformatic analysis on the current data in this thesis has been performed. It has been determined that ER and GR DynaLoad is functional in multiple cell lines; however, there are still a number of unanswered questions. The ENCODE consortium (Consortium, Bernstein et al. 2012), in addition to other studies, provides a multitude of publically available data whereby regions of transcription, TF association, chromatin structure, and histone modifications in the human genome have been mapped in cancer cells. However, it is beyond the scope of this PhD candidature to further investigate all avenues publically available. Further utilising these data sets may allow the detection of TF, histone modifications, or chromatin structural changes that mark regions that correspond to the changes in binding patterns identified in this thesis. Potential avenues, at these sites, that can be further explored include the analysis of H3K4me1 levels, the changes in histone modifications upon E2 stimulation, and changes in transcriptional factor binding upon treatment of cells with E2.

7.2.2 Further investigate the involvement of CTCF, histone modifications, and chromatin remodeller complexes in dictating DynaLoad.

The findings in chapter 6 of this thesis demonstrate that the DynaLoad mechanism is functional in multiple breast cancer cell lines; however, the complexity of this mechanism is more involved than previously suggested (Voss, Schiltz et al. 2011, Miranda, Voss et al. 2013). It has been shown that activation of multiple receptors can indeed modulate the response of other factors, including the pioneer factor FoxA1; however, the sites acquired are cell line specific. It was identified in MCF-7 cells, H3K27ac marks ER DynaLoad. ER DynaLoad sites identified in ZR-75-1 and T-47D cells were not found in MCF-7 cells, due the absence of H3K27ac. In addition, CTCF binding has been associated with GR DynaLoad sites in MCF-7 cells, and ER activated FoxA1 DynaLoad. To ascertain the true effect of these factors in deeming DynaLoad sites active, H3K27ac and CTCF ChIP-seq needs to be performed in ZR-75-1 and T-47D cells, thereby allowing the identification of a direct correlation of the two factors in multiple cell lines.

In addition, it has recently been shown that the chromatin remodelling proteins, Brg1, Snf2h, and ChD4 have the ability to open and close chromatin, individually or in a complex (Morris, Baek et al. 2014), which is contrary to previous notions that a unique remodelling system is recruited to a given DHS site (Hogan and Varga-Weisz 2007, Clapier and Cairns 2009). Since it is becoming apparent that SRs assert their response by a dynamic system, the identification of potential remodelling complexes involved in the acquisition of new ER, GR, and FoxA1

DynaLoad sites needs to be determined to further establish the mechanisms involved in DynaLoad binding.

The identification of a marker and remodelling complexes that denote new ER, GR, and FoxA1 binding sites may provide valuable information into the unknown actions of these proteins in breast cancer. Currently, in ER positive cancers, patients are treated with endocrine therapies such as Tamoxifen (Ali and Coombes 2002). However, women can become resistant to these therapies and relapse with a limitation of further treatment options (Clarke, Leonessa et al. 2001). Being able to identify new markers that indicate ER, GR, or FoxA1 mechanisms may provide new treatment targets and also provide new targets for endocrine therapy resistant cancers.

7.2.3 Further investigation into the mechanism behind GR lost sites by activation of ER in breast cancer cells.

In chapter 4, a massive inhibition of GR binding upon E2 stimulation in MCF-7 cells has been identified. This finding is not prevalent in breast cancer cells with either lower ER levels or higher GR levels. Determining the mechanism behind the loss of GR binding in ER dominant cancer may lead to further identification of the specific role GR plays in breast cancer progression. No change in DHS at these sites upon activation of ER is observed and the sites are not pre-marked with either H3K27ac, H3K4me3, H3K9me3, or H3K27me3 suggesting other mechanisms are involved. It has previously been demonstrated that PAD2, an enzyme that converts arginine and methylarginine residues to citrulline, is recruited to ER binding sites in MCF-7 cells resulting in the citullination of H3R26 at these binding elements. This results in chromatin decondensation

associated with gene transcription (Zhang, Bolt et al. 2012). To further characterise the loss of GR binding upon activation of ER, ER association with citrullination of H3R26 at GR lost sites could be determined. Further it has been shown that Dex does not induce citrullination of H3R26 (Guertin, Zhang et al. 2014). This would allow the identification of a potential mark associated with a loss of GR binding.

Previous studies have also determined that co-activation of ER and GR result in a decrease in GR binding to the MMTV reporter construct, despite the fact that ER cannot bind to that construct (Voss, Schiltz et al. 2011). It has been suggested that squelching of factors could be a probable mechanism for this finding. This needs to be investigated further as it has been determined in chapter 3 that there are higher levels of ER than GR in MCF-7 cells. In addition, a FoxA1 motif has been identified at these sites. Being able to determine a direct role for FoxA1 and ER in the inhibition of GR function may provide valuable clinical information. It has been determined that breast cancers that express high GR levels have a better prognosis in ER positive cancers compared with ER negative cancers, with an increased level of EMT activation, cell adhesion, and cell survival in the ER negative patients (Pan, Kocherginsky et al. 2011). This suggests that ER can potentially inhibit the negative effects of GR signalling in breast cancer. If a direct role can be determined between ER levels and FoxA1, in the inhibition of GR binding, FoxA1 could be used as an additional drug target that is used concurrently with ER inhibitors.

Further, to determine if GR and ER levels are the driving force into the redistribution of binding patterns, over expression of ER could be performed in

ZR-75-1 and T-47D cells which have been suggested to be a model where GR can function without being inhibited by ER. This will provide further evidence to indicate the mechanistic role GR is playing in breast cancer cells.

7.2.4 Further investigation of the effects of GR, ER, and FoxA1 crosstalk *in vivo.*

Studies in this thesis have shown that ER, GR, and FoxA1 DynaLoad is a mechanism that occurs in breast cancer cells lines, and that activation of multiple receptors can reprogram the binding landscape for other factors. However, these experiments have been performed in breast cancer cell lines where the hormone levels have been modulated. This may not accurately reflect the role of Dex and E2 signalling in breast cancer tissue *in vivo* and perhaps a more clinically relevant model, such as a mouse xenograft or explants model should be used to further our understanding of dual signalling in breast cancer cells.

Previous studies have demonstrated that female NMRI athymic nude mice can grow tumours from MCF-7, ZR-75-1, and T-47D cells suspended in Matrigel and transplanted by a subcutaneous injection into the left flank of the nude mice (Hoffmann, Bohlmann et al. 2004). Hormones can be administered by injection directly into tumours or by slow-release hormone pellets implanted subcutaneously. After tumour removal, ChIP-seq analysis can be performed on the tumour samples. Further, another viable approach could be the use of malignant human breast tissue in an explants culture model. This experimental system has been successfully established in a number of laboratories using different cancer tissues (Zhuang, Saaristo et al. 2003, Eigeliene, Harkonen et al. 2006, Centenera, Raj et al. 2013). By utilising this model, it has also been demonstrated that hormone stimulation can modulate SR signalling (Milewicz,

Gregoraszczuk et al. 2005, Ochnik, Moore et al. 2014). This model has multiple advantages as it utilises 3-dimensional human breast tissue compared with a clonal cell line. This results in the structure cell type of the breast tissue being retained, thereby inducing stromal and adipose tissue into the system (Zhuang, Saaristo et al. 2003). Utilising this model, to investigate GR, ER, and FoxA1 binding patterns upon dual activation of receptors at a genome-wide level will allow further investigation of the DynaLoad mechanism in a clinical relevant model of human malignant breast cancer. This will allow the assessment of SR levels and different types of breast cancers, and determine the potential involvement of other TF and histone modification in human samples.

7.3 Summary and Conclusion

The work completed in this thesis has provided novel insight into the crosstalk between GR, ER, and FoxA1 in a number of differing breast cancer cell models. It has been demonstrated that SRs have the ability to alter the response of one another upon dual activation, via a DynaLoad mechanism, demonstrating a unique and differing binding pattern compared with the single hormone treatment. Further, it has been identified that activated ER and GR have the ability to initiate a new subset of FoxA1 binding sites. FoxA1 has previously been thought of as a pioneer factor whoses function is to recruit TFs to closed chromatin in order to enable a transcriptional response. However, this thesis shows that other SRs can also regulate FoxA1 binding to the genome. Most importantly, it has been identified that the DynaLoad mechanism is functional in multiple breast cancer cells. Further, it is more complex than previously identified, whereby newly

identified sites are unique between cell lines, and histone modifications and other TF mark site specificity, in addition with the dual activation. It has also been shown that in an estrogenic system with high levels of activated ER, there is an alteration to the GR response by the massive inhibition of GR binding. This finding is not observed in cell lines with lower ER levels, suggesting ER has an ability to regulate the GR response. This has the ability to have implications in cancer prognosis due to ER being used as a target for therapy in the clinic. Collectively, the findings in this thesis indicate that multiple factors have the ability to function as drivers of SR and TF recruitment. This has provided a previous unknown mechanism controlling FoxA1 function challenging our current understanding of pioneer factors. The results generated in this thesis provide a framework for future investigations looking into dual SR signalling *in vivo*, and will provide further insight into mechanisms behind DynaLoad in breast cancer.

Appendix 1.

Appendix 1A: *De novo* motif analysis of remaining GR and ER clusters from chapter 4.

Cluster 1

Motif	Factor	*P* value
	FOXP1	1e-32
	NR class	1e-22
	TFAP2A	1e-18

Cluster 7

Motif	Factor	*P* value
	ER	1e-695
	FoxA1	1e-263
	NR class	1e-216

Cluster 3

Motif	Factor	*P* value
	AR half site	1e-18
	ER	1e-16
	Pbx1	1e-12

Cluster 8

Motif	Factor	*P* value
	FoxA1	1e-48
	ER	1e-30
	GR	1e-28

Cluster 4

Motif	Factor	*P* value
	PR	1e-31
	Gata-IR4	1e-15
	Gata-IR3	1e-15

Cluster 11

Motif	Factor	*P* value
	NR class	1e-11

Appendix 1B: *De novo* motif analysis of remaining PR and ER clusters from chapter 4.

Cluster 1

Motif	Factor	*P* value
	GR	1e-14
	Fox::Ebox	1e-12
	Sox13	1e-12

Cluster 5

Motif	Factor	*P* value
	ER	1e-30
	NR4A2	1e-18
	FoxA1	1e-12

Cluster 6

Motif	Factor	*P* value
	GR	1e-22
	FoxD1	1e-14
	Oct4	1e-12
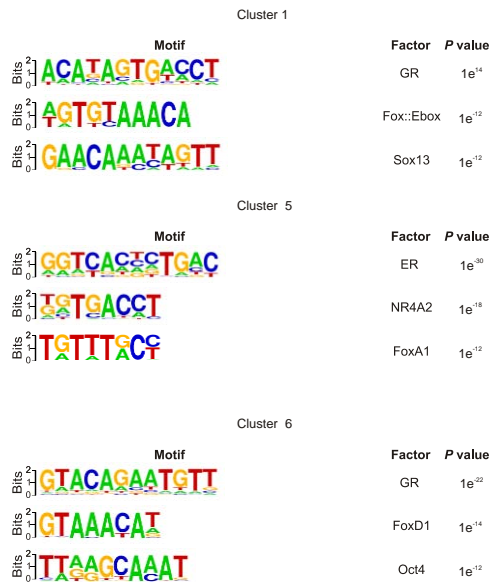
Appendix 1C: *De novo* **motif analysis of FoxA1 and ER cluster 1 from chapter 5.**
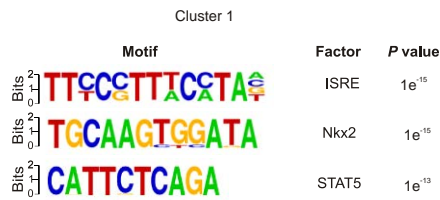
Appendix 1D: *De novo* **motif analysis of FoxA1 and PR cluster 1 from chapter 5.**
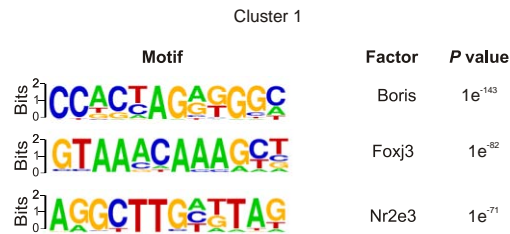
Appendix 1E: *De novo* **motif analysis of remaining GR and ER cluster from chapter 6.**
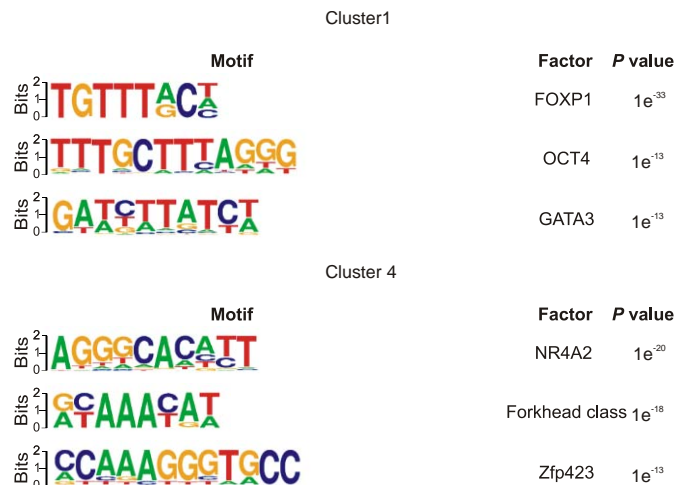
Appendix 1F: *De novo* motif analysis of remaining GR and ER clusters from chapter 6.

Cluster 1

Motif	Factor	*P* value
	GR	1e⁻⁸
	AR	1e⁻⁷
	PR	1e⁻²

Cluster 8

Motif	Factor	*P* value
	RARg	1e⁻³
	FOXA1	1e⁻³
	FOXH1	1e⁻³

Cluster 3

Motif	Factor	*P* value
	GR	1e⁻²
	AR	1e⁻²
	Srf	1e⁻²

Cluster 9

Motif	Factor	*P* value
	TEAD4	1e⁻²
	ETS	1e⁻²
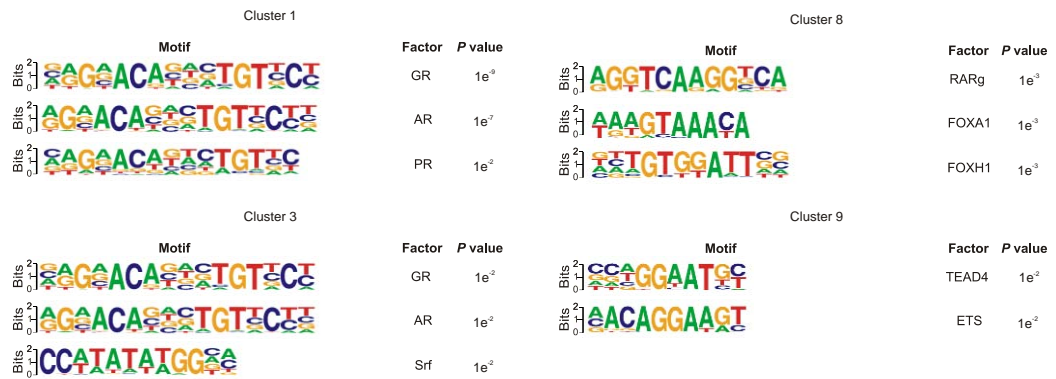
Appendix 1G: *De novo* motif analysis of remaining FoxA1 and GR clusters from chapter 6.

FoxA1 classical binding sites

Motif	Factor	*P* value
	FoxA1	1e⁻⁴⁴⁹⁵
	Ap2	1e⁻⁶⁰⁶
	GATA-IR3	1e⁻⁴⁴⁴

Cluster 1

Motif	Factor	*P* value
	FoxA1	1e⁻¹¹
	FoxA2	1e⁻⁹

Cluster 3

Motif	Factor	*P* value
	FoxA2	1e⁻¹⁵

Appendix 1H: *De novo* motif analysis of remaining FoxA1 and ER clusters from chapter 6

FoxA1 classical binding sites

Motif	Factor	P value
	FoxA1	1e^{-4286}
	Ap2	1e^{-614}
	GATA-IR3	1e^{-374}

Cluster 1

Motif	Factor	P value
	FoxP1	1e^{-9}

Cluster 4

Motif	Factor	P value
	FoxA1	1e^{-200}
	GATA-IR3	1e^{-31}
	Ap2	1e^{-25}

Appendix 2: Tables list high-throughput sequencing samples used in this thesis. Top table contains sample sets generated for this thesis. Bottom table lists the publically available ENCODE data analysed in this thesis.

Library	Cell Line	Treatment	Tags (replicate 1)	Tags (replicate 2)
GR ChIP-Seq	MCF-7	Untreated	30.57M	25.41M
GR ChIP-Seq	MCF-7	Plus Dex	41.03M	53.89M
GR ChIP-Seq	MCF-7	Plus E2	12.5M	19.84M
GR ChIP-Seq	MCF-7	Plus Dex and E2	15.94M	26.03M
ER ChIP-Seq	MCF-7	Untreated	43.01M	42.32M
ER ChIP-Seq	MCF-7	Plus Dex	28.96M	35.90M
ER ChIP-Seq	MCF-7	Plus E2	24.06M	30.13M
ER ChIP-Seq	MCF-7	Plus Dex and E2	29.72M	32.84M
ER ChIP-Seq	MCF-7	Plus P4	28.19M	27.84M
ER ChIP-Seq	MCF-7	Plus P4 and E2	48.72M	28.55M
FoxA1 ChIP-Seq	MCF-7	Untreated	25.35M	31.19M
FoxA1 ChIP-Seq	MCF-7	Plus Dex	23.2M	30.06M
FoxA1 ChIP-Seq	MCF-7	Plus E2	28.03M	31.88M
FoxA1 ChIP-Seq	MCF-7	Plus Dex and E2	27.21M	27.05M
PR ChIP-Seq	MCF-7	Untreated	31.14M	33.56M
PR ChIP-Seq	MCF-7	Plus P4	33.13M	30.18M
PR ChIP-Seq	MCF-7	Plus E2	32.64M	31.36M
PR ChIP-Seq	MCF-7	Plus P4 and E2	28.24M	32.08M
PolII ChIP-Seq	MCF-7	Untreated	25.47M	48.47M
PolII ChIP-Seq	MCF-7	Plus Dex	26.92M	27.13M
PolII ChIP-Seq	MCF-7	Plus E2	31.66M	20.24M
PolII ChIP-Seq	MCF-7	Plus Dex and E2	21.6M	28.14M
Input ChIP Seq	MCF-7	Plus Dex and E2	32.29M	38.28M
Input ChIP-Seq	MCF-7	Plus P4 and E2	14.79M	n/a
GR ChIP-Seq	T-47D	Untreated	22.45M	25.32M
GR ChIP-Seq	T-47D	Plus Dex	26.61M	26.08M
GR ChIP-Seq	T-47D	Plus E2	26.16M	20.51M
GR ChIP-Seq	T-47D	Plus Dex and E2	27.91M	37.77M
ER ChIP-Seq	T-47D	Untreated	24.22M	30.27M
ER ChIP-Seq	T-47D	Plus Dex	36.95M	36.87M
ER ChIP-Seq	T-47D	Plus E2	38.47M	34.30M
ER ChIP-Seq	T-47D	Plus Dex and E2	25.06M	28.27M
FoxA1 ChIP-Seq	T-47D	Untreated	31.90M	n/a
FoxA1 ChIP-Seq	T-47D	Plus Dex	29.66M	n/a
FoxA1 ChIP-Seq	T-47D	Plus E2	28.49M	n/a
FoxA1 ChIP-Seq	T-47D	Plus Dex and E2	28.61M	n/a
GR ChIP-Seq	ZR-75-1	Untreated	22.17M	26.27M
GR ChIP-Seq	ZR-75-1	Plus Dex	45.01M	32.53M
GR ChIP-Seq	ZR-75-1	Plus E2	31.98M	27.02M
GR ChIP-Seq	ZR-75-1	Plus Dex and E2	29.53M	28.36M
ER ChIP-Seq	ZR-75-1	Untreated	31.00M	21.56M
ER ChIP-Seq	ZR-75-1	Plus Dex	24.70M	23.77M
ER ChIP-Seq	ZR-75-1	Plus E2	26.56M	25.88M
ER ChIP-Seq	ZR-75-1	Plus Dex and E2	30.26M	32.96M
FoxA1 ChIP-Seq	ZR-75-1	Untreated	28.47M	26.04M
FoxA1 ChIP-Seq	ZR-75-1	Plus Dex	28.05M	30.07M
FoxA1 ChIP-Seq	ZR-75-1	Plus E2	29.57	29.88M
FoxA1 ChIP-Seq	ZR-75-1	Plus Dex and E2	26.63	36.79M
Input ChIP-Seq	ZR-75-1	Plus Dex and E2	29.42M	n/a

Library	Cell Line	Treatment	Tags (replicate 1)	Tags (replicate 2)	Source
DHS-Seq	MCF-7	Untreated	n/a	n/a	ENCODE:wgEncodeUwDnaseMcf7Estctrl0hAlnRep1
DHS-Seq	MCF-7	Untreated	n/a	n/a	ENCODE:wgEncodeUwDnaseMcf7Estctrl0hAlnRep2
DHS-Seq	MCF-7	Plus E2	n/a	n/a	ENCODE:wgEncodeUwDnaseMcf7Est100nmlhAlnRep2
DHS-Seq	MCF-7	Plus E2	n/a	n/a	ENCODE:wgEncodeUWDnaseMcf7Est100nM1hHotspotsRep2
H3K27ac ChIP-Seq	MCF-7	Untreated	n/a	n/a	ENCODE:wgEncodeSydhHistoneMcf7H3k27acUcdAlnRep1
H3K27ac ChIP-Seq	MCF-7	Untreated	n/a	n/a	ENCODE:wgEncodeSydhHistoneMcf7H3k27acUcdAlnRep2
H3K36me3 ChIP-Seq	MCF-7	Untreated	n/a	n/a	ENCODE:wgEncodeSydhHistoneMcf7H3k36me3bUcdAlnRep1
H3K36me3 ChIP-Seq	MCF-7	Untreated	n/a	n/a	ENCODE:wgEncodeSydhHistoneMcf7H3k36me3bUcdAlnRep2
H3K4me3 ChIP-Seq	MCF-7	Untreated	n/a	n/a	ENCODE:wgEncodeUwHistoneMcf7H3k4me3StdAlnRep1
H3K4me3 ChIP-Seq	MCF-7	Untreated	n/a	n/a	ENCODE:wgEncodeUwHistoneMcf7H3k4me3StdAlnRep2
H3K27me3 ChIP-Seq	MCF-7	Untreated	n/a	n/a	ENCODE:wgEncodeSydhHistoneMcf7H3k27me3bUcdAlnRep1
H3K27me3 ChIP-Seq	MCF-7	Untreated	n/a	n/a	ENCODE:wgEncodeSydhHistoneMcf7H3k27me3bUcdAlnRep2
H3K9me3 ChIP-Seq	MCF-7	Untreated	n/a	n/a	ENCODE:wgEncodeSydhHistoneMcf7H3k09me3UcdAlnRep1
H3K9me3 ChIP-Seq	MCF-7	Untreated	n/a	n/a	ENCODE:wgEncodeSydhHistoneMcf7H3k09me3UcdAlnRep2
CTCF ChIP-Seq	MCF-7	Untreated	n/a	n/a	ENCODE:wgEncodeOpenChromChipMcf7CtcfAlnRep1
CTCF ChIP-Seq	MCF-7	Untreated	n/a	n/a	ENCODE:wgEncodeOpenChromChipMcf7CtcfAlnRep2
CTCF ChIP-Seq	MCF-7	Plus E2	n/a	n/a	ENCODE:wgEncodeOpenChromChipMcf7CtcfEstroAlnRep1
CTCF ChIP-Seq	MCF-7	Plus E2	n/a	n/a	ENCODE:wgEncodeOpenChromChipMcf7CtcfEstroAlnRep2
MYC ChIP-Seq	MCF-7	Untreated	n/a	n/a	ENCODE:wgEncodeOpenChromChipMcf7CmycVehAlnRep1
MYC ChIP-Seq	MCF-7	Untreated	n/a	n/a	ENCODE:wgEncodeOpenChromChipMcf7CmycVehAlnRep2
MYC ChIP-Seq	MCF-7	Plus E2	n/a	n/a	ENCODE:wgEncodeOpenChromChipMcf7CmycEstroAlnRep1
MYC ChIP-Seq	MCF-7	Plus E2	n/a	n/a	ENCODE:wgEncodeOpenChromChipMcf7CmycEstroAlnRep2
GATA3 ChIP-Seq	MCF-7	Untreated	n/a	n/a	ENCODE:wgEncodeSydhTfbsMcf7Gata3UcdAlnRep1
GATA3 ChIP-Seq	MCF-7	Untreated	n/a	n/a	ENCODE:wgEncodeSydhTfbsMcf7Gata3UcdAlnRep2
P300 ChIP-Seq	MCF-7	Untreated	n/a	n/a	ENCODE:wgEncodeHaibTfbsMcf7P300V0422111AlnRep1
P300 ChIP-Seq	MCF-7	Untreated	n/a	n/a	ENCODE:wgEncodeHaibTfbsMcf7P300V0422111AlnRep2
HDAC2 ChIP-Seq	MCF-7	Untreated	n/a	n/a	ENCODE:wgEncodeHaibTfbsMcf7Hdac2sc6296V0422111AlnRep1
HDAC2 ChIP-Seq	MCF-7	Untreated	n/a	n/a	ENCODE:wgEncodeHaibTfbsMcf7Hdac2sc6296V0422111AlnRep2
CEBPB ChIP-Seq	MCF-7	Untreated	n/a	n/a	ENCODE:wgEncodeHaibTfbsMcf7Cebpbsc150V0422111AlnRep1
CEBPB ChIP-Seq	MCF-7	Untreated	n/a	n/a	ENCODE:wgEncodeHaibTfbsMcf7Cebpbsc150V0422111AlnRep2
ERG1 ChIP-Seq	MCF-7	Untreated	n/a	n/a	ENCODE:wgEncodeHaibTfbsMcf7Egr1V0422111AlnRep1
ERG1 ChIP-Seq	MCF-7	Untreated	n/a	n/a	ENCODE:wgEncodeHaibTfbsMcf7Egr1V0422111AlnRep2
ELF1 ChIP-Seq	MCF-7	Untreated	n/a	n/a	ENCODE:wgEncodeHaibTfbsMcf7Elf1V0422111AlnRep1
ELF1 ChIP-Seq	MCF-7	Untreated	n/a	n/a	ENCODE:wgEncodeHaibTfbsMcf7Elf1V0422111AlnRep1
FOSL2 ChIP-Seq	MCF-7	Untreated	n/a	n/a	ENCODE:wgEncodeHaibTfbsMcf7Fosl2V0422111AlnRep1
FOSL2 ChIP-Seq	MCF-7	Untreated	n/a	n/a	ENCODE:wgEncodeHaibTfbsMcf7Fosl2V0422111AlnRep2
FOXM1 ChIP-Seq	MCF-7	Untreated	n/a	n/a	ENCODE:wgEncodeHaibTfbsMcf7Foxm1sc502V0422111AlnRep1
FOXM1 ChIP-Seq	MCF-7	Untreated	n/a	n/a	ENCODE:wgEncodeHaibTfbsMcf7Foxm1sc502V0422111AlnRep2
GABP ChIP-Seq	MCF-7	Untreated	n/a	n/a	ENCODE:wgEncodeHaibTfbsMcf7GabpV0422111AlnRep1
GABP ChIP-Seq	MCF-7	Untreated	n/a	n/a	ENCODE:wgEncodeHaibTfbsMcf7GabpV0422111AlnRep2
JUND ChIP-Seq	MCF-7	Untreated	n/a	n/a	ENCODE:wgEncodeHaibTfbsMcf7JundV0422111AlnRep1
JUND ChIP-Seq	MCF-7	Untreated	n/a	n/a	ENCODE:wgEncodeHaibTfbsMcf7JundV0422111AlnRep2
MAX ChIP-Seq	MCF-7	Untreated	n/a	n/a	ENCODE:wgEncodeHaibTfbsMcf7MaxV0422111AlnRep1
MAX ChIP-Seq	MCF-7	Untreated	n/a	n/a	ENCODE:wgEncodeHaibTfbsMcf7MaxV0422111AlnRep2
NR2F2 ChIP-Seq	MCF-7	Untreated	n/a	n/a	ENCODE:wgEncodeHaibTfbsMcf7Nr2f2sc271940V0422111AlnRep1
NR2F2 ChIP-Seq	MCF-7	Untreated	n/a	n/a	ENCODE:wgEncodeHaibTfbsMcf7Nr2f2sc271940V0422111AlnRep2
NRSF ChIP-Seq	MCF-7	Untreated	n/a	n/a	ENCODE:wgEncodeHaibTfbsMcf7NrsfV0422111AlnRep1
NRSF ChIP-Seq	MCF-7	Untreated	n/a	n/a	ENCODE:wgEncodeHaibTfbsMcf7NrsfV0422111AlnRep2
PML ChIP-Seq	MCF-7	Untreated	n/a	n/a	ENCODE:wgEncodeHaibTfbsMcf7Pmlsc71910V0422111AlnRep1
PML ChIP-Seq	MCF-7	Untreated	n/a	n/a	ENCODE:wgEncodeHaibTfbsMcf7Pmlsc71910V0422111AlnRep2
RAD21 ChIP-Seq	MCF-7	Untreated	n/a	n/a	ENCODE:wgEncodeHaibTfbsMcf7Rad21V0422111AlnRep1
RAD21 ChIP-Seq	MCF-7	Untreated	n/a	n/a	ENCODE:wgEncodeHaibTfbsMcf7Rad21V0422111AlnRep2
RXL ChIP-Seq	MCF-7	Untreated	n/a	n/a	ENCODE:wgEncodeHaibTfbsMcf7RxlchV0422111AlnRep1
RXL ChIP-Seq	MCF-7	Untreated	n/a	n/a	ENCODE:wgEncodeHaibTfbsMcf7RxlchV0422111AlnRep2
RXL ChIP-Seq	MCF-7	Untreated	n/a	n/a	ENCODE:wgEncodeHaibTfbsMcf7RxlchV0422111AlnRep3
RXL ChIP-Seq	MCF-7	Untreated	n/a	n/a	ENCODE:wgEncodeHaibTfbsMcf7RxlchV0422111AlnRep4
SIN3Ak ChIP-Seq	MCF-7	Untreated	n/a	n/a	ENCODE:wgEncodeHaibTfbsMcf7Sin3ak20V0422111AlnRep1
SIN3Ak ChIP-Seq	MCF-7	Untreated	n/a	n/a	ENCODE:wgEncodeHaibTfbsMcf7Sin3ak20V0422111AlnRep2
SRF ChIP-Seq	MCF-7	Untreated	n/a	n/a	ENCODE:wgEncodeHaibTfbsMcf7SrfV0422111AlnRep1
SRF ChIP-Seq	MCF-7	Untreated	n/a	n/a	ENCODE:wgEncodeHaibTfbsMcf7SrfV0422111AlnRep2
TAF1 ChIP-Seq	MCF-7	Untreated	n/a	n/a	ENCODE:wgEncodeHaibTfbsMcf7Taf1V0422111AlnRep1
TAF1 ChIP-Seq	MCF-7	Untreated	n/a	n/a	ENCODE:wgEncodeHaibTfbsMcf7Taf1V0422111AlnRep2
TCF12 ChIP-Seq	MCF-7	Untreated	n/a	n/a	ENCODE:wgEncodeHaibTfbsMcf7Tcf12V0422111AlnRep1
TCF12 ChIP-Seq	MCF-7	Untreated	n/a	n/a	ENCODE:wgEncodeHaibTfbsMcf7Tcf12V0422111AlnRep2
TEAD4 ChIP-Seq	MCF-7	Untreated	n/a	n/a	ENCODE:wgEncodeHaibTfbsMcf7Tead4sc101184V0422111AlnRep1
TEAD4 ChIP-Seq	MCF-7	Untreated	n/a	n/a	ENCODE:wgEncodeHaibTfbsMcf7Tead4sc101184V0422111AlnRep2
HAE2F1 ChIP-Seq	MCF-7	Untreated	n/a	n/a	ENCODE:wgEncodeSydhTfbsMcf7Hae2f1UcdAlnRep1
HAE2F1 ChIP-Seq	MCF-7	Untreated	n/a	n/a	ENCODE:wgEncodeSydhTfbsMcf7Hae2f1UcdAlnRep2
TCF7L2 ChIP-Seq	MCF-7	Untreated	n/a	n/a	ENCODE:wgEncodeSydhTfbsMcf7Tcf7l2UcdAlnRep1
TCF7L2 ChIP-Seq	MCF-7	Untreated	n/a	n/a	ENCODE:wgEncodeSydhTfbsMcf7Tcf7l2UcdAlnRep2
ZNF217 ChIP-Seq	MCF-7	Untreated	n/a	n/a	ENCODE:wgEncodeSydhTfbsMcf7Znf217UcdAlnRep1
ZNF217 ChIP-Seq	MCF-7	Untreated	n/a	n/a	ENCODE:wgEncodeSydhTfbsMcf7Znf217UcdAlnRep2

Bibliography

Acevedo, M. L. and W. L. Kraus (2004). "Transcriptional activation by nuclear receptors." Essays Biochem **40**: 73-88.

AIHW (2007). Cancer in Australia: an overview, 2006. Canberra: AIHW. **Cat no. CAN 32**.

Ali, S. and R. C. Coombes (2002). "Endocrine-responsive breast cancer and strategies for combating resistance." Nat Rev Cancer **2**(2): 101-112.

Antonova, L. and C. R. Mueller (2008). "Hydrocortisone down-regulates the tumor suppressor gene BRCA1 in mammary cells: a possible molecular link between stress and breast cancer." Genes Chromosomes Cancer **47**(4): 341-352.

Archer, T. K., G. L. Hager and J. G. Omichinski (1990). "Sequence-specific DNA binding by glucocorticoid receptor "zinc finger peptides"." Proc Natl Acad Sci U S A **87**(19): 7560-7564.

Arora, V. K., E. Schenkein, R. Murali, S. K. Subudhi, J. Wongvipat, M. D. Balbas, N. Shah, L. Cai, E. Efstathiou, C. Logothetis, D. Zheng and C. L. Sawyers (2013). "Glucocorticoid receptor confers resistance to antiandrogens by bypassing androgen receptor blockade." Cell **155**(6): 1309-1322.

Aupperlee, M., A. Kariagina, J. Osuch and S. Z. Haslam (2005). "Progestins and breast cancer." Breast Dis **24**: 37-57.

Baek, S., M. H. Sung and G. L. Hager (2012). "Quantitative analysis of genome-wide chromatin remodeling." Methods Mol Biol **833**: 433-441.

Bain, D. L., A. F. Heneghan, K. D. Connaghan-Jones and M. T. Miura (2007). "Nuclear receptor structure: implications for function." Annu Rev Physiol **69**: 201-220.

Balfe, P. J., A. H. McCann, H. M. Welch and M. J. Kerin (2004). "Estrogen receptor beta and breast cancer." Eur J Surg Oncol **30**(10): 1043-1050.

Ballare, C., G. Castellano, L. Gaveglia, S. Althammer, J. Gonzalez-Vallinas, E. Eyras, F. Le Dily, R. Zaurin, D. Soronellas, G. P. Vicent and M. Beato (2013). "Nucleosome-driven transcription factor binding and gene regulation." Mol Cell **49**(1): 67-79.

Bardou, V. J., G. Arpino, R. M. Elledge, C. K. Osborne and G. M. Clark (2003). "Progesterone receptor status significantly improves outcome prediction over estrogen receptor status alone for adjuvant endocrine therapy in two large breast cancer databases." J Clin Oncol **21**(10): 1973-1979.

Beato, M. (1989). "Gene regulation by steroid hormones." Cell **56**(3): 335-344.

Beatson, G. T. (1983). "On The Treatment of Inoperable Cases of Carcinoma of the Mamma: Suggestions for a New Method of Treatment, with Illustrative Cases." CA Cancer J Clin **33**(2): 108-121.

Becker, M., C. Baumann, S. John, D. A. Walker, M. Vigneron, J. G. McNally and G. L. Hager (2002). "Dynamic behavior of transcription factors on a natural promoter in living cells." EMBO Rep **3**(12): 1188-1194.

Becker, P. B., B. Gloss, W. Schmid, U. Strahle and G. Schutz (1986). "In vivo protein-DNA interactions in a glucocorticoid response element require the presence of the hormone." Nature **324**(6098): 686-688.

Belikov, S., C. Astrand and O. Wrange (2009). "FoxA1 binding directs chromatin structure and the functional response of a glucocorticoid receptor-regulated promoter." Mol Cell Biol **29**(20): 5413-5425.

Belikov, S., P. H. Holmqvist, C. Astrand and O. Wrange (2012). "FoxA1 and glucocorticoid receptor crosstalk via histone H4K16 acetylation at a hormone regulated enhancer." Exp Cell Res **318**(1): 61-74.

Beral, V. (2003). "Breast cancer and hormone-replacement therapy in the Million Women Study." Lancet **362**(9382): 419-427.

Bernardo, G. M. and R. A. Keri (2012). "FOXA1: a transcription factor with parallel functions in development and cancer." Biosci Rep **32**(2): 113-130.

Birnbaumer, M., W. T. Schrader and B. W. O'Malley (1983). "Assessment of structural similarities in chick oviduct progesterone receptor subunits by partial proteolysis of photoaffinity-labeled proteins." J Biol Chem **258**(12): 7331-7337.

Birrell, S. N., R. E. Hall and W. D. Tilley (1998). "Role of the androgen receptor in human breast cancer." J Mammary Gland Biol Neoplasia **3**(1): 95-103.

Bosisio, D., I. Marazzi, A. Agresti, N. Shimizu, M. E. Bianchi and G. Natoli (2006). "A hyper-dynamic equilibrium between promoter-bound and nucleoplasmic dimers controls NF-kappaB-dependent gene activity." EMBO J **25**(4): 798-810.

Caizzi, L., G. Ferrero, S. Cutrupi, F. Cordero, C. Ballare, V. Miano, S. Reineri, L. Ricci, O. Friard, A. Testori, D. Cora, M. Caselle, L. Di Croce and M. De Bortoli (2014). "Genome-wide activity of unliganded estrogen receptor-alpha in breast cancer cells." Proc Natl Acad Sci U S A **111**(13): 4892-4897.

Cardiff, R. D. (1998). "Are the TDLU of the human the same as the LA of mice?" J Mammary Gland Biol Neoplasia **3**(1): 3-5.

Carroll, J. S., X. S. Liu, A. S. Brodsky, W. Li, C. A. Meyer, A. J. Szary, J. Eeckhoute, W. Shao, E. V. Hestermann, T. R. Geistlinger, E. A. Fox, P. A. Silver and M. Brown (2005). "Chromosome-wide mapping of estrogen receptor binding

reveals long-range regulation requiring the forkhead protein FoxA1." <u>Cell</u> **122**(1): 33-43.

Carroll, J. S., C. A. Meyer, J. Song, W. Li, T. R. Geistlinger, J. Eeckhoute, A. S. Brodsky, E. K. Keeton, K. C. Fertuck, G. F. Hall, Q. Wang, S. Bekiranov, V. Sementchenko, E. A. Fox, P. A. Silver, T. R. Gingeras, X. S. Liu and M. Brown (2006). "Genome-wide analysis of estrogen receptor binding sites." <u>Nat Genet</u> **38**(11): 1289-1297.

Centenera, M. M., G. V. Raj, K. E. Knudsen, W. D. Tilley and L. M. Butler (2013). "Ex vivo culture of human prostate tissue and drug development." <u>Nat Rev Urol</u> **10**(8): 483-487.

Chandy, M., J. L. Gutierrez, P. Prochasson and J. L. Workman (2006). "SWI/SNF displaces SAGA-acetylated nucleosomes." <u>Eukaryot Cell</u> **5**(10): 1738-1747.

Charn, T. H., E. T. Liu, E. C. Chang, Y. K. Lee, J. A. Katzenellenbogen and B. S. Katzenellenbogen (2010). "Genome-wide dynamics of chromatin binding of estrogen receptors alpha and beta: mutual restriction and competitive site selection." <u>Mol Endocrinol</u> **24**(1): 47-59.

Charpentier, A. H., A. K. Bednarek, R. L. Daniel, K. A. Hawkins, K. J. Laflin, S. Gaddis, M. C. MacLeod and C. M. Aldaz (2000). "Effects of estrogen on global gene expression: identification of novel targets of estrogen action." <u>Cancer Res</u> **60**(21): 5977-5983.

Chen, D., H. Ma, H. Hong, S. S. Koh, S. M. Huang, B. T. Schurter, D. W. Aswad and M. R. Stallcup (1999). "Regulation of transcription by a protein methyltransferase." <u>Science</u> **284**(5423): 2174-2177.

Cheung, E. and W. L. Kraus (2010). "Genomic analyses of hormone signaling and gene regulation." <u>Annu Rev Physiol</u> **72**: 191-218.

Chlebowski, R. T., G. L. Anderson, M. Gass, D. S. Lane, A. K. Aragaki, L. H. Kuller, J. E. Manson, M. L. Stefanick, J. Ockene, G. E. Sarto, K. C. Johnson, J. Wactawski-Wende, P. M. Ravdin, R. Schenken, S. L. Hendrix, A. Rajkovic, T. E. Rohan, S. Yasmeen and R. L. Prentice (2010). "Estrogen plus progestin and breast cancer incidence and mortality in postmenopausal women." <u>JAMA</u> **304**(15): 1684-1692.

Chlebowski, R. T., S. L. Hendrix, R. D. Langer, M. L. Stefanick, M. Gass, D. Lane, R. J. Rodabough, M. A. Gilligan, M. G. Cyr, C. A. Thomson, J. Khandekar, H. Petrovitch and A. McTiernan (2003). "Influence of estrogen plus progestin on breast cancer and mammography in healthy postmenopausal women: the Women's Health Initiative Randomized Trial." <u>JAMA</u> **289**(24): 3243-3253.

Chlebowski, R. T., L. H. Kuller, R. L. Prentice, M. L. Stefanick, J. E. Manson, M. Gass, A. K. Aragaki, J. K. Ockene, D. S. Lane, G. E. Sarto, A. Rajkovic, R. Schenken, S. L. Hendrix, P. M. Ravdin, T. E. Rohan, S. Yasmeen and G.

Anderson (2009). "Breast cancer after use of estrogen plus progestin in postmenopausal women." <u>N Engl J Med</u> **360**(6): 573-587.

Chlebowski, R. T., J. E. Manson, G. L. Anderson, J. A. Cauley, A. K. Aragaki, M. L. Stefanick, D. S. Lane, K. C. Johnson, J. Wactawski-Wende, C. Chen, L. Qi, S. Yasmeen, P. A. Newcomb and R. L. Prentice (2013). "Estrogen plus progestin and breast cancer incidence and mortality in the Women's Health Initiative Observational Study." <u>J Natl Cancer Inst</u> **105**(8): 526-535.

Cirillo, L. A., C. E. McPherson, P. Bossard, K. Stevens, S. Cherian, E. Y. Shim, K. L. Clark, S. K. Burley and K. S. Zaret (1998). "Binding of the winged-helix transcription factor HNF3 to a linker histone site on the nucleosome." <u>EMBO J</u> **17**(1): 244-254.

Clapier, C. R. and B. R. Cairns (2009). "The biology of chromatin remodeling complexes." <u>Annu Rev Biochem</u> **78**: 273-304.

Clarke, C. L. and J. D. Graham (2012). "Non-overlapping progesterone receptor cistromes contribute to cell-specific transcriptional outcomes." <u>PLoS One</u> **7**(4): e35859.

Clarke, R., F. Leonessa, J. N. Welch and T. C. Skaar (2001). "Cellular and molecular pharmacology of antiestrogen action and resistance." <u>Pharmacol Rev</u> **53**(1): 25-71.

Clemons, M. and P. Goss (2001). "Estrogen and the Risk of Breast Cancer." <u>N Engl J Med</u> **344**(4): 276-285.

Consortium, E. P., B. E. Bernstein, E. Birney, I. Dunham, E. D. Green, C. Gunter and M. Snyder (2012). "An integrated encyclopedia of DNA elements in the human genome." <u>Nature</u> **489**(7414): 57-74.

Core, L. J., J. J. Waterfall and J. T. Lis (2008). "Nascent RNA sequencing reveals widespread pausing and divergent initiation at human promoters." <u>Science</u> **322**(5909): 1845-1848.

Coser, K. R., J. Chesnes, J. Hur, S. Ray, K. J. Isselbacher and T. Shioda (2003). "Global analysis of ligand sensitivity of estrogen inducible and suppressible genes in MCF7/BUS breast cancer cells by DNA microarray." <u>Proc Natl Acad Sci U S A</u> **100**(24): 13994-13999.

Creighton, C. J., C. Kent Osborne, M. J. van de Vijver, J. A. Foekens, J. G. Klijn, H. M. Horlings, D. Nuyten, Y. Wang, Y. Zhang, G. C. Chamness, S. G. Hilsenbeck, A. V. Lee and R. Schiff (2009). "Molecular profiles of progesterone receptor loss in human breast tumors." <u>Breast Cancer Res Treat</u> **114**(2): 287-299.

Creyghton, M. P., A. W. Cheng, G. G. Welstead, T. Kooistra, B. W. Carey, E. J. Steine, J. Hanna, M. A. Lodato, G. M. Frampton, P. A. Sharp, L. A. Boyer, R. A. Young and R. Jaenisch (2010). "Histone H3K27ac separates active from poised

enhancers and predicts developmental state." <u>Proc Natl Acad Sci U S A</u> **107**(50): 21931-21936.

Cui, X., R. Schiff, G. Arpino, C. K. Osborne and A. V. Lee (2005). "Biology of progesterone receptor loss in breast cancer and its implications for endocrine therapy." <u>J Clin Oncol</u> **23**(30): 7721-7735.

Cvoro, A., C. Yuan, S. Paruthiyil, O. H. Miller, K. R. Yamamoto and D. C. Leitman (2011). "Cross talk between glucocorticoid and estrogen receptors occurs at a subset of proinflammatory genes." <u>J Immunol</u> **186**(7): 4354-4360.

Donegan, W. L. a. S., J.S. (1995). <u>Cancer of the Breast</u>, Saunders Company.

Dowsett, M., E. Folkerd, D. Doody and B. Haynes (2005). "The biology of steroid hormones and endocrine treatment of breast cancer." <u>Breast</u> **14**(6): 452-457.

Dundr, M., U. Hoffmann-Rohrer, Q. Hu, I. Grummt, L. I. Rothblum, R. D. Phair and T. Misteli (2002). "A kinetic framework for a mammalian RNA polymerase in vivo." <u>Science</u> **298**(5598): 1623-1626.

Eeckhoute, J., J. S. Carroll, T. R. Geistlinger, M. I. Torres-Arzayus and M. Brown (2006). "A cell-type-specific transcriptional network required for estrogen regulation of cyclin D1 and cell cycle progression in breast cancer." <u>Genes Dev</u> **20**(18): 2513-2526.

Eeckhoute, J., M. Lupien and M. Brown (2009). "Combining chromatin immunoprecipitation and oligonucleotide tiling arrays (ChIP-Chip) for functional genomic studies." <u>Methods Mol Biol</u> **556**: 155-164.

Eeckhoute, J., M. Lupien, C. A. Meyer, M. P. Verzi, R. A. Shivdasani, X. S. Liu and M. Brown (2009). "Cell-type selective chromatin remodeling defines the active subset of FOXA1-bound enhancers." <u>Genome Res</u> **19**(3): 372-380.

Eigeliene, N., P. Harkonen and R. Erkkola (2006). "Effects of estradiol and medroxyprogesterone acetate on morphology, proliferation and apoptosis of human breast tissue in organ cultures." <u>BMC Cancer</u> **6**: 246.

Engel, L. W., N. A. Young, T. S. Tralka, M. E. Lippman, S. J. O'Brien and M. J. Joyce (1978). "Establishment and characterization of three new continuous cell lines derived from human breast carcinomas." <u>Cancer Res</u> **38**(10): 3352-3364.

Evans, R. M. (1988). "The steroid and thyroid hormone receptor superfamily." <u>Science</u> **240**(4854): 889-895.

Fackenthal, J. D. and O. I. Olopade (2007). "Breast cancer risk associated with BRCA1 and BRCA2 in diverse populations." <u>Nat Rev Cancer</u> **7**(12): 937-948.

Fisher, B., C. Redmond, A. Brown, D. L. Wickerham, N. Wolmark, J. Allegra, G. Escher, M. Lippman, E. Savlov, J. Wittliff and et al. (1983). "Influence of tumor

estrogen and progesterone receptor levels on the response to tamoxifen and chemotherapy in primary breast cancer." <u>J Clin Oncol</u> **1**(4): 227-241.

Fisher, B., D. L. Wickerham, A. Brown and C. K. Redmond (1983). "Breast cancer estrogen and progesterone receptor values: their distribution, degree of concordance, and relation to number of positive axillary nodes." <u>J Clin Oncol</u> **1**(6): 349-358.

Foulds, C. E., Q. Feng, C. Ding, S. Bailey, T. L. Hunsaker, A. Malovannaya, R. A. Hamilton, L. A. Gates, Z. Zhang, C. Li, D. Chan, A. Bajaj, C. G. Callaway, D. P. Edwards, D. M. Lonard, S. Y. Tsai, M. J. Tsai, J. Qin and B. W. O'Malley (2013). "Proteomic analysis of coregulators bound to ERalpha on DNA and nucleosomes reveals coregulator dynamics." <u>Mol Cell</u> **51**(2): 185-199.

Franchimont, D. (2004). "Overview of the actions of glucocorticoids on the immune response: a good model to characterize new pathways of immunosuppression for new treatment strategies." <u>Ann N Y Acad Sci</u> **1024**: 124-137.

Frasor, J., J. M. Danes, B. Komm, K. C. Chang, C. R. Lyttle and B. S. Katzenellenbogen (2003). "Profiling of estrogen up- and down-regulated gene expression in human breast cancer cells: insights into gene networks and pathways underlying estrogenic control of proliferation and cell phenotype." <u>Endocrinology</u> **144**(10): 4562-4574.

Freedman, L. P., B. F. Luisi, Z. R. Korszun, R. Basavappa, P. B. Sigler and K. R. Yamamoto (1988). "The function and structure of the metal coordination sites within the glucocorticoid receptor DNA binding domain." <u>Nature</u> **334**(6182): 543-546.

Fryer, C. J. and T. K. Archer (1998). "Chromatin remodelling by the glucocorticoid receptor requires the BRG1 complex." <u>Nature</u> **393**(6680): 88-91.

Fu, X. D., M. S. Giretti, C. Baldacci, S. Garibaldi, M. Flamini, A. M. Sanchez, A. Gadducci, A. R. Genazzani and T. Simoncini (2008). "Extra-nuclear signaling of progesterone receptor to breast cancer cell movement and invasion through the actin cytoskeleton." <u>PLoS ONE</u> **3**(7): e2790.

Gaub, M. P., M. Bellard, I. Scheuer, P. Chambon and P. Sassone-Corsi (1990). "Activation of the ovalbumin gene by the estrogen receptor involves the fos-jun complex." <u>Cell</u> **63**(6): 1267-1276.

Gertz, J., D. Savic, K. E. Varley, E. C. Partridge, A. Safi, P. Jain, G. M. Cooper, T. E. Reddy, G. E. Crawford and R. M. Myers (2013). "Distinct properties of cell-type-specific and shared transcription factor binding sites." <u>Mol Cell</u> **52**(1): 25-36.

Gevry, N., S. Hardy, P. E. Jacques, L. Laflamme, A. Svotelis, F. Robert and L. Gaudreau (2009). "Histone H2A.Z is essential for estrogen receptor signaling." <u>Genes Dev</u> **23**(13): 1522-1533.

Ghayee, H. K. and R. J. Auchus (2007). "Basic concepts and recent developments in human steroid hormone biosynthesis." Rev Endocr Metab Disord **8**(4): 289-300.

Giangrande, P. H. and D. P. McDonnell (1999). "The A and B isoforms of the human progesterone receptor: two functionally different transcription factors encoded by a single gene." Recent Prog Horm Res **54**: 291-313; discussion 313-294.

Gill, P. G., W. D. Tilley, N. J. De Young, I. L. Lensink, P. D. Dixon and D. J. Horsfall (1991). "Inhibition of T47D human breast cancer cell growth by the synthetic progestin R5020: effects of serum, estradiol, insulin, and EGF." Breast Cancer Res Treat **20**(1): 53-62.

Grant, C. E., T. L. Bailey and W. S. Noble (2011). "FIMO: scanning for occurrences of a given motif." Bioinformatics **27**(7): 1017-1018.

Green, S., P. Walter, V. Kumar, A. Krust, J. M. Bornert, P. Argos and P. Chambon (1986). "Human oestrogen receptor cDNA: sequence, expression and homology to v-erb-A." Nature **320**(6058): 134-139.

Greene, G. L., P. Gilna, M. Waterfield, A. Baker, Y. Hort and J. Shine (1986). "Sequence and expression of human estrogen receptor complementary DNA." Science **231**(4742): 1150-1154.

Grontved, L., S. John, S. Baek, Y. Liu, J. R. Buckley, C. Vinson, G. Aguilera and G. L. Hager (2013). "C/EBP maintains chromatin accessibility in liver and facilitates glucocorticoid receptor recruitment to steroid response elements." EMBO J **32**(11): 1568-1583.

Guertin, M. J., X. Zhang, L. Anguish, S. Kim, L. Varticovski, J. T. Lis, G. L. Hager and S. A. Coonrod (2014). "Targeted H3R26 Deimination Specifically Facilitates Estrogen Receptor Binding by Modifying Nucleosome Structure." PLoS Genet **10**(9): e1004613.

Hah, N., C. G. Danko, L. Core, J. J. Waterfall, A. Siepel, J. T. Lis and W. L. Kraus (2011). "A rapid, extensive, and transient transcriptional response to estrogen signaling in breast cancer cells." Cell **145**(4): 622-634.

Hall, J. M., J. F. Couse and K. S. Korach (2001). "The multifaceted mechanisms of estradiol and estrogen receptor signaling." J Biol Chem **276**(40): 36869-36872.

Ham, J., A. Thomson, M. Needham, P. Webb and M. Parker (1988). "Characterization of response elements for androgens, glucocorticoids and progestins in mouse mammary tumour virus." Nucleic Acids Res **16**(12): 5263-5276.

Hardy, S., P. E. Jacques, N. Gevry, A. Forest, M. E. Fortin, L. Laflamme, L. Gaudreau and F. Robert (2009). "The euchromatic and heterochromatic

landscapes are shaped by antagonizing effects of transcription on H2A.Z deposition." <u>PLoS Genet</u> **5**(10): e1000687.

Harvie, M., L. Hooper and A. H. Howell (2003). "Central obesity and breast cancer risk: a systematic review." <u>Obes Rev</u> **4**(3): 157-173.

Hayes, D. F., Ed. (1993). <u>Atlas of Breast Cancer.</u> London, Mosby: Year book Europe Ltd.

He, H. H., C. A. Meyer, M. W. Chen, V. C. Jordan, M. Brown and X. S. Liu (2012). "Differential DNase I hypersensitivity reveals factor-dependent chromatin dynamics." <u>Genome Res</u> **22**(6): 1015-1025.

Heintzman, N. D., G. C. Hon, R. D. Hawkins, P. Kheradpour, A. Stark, L. F. Harp, Z. Ye, L. K. Lee, R. K. Stuart, C. W. Ching, K. A. Ching, J. E. Antosiewicz-Bourget, H. Liu, X. Zhang, R. D. Green, V. V. Lobanenkov, R. Stewart, J. A. Thomson, G. E. Crawford, M. Kellis and B. Ren (2009). "Histone modifications at human enhancers reflect global cell-type-specific gene expression." <u>Nature</u> **459**(7243): 108-112.

Heintzman, N. D., R. K. Stuart, G. Hon, Y. Fu, C. W. Ching, R. D. Hawkins, L. O. Barrera, S. Van Calcar, C. Qu, K. A. Ching, W. Wang, Z. Weng, R. D. Green, G. E. Crawford and B. Ren (2007). "Distinct and predictive chromatin signatures of transcriptional promoters and enhancers in the human genome." <u>Nat Genet</u> **39**(3): 311-318.

Heinz, S., C. Benner, N. Spann, E. Bertolino, Y. C. Lin, P. Laslo, J. X. Cheng, C. Murre, H. Singh and C. K. Glass (2010). "Simple combinations of lineage-determining transcription factors prime cis-regulatory elements required for macrophage and B cell identities." <u>Mol Cell</u> **38**(4): 576-589.

Heldring, N., A. Pike, S. Andersson, J. Matthews, G. Cheng, J. Hartman, M. Tujague, A. Strom, E. Treuter, M. Warner and J. A. Gustafsson (2007). "Estrogen receptors: how do they signal and what are their targets." <u>Physiol Rev</u> **87**(3): 905-931.

Herr, I. and J. Pfitzenmaier (2006). "Glucocorticoid use in prostate cancer and other solid tumours: implications for effectiveness of cytotoxic treatment and metastases." <u>Lancet Oncol</u> **7**(5): 425-430.

Hindle, W. M., K. (2009) "Global Library of Women's Medicine." DOI: 10.3843/GLOWM.10017.

Hissom, J. R. and M. R. Moore (1987). "Progestin effects on growth in the human breast cancer cell line T-47D--possible therapeutic implications." <u>Biochem Biophys Res Commun</u> **145**(2): 706-711.

Hoffmann, J., R. Bohlmann, N. Heinrich, H. Hofmeister, J. Kroll, H. Kunzer, R. B. Lichtner, Y. Nishino, K. Parczyk, G. Sauer, H. Gieschen, H. F. Ulbrich and M.

R. Schneider (2004). "Characterization of new estrogen receptor destabilizing compounds: effects on estrogen-sensitive and tamoxifen-resistant breast cancer." J Natl Cancer Inst **96**(3): 210-218.

Hogan, C. and P. Varga-Weisz (2007). "The regulation of ATP-dependent nucleosome remodelling factors." Mutat Res **618**(1-2): 41-51.

Hollenberg, S. M., C. Weinberger, E. S. Ong, G. Cerelli, A. Oro, R. Lebo, E. B. Thompson, M. G. Rosenfeld and R. M. Evans (1985). "Primary structure and expression of a functional human glucocorticoid receptor cDNA." Nature **318**(6047): 635-641.

Horseman, N. D. (1999). "Prolactin and mammary gland development." J Mammary Gland Biol Neoplasia **4**(1): 79-88.

Hsieh, C. C., D. Trichopoulos, K. Katsouyanni and S. Yuasa (1990). "Age at menarche, age at menopause, height and obesity as risk factors for breast cancer: associations and interactions in an international case-control study." Int J Cancer **46**(5): 796-800.

Htun, H., J. Barsony, I. Renyi, D. L. Gould and G. L. Hager (1996). "Visualization of glucocorticoid receptor translocation and intranuclear organization in living cells with a green fluorescent protein chimera." Proc Natl Acad Sci U S A **93**(10): 4845-4850.

Hundertmark, S., H. Buhler, M. Rudolf, H. K. Weitzel and V. Ragosch (1997). "Inhibition of 11 beta-hydroxysteroid dehydrogenase activity enhances the antiproliferative effect of glucocorticosteroids on MCF-7 and ZR-75-1 breast cancer cells." J Endocrinol **155**(1): 171-180.

Hurtado, A., K. A. Holmes, C. S. Ross-Innes, D. Schmidt and J. S. Carroll (2011). "FOXA1 is a key determinant of estrogen receptor function and endocrine response." Nat Genet **43**(1): 27-33.

Issar, M., S. Sahasranaman, P. Buchwald and G. Hochhaus (2006). "Differences in the glucocorticoid to progesterone receptor selectivity of inhaled glucocorticoids." Eur Respir J **27**(3): 511-516.

Ito, T., T. Ikehara, T. Nakagawa, W. L. Kraus and M. Muramatsu (2000). "p300-mediated acetylation facilitates the transfer of histone H2A-H2B dimers from nucleosomes to a histone chaperone." Genes Dev **14**(15): 1899-1907.

Jeltsch, J. M., Z. Krozowski, C. Quirin-Stricker, H. Gronemeyer, R. J. Simpson, J. M. Garnier, A. Krust, F. Jacob and P. Chambon (1986). "Cloning of the chicken progesterone receptor." Proc Natl Acad Sci U S A **83**(15): 5424-5428.

Jemal, A., F. Bray, M. M. Center, J. Ferlay, E. Ward and D. Forman (2011). "Global cancer statistics." CA Cancer J Clin **61**(2): 69-90.

Jin, C. and G. Felsenfeld (2007). "Nucleosome stability mediated by histone variants H3.3 and H2A.Z." Genes Dev **21**(12): 1519-1529.

Jin, C., C. Zang, G. Wei, K. Cui, W. Peng, K. Zhao and G. Felsenfeld (2009). "H3.3/H2A.Z double variant-containing nucleosomes mark 'nucleosome-free regions' of active promoters and other regulatory regions." Nat Genet **41**(8): 941-945.

John, S., P. J. Sabo, T. A. Johnson, M. H. Sung, S. C. Biddie, S. L. Lightman, T. C. Voss, S. R. Davis, P. S. Meltzer, J. A. Stamatoyannopoulos and G. L. Hager (2008). "Interaction of the glucocorticoid receptor with the chromatin landscape." Mol Cell **29**(5): 611-624.

John, S., P. J. Sabo, R. E. Thurman, M. H. Sung, S. C. Biddie, T. A. Johnson, G. L. Hager and J. A. Stamatoyannopoulos (2011). "Chromatin accessibility pre-determines glucocorticoid receptor binding patterns." Nat Genet **43**(3): 264-268.

Jonat, C., H. J. Rahmsdorf, K. K. Park, A. C. Cato, S. Gebel, H. Ponta and P. Herrlich (1990). "Antitumor promotion and antiinflammation: down-modulation of AP-1 (Fos/Jun) activity by glucocorticoid hormone." Cell **62**(6): 1189-1204.

Joseph, R., Y. L. Orlov, M. Huss, W. Sun, S. L. Kong, L. Ukil, Y. F. Pan, G. Li, M. Lim, J. S. Thomsen, Y. Ruan, N. D. Clarke, S. Prabhakar, E. Cheung and E. T. Liu (2010). "Integrative model of genomic factors for determining binding site selection by estrogen receptor-alpha." Mol Syst Biol **6**: 456.

Karmakar, S., Y. Jin and A. K. Nagaich (2013). "Interaction of glucocorticoid receptor (GR) with estrogen receptor (ER) alpha and activator protein 1 (AP1) in dexamethasone-mediated interference of ERalpha activity." J Biol Chem **288**(33): 24020-24034.

Kastner, P., A. Krust, B. Turcotte, U. Stropp, L. Tora, H. Gronemeyer and P. Chambon (1990). "Two distinct estrogen-regulated promoters generate transcripts encoding the two functionally different human progesterone receptor forms A and B." EMBO J **9**(5): 1603-1614.

Kent, W. J., C. W. Sugnet, T. S. Furey, K. M. Roskin, T. H. Pringle, A. M. Zahler and D. Haussler (2002). "The human genome browser at UCSC." Genome Res **12**(6): 996-1006.

Keydar, I., L. Chen, S. Karby, F. R. Weiss, J. Delarea, M. Radu, S. Chaitcik and H. J. Brenner (1979). "Establishment and characterization of a cell line of human breast carcinoma origin." Eur J Cancer **15**(5): 659-670.

Kininis, M., B. S. Chen, A. G. Diehl, G. D. Isaacs, T. Zhang, A. C. Siepel, A. G. Clark and W. L. Kraus (2007). "Genomic analyses of transcription factor binding, histone acetylation, and gene expression reveal mechanistically distinct classes of estrogen-regulated promoters." Mol Cell Biol **27**(14): 5090-5104.

Kinyamu, H. K. and T. K. Archer (2003). "Estrogen receptor-dependent proteasomal degradation of the glucocorticoid receptor is coupled to an increase in mdm2 protein expression." Mol Cell Biol **23**(16): 5867-5881.

Klokk, T. I., P. Kurys, C. Elbi, A. K. Nagaich, A. Hendarwanto, T. Slagsvold, C. Y. Chang, G. L. Hager and F. Saatcioglu (2007). "Ligand-specific dynamics of the androgen receptor at its response element in living cells." Mol Cell Biol **27**(5): 1823-1843.

Knotts, T. A., R. S. Orkiszewski, R. G. Cook, D. P. Edwards and N. L. Weigel (2001). "Identification of a phosphorylation site in the hinge region of the human progesterone receptor and additional amino-terminal phosphorylation sites." J Biol Chem **276**(11): 8475-8483.

Kong, S. L., G. Li, S. L. Loh, W. K. Sung and E. T. Liu (2011). "Cellular reprogramming by the conjoint action of ERalpha, FOXA1, and GATA3 to a ligand-inducible growth state." Mol Syst Biol **7**: 526.

Kraus, W. L., M. M. Montano and B. S. Katzenellenbogen (1993). "Cloning of the rat progesterone receptor gene 5'-region and identification of two functionally distinct promoters." Mol Endocrinol **7**(12): 1603-1616.

Kuiper, G. G., E. Enmark, M. Pelto-Huikko, S. Nilsson and J. A. Gustafsson (1996). "Cloning of a novel receptor expressed in rat prostate and ovary." Proc Natl Acad Sci U S A **93**(12): 5925-5930.

Kuiper, G. G. and J. A. Gustafsson (1997). "The novel estrogen receptor-beta subtype: potential role in the cell- and promoter-specific actions of estrogens and anti-estrogens." FEBS Lett **410**(1): 87-90.

Kumar, V. and P. Chambon (1988). "The estrogen receptor binds tightly to its responsive element as a ligand-induced homodimer." Cell **55**(1): 145-156.

Labrie, F. (2006). "Dehydroepiandrosterone, androgens and the mammary gland." Gynecol Endocrinol **22**(3): 118-130.

Labrie, F., V. Luu-The, C. Labrie, A. Belanger, J. Simard, S. X. Lin and G. Pelletier (2003). "Endocrine and intracrine sources of androgens in women: inhibition of breast cancer and other roles of androgens and their precursor dehydroepiandrosterone." Endocr Rev **24**(2): 152-182.

Labrie, F., R. Poulin, J. Simard, H. F. Zhao, C. Labrie, S. Dauvois, M. Dumont, A. C. Hatton, D. Poirier and Y. Merand (1990). "Interactions between estrogens, androgens, progestins, and glucocorticoids in ZR-75-1 human breast cancer cells." Ann N Y Acad Sci **595**: 130-148.

Lacroix, M. and G. Leclercq (2004). "Relevance of breast cancer cell lines as models for breast tumours: an update." Breast Cancer Res Treat **83**(3): 249-289.

Laganiere, J., G. Deblois, C. Lefebvre, A. R. Bataille, F. Robert and V. Giguere (2005). "From the Cover: Location analysis of estrogen receptor alpha target promoters reveals that FOXA1 defines a domain of the estrogen response." <u>Proc Natl Acad Sci U S A</u> **102**(33): 11651-11656.

Langlais, D., C. Couture, A. Balsalobre and J. Drouin (2012). "The Stat3/GR interaction code: predictive value of direct/indirect DNA recruitment for transcription outcome." <u>Mol Cell</u> **47**(1): 38-49.

Larson, B. L. a. S., V.R. (1978). <u>Lactation: A Comprehensive Treatise</u>. New York, Academic Press.

Laudet, V. (1997). "Evolution of the nuclear receptor superfamily: early diversification from an ancestral orphan receptor." <u>J Mol Endocrinol</u> **19**(3): 207-226.

Lee, D. Y., J. J. Hayes, D. Pruss and A. P. Wolffe (1993). "A positive role for histone acetylation in transcription factor access to nucleosomal DNA." <u>Cell</u> **72**(1): 73-84.

Lee, Y. K., Y. H. Choi, S. Chua, Y. J. Park and D. D. Moore (2006). "Phosphorylation of the hinge domain of the nuclear hormone receptor LRH-1 stimulates transactivation." <u>J Biol Chem</u> **281**(12): 7850-7855.

Lefterova, M. I., D. J. Steger, D. Zhuo, M. Qatanani, S. E. Mullican, G. Tuteja, E. Manduchi, G. R. Grant and M. A. Lazar (2010). "Cell-specific determinants of peroxisome proliferator-activated receptor gamma function in adipocytes and macrophages." <u>Mol Cell Biol</u> **30**(9): 2078-2089.

Leonhardt, S. A., V. Boonyaratanakornkit and D. P. Edwards (2003). "Progesterone receptor transcription and non-transcription signaling mechanisms." <u>Steroids</u> **68**(10-13): 761-770.

Lin, C. Y., V. B. Vega, J. S. Thomsen, T. Zhang, S. L. Kong, M. Xie, K. P. Chiu, L. Lipovich, D. H. Barnett, F. Stossi, A. Yeo, J. George, V. A. Kuznetsov, Y. K. Lee, T. H. Charn, N. Palanisamy, L. D. Miller, E. Cheung, B. S. Katzenellenbogen, Y. Ruan, G. Bourque, C. L. Wei and E. T. Liu (2007). "Whole-genome cartography of estrogen receptor alpha binding sites." <u>PLoS Genet</u> **3**(6): e87.

Lippman, M., G. Bolan and K. Huff (1976). "The effects of glucocorticoids and progesterone on hormone-responsive human breast cancer in long-term tissue culture." <u>Cancer Res</u> **36**(12): 4602-4609.

Luger, K., A. W. Mader, R. K. Richmond, D. F. Sargent and T. J. Richmond (1997). "Crystal structure of the nucleosome core particle at 2.8 A resolution." <u>Nature</u> **389**(6648): 251-260.

Lupien, M. and M. Brown (2009). "Cistromics of hormone-dependent cancer." Endocr Relat Cancer **16**(2): 381-389.

Lupien, M., J. Eeckhoute, C. A. Meyer, Q. Wang, Y. Zhang, W. Li, J. S. Carroll, X. S. Liu and M. Brown (2008). "FoxA1 translates epigenetic signatures into enhancer-driven lineage-specific transcription." Cell **132**(6): 958-970.

Mackay, A., N. Tamber, K. Fenwick, M. Iravani, A. Grigoriadis, T. Dexter, C. J. Lord, J. S. Reis-Filho and A. Ashworth (2009). "A high-resolution integrated analysis of genetic and expression profiles of breast cancer cell lines." Breast Cancer Res Treat **118**(3): 481-498.

Mauvais-Jarvis, P., F. Kuttenn, C. Malet and A. Gompel (1990). "Normal breast cells in culture. Effect of estrogens, progestins, and antiestrogens." Ann N Y Acad Sci **595**: 117-129.

McGuire, W. L. (1978). "Hormone receptors: their role in predicting prognosis and response to endocrine therapy." Semin Oncol **5**(4): 428-433.

McNally, J. G., W. G. Muller, D. Walker, R. Wolford and G. L. Hager (2000). "The glucocorticoid receptor: rapid exchange with regulatory sites in living cells." Science **287**(5456): 1262-1265.

Meijsing, S. H., C. Elbi, H. F. Luecke, G. L. Hager and K. R. Yamamoto (2007). "The ligand binding domain controls glucocorticoid receptor dynamics independent of ligand release." Mol Cell Biol **27**(7): 2442-2451.

Meyer, M. E., H. Gronemeyer, B. Turcotte, M. T. Bocquel, D. Tasset and P. Chambon (1989). "Steroid hormone receptors compete for factors that mediate their enhancer function." Cell **57**(3): 433-442.

Miesfeld, R., S. Okret, A. C. Wikstrom, O. Wrange, J. A. Gustafsson and K. R. Yamamoto (1984). "Characterization of a steroid hormone receptor gene and mRNA in wild-type and mutant cells." Nature **312**(5996): 779-781.

Miki, Y., J. Swensen, D. Shattuck-Eidens, P. A. Futreal, K. Harshman, S. Tavtigian, Q. Liu, C. Cochran, L. M. Bennett, W. Ding and et al. (1994). "A strong candidate for the breast and ovarian cancer susceptibility gene BRCA1." Science **266**(5182): 66-71.

Milewicz, T., E. L. Gregoraszczuk, K. Sztefko, K. Augustowska, J. Krzysiek and J. Rys (2005). "Lack of synergy between estrogen and progesterone on local IGF-I, IGFBP-3 and IGFBP-2 secretion by both hormone-dependent and hormone-independent breast cancer explants in vitro. Effect of tamoxifen and mifepristone (RU 486)." Growth Horm IGF Res **15**(2): 140-147.

Miranda, T. B., T. C. Voss, M. H. Sung, S. Baek, S. John, M. Hawkins, L. Grontved, R. L. Schiltz and G. L. Hager (2013). "Reprogramming the chromatin

landscape: interplay of the estrogen and glucocorticoid receptors at the genomic level." <u>Cancer Res</u> **73**(16): 5130-5139.

Mizuguchi, G., X. Shen, J. Landry, W. H. Wu, S. Sen and C. Wu (2004). "ATP-driven exchange of histone H2AZ variant catalyzed by SWR1 chromatin remodeling complex." <u>Science</u> **303**(5656): 343-348.

Moore, M. R., R. D. Hagley and J. R. Hissom (1988). "Progestin effects on lactate dehydrogenase and growth in the human breast cancer cell line T47D." <u>Prog Clin Biol Res</u> **262**: 161-179.

Moran, T. J., S. Gray, C. A. Mikosz and S. D. Conzen (2000). "The glucocorticoid receptor mediates a survival signal in human mammary epithelial cells." <u>Cancer Res</u> **60**(4): 867-872.

Morris, S. A., S. Baek, M. H. Sung, S. John, M. Wiench, T. A. Johnson, R. L. Schiltz and G. L. Hager (2014). "Overlapping chromatin-remodeling systems collaborate genome wide at dynamic chromatin transitions." <u>Nat Struct Mol Biol</u> **21**(1): 73-81.

Muse, G. W., D. A. Gilchrist, S. Nechaev, R. Shah, J. S. Parker, S. F. Grissom, J. Zeitlinger and K. Adelman (2007). "RNA polymerase is poised for activation across the genome." <u>Nat Genet</u> **39**(12): 1507-1511.

Nagy, L., H. Y. Kao, D. Chakravarti, R. J. Lin, C. A. Hassig, D. E. Ayer, S. L. Schreiber and R. M. Evans (1997). "Nuclear receptor repression mediated by a complex containing SMRT, mSin3A, and histone deacetylase." <u>Cell</u> **89**(3): 373-380.

Nardulli, A. M., G. L. Greene, B. W. O'Malley and B. S. Katzenellenbogen (1988). "Regulation of progesterone receptor messenger ribonucleic acid and protein levels in MCF-7 cells by estradiol: analysis of estrogen's effect on progesterone receptor synthesis and degradation." <u>Endocrinology</u> **122**(3): 935-944.

NCI (2007). NCI, N.C.I. Surveillance, Epidemiology, and End Results (SEER).

Need, E. F., L. A. Selth, T. J. Harris, S. N. Birrell, W. D. Tilley and G. Buchanan (2012). "Research resource: interplay between the genomic and transcriptional networks of androgen receptor and estrogen receptor alpha in luminal breast cancer cells." <u>Mol Endocrinol</u> **26**(11): 1941-1952.

Network, C. G. A. (2012). "Comprehensive molecular portraits of human breast tumours." <u>Nature</u> **490**(7418): 61-70.

Neve, R. M., K. Chin, J. Fridlyand, J. Yeh, F. L. Baehner, T. Fevr, L. Clark, N. Bayani, J. P. Coppe, F. Tong, T. Speed, P. T. Spellman, S. DeVries, A. Lapuk, N. J. Wang, W. L. Kuo, J. L. Stilwell, D. Pinkel, D. G. Albertson, F. M. Waldman, F. McCormick, R. B. Dickson, M. D. Johnson, M. Lippman, S. Ethier, A. Gazdar

and J. W. Gray (2006). "A collection of breast cancer cell lines for the study of functionally distinct cancer subtypes." <u>Cancer Cell</u> **10**(6): 515-527.

Ng, R. K. and J. B. Gurdon (2008). "Epigenetic memory of an active gene state depends on histone H3.3 incorporation into chromatin in the absence of transcription." <u>Nat Cell Biol</u> **10**(1): 102-109.

Ni, M., Y. Chen, E. Lim, H. Wimberly, S. T. Bailey, Y. Imai, D. L. Rimm, X. S. Liu and M. Brown (2011). "Targeting androgen receptor in estrogen receptor-negative breast cancer." <u>Cancer Cell</u> **20**(1): 119-131.

Norris, J. D., C. Y. Chang, B. M. Wittmann, R. S. Kunder, H. Cui, D. Fan, J. D. Joseph and D. P. McDonnell (2009). "The homeodomain protein HOXB13 regulates the cellular response to androgens." <u>Mol Cell</u> **36**(3): 405-416.

Ochnik, A. M., N. L. Moore, T. Jankovic-Karasoulos, T. Bianco-Miotto, N. K. Ryan, M. R. Thomas, S. N. Birrell, L. M. Butler, W. D. Tilley and T. E. Hickey (2014). "Antiandrogenic actions of medroxyprogesterone acetate on epithelial cells within normal human breast tissues cultured ex vivo." <u>Menopause</u> **21**(1): 79-88.

Ogawa, S., S. Inoue, T. Watanabe, A. Orimo, T. Hosoi, Y. Ouchi and M. Muramatsu (1998). "Molecular cloning and characterization of human estrogen receptor betacx: a potential inhibitor ofestrogen action in human." <u>Nucleic Acids Res</u> **26**(15): 3505-3512.

Orphanides, G. and D. Reinberg (2000). "RNA polymerase II elongation through chromatin." <u>Nature</u> **407**(6803): 471-475.

Orphanides, G. and D. Reinberg (2002). "A unified theory of gene expression." <u>Cell</u> **108**(4): 439-451.

Pan, D., M. Kocherginsky and S. D. Conzen (2011). "Activation of the glucocorticoid receptor is associated with poor prognosis in estrogen receptor-negative breast cancer." <u>Cancer Res</u> **71**(20): 6360-6370.

Perou, C. M., S. S. Jeffrey, M. van de Rijn, C. A. Rees, M. B. Eisen, D. T. Ross, A. Pergamenschikov, C. F. Williams, S. X. Zhu, J. C. Lee, D. Lashkari, D. Shalon, P. O. Brown and D. Botstein (1999). "Distinctive gene expression patterns in human mammary epithelial cells and breast cancers." <u>Proc Natl Acad Sci U S A</u> **96**(16): 9212-9217.

Perou, C. M., T. Sorlie, M. B. Eisen, M. van de Rijn, S. S. Jeffrey, C. A. Rees, J. R. Pollack, D. T. Ross, H. Johnsen, L. A. Akslen, O. Fluge, A. Pergamenschikov, C. Williams, S. X. Zhu, P. E. Lonning, A. L. Borresen-Dale, P. O. Brown and D. Botstein (2000). "Molecular portraits of human breast tumours." <u>Nature</u> **406**(6797): 747-752.

Ponta, H., A. C. Cato and P. Herrlich (1992). "Interference of pathway specific transcription factors." Biochim Biophys Acta **1129**(3): 255-261.

Poulin, R., J. M. Dufour and F. Labrie (1989). "Progestin inhibition of estrogen-dependent proliferation in ZR-75-1 human breast cancer cells: antagonism by insulin." Breast Cancer Res Treat **13**(3): 265-276.

Pratt, W. B. and D. O. Toft (1997). "Steroid receptor interactions with heat shock protein and immunophilin chaperones." Endocr Rev **18**(3): 306-360.

Rada-Iglesias, A., R. Bajpai, T. Swigut, S. A. Brugmann, R. A. Flynn and J. Wysocka (2011). "A unique chromatin signature uncovers early developmental enhancers in humans." Nature **470**(7333): 279-283.

Rae, J. M., M. D. Johnson, J. O. Scheys, K. E. Cordero, J. M. Larios and M. E. Lippman (2005). "GREB 1 is a critical regulator of hormone dependent breast cancer growth." Breast Cancer Res Treat **92**(2): 141-149.

Read, L. D., C. E. Snider, J. S. Miller, G. L. Greene and B. S. Katzenellenbogen (1988). "Ligand-modulated regulation of progesterone receptor messenger ribonucleic acid and protein in human breast cancer cell lines." Mol Endocrinol **2**(3): 263-271.

Reddy, T. E., J. Gertz, G. E. Crawford, M. J. Garabedian and R. M. Myers (2012). "The hypersensitive glucocorticoid response specifically regulates period 1 and expression of circadian genes." Mol Cell Biol **32**(18): 3756-3767.

Reddy, T. E., F. Pauli, R. O. Sprouse, N. F. Neff, K. M. Newberry, M. J. Garabedian and R. M. Myers (2009). "Genomic determination of the glucocorticoid response reveals unexpected mechanisms of gene regulation." Genome Res **19**(12): 2163-2171.

Redondo, M., T. Tellez, M. J. Roldan, A. Serrano, M. Garcia-Aranda, M. E. Gleave, M. L. Hortas and M. Morell (2007). "Anticlusterin treatment of breast cancer cells increases the sensitivities of chemotherapy and tamoxifen and counteracts the inhibitory action of dexamethasone on chemotherapy-induced cytotoxicity." Breast Cancer Res **9**(6): R86.

Reid, G., M. R. Hubner, R. Metivier, H. Brand, S. Denger, D. Manu, J. Beaudouin, J. Ellenberg and F. Gannon (2003). "Cyclic, proteasome-mediated turnover of unliganded and liganded ERalpha on responsive promoters is an integral feature of estrogen signaling." Mol Cell **11**(3): 695-707.

Rhen, T. and J. A. Cidlowski (2006). "Estrogens and glucocorticoids have opposing effects on the amount and latent activity of complement proteins in the rat uterus." Biol Reprod **74**(2): 265-274.

Richer, J. K., B. M. Jacobsen, N. G. Manning, M. G. Abel, D. M. Wolf and K. B. Horwitz (2002). "Differential gene regulation by the two progesterone receptor isoforms in human breast cancer cells." J Biol Chem **277**(7): 5209-5218.

Rigaud, G., J. Roux, R. Pictet and T. Grange (1991). "In vivo footprinting of rat TAT gene: dynamic interplay between the glucocorticoid receptor and a liver-specific factor." Cell **67**(5): 977-986.

Robinson, J. L., S. Macarthur, C. S. Ross-Innes, W. D. Tilley, D. E. Neal, I. G. Mills and J. S. Carroll (2011). "Androgen receptor driven transcription in molecular apocrine breast cancer is mediated by FoxA1." EMBO J **30**(15): 3019-3027.

Rosa, F. E., J. R. Caldeira, J. Felipes, F. B. Bertonha, F. C. Quevedo, M. A. Domingues, F. A. Moraes Neto and S. R. Rogatto (2008). "Evaluation of estrogen receptor alpha and beta and progesterone receptor expression and correlation with clinicopathologic factors and proliferative marker Ki-67 in breast cancers." Hum Pathol **39**(5): 720-730.

Roses, D. F. (1999). Breast cancer, Churchill Livingstone.

Rossouw, J. E., G. L. Anderson, R. L. Prentice, A. Z. LaCroix, C. Kooperberg, M. L. Stefanick, R. D. Jackson, S. A. Beresford, B. V. Howard, K. C. Johnson, J. M. Kotchen and J. Ockene (2002). "Risks and benefits of estrogen plus progestin in healthy postmenopausal women: principal results From the Women's Health Initiative randomized controlled trial." JAMA **288**(3): 321-333.

Rousseau-Merck, M. F., M. Misrahi, H. Loosfelt, E. Milgrom and R. Berger (1987). "Localization of the human progesterone receptor gene to chromosome 11q22-q23." Hum Genet **77**(3): 280-282.

Rubens, R. D., C. L. Tinson, R. E. Coleman, R. K. Knight, D. Tong, P. J. Winter and W. R. North (1988). "Prednisolone improves the response to primary endocrine treatment for advanced breast cancer." Br J Cancer **58**(5): 626-630.

Russo, J. and I. H. Russo (2006). "The role of estrogen in the initiation of breast cancer." J Steroid Biochem Mol Biol **102**(1-5): 89-96.

Sahu, B., M. Laakso, K. Ovaska, T. Mirtti, J. Lundin, A. Rannikko, A. Sankila, J. P. Turunen, M. Lundin, J. Konsti, T. Vesterinen, S. Nordling, O. Kallioniemi, S. Hautaniemi and O. A. Janne (2011). "Dual role of FoxA1 in androgen receptor binding to chromatin, androgen signalling and prostate cancer." EMBO J **30**(19): 3962-3976.

Sahu, B., M. Laakso, P. Pihlajamaa, K. Ovaska, I. Sinielnikov, S. Hautaniemi and O. A. Janne (2013). "FoxA1 specifies unique androgen and glucocorticoid receptor binding events in prostate cancer cells." Cancer Res **73**(5): 1570-1580.

Sartorius, C. A., M. Y. Melville, A. R. Hovland, L. Tung, G. S. Takimoto and K. B. Horwitz (1994). "A third transactivation function (AF3) of human progesterone receptors located in the unique N-terminal segment of the B-isoform." Mol Endocrinol **8**(10): 1347-1360.

Schaffner, W. (1988). "Gene regulation. A hit-and-run mechanism for transcriptional activation?" Nature **336**(6198): 427-428.

Schule, R., M. Muller, C. Kaltschmidt and R. Renkawitz (1988). "Many transcription factors interact synergistically with steroid receptors." Science **242**(4884): 1418-1420.

Schule, R., P. Rangarajan, S. Kliewer, L. J. Ransone, J. Bolado, N. Yang, I. M. Verma and R. M. Evans (1990). "Functional antagonism between oncoprotein c-Jun and the glucocorticoid receptor." Cell **62**(6): 1217-1226.

Schwartz, B. E. and K. Ahmad (2005). "Transcriptional activation triggers deposition and removal of the histone variant H3.3." Genes Dev **19**(7): 804-814.

Sharp, Z. D., M. G. Mancini, C. A. Hinojos, F. Dai, V. Berno, A. T. Szafran, K. P. Smith, T. P. Lele, D. E. Ingber and M. A. Mancini (2006). "Estrogen-receptor-alpha exchange and chromatin dynamics are ligand- and domain-dependent." J Cell Sci **119**(Pt 19): 4101-4116.

Shogren-Knaak, M., H. Ishii, J. M. Sun, M. J. Pazin, J. R. Davie and C. L. Peterson (2006). "Histone H4-K16 acetylation controls chromatin structure and protein interactions." Science **311**(5762): 844-847.

Siersbaek, R., R. Nielsen, S. John, M. H. Sung, S. Baek, A. Loft, G. L. Hager and S. Mandrup (2011). "Extensive chromatin remodelling and establishment of transcription factor 'hotspots' during early adipogenesis." EMBO J **30**(8): 1459-1472.

Simpson, E. R. (2003). "Sources of estrogen and their importance." J Steroid Biochem Mol Biol **86**(3-5): 225-230.

Simpson, E. R. and S. R. Davis (2001). "Minireview: Aromatase and the Regulation of Estrogen Biosynthesis--Some New Perspectives." Endocrinology **142**(11): 4589-4594.

Slamon, D. J., G. M. Clark, S. G. Wong, W. J. Levin, A. Ullrich and W. L. McGuire (1987). "Human breast cancer: correlation of relapse and survival with amplification of the HER-2/neu oncogene." Science **235**(4785): 177-182.

Smith, R. A., R. A. Lea, J. E. Curran, S. R. Weinstein and L. R. Griffiths (2003). "Expression of glucocorticoid and progesterone nuclear receptor genes in archival breast cancer tissue." Breast Cancer Res **5**(1): R9-12.

Smith, R. A., R. A. Lea, S. R. Weinstein and L. R. Griffiths (2007). "Progesterone, glucocorticoid, but not estrogen receptor mRNA is altered in breast cancer stroma." Cancer Lett **255**(1): 77-84.

So, A. Y., C. Chaivorapol, E. C. Bolton, H. Li and K. R. Yamamoto (2007). "Determinants of cell- and gene-specific transcriptional regulation by the glucocorticoid receptor." PLoS Genet **3**(6): e94.

Sorlie, T., C. M. Perou, R. Tibshirani, T. Aas, S. Geisler, H. Johnsen, T. Hastie, M. B. Eisen, M. van de Rijn, S. S. Jeffrey, T. Thorsen, H. Quist, J. C. Matese, P. O. Brown, D. Botstein, P. E. Lonning and A. L. Borresen-Dale (2001). "Gene expression patterns of breast carcinomas distinguish tumor subclasses with clinical implications." Proc Natl Acad Sci U S A **98**(19): 10869-10874.

Soule, H. D., J. Vazquez, A. Long, S. Albert and M. Brennan (1973). "A human cell line from a pleural effusion derived from a breast carcinoma." J Natl Cancer Inst **51**(5): 1409-1416.

Stender, J. D., J. Frasor, B. Komm, K. C. Chang, W. L. Kraus and B. S. Katzenellenbogen (2007). "Estrogen-regulated gene networks in human breast cancer cells: involvement of E2F1 in the regulation of cell proliferation." Mol Endocrinol **21**(9): 2112-2123.

Takai, H., H. Matsumura, S. Matsui, K. M. Kim, M. Mezawa, Y. Nakayama and Y. Ogata (2014). "Unliganded estrogen receptor alpha stimulates bone sialoprotein gene expression." Gene **539**(1): 50-57.

Takimoto, G. S., L. Tung, H. Abdel-Hafiz, M. G. Abel, C. A. Sartorius, J. K. Richer, B. M. Jacobsen, D. L. Bain and K. B. Horwitz (2003). "Functional properties of the N-terminal region of progesterone receptors and their mechanistic relationship to structure." J Steroid Biochem Mol Biol **85**(2-5): 209-219.

Thurman, R. E., E. Rynes, R. Humbert, J. Vierstra, M. T. Maurano, E. Haugen, N. C. Sheffield, A. B. Stergachis, H. Wang, B. Vernot, K. Garg, S. John, R. Sandstrom, D. Bates, L. Boatman, T. K. Canfield, M. Diegel, D. Dunn, A. K. Ebersol, T. Frum, E. Giste, A. K. Johnson, E. M. Johnson, T. Kutyavin, B. Lajoie, B. K. Lee, K. Lee, D. London, D. Lotakis, S. Neph, F. Neri, E. D. Nguyen, H. Qu, A. P. Reynolds, V. Roach, A. Safi, M. E. Sanchez, A. Sanyal, A. Shafer, J. M. Simon, L. Song, S. Vong, M. Weaver, Y. Yan, Z. Zhang, Z. Zhang, B. Lenhard, M. Tewari, M. O. Dorschner, R. S. Hansen, P. A. Navas, G. Stamatoyannopoulos, V. R. Iyer, J. D. Lieb, S. R. Sunyaev, J. M. Akey, P. J. Sabo, R. Kaul, T. S. Furey, J. Dekker, G. E. Crawford and J. A. Stamatoyannopoulos (2012). "The accessible chromatin landscape of the human genome." Nature **489**(7414): 75-82.

Tortora, G. J. (1995). The reproductive systems. Principles of Human Anatomy, Harper Collins College Publishers.

Truss, M., J. Bartsch, A. Schelbert, R. J. Hache and M. Beato (1995). "Hormone induces binding of receptors and transcription factors to a rearranged nucleosome on the MMTV promoter in vivo." EMBO J **14**(8): 1737-1751.

Tsai, S. Y., J. Carlstedt-Duke, N. L. Weigel, K. Dahlman, J. A. Gustafsson, M. J. Tsai and B. W. O'Malley (1988). "Molecular interactions of steroid hormone receptor with its enhancer element: evidence for receptor dimer formation." Cell **55**(2): 361-369.

Uht, R. M., C. M. Anderson, P. Webb and P. J. Kushner (1997). "Transcriptional activities of estrogen and glucocorticoid receptors are functionally integrated at the AP-1 response element." Endocrinology **138**(7): 2900-2908.

Umesono, K. and R. M. Evans (1989). "Determinants of target gene specificity for steroid/thyroid hormone receptors." Cell **57**(7): 1139-1146.

Vaidya, J. S., G. Baldassarre, M. A. Thorat and S. Massarut (2010). "Role of glucocorticoids in breast cancer." Curr Pharm Des **16**(32): 3593-3600.

van der Burg, B., E. Kalkhoven, L. Isbrucker and S. W. de Laat (1992). "Effects of progestins on the proliferation of estrogen-dependent human breast cancer cells under growth factor-defined conditions." J Steroid Biochem Mol Biol **42**(5): 457-465.

van Landeghem, A. A. J., J. Poortman, M. Nabuurs and J. H. H. Thijssen (1985). "Endogenous Concentration and Subcellular Distribution of Estrogens in Normal and Malignant Human Breast Tissue." Cancer Res **45**(6): 2900-2906.

Vienonen, A., S. Miettinen, T. Manninen, L. Altucci, E. Wilhelm and T. Ylikomi (2003). "Regulation of nuclear receptor and cofactor expression in breast cancer cell lines." Eur J Endocrinol **148**(4): 469-479.

Vilasco, M., L. Communal, N. Mourra, A. Courtin, P. Forgez and A. Gompel (2011). "Glucocorticoid receptor and breast cancer." Breast Cancer Res Treat **130**(1): 1-10.

Voss, T. C., R. L. Schiltz, M. H. Sung, P. M. Yen, J. A. Stamatoyannopoulos, S. C. Biddie, T. A. Johnson, T. B. Miranda, S. John and G. L. Hager (2011). "Dynamic exchange at regulatory elements during chromatin remodeling underlies assisted loading mechanism." Cell **146**(4): 544-554.

Walker, D., H. Htun and G. L. Hager (1999). "Using inducible vectors to study intracellular trafficking of GFP-tagged steroid/nuclear receptors in living cells." Methods **19**(3): 386-393.

Walsh, D. and J. Avashia (1992). "Glucocorticoids in clinical oncology." Cleve Clin J Med **59**(5): 505-515.

Wang, Q., W. Li, X. S. Liu, J. S. Carroll, O. A. Janne, E. K. Keeton, A. M. Chinnaiyan, K. J. Pienta and M. Brown (2007). "A hierarchical network of transcription factors governs androgen receptor-dependent prostate cancer growth." <u>Mol Cell</u> **27**(3): 380-392.

Wang, Q., W. Li, Y. Zhang, X. Yuan, K. Xu, J. Yu, Z. Chen, R. Beroukhim, H. Wang, M. Lupien, T. Wu, M. M. Regan, C. A. Meyer, J. S. Carroll, A. K. Manrai, O. A. Janne, S. P. Balk, R. Mehra, B. Han, A. M. Chinnaiyan, M. A. Rubin, L. True, M. Fiorentino, C. Fiore, M. Loda, P. W. Kantoff, X. S. Liu and M. Brown (2009). "Androgen receptor regulates a distinct transcription program in androgen-independent prostate cancer." <u>Cell</u> **138**(2): 245-256.

Webb, P., G. N. Lopez, R. M. Uht and P. J. Kushner (1995). "Tamoxifen activation of the estrogen receptor/AP-1 pathway: potential origin for the cell-specific estrogen-like effects of antiestrogens." <u>Mol Endocrinol</u> **9**(4): 443-456.

Wei, L. L., N. L. Krett, M. D. Francis, D. F. Gordon, W. M. Wood, B. W. O'Malley and K. B. Horwitz (1988). "Multiple human progesterone receptor messenger ribonucleic acids and their autoregulation by progestin agonists and antagonists in breast cancer cells." <u>Mol Endocrinol</u> **2**(1): 62-72.

Weinberger, C., S. M. Hollenberg, E. S. Ong, J. M. Harmon, S. T. Brower, J. Cidlowski, E. B. Thompson, M. G. Rosenfeld and R. M. Evans (1985). "Identification of human glucocorticoid receptor complementary DNA clones by epitope selection." <u>Science</u> **228**(4700): 740-742.

Welboren, W. J., M. A. van Driel, E. M. Janssen-Megens, S. J. van Heeringen, F. C. Sweep, P. N. Span and H. G. Stunnenberg (2009). "ChIP-Seq of ERalpha and RNA polymerase II defines genes differentially responding to ligands." <u>EMBO J</u> **28**(10): 1418-1428.

Whirledge, S., D. Dixon and J. A. Cidlowski (2012). "Glucocorticoids regulate gene expression and repress cellular proliferation in human uterine leiomyoma cells." <u>Horm Cancer</u> **3**(3): 79-92.

WHO (2008). W.H.O World Health Statistics.

Wittliff, J. L. (1984). "Steroid-hormone receptors in breast cancer." <u>Cancer</u> **53**(3 Suppl): 630-643.

Wolffe, A. P. and J. J. Hayes (1999). "Chromatin disruption and modification." <u>Nucleic Acids Res</u> **27**(3): 711-720.

Wrange, O., S. Okret, M. Radojcic, J. Carlstedt-Duke and J. A. Gustafsson (1984). "Characterization of the purified activated glucocorticoid receptor from rat liver cytosol." <u>J Biol Chem</u> **259**(7): 4534-4541.

Xu, J. and Q. Li (2003). "Review of the in vivo functions of the p160 steroid receptor coactivator family." <u>Mol Endocrinol</u> **17**(9): 1681-1692.

Yamaguchi, N., E. Ito, S. Azuma, R. Honma, Y. Yanagisawa, A. Nishikawa, M. Kawamura, J. Imai, K. Tatsuta, J. Inoue, K. Semba and S. Watanabe (2008). "FoxA1 as a lineage-specific oncogene in luminal type breast cancer." Biochem Biophys Res Commun **365**(4): 711-717.

Yamamoto, K. R. (1985). "Steroid receptor regulated transcription of specific genes and gene networks." Annu Rev Genet **19**: 209-252.

Yang-Yen, H. F., J. C. Chambard, Y. L. Sun, T. Smeal, T. J. Schmidt, J. Drouin and M. Karin (1990). "Transcriptional interference between c-Jun and the glucocorticoid receptor: mutual inhibition of DNA binding due to direct protein-protein interaction." Cell **62**(6): 1205-1215.

Zaret, K. S. and J. S. Carroll (2011). "Pioneer transcription factors: establishing competence for gene expression." Genes Dev **25**(21): 2227-2241.

Zhang, X., M. Bolt, M. J. Guertin, W. Chen, S. Zhang, B. D. Cherrington, D. J. Slade, C. J. Dreyton, V. Subramanian, K. L. Bicker, P. R. Thompson, M. A. Mancini, J. T. Lis and S. A. Coonrod (2012). "Peptidylarginine deiminase 2-catalyzed histone H3 arginine 26 citrullination facilitates estrogen receptor alpha target gene activation." Proc Natl Acad Sci U S A **109**(33): 13331-13336.

Zhang, Y., J. Liang, Y. Li, C. Xuan, F. Wang, D. Wang, L. Shi, D. Zhang and Y. Shang (2010). "CCCTC-binding factor acts upstream of FOXA1 and demarcates the genomic response to estrogen." J Biol Chem **285**(37): 28604-28613.

Zhou, F., B. Bouillard, M. O. Pharaboz-Joly and J. Andre (1989). "Non-classical antiestrogenic actions of dexamethasone in variant MCF-7 human breast cancer cells in culture." Mol Cell Endocrinol **66**(2): 189-197.

Zhuang, Y. H., R. Saaristo and T. Ylikomi (2003). "An in vitro long-term culture model for normal human mammary gland: expression and regulation of steroid receptors." Cell Tissue Res **311**(2): 217-226.